Operation and Control of Electric Energy Processing Systems

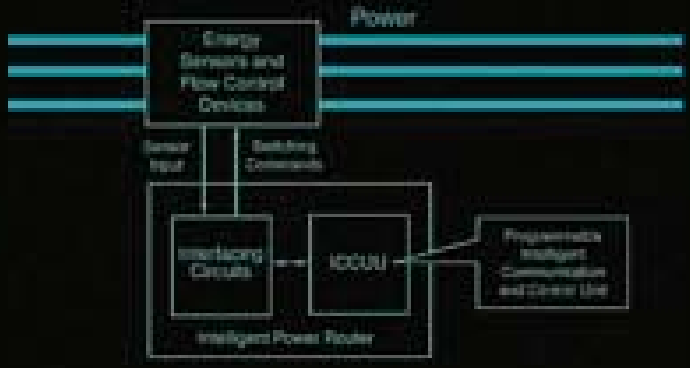

JAMES MOMOH • LAMINE MILI

WILEY
IEEE
IEEE PRESS
Mohamed E. El-Hawary, *Series Editor*

OPERATION AND CONTROL OF ELECTRIC ENERGY PROCESSING SYSTEMS

IEEE Press
445 Hoes Lane
Piscataway, NJ 08854

Technical Reviewers
Peter Sutherland
GE Energy Services

Fred Denny
McNeese State University

OPERATION AND CONTROL OF ELECTRIC ENERGY PROCESSING SYSTEMS

Edited by

James Momoh
Lamine Mili

Mohamed E. El-Hawary, *Series Editor*

IEEE PRESS

A JOHN WILEY & SONS, INC., PUBLICATION

Published by John Wiley & Sons, Inc., Hoboken, New Jersey.
Published simultaneously in Canada.

Library of Congress Cataloging-in-Publication Data:

Momoh, James A., 1950-
Operation and control of electric energy processing systems / James Momoh, Lamine Mili.
p. cm.
ISBN 978-0-470-47209-5 (cloth)
1. Electric power systems–Control. 2. Electric power-plants–Management. 3. Electric utilities–Management. I. Mili, Lamine. II. Title.
TK1191.M55 2009
621.3–dc22

2009040165

Printed in the United States of America.

10 9 8 7 6 5 4 3 2 1

CONTENTS

PREFACE ix

CONTRIBUTORS xi

1 A FRAMEWORK FOR INTERDISCIPLINARY RESEARCH AND EDUCATION 1
James Momoh

1.1 Introduction 1
1.2 Power System Challenges 4
1.2.1 The Power System Modeling and Computational Challenge 5
1.2.2 Modeling and Computational Techniques 6
1.2.3 New Interdisciplinary Curriculum for the Electric Power Network 6
1.3 Solution of the EPNES Architecture 6
1.3.1 Modular Description of the EPNES Architecture 6
1.3.2 Some Expectations of Studies Using EPNES Benchmark Test Beds 7
1.4 Test Beds for EPNES 8
1.4.1 Power System Model for the Navy 8
1.4.2 Civil Test Bed—179-Bus WSCC Benchmark Power System 10
1.5 Examples of Funded Research Work in Response to the EPNES Solicitation 10
1.5.1 Funded Research by Topical Areas/Groups under the EPNES Award 10
1.5.2 EPNES Award Distribution 12
1.6 Future Directions of EPNES 13
1.7 Conclusions 14

2 DYNAMICAL MODELS IN FAULT-TOLERANT OPERATION AND CONTROL OF ENERGY PROCESSING SYSTEMS 15
Christoforos N. Hadjicostis, Hugo Rodríguez Cortés, Aleksandar M. Stankovic

2.1 Introduction 15
2.2 Model-Based Fault Detection 16

2.2.1 Fault Detection via Analytic Redundancy 17
2.2.2 Failure Detection Filters 17
2.3 Detuning Detection and Accommodation on IFOC-Driven Induction Motors 19
2.3.1 Detuned Operation of Current-Fed Indirect Field-Oriented Controlled Induction Motors 20
2.3.2 Detection of the Detuned Operation 24
2.3.3 Estimation of the Magnetizing Flux 26
2.3.4 Accommodation of the Detuning Operation 27
2.3.5 Simulations 28
2.4 Broken Rotor Bar Detection on IFOC-Driven Induction Motors 28
2.4.1 Squirrel Cage Induction Motor Model with Broken Rotor Bars 29
2.4.2 Broken Rotor Bar Detection 31
2.5 Fault Detection on Power Systems 35
2.5.1 The Model 35
2.5.2 Class of Events 37
2.5.3 The Navy Electric Ship Example 38
2.5.4 Fault Detection Scheme 39
2.5.5 Numerical Simulations 41
2.6 Conclusions 43

3 INTELLIGENT POWER ROUTERS: DISTRIBUTED COORDINATION FOR ELECTRIC ENERGY PROCESSING NETWORKS 47

Agustín A. Irizarry-Rivera, Manuel Rodríguez-Martínez, Bienvenido Vélez, Miguel Vélez-Reyes, Alberto R. Ramirez-Orquin, Efraín O'Neill-Carrillo, José R. Cedeño

3.1 Introduction 47
3.2 Overview of the Intelligent Power Router Concept 48
3.3 IPR Architecture and Software Module 50
3.4 IPR Communication Protocols 55
3.4.1 State of the Art 55
3.4.2 Restoration of Electrical Energy Networks with IPRs 59
3.4.3 Mathematical Formulation 60
3.4.4 IPR Network Architecture 60
3.4.5 Islanding-Zone Approach via IPR 61
3.4.6 Negotiation in Two Phases 62
3.4.7 Experimental Results 65
3.5 Risk Assessment of a System Operating with IPR 65
3.5.1 IPR Components 65
3.5.2 Configuration 66
3.5.3 Example 66
3.6 Distributed Control Models 71
3.6.1 Distributed Control of Electronic Power Distribution Systems 71

3.6.2 Integrated Power System in Ship Architecture 74
3.6.3 DC Zonal Electric Distribution System 76
3.6.4 Implementation of the Reconfiguration Logic 77
3.6.5 Conclusion 77
3.7 Reconfiguration 79
3.8 Economics Issues of the Intelligent Power Router Service 79
3.8.1 The Standard Market Design (SMD) Environment 80
3.8.2 The Ancillary Service (A/S) Context 81
3.8.3 Reliability Aspects of Ancillary Services 81
3.8.4 The IPR Technical/Social/Economical Potential for Optimality 81
3.8.5 Proposed Definition for the Intelligent Power Router Ancillary Service 82
3.8.6 Summary 82
3.9 Conclusions 82

4 POWER CIRCUIT BREAKER USING MICROMECHANICAL SWITCHES 87
George G. Karady, Gerald T. Heydt, Esma Gel, Norma Hubele

4.1 Introduction 87
4.2 Overview of Technology 88
4.2.1 Medium Voltage Circuit Breaker 88
4.2.2 Micro-Electro-Mechanical Switches (MEMS) 90
4.3 The Concept of a MEMS-Based Circuit Breaker 92
4.3.1 Circuit Description 92
4.3.2 Operational Principle 93
4.3.3 Current Interruption 94
4.3.4 Switch Closing 94
4.4 Investigation of Switching Array Operation 95
4.4.1 Model Development 97
4.4.2 Analysis of Current Interruption and Load Energization 97
4.4.3 Effect of Delayed Opening of Switches 100
4.4.4 A Block of Switch Fails to Open 102
4.4.5 Effect of Delayed Closing of Switches 103
4.4.6 One Set of Switches Fails to Close 103
4.4.7 Summary of Simulation Results 104
4.5 Reliability Analyses 105
4.5.1 Approximations to Estimate Reliability 106
4.5.2 Computational Results 108
4.6 Proof of Principle Experiment 109
4.6.1 Circuit Breaker Construction 109
4.6.2 Control Circuit 111
4.7 Circuit Breaker Design 114
4.8 Conclusions 115

5 GIS-BASED SIMULATION STUDIES FOR POWER SYSTEMS EDUCATION **119**
Ralph D. Badinelli, Virgilio Centeno, Boonyarit Intiyot

5.1 Overview 119
5.1.1 Case Studies 121
5.1.2 Generic Decision Model Structure 123
5.1.3 Simulation Modeling 126
5.1.4 Interfacing 130
5.2 Concepts for Modeling Power System Management and Control 133
5.2.1 Large-Scale Optimization and Hierarchical Planning 133
5.2.2 Sequential Decision Processes and Adaptation 137
5.2.3 Stochastic Decisions and Risk Modeling 140
5.2.4 Group Decision Making and Markets 141
5.2.5 Power System Simulation Objects 142
5.3 Grid Operation Models and Methods 143
5.3.1 Randomized Load Simulator 144
5.3.2 Market Maker 146
5.3.3 The Commitment Planner 150
5.3.4 Implementation 153

6 DISTRIBUTED GENERATION AND MOMENTUM CHANGE IN THE AMERICAN ELECTRIC UTILITY SYSTEM: A SOCIAL-SCIENCE SYSTEMS APPROACH **157**
Richard F. Hirsh, Benjamin K. Sovacool, Ralph D. Badinelli

6.1 Introduction 157
6.2 Overview of Concepts 158
6.2.1 Using the Systems Approach to Understand Change in the Utility System 158
6.2.2 Origins and Growth of Momentum in the Electric Utility System 159
6.2.3 Politics and System Momentum Change 161
6.3 Application of Principles 163
6.3.1 The Possibility of Distributed Generation and New Momentum 164
6.3.2 Impediments to Decentralized Electricity Generation 166
6.4 Practical Consequences: Distributed Generation as a Business Enterprise 168
6.5 Aggregated Dispatch as a Means to Stimulate Economic Momentum with DG 170
6.6 Conclusion 172

INDEX **177**

PREFACE

This is the second graduate textbook of a two-volume series that relate the interdisciplinary research activities carried out by researchers in power engineering, economics, and systems engineering funded by NSF-ONR EPNES. The NSF-ONR EPNES initiative has enabled researchers, university professors, and graduate students to engage in interdisciplinary work in all the aforementioned areas. The contributors to both volumes have expertise in economics, social sciences, and electric power systems.

Nevertheless, there remain barriers between intellectual disciplines relevant to development of efficient and secure power networks. Innovative and integrated curricula and pedagogy that incorporate advanced systems theory, economics, environmental science, policy, and technical issues must be developed. These two volumes address this need. We hope that this appeal will reach a broad audience of policy makers, executives and engineers of electric utilities, university faculty members and graduate students as well as researchers working in cross-cutting areas related to electric power systems, economics, and social sciences. To our best knowledge, there is no book that combines all these fields. The purpose of these two volumes is to provide working knowledge as well as the latest research in electric power systems theory and applications.

The companion volume of this two-volume series addresses the economic, social, and security aspects of the operation and planning of restructured electric power systems. In the present volume we focus on the operation and control of electric energy processing systems. The multidisciplinary research collected in this volume should well prepare engineers, economists, and social scientists to plan and operate secure and efficient power systems. The contributors emphasize the importance of design in achieving robust power networks that meet resiliency and sustainability requirements.

The present volume is organized in six chapters. Chapter 1, which is authored by J. Momoh, introduces the EPNES initiative. Chapter 2, which is authored by C. N. Hadjicostis, H. Rodríguez Cortés, and A. M. Stankovic, investigates several dynamical models in fault tolerant operation and control of energy processing systems. Chapter 3, which is authored by A. A. Irizarry-Rivera, M. Rodríguez-Martínez, B. Vélez, M. Vélez-Reyes, A. R. Ramirez-Orquin, E. O'Neill-Carrillo, and J. R. Cedeño, develops intelligent power routers for distributed coordination of electric energy processing networks. Chapter 4, which is authored by G. G. Karady, G. T. Heydt, E. Gel, and N. Hubele, deals with the design of power circuit breakers using an array of small micro-electro-mechanical (MEMS) switches together with diodes for faster operation

and smaller equipment size aimed at reducing the vulnerability of a power system to faults. Chapter 5, which is authored by R. D. Badinelli, V. Centeno, and B. Intiyot, develops a GIS-based market simulation studies for power systems education. Finally, Chapter 6, which is authored by R. F. Hirsh, B. K. Sovacool, and R. D. Badinelli, employs a social-sciences approach to help understand the development and use of distributed generation (DG) technologies—small-scale generators that produce power near their loads—in the electric power system.

We are grateful to Katherine Drew from ONR for financial and moral support, Ed Zivi from ONR for the benchmarks, and colleagues from ONR and NSF for fostering a congenial environment that allowed this work to grow and flourish. We thank former NSF division directors, Dr. Rajinder Khosla and Dr. Vasu Varadan, who provided seed funding for this initiative. We also thank Dr. Paul Werbos and Dr. Kishen Baheti from NSF for facilitating interdisciplinary discussions on power systems reliability and education. We are thankful to NSF-DUE program directors, Prof. Roger E. Salters from the NSF Division of Undergraduate Education and Dr. Bruce Hamilton of NSF BES Division.

We acknowledge the contributions of our graduate students at Howard University and at Virginia Tech who helped prepare these volumes for publication.

James Momoh
Department of Electrical and Computer Engineering
Howard University
Washington, DC
jmomoh@howard.edu

Lamine Mili
Department of Electrical and Computer Engineering
Virginia Tech
Falls Church, VA
lmili@vt.edu

CONTRIBUTORS

Ralph D. Badinelli, Pamplin College of Business, Virginia Tech, Blacksburg, VA, USA

Efraín O'Neill-Carrillo, University of Puerto Rico at Mayagüez, Mayagüez, Puerto Rico

José R. Cedeño, University of Puerto Rico at Mayagüez, Mayagüez, Puerto Rico

Virgilio Centeno, Department of Electrical and Computer Engineering, Virginia Tech, Blacksburg, VA, USA

Hugo Rodríguez Cortés, Northeastern University, Boston, MA, USA

Esma Gel, Arizona State University, Tempe, AZ, USA

Christoforos N. Hadjicostis, Associate Professor, University of Cyprus, Nicosia, Cyprus, and University of Illinois at Urbana-Champaign, IL, USA

Gerald T. Heydt, Department of Electrical Engineering, Arizona State University, Tempe, AZ, USA

Richard F. Hirsh, Department of History, Virginia Tech, Blacksburg, VA, USA

Norma Hubele, Industrial Engineering, Arizona State University, Tempe, AZ, USA

Boonyarit Intiyot, Virginia Tech, Blacksburg, VA, USA

George G. Karady, Salt River Chair Professor, Department of Electrical Engineering, Arizona State University, Tempe, AZ, USA

Manuel Rodríguez-Martínez, University of Puerto Rico at Mayagüez, Mayagüez, Puerto Rico

Lamine Mili, Professor and NVC-Electrical and Computer Engineering Program Director, Department of Electrical and Computer Engineering, Virginia Tech, Northern Virginia Center, Falls Church, VA, USA

James Momoh, Professor and Director of CESaC, Department of Electrical and Computer Engineering, Howard University, Washington, DC, USA

Alberto R. Ramirez-Orquin, University of Puerto Rico at Mayagüez, Mayaguez, Puerto Rico

Miguel Vélez-Reyes, Director, Tropical Center for Earth and Space Studies, University of Puerto Rico at Mayagüez, Mayagüez, Puerto Rico

Agustín A. Irizarry-Rivera, Catedrático Asociado, Department of Electrical and Computer Engineering, University of Puerto Rico at Mayagüez, Mayagüez, Puerto Rico

Benjamin K. Sovacool, Virginia Tech, Blacksburg, VA, USA

Aleksandar M. Stankovic, Department of Electrical and Computer Engineering, Northeastern University, Boston, MA, USA

Bienvenido Vélez, University of Puerto Rico at Mayagüez, Mayagüez, Puerto Rico

1

A FRAMEWORK FOR INTERDISCIPLINARY RESEARCH AND EDUCATION

James Momoh

Howard University

1.1 INTRODUCTION

Electric power networks efficiency and security (EPNES) deals with fundamental issues of understanding the security, efficiency, and behavior of large electric power systems, including utility and US Navy power system topologies, under varying disruptive or catastrophic events. Because the US Navy ship power system is an integrated power system (IPS) consisting of AC/DC components and several operational frequencies, they require different modeling and simulation tools than those being using in standard industrial or bulk AC power systems. Accurate contingency evaluation of the Naval Integrated Power System should be based on a comprehensive system model of the naval ship system. For both systems, robustness characteristics are to be measured in terms of various attributes such as survivability, security, efficiency, sustainability, and affordability.

There is an urgent need for the development of innovative methods and conceptual frameworks for analysis, planning, and operation of complex, efficient, and secure electric power networks. If this need is to be met and sustained in the long run, there must be appropriate educational resources developed and available to teach those who will design, develop, and operate those networks. Hence educational pedagogy and

Operation and Control of Electric Energy Processing Systems, Edited by James Momoh and Lamine Mili

curricula improvement must be a natural part of this endeavor. The next generation of high-performance dynamic and adaptive nonlinear networks, of which power systems are an application, will be designed and upgraded with the interdisciplinary knowledge required to achieve improved survivability, security, reliability, reconfigurability, and efficiency.

Additionally, in order to increase interest in power engineering education and to address workforce issues in the deregulated power industry, an interdisciplinary research-based curriculum that prepares engineers, economists, and scientists to plan and operate power networks is necessary. To accomplish this goal, it must be recognized that these networks are sociotechnical systems, meaning that successful functioning depends as much on social factors as technical characteristics. Robust power networks are a critical component of larger efforts to achieve sustainable economic growth on a global scale.

The continued security of electric power networks can be compromised not only by technical breakdowns but also by deliberate sabotage, misguided economic incentives, regulatory difficulties, the shortage of energy production and transmission facilities, and the lack of appropriately trained engineers, scientists, and operations personnel.

Addressing these issues requires an interdisciplinary approach that brings researchers from engineering, environmental, and social-economic sciences together. NSF anticipates that the research activities funded by this program will increase the likelihood that electric power will be available throughout the United States at all times, at reasonable prices, and with minimal deleterious environmental impacts. It is hoped that a convergence of socioeconomic principles with new system theories and computational methods for systems analysis will lead to development of a more efficient, robust, and secure distributed network system. Figure 1.1 depicts the unification of knowledge through research and education.

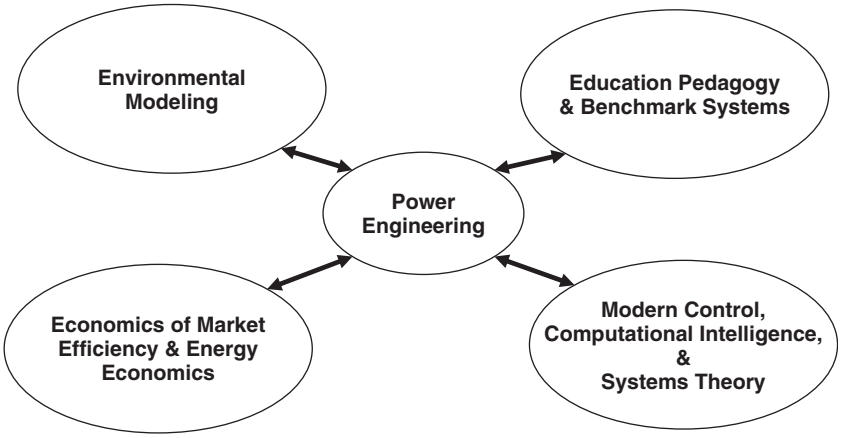

Figure 1.1 Unification of knowledge through research and education.

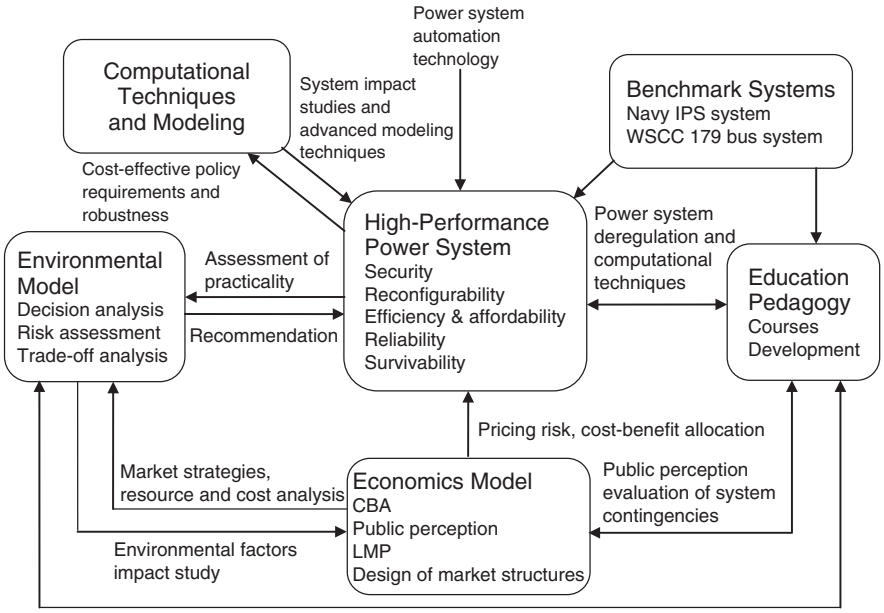

Figure 1.2 Modular representation of the EPNES framework.

Research is needed to develop the power system automation technology that meets all of the technical, economic, and environmental constraints. Research in the individual disciplines has been performed without the unification of the overall research theme across boundaries. This may be due to lack of unifying educational pedagogy and collaborative problem solving among domain experts, both of which could provide deeper understating of power systems under different conditions.

In order to overcome the existing barriers between intellectual disciplines relevant to development of efficient and secure power networks, innovative and integrated curricula and pedagogy that incorporate advanced systems theory, economics, environmental science, policy and technical issues must be developed. These new curriculum will motivate both students and faculty to think in a multidisciplinary manner, in order to better prepare the workforce for the power industry of the future. The EPNES solicitation therefore embraces a multidisciplinary approach in both proposed research and education activities. Some potential cross-cutting courses are financial engineering, power market and cost-benefit analysis, and power environment, advanced system theory and computational intelligence, power economics, and computational tools for deregulated power industry.

We recommend that all multidisciplinary courses use canonical benchmark systems for verification/validation of developed theories and tools. When possible, the courses should be jointly taught by professors across disciplines. To promote broader dissemination of knowledge and understanding, courses should be developed for both undergraduate and graduate students. These courses should also be made available through workshops and lectures, electronically, and be posted on the host institution's

website. Furthermore an assessment strategy should be applied on an ongoing basis to ensure sustainability of the program and its impact in attracting students and improving workforce competencies in developing efficient and reliable power systems.

1.2 POWER SYSTEM CHALLENGES

The EPNES initiative is designed to engender major advances in the integration of new concepts in control, modeling, component technology, and social and economic theories for electrical power networks' efficiency and security [1,2]. It challenges educators and scientists to develop new interdisciplinary research-based curricula and pedagogy that will motivate students' learning and increase their retention across affected disciplines. As such, interdisciplinary research teams of engineers, scientists, social scientists, economists, and environmental experts are required to collaborate on the grand challenges. These challenges include but are not limited to the following categories.

A. Systems and Security

- Advanced Systems Theory: Advanced theories and computer-aided modeling tools to support and validate complex modeling and simulation, advanced adaptive control theory, and intelligent-distributed learning agents with relevant controls for optimal handling of systems complexity and uncertainty.
- Robust Systems Architectures and Configurations: Advanced analytical methods and tools for optimizing and testing configurations of functional elements/architectures to include control of power electronics and systems components, complexity analysis, time-domain simulation, dynamic priority load shedding for survivability, and gaming strategies under uncertainties.
- Security and High-Confidence Systems Architecture: New techniques and innovative tools for fault-tolerant and self-healing networks, situational awareness, smart sensors, and analysis of structural changes. Applications include adaptive control algorithms, systems and component security, and damage control systems for continuity of service during major disruptions.

B. Economics, Efficiency, and Behavior

- Regulatory Constraints and Incentives: New research ideas that explore the influence of regulations on the economics of electric networks.
- Risk Assessment, Risk Perceptions, and Risk Management: Novel methods and applications for linking technical risk assessments, public risk perceptions, and risk management decisions.
- Public Perceptions, Consumer Behavior, and Public Information: Innovative approaches that improve public perception of electric power systems through increased publicity and education about the electric power networks.

C. Environmental Issues

- Environmental Systems and Control: Innovative environmental sensing techniques for system operation and maintenance, improvements in emission

control technologies, and/or network operation for minimization of environmental impact, among others. The interplay of these factors with the other topics in this solicitation is a requirement.

- Technology for Global Sustainability: Cross-disciplinary efforts that contribute to resource and environments transitions and are needed to ensure long-term sustainability of global economic growth.

D. New Curricula and Pedagogy

New Curricula and Pedagogy: Innovative and integrated curricula and pedagogy incorporating advanced system theory, economics, and other social science perspectives, as well as environmental science, policy, and technical issues, are desirable. New and innovative curricula to raise interest levels of both students and faculty, and to better prepare the workforce of the future are also desirable. Pedagogy and curricula must be developed at both the undergraduate and graduate students' level.

E. Benchmark Test Systems

Benchmark Test Systems: These are required for validation of models, advanced theories, algorithms, numerical and computational efficiency, distributed learning agents, robust situational awareness for hierarchical and/or decentralized systems, adaptive controls, self-healing networks, and continuity of service despite faults. A Navy power systems baseline ship architecture is available at the United States Naval Academy, website, http://www.usna.edu/EPNES.
Both civil and Navy test beds will be available from the Howard University website: http://www.cesac.howard.edu/ [3].

1.2.1 The Power System Modeling and Computational Challenge

Power system architectures today are being made more complex as they are enhanced with new grid technology or new devices such as flexible AC transmission system devices (FACTS), distributed generation (DG), automatic voltage regulator (AVR), and advanced control systems. The introduction of these systems will affect overall network performance. Performance assessments to be done can be of two types, either static and dynamic, or quasi-static dynamic behaviors under different (N-1) and (N-2) contingencies.

Several methods are commonly used for evaluating the performance of power systems under different conditions. For small and large disturbances, the methods include Lyapunov stability analysis, power flow, Bode plots, reliability stability assessment, and other frequency response techniques. These tools allow us to determine the various capabilities of the power system in an online or offline mode.

The tools will enable us to achieve better performance analyses, even to take into account other interconnecting networks on the power systems. These can include wireless communication devices, distributed generation, and control devices such as generation schedulers, phase shifters, tap changing transformers, and FACTS devices. In addition to new modeling techniques that incorporate uncertainties, advanced simulation tools are needed.

1.2.2 Modeling and Computational Techniques

Develop techniques that consider all canonical devices, as well as new devices and technologies for power systems, such as FACTS and distributed generation, transformer taps, phase shifters with generation, load, transmission lines, DC/AC converters and their optimal location within the power system. The development of new load flow programs for DC/AC systems for ship and utility systems taking into consideration the peculiarities of both systems is desirable.

1.2.3 New Interdisciplinary Curriculum for the Electric Power Network

EPNES supports research that is performed in interdisciplinary groups with the objective of generating new concepts and approaches stimulated by the interaction of diverse disciplines. This will foster the development of pedagogy and educational material for undergraduate and graduate level students. The initiative supports outreach and curriculum improvements to most effectively educate the future workforce via an interdisciplinary research scope with intellectual merit and broader impacts to the country as well as the global scientific community.

1.3 SOLUTION OF THE EPNES ARCHITECTURE

The explanation of the interaction of different phases of the EPNES framework is presented in terms of the sustainability, survivability, efficiency, and behavior. It satisfies the economic, technical, and environmental constraints, and other social risk factors under different contingencies. It is modeled using advanced systems concepts and accommodates new technology and testable data using the utility and military systems.

1.3.1 Modular Description of the EPNES Architecture

Module 1: High-Performance Electric Power Systems (HPEPS) This is the ultimate automated power systems architecture to be built with the attributes of survivability, security, affordability, and sustainability. The tools developed in the modules below are needed to achieve the proposed HPEPS.

Module 2: Mathematical Analysis Toolkit This module is dedicated to providing models of devices using the elements of advanced system theory and concepts, intelligent distributed learning agents and controls for optimal handling of systems complexity, robust architectures and reconfiguration, and secure, high-confidence systems architecture. The toolkit will require development of new techniques and innovative tools for the optimization and testing of functional elements for electronics and systems components, complexity analysis, time domain simulation, dynamic priority load shedding for survivability, and gaming strategies under uncertainties. Additionally, for secured and high-confidence systems architectures, these tools develop new techniques and analysis techniques for self-healing networks, situational awareness,

smart sensors, and structural changes. This toolkit will also utilize adaptive controls, component security and damage control systems for continuity of service during major disruptions.

Module 3: Behavior and Market Model Tool This module is to be designed based on the design parameters and cost data from the mathematical analysis tool, in order to define the economic and public perception for HPEPS. The module computes regulatory constraints and incentives that economically influence the operation of electric networks. The module provides innovative methods for linking risk assessments, public perceptions, and risk management decisions. The computation of risk indexes based on uncertainties and adequate pricing mechanisms is performed in this module. The computation of cost benefit analysis of different strategies is also to be included.

Module 4: Environment Issues and Control This module utilizes innovative environmental sensing techniques for system operation and maintenance. Improvements in emission controls techniques for minimization of environmental impact are required. To achieve this objective, several indexes are needed to compute the environmental constraints that will be included in the global optimization for developing the risk assessment and cost-benefit analysis tools. The trade-off computed in this module will be used to determine new input for optimizing the HPEPS.

Module 5: Benchmark Test System The validation of the models, advanced algorithms, numerical methods, and computational efficiency will be done using the tools developed in the previous modules using the benchmark systems. Representative test beds and some useful associated models will be described in a later section of the paper. Different performance parameters or attributes of the HPEPS will be analyzed using appropriate models based on hierarchical and decentralized control systems, to ensure continuity of service and abilities in the design and operation of the proposed power system.

1.3.2 Some Expectations of Studies Using EPNES Benchmark Test Beds

Two test beds, involving civilian and military ship power systems, are proposed to support the evaluation of the performance, behavior, efficiency, and security of the power systems as designed. The first is a representative civilian utility system that can be a US utility system or the EPRI/WSCC 180-bus system [4]. Also the US Navy benchmark integrated power system (IPS) system designed by Professor Edwin Zivi of the US Navy Academy is a representative Navy test-bed example. Both systems consist of generator models, transmission networks and interties, various types of loads and controls, and new technology control devices such as FACTS, AC/DC transmission, and distributed generation. To ensure that all elements of EPNES are considered by the researchers, including the issues of environmental constraints (e.g., emission from generator plant devices), public perception, and pricing and cost parameters for economic and risk assessment.

Using studies done on the benchmark systems, we plan to assess the security and reliability of the systems in different scenarios. For the economics studies we plan to assess the cost-benefit analysis acquisition trade-off (cost versus security) and also determine the optimum market structures that will enhance the efficiency of the power system production and delivery. We plan to evaluate the risk assessment and public perception of different operational planning scenarios, given the environmental constraints. The "why" and "how" of the analysis of multiple objectives and constraints will be done using the advanced optimization techniques. We expect that researchers will take advantage of distributed controls and hierarchical structures to handle the challenges of designing the best automation scheme for future power systems that are capable of adapting to different situations, self-reconfiguring, and sustaining faults and yet prove to remain reliable and affordable.

1.4 TEST BEDS FOR EPNES

1.4.1 Power System Model for the Navy

To build a high-performance electric power system (HPEPS) model for the US Navy ship system, a detailed physical model and mathematical model of each component of the ship system is needed. For an integrated power system, at minimum, the generator model, the AC/DC converter, DC/AC inverter and various ship service loads need to be modeled. Because the Navy ship power system is an integrated power system (IPS), an AC/DC power flow program needs to be specially designed for the performance evaluation and security assessment of the naval ship system. Accurate contingency evaluation of the naval integrated power system should be based on a comprehensive system model of the naval ship system.

Figure 1.3 is the AC generation and propulsion test bed. It comprises the following elements:

- The prime mover and governor is a 150 Hp four-quadrant dynamometer system
- The synchronous machine (SM) is a Leroy Somer two-bearing alternator, part number LSA432L7. It is rated for 59 kW (continuous duty) with an output line-to-line voltage of 520 to 590 V_{rms}. The machine is equipped with a brushless excitation system and a voltage regulator.
- The propulsion load consists of the propulsion power converter, induction motor, and load emulator:
  - The inverter propulsion power converter has a rectified, DC link.
  - The propulsion motor is a 460 V_{rms} L-L, 37 kW, 1800 rpm, Baldor model number ZDM4115T-AM1 induction machine (IM).
  - The load emulator is a 37 kW four-quadrant dynamometer.
- The 15 KW ship service power supply (PS) consists of 480 V 3-phase AC diode rectifier bridge feeding a buck converter to produce 500 V DC. These converters provide the logical interconnection of the AC and the DC test beds. In the future an alternative, thyristor-based active rectifier converter may be available.

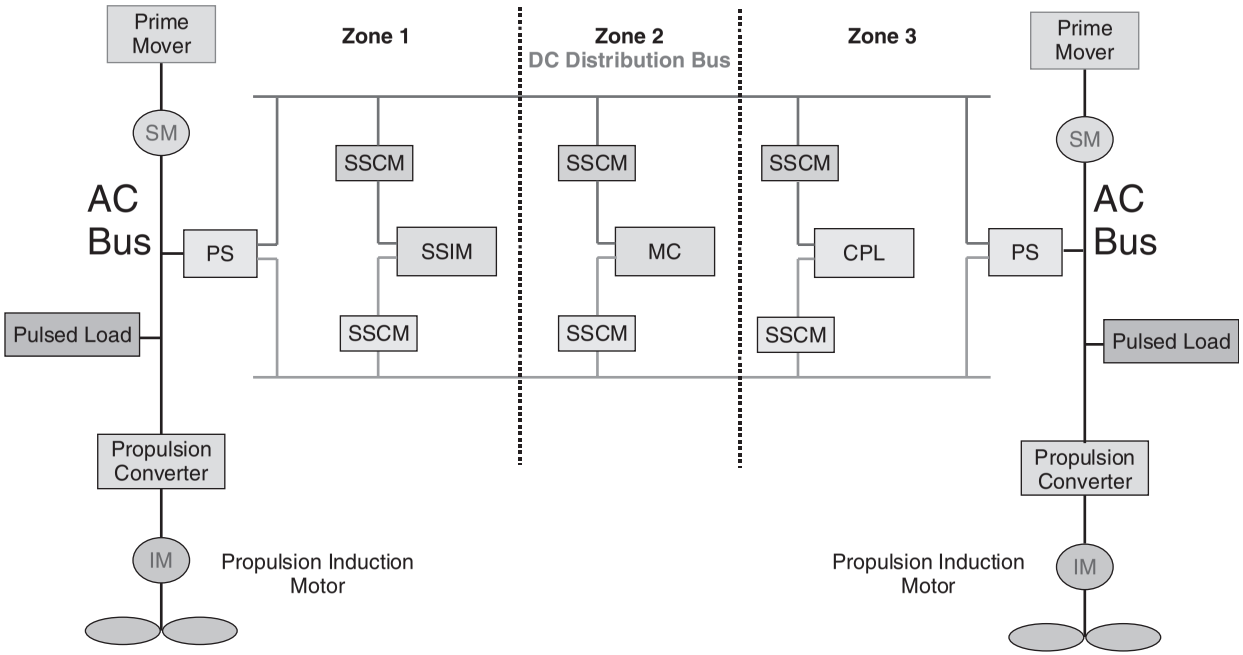

Figure 1.3 Navy power system topology.

- A pulsed load is a purely AC load connected close to the generator terminal for representation of the pulse weaponry. It operates on a base power of 1 KW and requires 100 kW, when fired, from the AC zone of the ship power system.
- The harmonic filter (HF) is a wye-connected LC arrangement. The effective capacitance is 50 μF (which is implemented with two 660 V_{rms} 25 μF capacitors in series) and the design value of inductance is 5.6 mH (rated for a 40 A peak, without saturating.

Also in Figure 1.3, the DC zonal ship service distribution test bed is shown. It is composed of the following elements:

- Each 15 kW ship service power supply consists of a 480 V 3-phase AC diode rectifier bridge feeding a buck converter to produce 500 V DC. These converters provide the logical interconnection of the AC and DC test beds. In the future an alternative, thyristor-based active rectifier converter may be available.
- The 5 kW ship service converter modules convert 500 V DC distribution power to intrazone distribution of approximately 400 VDC
- The 5 kW ship service inverter modules convert the intrazone 400 V DC to three-phase 230 V AC powers.
- The motor controller (MC) is a three-phase inverter rated at 5 kW
- The constant power load (CPL) is a buck converter rated at 5 kW.

1.4.2 Civil Test Bed—179-Bus WSCC Benchmark Power System

The WSCC benchmark system contains 179 buses, 205 transmission lines, 58 generators, and 104 *equivalenced* loads on the high-voltage transmission circuits. The system is operated at 230, 345, and 500 kV [4]. Figure 1.4 shows a HV single line diagram of this system. Also embedded in this system are several control devices/options, including ULTC transformers, fixed series compensators, switchable series compensators, static tap changers/phase regulators, generation control, and 3-winding transformers. At the 100 MVA system base, the total generation is 681.79 + j156.34 p.u. and the total load is 674.10 + j165.79 p.u.

1.5 EXAMPLES OF FUNDED RESEARCH WORK IN RESPONSE TO THE EPNES SOLICITATION

1.5.1 Funded Research by Topical Areas/Groups under the EPNES Award

The awarded research topical areas are grouped in four areas: (1) Group A: system theory, security technology/communications, micro-electro-mechanical systems (MEMS); (2) Group B: economic market efficiency; (3) Group C: interdisciplinary research in systems, economics, and environment; (4) Group D: interdisciplinary education. The titled of the awards for each of these groups are listed below. The four joint NSF/ONR awards are marked with a star (*).

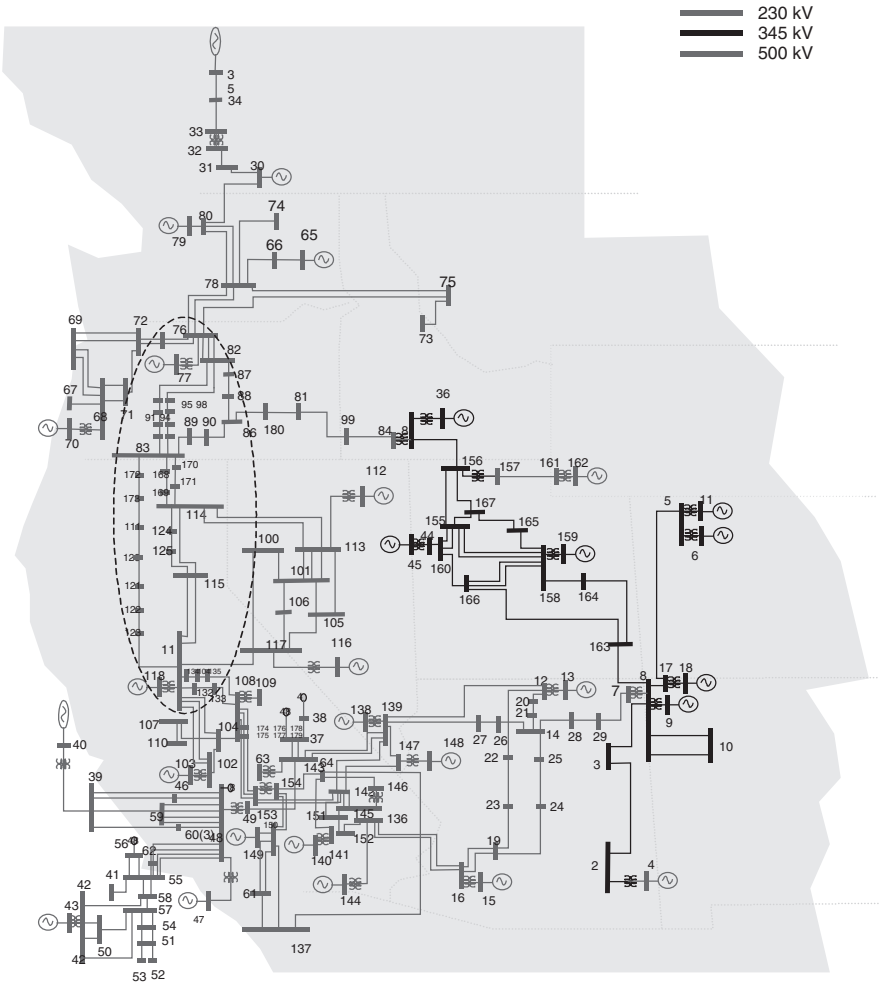

Figure 1.4 One-line diagram of the 179-bus reduced WSCC electric power system.

Group A: Systems Theory, Security, Technology/Communications, Micro-Electro-Mechanical Systems (MEMS)

- University integrated micro-electro-mechanical systems (MEMS) and advance technology for the next generation/power distribution.
- *Dynamic models in fault-tolerant operation and control of energy-processing systems.
- Unified power and communication infrastructure for high-security electricity supply.
- Intelligent power router for distributed coordination in electric energy-processing networks.

- *High confidence control of the power networks using dynamic incentive mechanism.
- Planning reconfigurable power systems control for transmission enhancement with cost recovery systems.

Group B: Economic Market Efficiency

- Forward contracts, multi-settlement equilibrium and risk management in competitive electricity markets.
- Dynamic game theoretic models of electric power markets and their vulnerability.
- Security of supply and strategic learning in restructured power markets.
- Robustness, efficiency, and security of electric power grid in a market environment.
- *Dynamic transmission provision and pricing for electric power systems.
- Pricing transmission congestion to alleviate stability constraints in bulk power planning.

Group C: Interdisciplinary Research in Systems, Economics, and Environment

- Designing an efficient and secure power system using an interdisciplinary research and education approach.
- *Integrating electrical, economics, and environmental factors into flexible power system engineering.
- Modeling the interconnection between technical, social, economics, and environmental components of large scale electric power systems.
- A holistic approach to the design and management of a secure and efficient distributed generation power system.
- Power security enhancement via equilibrium modeling and environmental assessment (collaborative effort among three universities).
- Decentralized resources and decision making.

Group D: Interdisciplinary Education Component of EPNES Initiative

- Development of an undergraduate engineering course in market engineering with application to electricity markets.
- Educational component: Modeling the interaction between the technical, social, economic and environmental components of large-scale electric power systems.
- A technological tool and case studies for education in the design and management of a secure and efficient distributed generation power system.

1.5.2 EPNES Award Distribution

To date, a total of 17 awards, valuing over U.S.$19 million were granted to the winning proposals from 21 universities under the EPNES initiative, supporting the research activities of faculty and students. The topical areas and involved schools are

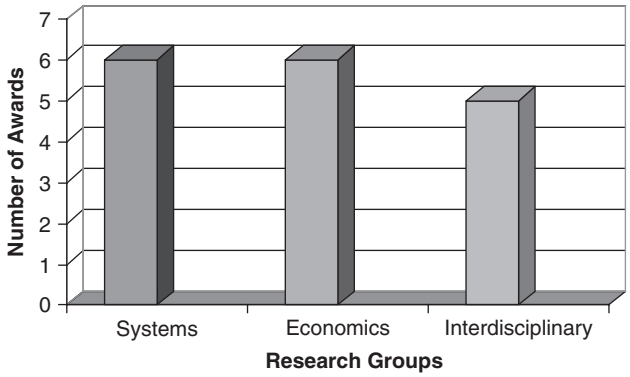

Figure 1.5 Distribution of EPNES awards among interdisciplinary research groups.

listed in the previous section of this paper. Figure 1.5 shows the distribution among the systems, economics, and interdisciplinary groups. These three groups are spanned by the requirements of education and benchmark systems.

1.6 FUTURE DIRECTIONS OF EPNES

1. Promote the implementation of the current EPNES goals by researchers for adoption in the private sector and the Navy. The underlying objective of EPNES is to unify cross-disciplinary research in systems theory, economics principles, and environmental science for the electric power system of the future.
2. Continue to involve industry and government agencies as partners. For example, utilize EPNES as a vehicle for collaboration with US Department of Energy in addressing future needs of the industry such as blackouts, intelligent networks, and power network efficiency.
3. Include more mathematics and system engineering concepts in the scope of EPNES. This includes development of an initiative that is geared to include applied mathematics, systems theory, and security in addressing the needs of the power networks.
4. Extend the economic foundations from markets to cost-benefit analysis and pricing mechanisms for the new age high-performance power networks, both terrestrial and naval.
5. Continue to support reform in power systems with better education pedagogy and more adequate curricula in the colleges and universities. Enforce "learning and research" via collaboration for increased activities that cut across engineering, science, mathematics, environmental, and social science disciplines. Promote and distribute the new education programs throughout the universities and colleges.
6. Use EPNES as a benchmark for proposal requirements of other NSF initiatives. Subsequent proposals submitted by principal investigators to an NSF

multidisciplinary announcement should not be limited to the component level of problem-solving but should reflect a broader and more comprehensive interdisciplinary thinking, together with a plan for real-time implementation of the research by the private sector. Future initiatives would be structured toward the areas of human social dynamics (HSD), critical cyber infrastructure (CCI), and information technology research (ITR).

1.7 CONCLUSIONS

In the electric power networks security and efficiency (EPNES) initiative we have described, we envision a framework of interdisciplinary research work. EPNES has many challenging research and education tasks that will require state-of-the-art knowledge and technologies to complete. Already the research results of the EPNES project hold promise for the improvement of both terrestrial and naval power system performance in terms of survivability, sustainability, efficiency, and security as well as for protection of the environment.

The funded research under the EPNES collaboration demonstrates much breadth of initiative. We believe that these research results will significantly contribute to the education of future engineers, scientists, and economists.

ACKNOWLEDGMENTS

On behalf of the National Science Foundation (NSF) and the Office of Naval Research (ONR), the author would like to acknowledge the participation of all the principal investigators who submitted winning proposals from various educational institutions. They have effectively risen to the challenges of the EPNES initiative.

The author acknowledges the support of the Office of Naval Research in the definition, execution, and partial funding of the EPNES collaboration, in particular, Katherine Drew of the Engineering and Physical Sciences Department.

In addition, the author acknowledges Prof. Edwin Zivi of the United States Naval Academy for his formulation and definition of the Naval benchmark test-bed system.

The author also would like to extend his gratitude to the supporting management teams and staff of NSF.

BIBLIOGRAPHY

1. Program Solicitation for NSF/ONR Partnership in Electric Power Networks Efficiency and Security (EPNES). NSF-02-041. National Science Foundation. http://www.cesac.howard.edu/NSF_proposals/nsf02041.htm.
2. ONR/NSF EPNES Control Challenge Problem Website. United States Naval Academy. http://www.usna.edu/EPNES.
3. Center for Energy Systems and Control (CESaC). Howard University. http://www.cesac.howard.edu/.
4. Power System Data Information. Arizona State University. http://www.public.asu.edu/~huini/WsccDataFiles.htm.

2

DYNAMICAL MODELS IN FAULT-TOLERANT OPERATION AND CONTROL OF ENERGY PROCESSING SYSTEMS

Christoforos N. Hadjicostis,[1] Hugo Rodríguez Cortés,[2]
Aleksandar M. Stankovic[2]

[1] *University of Cyprus and University of Illinois at Urbana-Champaign*
[2] *Northeastern University*

2.1 INTRODUCTION

Our main research goal was to develop a comprehensive framework for fault tolerance enhancement in electric drives and power systems. This framework was to serve as a general tool for analysis and fault-tolerant operation. Its development led us to re-examine the foundations of fault detection and accommodation in energy-processing systems.

Energy processing systems share a number of features with other large, complex engineered systems, including the possibility of failure of components and links. Present technology tends to emphasize the role of automation in detecting and accommodating equipment failures and in maintaining system integrity. In power systems the problem of component failure is addressed in the framework of security. The main premise is that the analyst can generate a list of likely (credible) outages, and then study the effects of each of these outages using the best available information about the state of the system at the time of interest. In utility practice the list of outages typically includes faults of major (single) pieces of equipment,

Operation and Control of Electric Energy Processing Systems, Edited by James Momoh and Lamine Mili

like generators, transmission lines, loads, and transformers. Under the assumption that the system protection correctly identifies the faulted piece, a static (load-flow) analysis is performed on the remaining system (with the faulted piece disconnected) to ensure that the system continues to operate within acceptable performance and safety limits. The models used in the process often come from system design studies, and they have not been verified by specific experiments. The US Navy uses a similar procedure: the damage tolerance analysis includes a generation of the list of failed components (often as a part of weapons damage assessment), followed by a static analysis of line flows and node voltages.

Neither utility nor Navy experts are completely satisfied with the present state of affairs. Months of studies and model tuning are often necessary to only qualitatively capture the main features of systemwide outages, such as in California in 1996. Improvements that have been considered (mostly in the research literature) include the use of dynamical models for assessment of prefault states (dynamic state estimation) and of transients following the outage (the so-called dynamic security assessment). Two main stumbling blocks with this approach are the need to tailor the level of detail for component models (so as to keep the overall model tractable) and the need to include the effects (and possible misfiring) of protection in a systematic fashion.

In our research we developed dynamic models for various tasks, including component protection, dynamic fault detection, and accommodation, and made novel connections with traditional fault detection techniques. Toward this end, in Section 1.2 we review model-based fault detection techniques. The review covers failure detection filtering approaches, starting from the pioneering work of Beard and Jones and ending at the detection schemes based on differential geometry techniques. The rest of the chapter is devoted to the solution of fault detection problems in energy processing systems. We begin in Section 1.3 with a monitoring scheme to detect detuned operation in IFOC driven induction motors. In Section 1.3 we propose a monitoring scheme to detect broken rotor bars on IFOC-driven squirrel cage induction motors. Finally, in Section 1.5 we propose a monitoring scheme to detect bus load changes, symmetric line short circuits, and lost lines on the power system of the Navy electric ship.

2.2 MODEL-BASED FAULT DETECTION

The basic function of a fault detection scheme is to produce an alarm when a fault occurs in the monitored system, and in a second stage to identify the failed component. Ideally the alarm should be a binary signal announcing that a fault is influencing the system or that no fault is hampering the system. Another important characteristic for the alarm is the speed of detection. It is desirable to have a fault detection scheme that produces an alarm immediately after the occurrence of the fault. Finally, the most important characteristic of the alarm is the rate of false alarms, as false alarms deteriorate the performance of fault detection schemes. Thus a great effort in the design of fault detection schemes focuses on the problem of generation of alarms providing effective discrimination between different faults, system disturbances and modeling uncertainties.

2.2.1 Fault Detection via Analytic Redundancy

Residuals, also denoted as alarms, are quantities expressing the difference between the actual plant outputs and those expected on the basis of the applied inputs and the mathematical model. They are obtained by exploiting dynamic or static relationships among sensor outputs and actuator inputs. An important characteristic for residuals is that they need to be robust with respect to the effect of nuisance faults; otherwise, nuisance faults will obscure the residual's performance by acting as a source of false alarms.

The general procedure of fault detection, isolation and accommodation (FDIA) in dynamic systems with the aid of analytical redundancy consists of the following three steps [20]:

1. Generation of functions that carry information about the faults, so-called residuals.
2. Decision about the occurrence of a fault and localization of the fault, so-called isolation.
3. Accommodation of the faulty process, and transition to normal operation.

To date, much of the work on the generation of residuals mostly performed within the analytic redundancy framework observes two important tendencies: failure detection filters and parity relations. The similarities between these two approaches lead to the same residuals being applicable for linear systems and for some nonlinear systems [8].

2.2.2 Failure Detection Filters

Beard [2] was the first to propose a fault detection filter, refined later by Jones [10]. In this filter, known as the Beard–Jones detection (BJD) filter, the reachable subspaces of each fault are placed into invariant independent subspaces. Then, when a nonzero residual is detected, the fault is identified by projecting the residual onto the reachable subspaces of faults and comparing the projection against a threshold. Even though multiple faults can be detected with this filter, the approach is very restrictive as faults have to satisfy a mutual detectability condition [15].

Further improvements to the BJD filter were suggested in [16] with the restricted diagonal detection (RDD) filter. In this approach faults are divided into faults that need to be detected (so-called target faults) and nuisance faults (e.g., parameter uncertainties, changes in system parameters, and noise). Nuisance faults are projected onto the unobservable space of residuals while maintaining observability of target faults; then target faults are identified as in the BJD filter. When every fault is detected, BJD and RDD filters are equivalent.

The most recent version of the BJD filter, the so-called unknown input (UI) observer approach, was proposed in [20] using the eigenstructure assignment and the Kronecker canonical form as design methods, and in [16] using geometric techniques. In the UI observer approach, nuisance faults are projected onto the unobservable subspace so that residuals are influenced only by the target fault, simplifying in this way the decision task. It should be pointed out that even though the use of UI observers

in fault detection and isolation was first proposed in [16–20], UI observers have received significant attention only after the pioneering work of Basille and Marro, presented for instance in [1]. In this chapter we consider the UI observer approach with geometric techniques.

In the nonlinear setting, the residual generation problem using analytic redundancy has been addressed in [9] for state-affine systems and lately in [6] for input-affine systems. In these works residual generator construction is based, under some mild additional assumptions, on the existence of an unobservability subspace (distribution) leading to a subsystem unaffected by all fault signals but the fault of interest; then an asymptotic observer for such a subsystem, which in the nonlinear case may not exist, yields the residual generator.

Consider the nonlinear system

$$\begin{aligned} \dot{x} &= f(x) + g(x)u + l_N(x)m_N + l_T(x)m_T \\ y &= h(x) \end{aligned} \tag{2.1}$$

where $x \in R^n$ is the state, $y \in R^k$ is the measurable output, $m_N \in R^{l1}$ and $m_T \in R^{l2}$ are arbitrary functions of time representing the nuisance and target failure modes respectively. During fault free operation the failure modes are equal to zero. The columns of $f(x), g(x), h(x), l_T(x)$, and $l_T(x)$ are smooth vector fields. The matrices $l_T(x)$ and $l_N(x)$ denote the failure signatures.

Problem 1: Consider the energy processing system described by equation (2.1) Design a dynamic residual generator with state $\hat{x} \in R^e$, of the form

$$\begin{aligned} \dot{\hat{x}} &= F(\hat{x}, y) + E(\hat{x}, y)u \\ r &= M(\hat{x}, y) \end{aligned} \tag{2.2}$$

where $F(\hat{x}, y), E(\hat{x}, y)$, and $M(\hat{x}, y)$ are smooth vector fields, that takes y and u as inputs and generates the residual signal r with the following local properties:

I. When the target failure is not present, r decays asymptotically to zero; that is, the transmission from u and nuisance faults is zero and r is asymptotically stable.

II. For a nonzero target fault, the residual is nonzero.

Condition I considers the stability of the residual generator and ensures that the input signal u and the nuisance faults m_N do not affect the residual r. Condition II guarantees that the target fault affects the residual.

In [6] a necessary condition for the existence of a solution to Problem 1 is given. This condition, under some mild assumptions, leads to a subsystem driven only by the fault of interest. Thus the solution to Problem 1 can be found provided there is an observer for such a subsystem. Specifically, assume that the minimal unobservability distribution of (2.1), denoted by S^*, that contains the image of the nuisance fault signature is locally nonsingular. Then it can be shown that if

$$S^* \cap \text{ span}\{\mathrm{l_T(x)}\} = \{0\} \tag{2.3}$$

it is possible to find a state diffeomorphism and an output diffeomorphism

$$\begin{bmatrix} z_1 \\ z_2 \\ z_3 \end{bmatrix} = \phi(x), \quad \begin{bmatrix} w_1 \\ w_2 \end{bmatrix} = \psi(y) \tag{2.4}$$

such that in the new coordinates the system (2.1) is described by equations of the form

$$\begin{aligned} \dot{z}_1 &= f_1(z_1, z_2) + g_1(z_1, z_2) + l_{T1}(z)m_T \\ \dot{z}_2 &= f_2(z) + g_2(z) + l_{N2}(z)m_N + L_{T2}(z)m_T \\ \dot{z}_3 &= f_3(z) + g_3(z) + l_{N3}(z)m_N + L_{T3}(z)m_T \\ w_1 &= h_1(z_1) \\ w_2 &= z_2 \end{aligned}$$

From these equations it is possible to extract a subsystem driven only by the fault of interest (target fault) as

$$\begin{aligned} \dot{z}_1 &= f_1(z_1, z_2) + g_1(z_1, z_2) + l_{T1}(z)m_T \\ w_1 &= h_1(z_1) \end{aligned} \tag{2.5}$$

Clearly, when it is possible to design an observer for (2.5), the residual generation problem is solvable. The minimal unobservability distribution S^* containing the image of the nuisance fault signature can be computed as the last element of the sequence

$$\begin{aligned} S_0 &= W^* + \text{Ker}\{dh\} \\ S_k &= W^* + [f, S_{k-1} \cap \text{Ker}\{\text{d}h\}] + [g, S_{k-1} \cap \text{Ker}\{\text{d}h\}], \qquad i = 1, \ldots, k \end{aligned} \tag{2.6}$$

where $k \leq n-1$ is determined by the condition $S_k = S_{k-1}$. Concerning W^*, it is computed as the last element of the following sequence:

$$\begin{aligned} W_0 &= \overline{P} \\ W_i &= \overline{W}_{i-1} + [f, \overline{W}_{i-1} \cap \text{Ker}\{\text{d}h\}] + [g, \overline{W}_{i-1} \cap \text{Ker d}h], \qquad i = 1, \ldots, k \end{aligned} \tag{2.7}$$

with $i \leq n-1$ determined by the condition $W_{i+1} = W_i$. In (2.6) and (2.7) the $[.,.]$ denotes the Lie product, $\overline{X}$ denotes the involutive closure of X, and $\boldsymbol{P} = \text{span}\{\boldsymbol{l}_N(x)\}$.

Finally, we consider nonlinear systems with unstructured failure modes described by equations of the form

$$\begin{aligned} \dot{x} &= f(x, m_T, m_N) + g(x, m_T, m_N)u \\ y &= h(x) \end{aligned} \tag{2.8}$$

2.3 DETUNING DETECTION AND ACCOMMODATION ON IFOC-DRIVEN INDUCTION MOTORS

In most high-performance applications of electric drives (e.g., speed and position servos), the control structure utilized is the so-called field oriented (vector) control. It allows for (almost) decoupled control of torque and flux, and yields a very fast

transient response. In the case of a well-tuned controller, the main performance limitations come from the current bandwidth of the drive. With modern power electronic switching devices (e.g., IGBT) that bandwidth is well above a kHz, resulting in outstanding electromechanical response. In the case of a detuned operation, however, the performance can degrade substantially, both in transients (torque command following) and in steady state (efficiency). If the detuning is caused by a typically nonmonitored process (e.g., rotor time constant variation, or a slow degradation of the shaft position sensor information), it may go undetected for a while, and lead to drastic efficiency reduction, or even a hard fault. In this chapter we propose model-based scheme to detect the detuning process in a general purpose field-oriented induction drive motor. It is based on differential geometric considerations, and it is immune to a number of transients that normally occur in a high-performance drive, like load torque variations.

2.3.1 Detuned Operation of Current-Fed Indirect Field-Oriented Controlled Induction Motors

It is well known that mechanical commutation simplifies significantly the control task in DC motors. The action of the commutator is to reverse the direction of the armature winding currents as the coils pass the brush position so that the armature current distribution is fixed in space regardless of the rotor speed. Thus the field flux produced by the stator and the magneto-motive force (MMF) created by the current in the armature winding are maintained in a mutually perpendicular orientation independent of the rotor speed. The result of this orthogonality is that the field flux is practically unaffected by the armature current, as a result when the field flux is kept constant, the produced electromechanical torque is proportional to the armature current. High dynamic performance can be obtained using two linear control loops, one (slow) controlling the field flux and the other (fast) one controlling the armature current.

In induction motors field flux and armature MMF distributions are not orthogonal, rendering the analysis and control of these devices more complicated. However, the action of the commutator of a DC machine in holding a fixed orthogonal spatial angle between the field flux and the armature MMF can be emulated in induction machines by orienting the stator current with respect to the rotor flux so as to attain practically independent controlled flux and torque. Such controllers are called field-oriented controllers and they require independent control of both magnitude and phase of the AC quantities.

An understanding of the decoupled flux and torque control resulting from field orientation can be attained from the model of an induction machine in the fixed stator frame [13,18,19]

$$
\begin{aligned}
\sigma \frac{d}{dt} i_{\alpha s} &= -\left(r_s + \frac{L_m}{L_r \tau_r}\right) i_{\alpha s} + \omega_r \frac{L_m}{L_r} \lambda_{\beta r} + \frac{L_m}{L_r \tau_r} \lambda_{\alpha r} + v_{\alpha s} \\
\sigma \frac{d}{dt} i_{\beta s} &= -\left(r_s + \frac{L_m}{L_r \tau_r}\right) i_{\beta s} - \omega_r \frac{L_m}{L_r} \lambda_{\alpha r} + \frac{L_m}{L_r \tau_r} \lambda_{\beta r} + v_{\beta s} \\
\frac{d}{dt} \lambda_{\alpha r} &= -\frac{1}{\tau_r} \lambda_{\alpha r} - \omega_r \lambda_{\beta r} + \frac{L_m}{\tau_r} i_{\alpha s}
\end{aligned}
\tag{2.9}
$$

$$\frac{d}{dt}\lambda_{\beta r} = -\frac{1}{\tau_r}\lambda_{\beta r} + \omega_r \lambda_{\alpha r} + \frac{L_m}{\tau_r} i_{\beta s}$$

$$\frac{2J}{P}\frac{d}{dt}\omega_r = \frac{P}{2}\frac{L_m}{L_r}(\lambda_{\alpha r} i_{\beta s} - \lambda_{\beta r} i_{\alpha s}) - \tau_L$$

where $i_{\alpha\beta s}$ are the stator currents, $\lambda_{\alpha\beta r}$ are the rotor flux linkages, $v_{\alpha\beta s}$ are the stator voltages, $\omega_r(P/2)$ is the mechanical velocity, P is the number of poles in the machine, J is the rotational inertia, τ_L is the torque load, r_s, r_r are the stator and rotor resistances, L_s, L_r, L_m are the stator, rotor and mutual inductances, $\tau_r = L_r/r_r$ and $\sigma = L_s - L_m^2/L_r$.

The field orientation concept implies that the current components supplied to the machine should be oriented in phase (flux components) and in quadrature (torque component) to the rotor flux vector $\lambda_{\alpha\beta r}$. This can be accomplished by choosing ω_e to be the instantaneous speed of $\lambda_{\alpha\beta r}$ and locking the phase of the reference system to the direction of the magnetizing flux λ_M; that is,

$$\begin{bmatrix} \lambda_M \\ 0 \end{bmatrix} = e^{-J\theta_e} \begin{bmatrix} \lambda_{\alpha r} \\ \lambda_{\beta r} \end{bmatrix} \tag{2.10}$$

where

$$e^{J\theta_e} = \begin{bmatrix} \cos(x) & -\sin(\theta_e) \\ \sin(x) & \cos(x) \end{bmatrix}.$$

When the machine is supplied from a current-regulated source, the stator equations can be omitted; the rotor dynamics, in terms of stator currents and rotor flux, in a rotor field-oriented frame is described by the equations

$$\frac{d}{dt}\lambda_M = -\frac{1}{\tau_r}\lambda_M + \frac{L_m}{\tau_r} i_{ds} \tag{2.11}$$

$$\omega_e = \omega_r + \frac{L_m}{\tau_r}\frac{i_{\beta s}}{\lambda_M} \tag{2.12}$$

$$\frac{2J}{P}\frac{d}{dt}\omega_r = \frac{P}{2}\frac{L_m}{L_r}\lambda_M i_{qs} - \tau_L \tag{2.13}$$

with $i_{dqs} = e^{-J\theta_e} i_{\alpha\beta s}$

Equations (2.11) to (2.13) describe the dynamic response of a field-oriented induction machine and essentially parallel the DC machine dynamics. Equation (2.11) corresponds to the field circuit on a DC machine. Equation (2.12) defines what is commonly called the slip frequency $\omega_s = \omega_e - \omega_r$ which is inherently associated with the division of the input stator current into the desired flux and torque components. The electromechanical torque in (2.13) shows the desired torque control property of providing a torque proportional to the torque command current i_{qs}.

The implementation of field orientation can be easily carried out provided that the position angle of the rotor flux θ_e is known. There are two basic approaches to determine θ_e: direct schemes, which determine the angle from flux measurements, and

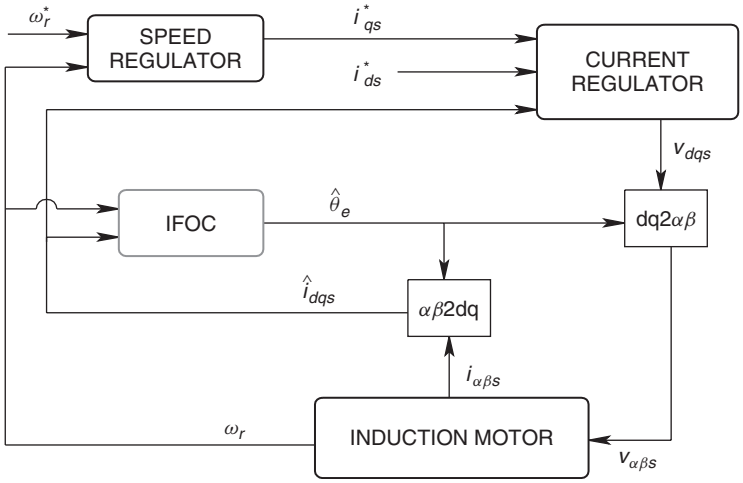

Figure 2.1 Indirect field-oriented control diagram.

indirect schemes, which measure the rotor velocity and utilize the slip frequency to compute the angle of the rotor flux relative to the rotor. The indirect method uses the fact that a necessary condition to produce field orientation is to satisfy the slip relation. An indirect field-oriented controller is described by the equations

$$\begin{aligned} \frac{d}{dt}\hat{\lambda}_M &= -\frac{1}{\hat{\tau}_r}\hat{\lambda}_M + \frac{L_m}{\hat{\tau}_r}\hat{i}_{ds} \\ \hat{\omega}_e &= \omega_r + \frac{L_m}{\hat{\tau}_r}\frac{\hat{i}_{\beta s}}{\hat{\lambda}_M} \end{aligned} \tag{2.14}$$

where $\hat{\omega}_e$ is the estimated synchronous velocity, $\hat{\lambda}_M$ is the estimated rotor flux linkage, $\hat{\tau}_r$ is the estimated rotor time constant, and $\hat{i}_{dqs}$ are the measured stator currents. The indirect field-oriented controller together with the current controller and the speed controller are shown in Figure 2.1. From (2.11), (2.12), and (2.14) we observe that $\hat{\omega}_e = \omega_e$ and $\hat{\lambda}_M = \lambda_M$ provided that all parameters are accurately known. As a result $\theta_e = \hat{\theta}_e$ and the measured stator currents $\hat{i}_{dqs}$ are equal to the actual stator currents i_{dqs}. It is reasonable to assume that we have a good estimate of L_m; however, the rotor time constant is usually not exactly known as it changes because of motor heating, mismatch in manufacturing, or other variations. A mismatch in the rotor time constant results in a loss of the correct field orientation, labeled as detuning of the controller. The main consequences of detuning are a flux level that is not properly maintained, a resulting steady state that is not the commanded value, a torque response that is degraded, and a degraded efficiency and increased motor heating.

Next, we obtain a dynamic model that accounts for the detuning effect. Although the true field-oriented induction motor dynamics (2.11)–(2.13) exist in the motor, its states cannot be measured directly. In fact the only measurable outputs of the

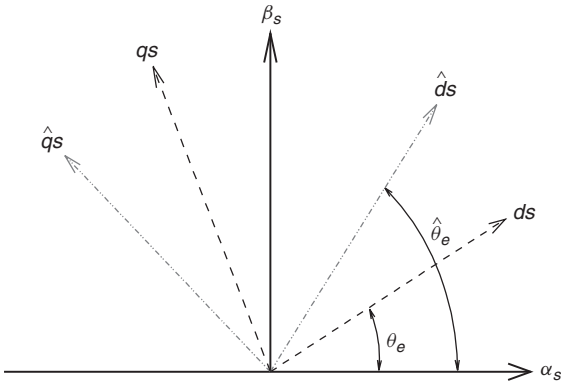

Figure 2.2 Fixed frame and rotating frames.

induction motor are the stator currents in the *abc* frame and the mechanical rotor speed ω_r. Since it is assumed that the induction motor is wye connected, the currents $i_{\alpha\beta s}$ can be obtained from i_{abcs} as follows:

$$\begin{aligned} i_{\alpha s} &= \sqrt{\frac{3}{2}} i_{as} \\ i_{\beta s} &= \frac{1}{\sqrt{2}}(i_{bs} - i_{cs}) \end{aligned} \tag{2.15}$$

As observed in Figure 2.2, the relation between currents $i_{\alpha\beta s}$ and currents i_{dqs} is defined by

$$i_{\alpha\beta s} = e^{J\theta_e} i_{dqs} \tag{2.16}$$

Note now that in a detuned condition ($\theta_e \neq \hat{\theta}_e$) stator currents are given as

$$i_{dqs} = e^{-J\hat{\theta}_e} i_{\alpha\beta s} \tag{2.17}$$

thus from (1.16) and (1.17) we conclude that

$$i_{dqs} = e^{-J\tilde{\theta}_e} \hat{i}_{dqs} \tag{2.18}$$

with $\tilde{\theta}_e = \theta_e - \hat{\theta}_e$.

Replacing (2.18) into (2.11) to (2.13) and reordering terms, we get an indirect field-oriented controlled induction motor model that includes detuning effects and is described by the following equations:

$$\frac{d}{dt}\lambda_M = -\frac{1}{\tau_r}\lambda_M + \frac{L_m}{\tau_r}\left[\cos(\tilde{\theta}_e)\hat{i}_{ds} + \sin(\tilde{\theta}_e)\hat{i}_{qs}\right]$$

$$\frac{d}{dt}\tilde{\theta}_e = \frac{L_m}{\tau_r}\frac{\cos(\tilde{\theta}_e)\hat{i}_{qs} - \sin(\tilde{\theta}_e)\hat{i}_{ds}}{\lambda_M} - \frac{L_m}{\hat{\tau}_r}\frac{\hat{i}_{ds}}{\hat{\lambda}_M}$$

$$\begin{aligned}\frac{d}{dt}\hat{\lambda}_M &= -\frac{1}{\hat{\tau}_r}\hat{\lambda}_M + \frac{L_m}{\hat{\tau}_r}\hat{i}_{ds} \\ \frac{2J}{P}\frac{d}{dt}\omega_r &= \frac{P}{2}\frac{L_m}{L_r}\lambda_M\left[\cos(\tilde{\theta}_e)\hat{i}_{qs} - \sin(\tilde{\theta}_e)\hat{i}_{ds}\right] - \tau_L\end{aligned} \tag{2.19}$$

where $\frac{d}{dt}\theta_e = \omega_e - \hat{\omega}_e$. Note now that in steady state, from equation (2.19) we have that

$$\frac{1}{\tau_r}\frac{\cos(\tilde{\theta}_e)\hat{i}_{qs} - \sin(\tilde{\theta}_e)\hat{i}_{ds}}{\cos(\tilde{\theta}_e)\hat{i}_{ds} + \sin(\tilde{\theta}_e)\hat{i}_{qs}} = \frac{1}{\hat{\tau}_r}\frac{\hat{i}_{qs}}{\hat{i}_{ds}} \tag{2.20}$$

This gives

$$\tan(\tilde{\theta}_e) = \frac{\left(1 - \frac{\tau_r}{\hat{\tau}_r}\right)\frac{\hat{i}_{qs}}{\hat{i}_{ds}}}{1 + \frac{\tau_r}{\hat{\tau}_r}\left(\frac{\hat{i}_{qs}}{\hat{i}_{ds}}\right)^2}$$

thus $\tilde{\theta}_e = 0$ provided that $\tau_r = \hat{\tau}_r$.

2.3.2 Detection of the Detuned Operation

Next we design a residual generator to detect detuned indirect field-oriented controllers following the model-based fault detection method outlined in the previous section. We consider $\tilde{\theta}_e$ in (2.19) as an externally generated signal, and for fault detection we consider the following system:

$$\begin{aligned}\frac{d}{dt}\lambda_M &= -\frac{1}{\tau_r}\lambda_M + \frac{L_m}{\tau_r}[\cos(\tilde{\theta}_e)\hat{i}_{ds} + \sin(\tilde{\theta}_e)\hat{i}_{qs}] \\ \frac{2J}{P}\frac{d}{dt}\omega_r &= \frac{P}{2}\frac{L_m}{L_r}\lambda_M[\cos(\tilde{\theta}_e)\hat{i}_{qs} - \sin(\tilde{\theta}_e)\hat{i}_{ds}] - \tau_L\end{aligned} \tag{2.21}$$

Note now that to express the dynamics in (2.21) in terms of the system (2.1), we need to identify the target and nuisance faults. Since the load torque τ_L is also an unknown quantity that may vary over a wide range depending on the motor application, we consider it as a nuisance fault; that is,

$$l_N = \begin{bmatrix} 0 \\ -\frac{P}{2J} \end{bmatrix}$$

Note that now the information about detuning ($\tilde{\theta}_e \neq 0$) is contained on the trigonometric functions of (2.21). So, by defining,

$$m_T = \begin{bmatrix} \cos(\tilde{\theta}_e) - 1 \\ \sin(\tilde{\theta}_e) \end{bmatrix}$$

we have

$$l_T = \begin{bmatrix} \frac{L_m}{\tau_r}\hat{i}_{ds} & \frac{L_m}{\tau_r}\hat{i}_{qs} \\ \frac{P^2}{4J}\frac{L_m}{L_r}\lambda_M\hat{i}_{qs} & -\frac{P^2}{4J}\frac{L_m}{L_r}\lambda_M\hat{i}_{ds} \end{bmatrix},$$

$$f = \begin{bmatrix} -\frac{1}{\tau_r}\lambda_M \\ 0 \end{bmatrix}, \quad g = \begin{bmatrix} \frac{L_m}{\tau_r} & 0 \\ 0 & \frac{P^2}{4J}\frac{L_m}{L_r}\lambda_M \end{bmatrix}$$

and $u = [\hat{i}_{ds} \quad \hat{i}_{qs}]$.

As was stated previously, the only measurable quantity in (2.21) is the rotor speed ω_r; that is,

$$y = \omega_r \tag{2.22}$$

Straightforward computations show that for (2.22) the minimal unobservability distribution is given as

$$S^*_{\omega_r} = \text{span}\left\{ \begin{matrix} 0 & \frac{1}{\tau_r} \\ -\frac{P}{2J} & 0 \end{matrix} \right\}$$

and condition (2.3) is not satisfied.

Consider further the magnetizing flux as the output of the system:

$$y_1 = \lambda_M \tag{2.23}$$

Analogous computations show that

$$S^*_{\lambda_M} = \text{span}\left\{ \begin{matrix} 0 \\ -\frac{P}{2J} \end{matrix} \right\}$$

and condition (2.3) is satisfied.

By inspection we see that in this case the subsystem (2.5), with $z_1 = \lambda_M$ and $w_1 = y_1$, reads as

$$\dot{\lambda}_M = -\frac{1}{\tau_r}\lambda_M + \frac{L_m}{\tau_r}\hat{i}_{ds} + \frac{L_m}{\tau_r}\hat{i}_{ds}m_{t1} + \frac{L_m}{\tau_r}\hat{i}_{qs}m_{t2}$$

Hence we have a solution to Problem 1 by designing an observer for subsystem (2.24). Note that in (2.24) the rotor time constant is unknown. However, the residual generator

$$\begin{aligned} \dot{\bar{\lambda}}_M &= -\frac{1}{\hat{\tau}_r}\bar{\lambda}_M + \frac{L_m}{\hat{\tau}_r}\hat{i}_{ds} - \Gamma(\bar{\lambda}_M - \lambda_M) \\ r &= \bar{\lambda}_M - \lambda_M \end{aligned} \tag{2.24}$$

where $\Gamma > 0$ solves Problem 1.

To verify that a solution to Problem 1 is given by (2.24), note that the dynamics of the residual is described by the equation

$$\dot{r} = -\Gamma r - \left(\frac{1}{\hat{\tau}_r} - \frac{1}{\tau_r}\right)(\lambda_M - L_m \hat{i}_{ds}) - \frac{L_m}{\tau_r}\hat{i}_{ds} m_{t1} - \frac{L_m}{\tau_r}\hat{i}_{qs} m_{t2} \tag{2.25}$$

The second right-hand term in (2.25) is somewhat unexpected; however, we notice that this term will be zero provided m_{t1} and m_{t2} are equal to zero. This term, in fact, also represents the detuning problem expressed as the difference between the estimated rotor time constant and the actual rotor time constant. Hence we have established that (2.24) is a solution to Problem 1.

2.3.3 Estimation of the Magnetizing Flux

Note that to compute the residual, we need to have access to the magnetizing flux λ_M, which is not typically available. As stated in [17], this flux can be computed as follows. Assuming that the rotor dynamics is in steady state, we have

$$\sigma\left[i_{\beta s}\frac{d}{dt}i_{\alpha s} - i_{\alpha s}\frac{d}{dt}i_{\beta s}\right] = \frac{\hat{\omega}_e}{L_r}\lambda_M^2 + q \tag{2.26}$$

where $q = v_{\alpha s} i_{\beta s} - v_{\beta s} i_{\alpha s}$. Define now

$$\theta = \arctan\left(\frac{i_{\alpha s}}{i_{\beta s}}\right) \tag{2.27}$$

thus (2.26) can be written as

$$\dot{\theta} = \frac{\frac{\hat{\omega}_e}{L_r}\lambda_M^2 + q}{\sigma(i_{\alpha s}^2 + i_{\beta s}^2)} \tag{2.28}$$

Under the assumption above λ_M is a constant in (2.28). In order to estimate λ_M, we follow the general results presented in [11]. Define the estimation error

$$z = \Lambda - \lambda_M^2 + \beta(\theta) \tag{2.29}$$

thus we have

$$\dot{z} = \dot{\Lambda} + \frac{\partial \beta}{\partial \theta}\frac{\frac{\hat{\omega}_e}{L_r}(\Lambda - z + \beta(\theta)) + q}{\sigma(i_{\alpha s}^2 + i_{\beta s}^2)}$$

Defining

$$\beta(\theta) = K\sigma\theta, \dot{\Lambda} = -K\frac{\frac{\hat{\omega}_e}{L_r}(\Lambda - z + \beta(\theta)) + q}{\sigma(i_{\alpha s}^2 + i_{\beta s}^2)} \tag{2.30}$$

with $K > 0$, we can describe the estimation error dynamics by

$$\dot{z} = -\frac{K}{L_r}\frac{\hat{\omega}_e}{(i_{\alpha s}^2 + i_{\beta s}^2)}z$$

thus z converges exponentially to zero and

$$\lim_{t\to\infty}(\Lambda - \lambda_M^2 + K\sigma\theta) = 0 \tag{2.31}$$

Finally, from (2.31) we have that

$$\lambda_M = \sqrt{|\Lambda + K\sigma\theta|}$$

We can also estimate the magnetizing flux from stator steady state values. To see this, note that

$$i_{\beta s}\frac{d}{dt}i_{\alpha s} - i_{\alpha s}\frac{d}{dt}i_{\beta s} = i_{qs}\frac{d}{dt}i_{ds} - i_{ds}\frac{d}{dt}i_{qs} - \omega_e[i_{\alpha s}^2 + i_{\beta s}^2] \tag{2.32}$$

Thus, by replacing (2.32) into (2.26) and assuming that the stator dynamics is in steady state, we have

$$\lambda_M = \sqrt{\left|\frac{L_r}{\omega_e}(v_{\beta s}i_{\alpha s} - v_{\alpha s}i_{\beta s}) - \sigma L_r(i_{\alpha s}^2 + i_{\beta s}^2)\right|}$$

2.3.4 Accommodation of the Detuning Operation

In steady state we have

$$i_{ds} = \frac{\lambda_M}{L_m}$$

Moreover, since (2.18) implies

$$\|i_{dqs}\| = \|\hat{i}_{dqs}\|$$

we can compute i_{qs} as

$$i_{qs} = \sqrt{\hat{i}_{ds}^2 + \hat{i}_{qs}^2 + i_{ds}^2} \tag{2.33}$$

Finally, from (1.20) we have

$$\tau_r = \hat{\tau}_r\frac{i_{qs}}{i_{ds}}\frac{\hat{i}_{ds}}{\hat{i}_{qs}} \tag{2.34}$$

For accommodation of the detuning operation, we define a threshold $r_m > 0$ for the residual in such a way that the IFOC is detuned provided that $|r| > r_m$. This threshold reduces the effect of noise and other nonmodeled dynamics on the decision.

Once it is decided that the IFOC is detuned, the accommodation procedure waits for the system to achieve a steady state operation. Then it computes the new rotor time constant from (1.34), and sends it to the IFOC scheme.

TABLE 2.1 Parameters of the induction motor

Parameter	Motor (3 HP)
$L_s, L_r (H)$	0.3826,0.3808
$L_m (H)$	0.3687
$r_r, r_s (\Omega)$	1.34, 1.77
P	4

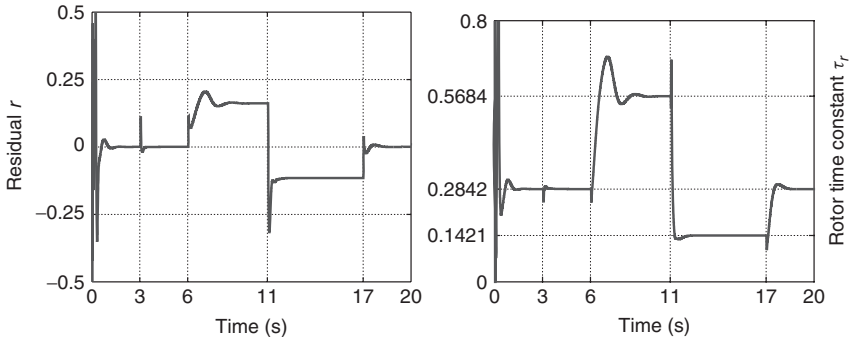

Figure 2.3 (Left) Residual behavior; (right) computed rotor time constant.

2.3.5 Simulations

We now validate the residual generator and the computation of the actual time rotor constant via numerical simulations. We consider an induction motor with the parameters shown in Table 2.1. In all the simulations we select $\Gamma = 10$. In the following simulations the accommodation procedure is not completed; we only compute the actual time rotor constant without correcting it on the IFOC scheme. In order to demonstrate that the residual is not asymptotically affected by changes of the load torque, at $t = 3$ s we reduce the load torqued by 50%. The residual converges to zero as shown in Figure 2.3.

In order to show that the residual detects changes of the rotor time constant, we change at $t = 6$ s, the time rotor constant to twice the nominal value. Note that the residual detects the detuning condition by going to a nonzero equilibrium. At $t = 10$ s, the computed rotor time constant is $\tau_r = 0.56836$; see Figure 2.3. At $t = 11$ s, the time rotor constant is changed to half the nominal value, as we observe that the detuning is detected. We compute the rotor time constant as $\tau_r = 0.14208$. Finally, at $t = 17$ s, the time rotor constant is restored to its nominal value. We observe that the residual goes back to zero.

2.4 BROKEN ROTOR BAR DETECTION ON IFOC-DRIVEN INDUCTION MOTORS

Industrial experience has shown that broken rotor bars can be a serious problem for certain induction motors with demanding work cycles. Although broken rotor bars do not initially cause an induction motor to fail, they can have serious secondary effects. The fault may result in broken parts of the bar hitting stator windings at high speed.

This in turn can cause a serious damage to the induction motor; therefore faulty rotor bars need to be detected as early as possible.

Broken rotor bars cause disturbances of the flux pattern in induction machines. These non-uniform magnetic field components influence machine torque and stator terminal quantities, and are thus detectable, in principle, by monitoring schemes. To date, different methods have been proposed for broken rotor bar detection. The most well known approach is the non−model-based motor current signature analysis (MCSA) method [26]. This method monitors the spectrum of a single phase of the stator current for frequency components associated with broken rotor bars. The main disadvantage of the MCSA method is that it relies on the interpretation of the frequency components of the stator current spectrum that are influenced by many factors, including variations in electric supply and in static and dynamic load conditions. These conditions can lead to errors in the fault detection task [3]. On the other hand, a practical advantage of MCSA is that only stator currents need to be measured. Efforts to eliminate the influence of load conditions have been presented, for instance, in [24] where it is shown that the direct component of the stator currents in a synchronous frame is not affected by load conditions; thus it is proposed to monitor the spectrum of that stator current component. It turns out that in our proposed monitoring scheme we monitor a state closely related to the direct component of the stator current. However, we discovered our signal selection using geometric techniques. Fuzzy logic [22] and neural network [7] techniques have been also proposed to handle load-related ambiguous frequency components. The MCSA method has been the main approach used for detecting broken rotor bars on induction motors operating in open-loop. However, spectral analysis techniques applicable under variable speed conditions have also been presented in the literature (e. g., [4,27]).

Despite the extensive work on broken rotor bar detection, model-based techniques have not received much attention. Main reasons are that fault-related induction motor parameters are not well known, and available models are quite complicated to be tractable with model-based fault detection techniques. However, by making a compromise between a better tracking of the fault-related signals (by using dynamic models) and a reduced domain of applicability of the results (due to assumptions about the induction motor parameters), model-based broken rotor bar detection techniques have been recently proposed. One such example is the Vienna monitoring method (VMM) presented in [12]. The VMM is based on the comparison of the computed electromechanical torque from two real-time machine models. A healthy induction motor leads to equal values computed by the two models, whereas a faulted induction motor excites the models in a different way, leading to a difference between computed torque values. This difference is used to determine the existence of broken rotor bars. The VMM has one disadvantage, which is also present in our proposed monitoring scheme: variations on the time rotor constant deteriorate the performance of the fault detection scheme.

2.4.1 Squirrel Cage Induction Motor Model with Broken Rotor Bars

We present now an induction motor model with broken rotor bars. The proposed model is less detailed than the models presented, for instance, in [14] and [29]. A novel feature is that the effect of broken rotor bars is taken into account by adding only

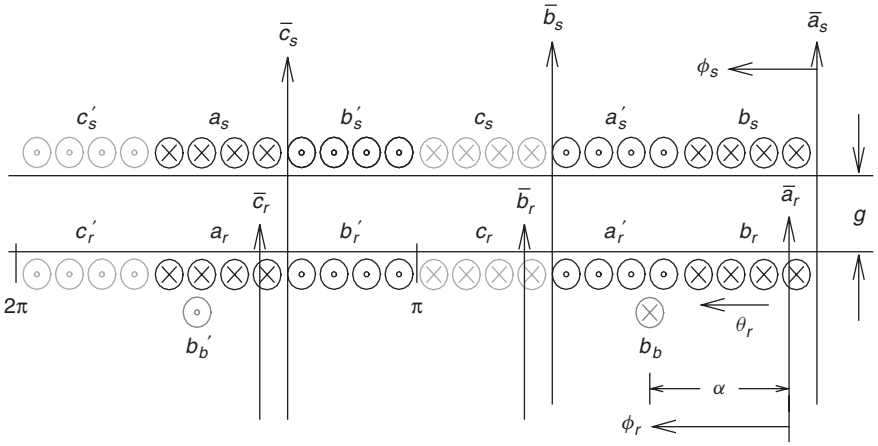

Figure 2.4 Developed diagram of the cross-sectional view.

one state to the classical induction motor model (e.g., in [13]). This way tractability is achieved.

The proposed model is based on the idea that the superimposition of an extra set of rotor currents on those normally found in a healthy motor may account for the effect of broken rotor bars [29]. Our main assumptions are summarized as follows; refer to Figure 2.4.

Because of the high permeability of steel, magnetic fields exist only in the air gap g and have radial direction $\overline{a}_r$ (remember, the air gap is small relative to the inside diameter of the stator). The stator windings $a_s - a_s', b_s - b_s'$, and $c_s - c_s'$ are identical in that each winding has the same resistance and the same number of turns. The rotor windings $a_r - a_r', b_r - b_r'$, and $c_r - c_r'$ are identical in the same sense. All windings have sinusoidal distribution. The extra set of rotor currents (representing the broken bar) is included by adding an extra winding, denoted by $b_b - b_b'$, to the original rotor windings. Magnetic saturation, eddy-currents, and friction losses are not included in our analysis.

In Figure 2.4, $\overline{a}_s, \overline{b}_s, \overline{c}_s$ and $\overline{a}_r, \overline{b}_r, \overline{c}_r$ denote the positive direction of the fluxes produced by each winding. $\otimes$ indicates the positive direction of current. The angular displacement of the rotor relative to $\overline{a}_r$ is denoted by θ_r, the stator angular displacement relative to $\overline{a}_s$ is denoted by ϕ_s, while the rotor angular displacement relative to the $\overline{a}_r$ axis is denoted by ϕ_r. The angular displacements θ_r, ϕ_s, and ϕ_s are related via

$$\phi_s = \phi_r + \theta_r.$$

Following the modeling procedure of [13], we have that the dynamic model of a squirrel cage induction motor with broken bars as described by

$$\begin{aligned} \dot{\lambda}_{abcs} &= -R_s i_{abcs} + v_{abcs} \\ \dot{\lambda}_{abcr} &= -R_r i_{abcr} \\ \dot{\lambda}_b &= -r_b i_b, \end{aligned} \tag{2.35}$$

where $\lambda_{abcs}, \lambda_{abcr}$ are the stator and rotor flux linkages, i_{abcs}, i_{abcr} are the stator and rotor currents, v_{abcs} is the stator voltage, λ_b, i_b are the broken bar flux linkage and current, $R_r = \text{diag}\{r_r\}$ is the rotor resistance, and $R_s = \text{diag}\{r_s\}$ is the stator resistance. Flux linkages and currents are related as

$$\begin{bmatrix} i_{abcs} \\ i_{abcr} \\ i_b \end{bmatrix} = \begin{bmatrix} \mathbf{L}_s & \mathbf{L}_{sr} & \mathbf{L}_{bs} \\ \mathbf{L}_{sr}^T & \mathbf{L}_r & \mathbf{L}_{br} \\ \mathbf{L}_{bs}^T & \mathbf{L}_{br}^T & \mathbf{L}_b \end{bmatrix}^{-1} \begin{bmatrix} \lambda_{abcs} \\ \lambda_{abcr} \\ \lambda_b \end{bmatrix} \tag{2.36}$$

where

$$\begin{aligned}
\mathbf{L}_{bs} &= -L_{bs}\left[\cos(\alpha)\cos\left(\alpha - \frac{2\pi}{3}\right)\cos\left(\alpha + \frac{2\pi}{3}\right)\right] \\
\mathbf{L}_{br} &= -L_{br}\left[\cos(\theta_r - \alpha)\cos\left(\theta_r - \alpha - \frac{2\pi}{3}\right)\cos\left(\theta_r - \alpha + \frac{2\pi}{3}\right)\right] \\
\mathbf{L}_s &= \begin{bmatrix} L_{ls} + L_{ms} & -\frac{L_{ms}}{2} & -\frac{L_{ms}}{2} \\ -\frac{L_{ms}}{2} & L_{ls} + L_{ms} & -\frac{L_{ms}}{2} \\ -\frac{L_{ms}}{2} & -\frac{L_{ms}}{2} & L_{ls} + L_{ms} \end{bmatrix} \\
\mathbf{L}_{sr} &= L_{sr}\begin{bmatrix} \cos(\theta_r) & \cos\left(\theta_r + \frac{2\pi}{3}\right) & \cos\left(\theta_r - \frac{2\pi}{3}\right) \\ \cos\left(\theta_r - \frac{2\pi}{3}\right) & \cos(\theta_r) & \cos\left(\theta_r + \frac{2\pi}{3}\right) \\ \cos\left(\theta_r + \frac{2\pi}{3}\right) & \cos\left(\theta_r - \frac{2\pi}{3}\right) & \cos(\theta_r) \end{bmatrix}
\end{aligned} \tag{2.37}$$

In equations (2.36) and (2.37), L_{ls}, L_{ms} are the stator leakage and self inductance, L_{lr}, L_{mr} are the rotor leakage and self-inductance, $L_{sr} = L_{ms}$ is the stator–rotor mutual inductance, $L_{br}, L_{bs} = L_{br}$ are the broken bar–stator and broken bar–rotor mutual inductance, respectively, L_b is the broken bar self-inductance, and α is the angular position of the broken bar. Finally, the mechanical dynamics is described by

$$J\dot{\omega}_m = \frac{P}{2}\frac{d}{d\theta_r}\left(i_{abcs}^T \mathbf{L}_{sr} i_{abcr} + i_{abcs}^T \mathbf{L}_{bs} i_{bb}\right) - \tau_L \tag{2.38}$$

Note that the inductances L_{br}, L_{bs}, the resistance of the broken rotor bar and the angular position α are unknown parameters, since it is not possible to know in advance the number and the position of broken rotor bars.

2.4.2 Broken Rotor Bar Detection

Now we design a residual generator to detect broken rotor bars on an IFOC-driven squirrel cage induction motor. To this end, by considering i_b as an externally generated

signal, we express the induction motor dynamics (2.1) in terms of a frame with phase locked with the direction of the rotor-magnetizing flux rotating at synchronous speed ω_e. Thus we have

$$\begin{aligned}
\dot{\lambda}_{qs} &= -r_s i_{qs} - \omega_e \psi_{ds} + v_{qs} \\
\dot{\lambda}_{ds} &= -r_s i_{ds} + \omega_e \psi_{qs} + v_{ds} \\
\dot{\lambda}_M &= -\frac{1}{\tau_r}\lambda_M + \frac{L_m}{\tau_r} i_{qs} - \frac{L_{br}}{\tau_r}\cos(\theta_s - \alpha) i_b \\
\omega_e &= \omega_r + \frac{L_m}{\tau_r}\frac{i_{qs}}{\lambda_M} - \frac{L_{br}}{\tau_r}\sin(\theta_s - \alpha)\frac{i_b}{\lambda_M} \\
J\dot{\omega}_r &= \frac{3}{2}\frac{P^2}{4}\left[\frac{L_m}{L_r} i_{qs}\lambda_M + L_{bs}\cos(\theta_s + \alpha) i_{ds} i_b - L_{bs}\sin(\theta_s + \alpha) i_{qs} i_b\right] - \tau_L
\end{aligned} \tag{2.39}$$

where $\tau_r = (L_{lr} + L_{mr})/r_r$ is the rotor time constant, $\omega_r = 2\omega_m/P$ is the rotor angular frequency and $\theta_s = \theta_e - \theta_r$ is the slip angular frequency.

Because the induction motor may be assumed to be fed by current inverters with fast current controllers in an IFOC scheme, the induction motor dynamics that we consider for fault detection reads as

$$\begin{aligned}
\dot{\lambda}_M &= -\frac{1}{\tau_r}\lambda_M + \frac{L_m}{\tau_r} i_{ds} - \frac{L_{br}}{\tau_r}\sin(\theta_s - \alpha) i_b \\
\dot{\theta}_r &= \omega_r \\
J\dot{\omega}_r &= \frac{3}{2}\frac{P^2}{4}\left[\frac{L_m}{L_r} i_{qs}\lambda_M + L_{bs}\cos(\theta_s + \alpha) i_{ds} i_b - L_{bs}\sin(\theta_s + \alpha) i_{qs} i_b\right] - \tau_L \\
\dot{\theta}_e &= \omega_r + \frac{L_m}{\tau_r}\frac{i_{qs}}{\lambda_M} - \frac{L_{br}}{\tau_r}\cos(\theta_s - \alpha)\frac{i_b}{\lambda_M}
\end{aligned} \tag{2.40}$$

where i_{ds} and i_{qs} are the stator currents components controlled by the current controllers.

To write the rotor flux dynamics (1.40) in terms of (1.1), we first identify the target and nuisance faults. Because we want to design a broken rotor bar detector that is not influenced by load conditions, τ_L and i_b in (1.40) are identified as the nuisance and target fault modes respectively:

$$l_n = \begin{bmatrix} 0 \\ 0 \\ -\dfrac{1}{J} \\ 0 \end{bmatrix}, \quad l_t = \begin{bmatrix} -\dfrac{L_{br}}{\tau_r}\sin(\theta_s - \alpha) \\ 0 \\ \dfrac{3P^2}{8J} L_{bs}[\cos(\theta_s + \alpha) i_{ds} + \sin(\theta_s + \alpha) i_{qs}] \\ -\dfrac{L_{br}\cos(\theta_s - \alpha)}{\tau_r \lambda_M} \end{bmatrix}$$

Moreover we have

$$f = \begin{bmatrix} -\dfrac{1}{\tau_r}\lambda_M \\ \omega_r \\ 0 \\ \omega_r \end{bmatrix}, \quad g_1 = \begin{bmatrix} \dfrac{L_m}{\tau_r} \\ 0 \\ 0 \\ 0 \end{bmatrix}, \quad g_2 = \begin{bmatrix} 0 \\ 0 \\ \dfrac{3P^2}{8J}\lambda_M \\ \dfrac{L_m}{\tau_r \lambda_M} \end{bmatrix}$$

From a practical standpoint, it is desirable to design a residual generator using the rotor speed, as it is an easily measurable state. However, it can be shown that with the rotor speed as the output of (1.40) the corresponding minimal unobservability distribution intersects the image of the nuisance fault signature; that is, the load condition effects cannot be removed from the residual. So, if we consider the rotor flux λ_M as the output of (1.40), the minimal unobservability distribution S^* is computed as

$$S^* = \text{span} \begin{Bmatrix} 0 & 0 & 0 \\ 1/J & 0 & 0 \\ 0 & 1/J & 0 \\ 0 & 0 & 1/J \end{Bmatrix}. \tag{2.41}$$

Clearly, (2.3) is satisfied for $\theta_s - \alpha \neq 0$, and we can go further to find the diffeomorphism (2.4). By inspection, we note that (2.5), with $w_1 = y$, reads as

$$\begin{aligned} \dot{\lambda}_M &= -\frac{1}{\tau_r}\lambda_M + \frac{L_m}{\tau_r} i_{ds} - \frac{L_{br}}{\tau_r} \sin(\theta_s - \alpha) i_b \\ y &= \lambda_M \end{aligned} \tag{2.42}$$

As a result we have that Problem 1 is solvable with the residual generator dynamics described by

$$\begin{aligned} \dot{\hat{\lambda}}_M &= -\Gamma \hat{\lambda}_M - \left(\frac{1}{\tau_r} - \Gamma\right)\lambda_M + \frac{L_m}{\tau_r} i_{ds} \\ r &= \hat{\lambda}_M - \lambda_M \end{aligned} \tag{2.43}$$

where $\Gamma > 0$. Furthermore, from residual dynamics described by

$$\dot{r} = -\Gamma r + \frac{L_{br}}{\tau_r} \sin(\theta_s - \alpha) i_b \tag{2.44}$$

it is possible to verify that conditions I and II are satisfied. This is because for $i_b = 0$ the residual goes exponentially to zero and is not affected by the nuisance fault (load torque). Moreover for $i_b \neq 0$ the residual will move away from zero.

In [24] it is shown that an induction motor state that is not influenced by load conditions is the current i_{ds}, so we suggest that the spectrum of i_{ds} be monitored. Note that in steady state $\lambda_M = L_m i_{ds}$. Note that we arrived at this conclusion using nonlinear

TABLE 2.2 Induction motor parameters

Parameter	Motor 1(3 HP)	Motor 2 (100 HP)
L_{ls}, L_{lr} (H)	0.024, 0.013	0.0004, 0.006
L_{ms} (H)	0.245	0.0096
$r_r, r_s\,(\Omega)$	1.34, 1.77	0.037, 0.025
P	4	4
$J\,(\mathrm{Kgm}^2)$	0.025	0.863
τ_L (Nm)	12	90

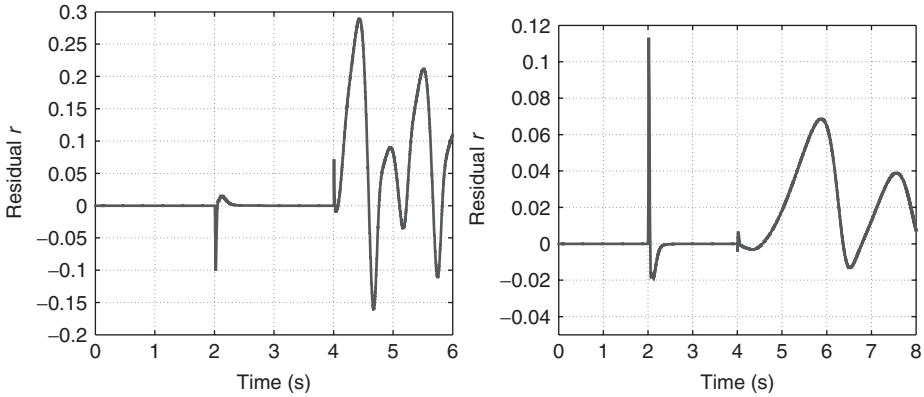

Figure 2.5 (Left) Residual behavior for motor 1; (right) residual behavior for Motor 2.

geometric techniques. We can verify the performance of the broken rotor bar detector via numerical simulations. In all simulations we consider the induction motor model introduced in [28] with parameters as indicated in Table 2.2. The residual behavior for motor 1 is shown in Figure 2.5. To verify that the residual is not affected asymptotically by changes on the load torque, at $t = 2$ s we increase the load torque by 50%.

Note that the residual is not asymptotically affected. To show that the residual actually detects the effect of broken rotor bars, at $t = 4$ s we "break" one rotor bar. Then the residual, as predicted, detects this effect. The residual behavior for motor 2 is also shown in Figure 2.5. At $t = 2$ s, we reduce the load torque by 50%. Notice that the residual is not asymptotically affected. At t = 4 s, one rotor bar is broken. As predicted by our computations, the residual reacts to the target fault. However, note that if the rotor time constant is not exactly known, deviations from the value used in the residual generator will produce a reaction of the fault detector. Since changes on the rotor time constant are mainly due to the rise of the temperature of the motor, the reaction of the fault detector to this mismatch should be slow. This problem also occurs in the Vienna monitoring method, as it is assumed that the rotor time constant is known exactly. Noisy measurements can also disturb the detector's performance. However, our initial analysis indicates that it is possible to distinguish between noisy measurements and broken rotor bar driven residuals.

Clearly, the limitations of the developed induction motor model will affect the fault detector scheme. But because we consider ideally distributed stator and rotor windings, it is not possible to determine the influence of other current harmonics on the residual.

2.5 FAULT DETECTION ON POWER SYSTEMS

In the new highly interconnected electricity markets, state estimation is the key function in determining real-time network operating conditions. Operators justify technical and economical decisions based on the network operation conditions, such as managing congestion and uncovering potential operation problems. As a consequence more accurate and reliable state estimators are needed.

In power systems practice, state estimation is currently performed in a non–model-based framework. So state estimation is mainly used to filter redundant data, to eliminate incorrect measurements, and to allow for the determination of the power flows in parts of the network that are not directly metered. There are some state estimation procedures that include a simplified dynamics (a first-order dynamic equation driven by noise) to add pseudomeasurements that help in filtering bad analog data that may arise during parameter estimation; observability conditions improve in situations where the meter configuration may change during the process. Recently some dynamic model-based state estimation approaches have been introduced. For instance, in [5] a gain-scheduled nonlinear observer is introduced to estimate the machine angle in a single machine infinite bus configuration. In [25] the multimachine state estimation problem is addressed and solved with a linear observer.

In this section we propose a model-based fault detection scheme for embedded power systems. Traditionally fault detection problems in power systems have been addressed in a model-free framework. A carefully selected signal is monitored in time or frequency domain in order to track deviations from its expected value. More elaborated monitoring schemes include the identification of false alarms. Since false alarms could cause costly shutdowns, this state of affairs is not completely satisfactory. Since the state estimation is the cornerstone for model-based fault detection, the proposed monitoring scheme relies in a model-based state estimation process. Two main stumbling blocks remain on this approach: one is the need to tailor the level of detail for component models (as to keep the overall model tractable) and the other is the need to discriminate the sources of possible misfirings in a systematic fashion. We consider the dynamics of a power system associated to the swing model, assuming that line parameters, generator parameters, bus voltage magnitudes, and generator speed are known. A nonlinear observer is used to estimate a quantity related to the generator angles, which in turn is used to generate a residual signal. To illustrate the idea, we consider a very simplified version of the power system of the electric ship presented in [21].

2.5.1 The Model

We consider the structure-preserving internal-node classical swing model [23]. In this model the generator is described by the swing equations, and its effect on the network

is considered as a constant voltage source behind a transient reactance, so that the power system is described by the differential equations

$$\begin{aligned} \frac{d\delta_i}{dt} &= \omega_i - \omega_s \\ \frac{2H_i}{\omega_s}\frac{d\omega_i}{dt} &= T_{Mi} - \mathrm{Re}(E_{qi} I_{Gi}^*) - D_i(\omega_i - \omega_s) \\ E_{qi} e^{j\delta_i} &= jX'_{di} I_{Gi} + V_i e^{j\theta_i}, \qquad i = 1, \ldots, m \end{aligned} \tag{2.45}$$

and the load-flow equations

$$\begin{aligned} V_i e^{j\theta_i} I_{Gi}^* + P_{Li} + jQ_{Li} &= \sum_{k=1}^{n} V_i V_k Y_{ik} e^{j(\theta_i - \theta_k - \alpha_{ik})}, \qquad i = 1, \ldots, m \\ P_{Li} + jQ_{Li} &= \sum_{k=1}^{n} V_i V_k Y_{ik} e^{j(\theta_i - \theta_k - \alpha_{ik})}, \qquad i = m+1, \ldots, n \end{aligned} \tag{2.46}$$

where $\delta_i \ i = 1, \ldots, m$ are the generator angles, $\omega_i \ i = 1, \ldots, m$ are the generator speeds, ω_s is the synchronous speed in p.u., H_i is the inertia in p.u. of generator i, D_i is the damping constant in p.u. of generator i, X'_{di} is the transient impedance of generator i, T_{Mi} is the mechanical torque applied to the generator shaft, $E_{qi} e^{j\delta_i}$ is the internal voltage of generator i, I_{Gi} is the internal current of generator $i, V_i e^{j\theta_i}$ is the voltage at bus i, P_{Li} is the active power load at bus i, Q_{Li} is the reactive power load at bus i, and $Y_{ik} e^{-j\alpha_{ik}}$ is the i, k element of the admittance bus matrix.

Assuming constant load impedances, we can write the differential algebraic equations (2.45)-(2.46) as

$$\begin{aligned} \frac{d\delta_i}{dt} &= \omega_i - \omega_s \\ \frac{2H_i}{\omega_s}\frac{d\omega_i}{dt} &= T_{Mi} - Re(E_{qi} I_{Gi}^*) - D_i(\omega_i - \omega_s) \\ \begin{bmatrix} I_G \\ 0 \end{bmatrix} &= \begin{bmatrix} Y_G & Y_B \\ Y_B^T & Y_C \end{bmatrix} \begin{bmatrix} E \\ \overline{V} \end{bmatrix} \end{aligned} \tag{2.47}$$

where

$$\begin{aligned} I_G &= \begin{bmatrix} I_{G1} & \ldots & I_{Gm} \end{bmatrix} \\ E &= \begin{bmatrix} E_{q1} e^{j\delta_1} & \ldots & E_{qm} e^{j\delta_m} \end{bmatrix} \\ \overline{V} &= \begin{bmatrix} V_1 e^{j\theta_1} & \ldots & V_m e^{j\theta_m} \end{bmatrix} \\ Y_G &= \mathrm{diag} \left\{ \frac{1}{jX'_{d1}} \quad \cdots \quad \frac{1}{jX'_{dm}} \right\} \end{aligned}$$

$$Y_B = \begin{bmatrix} -Y_G & 0 \end{bmatrix}$$

$$Y_C = Y_{bus} + \begin{bmatrix} Y_G & 0 \\ 0 & 0 \end{bmatrix} + \text{diag}\{y_{L1} \quad \dots \quad y_{Ln}\}$$

with Y_{bus} the network admittance matrix and

$$y_{Li} = \frac{P_{Li} - jQ_{Li}}{V_i^2}, \qquad i = 1, \dots, n$$

2.5.2 Class of Events

Here we model three classes of events: bus load changes, symmetrical line short circuits, and lost lines.

1. Bus load change. A load change at bus i is modeled adding to the nominal admittance matrix Y_C a matrix with all entries equal to zero but the entry (i, i):

$$Y_{Flc} = \begin{matrix} \\ \\ i \\ \\ \\ \end{matrix} \begin{bmatrix} 0 & 0 & 0 & 0 \\ 0 & \Delta y_{bi} & 0 & 0 \\ 0 & 0 & 0 & 0 \\ 0 & 0 & 0 & 0 \end{bmatrix} \begin{matrix} \\ \\ \\ \\ \\ \end{matrix} \qquad (2.48)$$
$$\begin{matrix} & & i & & \end{matrix}$$

   where

$$\Delta y_{bi} = \frac{\Delta P_{Li} - j\,\Delta Q_{Li}}{V_i^2}$$

   with ΔP_{Li} and ΔQ_{Li} as the active and reactive power changes, respectively.

2. Symmetrical line short circuit. A symmetrical line short circuit is modeled by adding a virtual bus at the point of the short circuit and by connecting to the virtual bus a load with very high admittance. For instance, if the short circuit occurs between buses s and t at $\frac{1}{\beta}$ the length of the line from bus s, the following admittance matrix is added to Y_C:

$$Y_{Fsc} = \begin{matrix} \\ s \\ \\ t \\ \\ n+1 \\ \end{matrix} \begin{bmatrix} 0 & 0 & 0 & 0 & 0 & 0 \\ 0 & -\alpha y_{li} & 0 & y_{li} & 0 & -\alpha y_{li} \\ 0 & 0 & 0 & 0 & 0 & 0 \\ 0 & y_{li} & 0 & -(1-\alpha) y_{li} & 0 & -(1-\alpha) y_{li} \\ 0 & 0 & 0 & 0 & 0 & 0 \\ 0 & -\alpha y_{li} & 0 & -(1-\alpha) y_{li} & 0 & y_{li} + y_0 \end{bmatrix} \qquad (2.49)$$
$$\begin{matrix} & s & & t & & n+1 \end{matrix}$$

   where $\alpha = 1/\beta$ and y_0 represents the added high admittance.

3. Lost line. The effect of losing a line is modeled by removing the line's admittance from the admittance bus matrix. For instance, if the line from bus s

to bus t, with admittance y_{li}, is lost, the following matrix is added to the admittance bus matrix Y_C:

$$Y_{Fll} = \begin{matrix} \\ s \\ \\ t \\ \\ \end{matrix} \begin{matrix} \begin{bmatrix} 0 & 0 & 0 & 0 & 0 \\ 0 & -y_{li} & 0 & y_{li} & 0 \\ 0 & 0 & 0 & 0 & 0 \\ 0 & y_{li} & 0 & -y_{li} & 0 \\ 0 & 0 & 0 & 0 & 0 \end{bmatrix} \\ \begin{matrix} \quad & s & \quad & t & \quad \end{matrix} \end{matrix} \tag{2.50}$$

Since the events have been modeled as admittance changes, their effects on the power system dynamics enter through the admittance matrices Y_B and Y_C. In this chapter we consider only two events: a load bus change and a lost line. Thus the faulted admittance matrix $\tilde{Y}_C$ is defined as

$$\tilde{Y}_C = Y_C + aY_{Flc} + bY_{Fll} \tag{2.51}$$

where a and b take the value 1 when the event is present and the value 0 when it is not.

2.5.3 The Navy Electric Ship Example

Consider the simplified version, shown in Figure 2.6, of the ship power system introduced in [21]. The bus admittance matrix Y_{bus} is defined as

$$Y_{bus} = \begin{bmatrix} 2y_a & 0 & -2y_a \\ 0 & 2y_b & -2y_b \\ -2y_a & -2y_b & 2(y_a + y_b) \end{bmatrix} \tag{2.52}$$

On the other hand, we have

$$Y_G = \begin{bmatrix} \dfrac{1}{jX'_{d1}} & 0 \\ 0 & \dfrac{1}{jX'_{d2}} \end{bmatrix}, \quad Y_B = \begin{bmatrix} \dfrac{1}{jX'_{d1}} & 0 & 0 \\ 0 & \dfrac{1}{jX'_{d2}} & 0 \end{bmatrix}$$

$$Y_C = \begin{bmatrix} \dfrac{X'_{d1}(2y_a + y_{M1}) - j}{X'_{d1}} & 0 & -2y_a \\ 0 & \dfrac{X'_{d2}(2y_b + y_{M2}) - j}{X'_{d2}} & -2y_b \\ -2y_a & -2y_b & 2y_{ab} + y_{L3} \end{bmatrix} \tag{2.53}$$

where $y_{ab} = y_a + y_b$. From the last two equations of (2.47) we have

$$I_G = ZE, \quad Z = Y_G - Y_B Y_C^{-1} Y_B^T \tag{2.54}$$

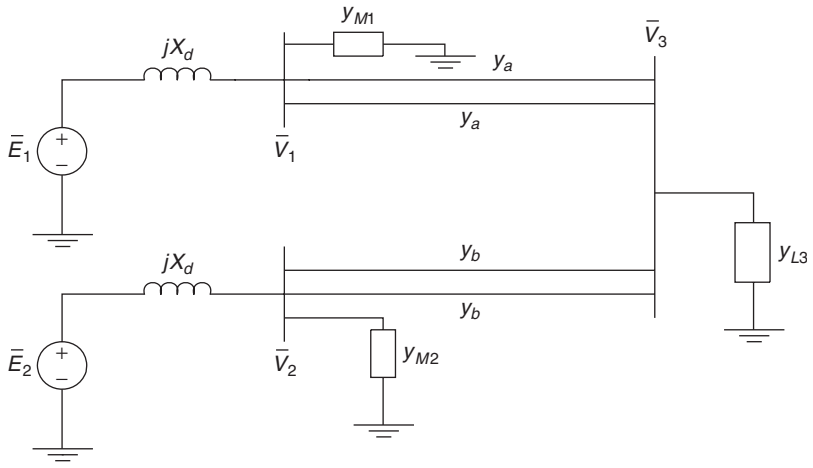

Figure 2.6 Power system diagram of the Navy electric ship.

Then equation (2.47) for the power system of Figure 2.6 reads as follows:

$$\begin{aligned}
\frac{d\delta_1}{dt} &= \omega_1 - \omega_s \\
\frac{2H_1}{\omega_s}\frac{d\omega_1}{dt} &= T_{M1} - Z_{11}^r E_{q1}^2 - E_{q1}E_{q2}Z_{12}^r \cos(\delta_1 - \delta_2) \\
&\quad - E_{q1}E_{q2}Z_{12}^i \sin(\delta_1 - \delta_2) - D_1(\omega_1 - \omega_s) \\
\frac{d\delta_2}{dt} &= \omega_2 - \omega_s \\
\frac{2H_2}{\omega_s}\frac{d\omega_2}{dt} &= T_{M2} - Z_{22}^r E_{q2}^2 - E_{q1}E_{q2}Z_{21}^r \cos(\delta_1 - \delta_2) \\
&\quad + E_{q1}E_{q2}Z_{21}^i \sin(\delta_1 - \delta_2) - D_2(\omega_2 - \omega_s)
\end{aligned} \tag{2.55}$$

where $Z_{ij}^r = Re(Z_{ij})$ and $Z_{ij}^r = Im(Z_{ij})$ with Z_{ij} the (i,j) element of Z.

Next we consider a load change at bus 1 followed by a loss of the line between bus 1 and bus 3. These two events are modeled by the following matrices:

$$Y_{Flc} = \begin{bmatrix} \Delta y_{b1} & 0 & 0 \\ 0 & 0 & 0 \\ 0 & 0 & 0 \end{bmatrix}, \quad Y_{Fll} = \begin{bmatrix} -y_a & 0 & y_a \\ 0 & 0 & 0 \\ y_a & 0 & -y_a \end{bmatrix} \tag{2.56}$$

2.5.4 Fault Detection Scheme

Assuming that the events occur independently, we propose the following residual candidate:

$$r = (Y_B^T E + Y_C \overline{V})e^{-j\delta_2} \tag{2.57}$$

the term in parenthesis, under fault free conditions, is equal to zero. Expanding (2.57), we have

$$\begin{aligned} r_1 &= -\frac{1}{jX'_{d1}}E_{q1}e^{j(\delta_1-\delta_2)} + Y_{C11}V_1e^{j(\theta_1-\delta_2)} + Y_{C13}V_3e^{j(\theta_3-\delta_2)} \\ r_2 &= -\frac{1}{jX'_{d2}}E_{q2} + Y_{C22}V_2e^{j(\theta_2-\delta_2)} + Y_{C23}V_3e^{j(\theta_3-\delta_2)} \\ r_3 &= Y_{C31}V_1e^{j(\theta_1-\delta_2)} + Y_{C32}V_2e^{j(\theta_2-\delta_2)} + Y_{C33}V_3e^{j(\theta_3-\delta_2)} \end{aligned} \tag{2.58}$$

The unknown quantities in (2.58) are $\delta_1 - \delta_2$ and $\overline{V}e^{-j\delta_2}$. In order to compute $\overline{V}e^{-j\delta_2}$, we consider the relation

$$0 = Y_B^T E e^{-j\delta_2} + Y_C \overline{V} e^{-j\delta_2} \tag{2.59}$$

which gives

$$\overline{V}e^{-j\delta_2} = -Y_C^{-1}Y_B^T E e^{-j\delta_2}$$

Substituting the above into (2.57), we have

$$r = Y_B^T E e^{-j\delta_2} + Y_C(-Y_C^{-1}Y_B^T E e^{-j\delta_2}) \tag{2.60}$$

that is $r = 0$. However, in the faulty case, the admittance matrix Y_C is replaced by $\tilde{Y}_C$ defined in (2.51), so (2.60) becomes

$$r = Y_B^T E e^{-j\delta_2} + (Y_C + aY_{Flc} + bY_{Fll})(-Y_C^{-1}Y_B^T E e^{-j\delta_2})$$

As a consequence the residual candidate r moves away from zero, satisfying the basic requirements to be considered a true residual. Now, in order to distinguish between the two events, we redefine the residual signal as follows:

$$\begin{aligned} r_{s1} &= v_1 r, \\ r_{s2} &= v_2 r \end{aligned}$$

with

$$\begin{aligned} v_1 Y_{Flc} \neq 0, \quad v_1 Y_{Fll} = 0 \\ v_2 Y_{Fll} \neq 0, \quad v_2 Y_{Flc} = 0 \end{aligned} \tag{2.61}$$

so that $r_{s2} \neq 0$ implies that a line between bus 1 and bus 3 is lost and $r_{s1} \neq 0$ implies that the load at bus 1 has changed. Note that for our example the vectors

$$v_1 = [1 \quad 0 \quad 1], \quad v_2 = [0 \quad 0 \quad 1]$$

satisfy (2.61). Then for $r_{s1}, m_t = a$ and $m_n = b$ while for r_{s2} we have $m_t = b$ and $m_n = a$.

In order to compute the angle $\delta_1 - \delta_2$, we design an observer. To begin, we define

$$\begin{aligned} \delta_{12} &= \delta_1 - \delta_2 \\ \omega_{12} &= \omega_1 - \omega_2 \end{aligned} \tag{2.62}$$

Straightforward computations show that in the coordinates (2.62), the power system dynamic equations (2.55) can be rewritten as

$$\begin{aligned} \frac{d\delta_{12}}{dt} &= \omega_{12} \\ \frac{d\omega_{12}}{dt} &= a_1 + a_2 \cos(\delta_{12}) + a_3 \sin(\delta_{12}) \end{aligned} \tag{2.63}$$

where

$$\begin{aligned} a_1 &= \frac{\omega_s}{2H_1}[T_{M1} - Z_{11}^r E_{q1}^2] - \frac{\omega_s}{2H_2}[T_{M2} - Z_{22}^r E_{q2}^2] \\ a_2 &= \frac{\omega_s}{2} E_{q1} E_{q2} \left(\frac{Z_{21}^r}{H_2} - \frac{Z_{12}^r}{H_1} \right) \\ a_3 &= -\frac{\omega_s}{2} E_{q1} E_{q2} \left(\frac{Z_{12}^i}{H_1} + \frac{Z_{21}^i}{H_2} \right) \end{aligned} \tag{2.64}$$

and we have disregarded the damping terms.

We propose an observer with the following structure:

$$\begin{aligned} \frac{d\hat{\delta}_{12}}{dt} &= \hat{\omega}_{12} + \Gamma_1(\omega_{12} - \hat{\omega}_{12}) \\ \frac{d\hat{\omega}_{12}}{dt} &= a_1 + a_2 \cos(\hat{\delta}_{12}) + a_3 \sin(\hat{\delta}_{12}) + \Gamma_2(\omega_{12} - \hat{\omega}_{12}) \end{aligned} \tag{2.65}$$

By linearization it can be shown that for $\Gamma_1 < 1$ and $\Gamma_2 > 0$ the observation errors $e_\delta = \delta_{12} - \hat{\delta}_{12}$ and $e_\omega = \omega_{12} - \hat{\omega}_{12}$ go asymptotically to zero.

2.5.5 Numerical Simulations

To verify the performance of the monitoring scheme, we carried out numerical simulations. The power system parameters are given in Tables 2.3 and 2.4. In all simulations it is assumed that events do not occur simultaneously and that the power system is initially at a given equilibrium point. The events occur during $1 \leq t \leq 3$ s.

First, we consider the ideal case; that is, we assume that machine and bus angles are available. Figure 2.7 shows the residual behavior for a load change of 0.5 p.u. at bus 1. As expected, the residual signal r_{s1} moves away from zero while r_{s2} remains equal to zero.

The picture at the right in Figure 2.7 shows the residual behavior in the event of losing a line between bus 1 and 3. Note that as expected, the residual signal r_{s2}

TABLE 2.3 Machine parameters

Parameter	Machine 1	Machine 2
H (p.u.)	12	8.75
jXd (p.u.)	j0.1333	j0.14
D (p.u.)	6	6.25
TM (p.u.)	2.5459	2.00

TABLE 2.4 Network parameters

y_a	0.4367−j3.2751
y_b	0.7335−j4.8900
y_{M1}	1.5−j0.5
y_{M2}	1.0−j0.3
y_{L3}	2.3203−j0.8121

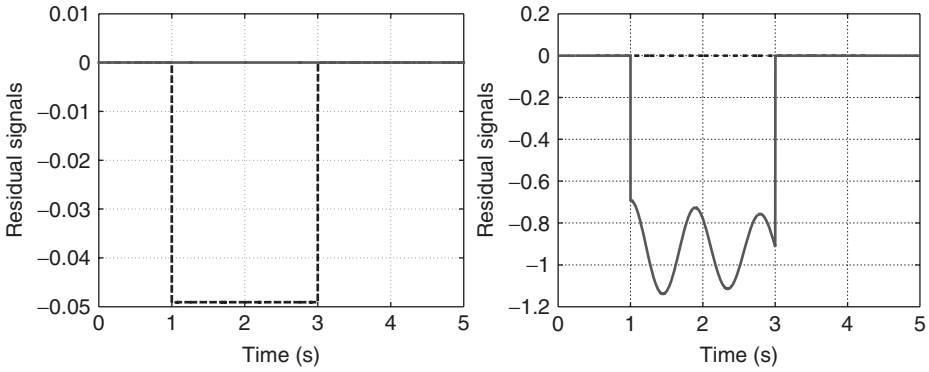

Figure 2.7 (Left) Bus load change, r_{s1} (dashed line), r_{s2} (continuous line); (right) lost line, r_{s1}(dashed line), r_{s2} (continuous line).

detects the event. This shows that in the ideal case our monitoring scheme is able to detect and distinguish between the two events.

Now we consider the case where machine and bus angles are not available. The observer gains are $\Gamma_1 = 0.987$ and $\Gamma_2 = 40$. Figure 2.8 shows the residual behavior for event 1 (load change at bus 1). Note that the both residual signal are affected by the event. However, as the effect of the event on r_{s1} is bigger, it is possible identify the event.

The picture at the right in Figure 2.8 shows the observer error e_δ for this event. Figure 2.9 shows the residual behavior for event 2. As can be observed, the event affects both residual signals and it is difficult to conclude which event is present. The observer error e_δ is shown in Figure 2.9. Note that for event 2 the observer error e_δ is considerably larger compared to the observer error in Figure 2.8. This explains why the distinguishability between the events is degraded.

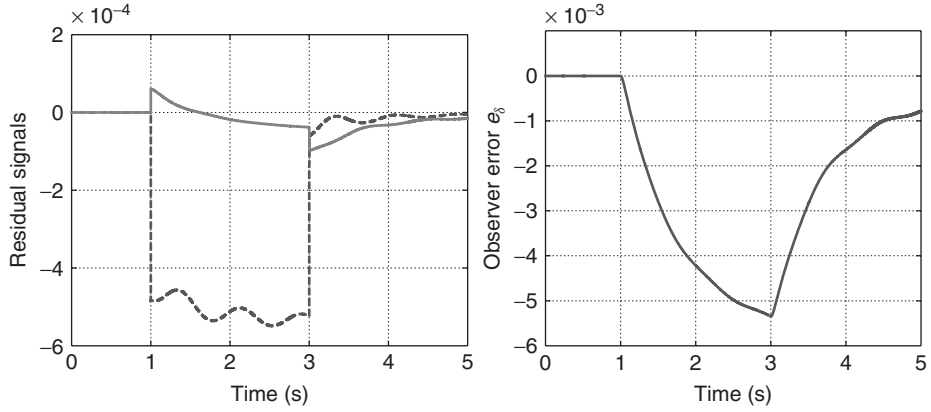

Figure 2.8 (Left) Bus load change, r_{s1} (dashed line), r_{s2} (continuous line); (right) observer error e_δ.

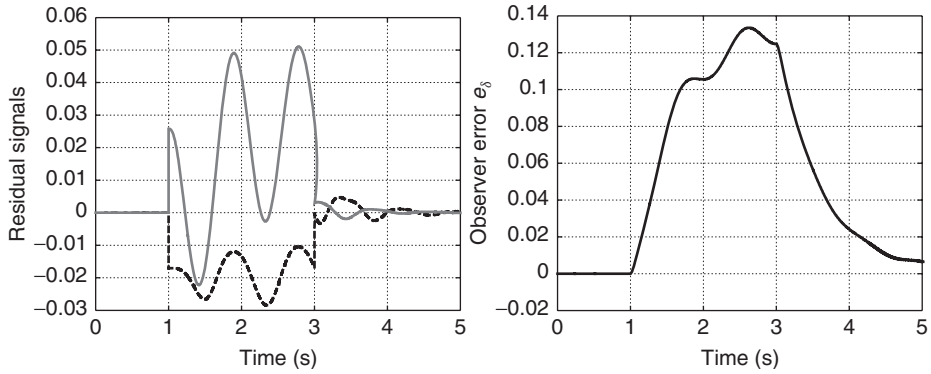

Figure 2.9 (Left) Lost line, r_{s1} (dashed line), r_{s2} (continuous line); (right) Observer error e_δ.

2.6 CONCLUSIONS

We have presented a monitoring scheme to detect detuning operation on indirect field-oriented controlled current-fed induction motors. The key for fault detection is the development of a model based on the detuning interpretation introduced in [17]. The model expresses the detuning effect in terms of the difference between the real and the estimated rotating frames, and the selection of the induction motor state to monitor based on techniques from differential theory. It was shown how the fault can be accommodated. Numerical simulations were used to validate the monitoring scheme, and the results clearly show that the monitoring scheme is not affected by changes on the load torque.

We also developed a simplified model for a squirrel cage induction motor that includes broken rotor bars effects. Relying on differential geometry techniques, we have proposed a model-based solution to the broken rotor bar detection problem on IFOC-driven squirrel cage induction motors. We show that load torque conditions will not lead to errors in the detection, as the fault detector is not affected by the load torque. Numerical simulations of very different induction motors validate the model and the performance of the monitoring scheme.

Finally, we addressed the fault detection problem in an embedded power system and proposed a model-based solution. The distinguishability is achieved in the ideal case. However, as shown by our numerical simulation the capability to distinguish between the two events is degraded by the observer performance, ongoing efforts are directed toward the design of an adaptive observer.

BIBLIOGRAPHY

1. Basille, G., and Marro, G. *Controlled and Conditioned Invariants in Linear Systems Theory*. Prentice Hall, 1992, ISBN 0-13-172974-8.
2. Beard, R. V. *Failure Accommodation in Linear Systems through Self-Reorganization*. PhD dissertation. MIT, Cambridge, February 1971.
3. Benbouzid, M. H., and Kliman, G. B. "What Stator Current Processing-Based Technique to Use for Induction Motor Rotor Fault Diagnosis?" *IEEE Trans. Energy Conversion*, 18(2): 238–244, 2003.
4. Burnett, R., Watson, J. F., and Elder S. "The Detection and Location of Rotor Faults within Three Phase Induction Motors." *Proc. Int. Conf. Electric Machinery*, pp. 288–293, 1994.
5. Chang, J., Taranto, G., and Chow, J. "Dynamic State Estimation in Power System Using High Gain-Scheduled Nonlinear Observer." *Proc. 4th IEEE Conf. on Control Applications*, pp. 221–226, 1995.
6. De Persis, C., and Isidori A. "A Geometric Approach to Nonlinear Fault Detection and Isolation." *IEEE Trans. on Automatic Control*, 46(6): 853–865, 2001.
7. Filippetti, F., Franchescini, G., and Tassoni, C. "Neural Network Aided On-line Diagnosis of Induction Motor Rotor Faults." *IEEE Trans. Industrial Applications*, 31(4): 892–899, 1995.
8. Gertler, J., All Linear Methods are Equal and Extendible to (Some) Nonlinearities.'' *Int. J. Robust Nonlinear Control*, 12: 629–648, 2002.
9. Hammouri, H., Kinnaert, M., and El Yaagoubi, E. H. "Fault Detection and Isolation for State Affine Systems." *European Journal of Control*, 4(11): 2–16, 1998.
10. Jones, H. L. *Failure Detection in Linear Systems*. PhD dissertation. MIT, 1973.
11. Karagiannis, D., Astolfi, A., and Ortega, R. "Two Results for Adaptive Output Feedback Stabilization of Nonlinear Systems." *Automatica*, 39(5): 857–866, 2003.
12. Kral, C., Pirker, F., and Pascoli, G. "Detection of Rotor Faults in Squirrel-Cage Induction Machines at Standstill for Batch Test by Means of the Vienna Monitoring Method." *IEEE Trans. Industry Applications*, 38(3): 618–624, 2002.
13. Krause, C. P., Wasynczuk, O. and Sudho, D. S. *Analysis of Electric Machinery*. IEEE Press, New York, 1995.

14. Manolas, S. T. J., and Tegopoulos, J. A., "Analysis of Squirrel Cage Induction Motors with Broken Bars and Rings." *IEEE Trans. Energy Conversion*, 14(4): 1300–1305, 1999.
15. Massoumnia, M. "A Geometric Approach to the Synthesis of Failure Detection Filters." *IEEE Trans. Automatic Control*, 31(9): 839–846, 1986.
16. Massoumnia, M., Verghese, G., and Willsky, A. "Failure Detection and Identification." *IEEE Trans. Automatic Control*, 34(3): 316–321, 1989.
17. Mijalkovic, M. *Sensitivity Analysis for Nonlinear Magnetics*. Northeastern University Internal Report, May, 2002.
18. Mohan, N. *Advanced Electric Drives*. MNPERE, Minneapolis, MN, 2001.
19. Novotny, D. W., and Lipo, T. A. *Vector Control and Dynamics of AC Drives*. Clarendon Press, New York, 1996.
20. Patton, R., Frank, P., and Clark R. *Fault Diagnosis in Dynamic Systems Theory and Application*. Prentice Hall, Upper Saddle River, NJ, 1989.
21. Pekarek, S., Tichenor, J., Benavides, N., Koeing, A., Wang, H., Sudho, S., Kuhn, B., Glover, S., Aliprantis, D., Byoun, J., and Sauer, J. *Development of a Test Bed for Design and Evaluation of Power Electronic Based Systems*. Society of Automotive Engineers, Troy, MI, 2002.
22. Ritchie, E., Deng, X., and Jokinen, T. "Diagnosis of Rotor Faults in Squirrel Cage Induction Motors Using a Fuzzy Logic Approach." *Proc. Int. Conf. Electric Machinery*, Paris, France, pp. 348–352, 1994.
23. Sauer, P. W., and Pai, M. A. *Power System Dynamics and Stability*. Prentice Hall, Upper Saddle River, NJ, 1998.
24. Schoen, R. R., and Hableter, G. T. "Evaluation and Implementation of a System to Eliminate Arbitrary Load Effects in Current–Based Monitoring of Induction Machines." *IEEE Trans. Industry Applications*, 33(6):, 1997.
25. Scholtz, E., Sonthikorn, P., Verghese, G. C., and Leisure, B. C. "Observers for Swing State Estimation of Power Systems." Proc. *North American Power Symp*., October, 2002.
26. Thomson, W. T., and Fenger, M. "Current Signature Analysis to Detect Induction Motor Faults." *IEEE Industry Applications*, July–August: 26–34, 2001.
27. Watson, J. F., and Elder, S. "Transient Analysis of the Line Current as a Fault Detection Technique for 3-phase Induction Motors." *Proc. Int. Conf. Electric Machinery*, pp. 1241–1245, 1992.
28. Welsh, M. S. *Detection of Broken Rotor Bars in Induction Motors Using Stator Measurements*. PhD dissertation. MIT, Cambridge, May 1988.
29. Williamson, S., and Smith A. C. "Steady-State Analysis of 3-phase Cage Motors with Rotor Bar and End Ring Faults." *Proc. Institute of Electrical Engineering*, 2(3B): 93–100, 1982.

3

INTELLIGENT POWER ROUTERS: DISTRIBUTED COORDINATION FOR ELECTRIC ENERGY PROCESSING NETWORKS

Agustín A. Irizarry-Rivera, Manuel Rodríguez-Martínez, Bienvenido Vélez, Miguel Vélez-Reyes, Alberto R. Ramirez-Orquin, Efraín O'Neill-Carrillo, José R. Cedeño

University of Mayaguez, Puerto Rico

3.1 INTRODUCTION

The intelligent power router (IPR), a concept based on scalable coordination, is proposed to control the next generation power network. Our goal is to show that by distributing network intelligence and control functions using the IPR, we will be capable of achieving improved survivability, security, reliability, and re-configurability. Each IPR has embedded intelligence that allows it to switch power lines, shed load, and receive/broadcast local state variable information to and from other IPR. The information exchange capability of the routers will provide coordination among them to reconfigure the network when subject to a natural or human-made disaster.

In this chapter we report our progress on six different activities around the creation of the IPR: IPR architecture, communication protocols among IPRs, distributed controls, risk assessment of a system operated with and without IPR, power system reconfiguration based on a controlled islanding scheme using IPR, and power routing as an ancillary service since the IPR may provide improved efficiency and security in the context of a realistic market structure such as the standard market design, with LMP pricing algorithm.

Operation and Control of Electric Energy Processing Systems, Edited by James Momoh and Lamine Mili

3.2 OVERVIEW OF THE INTELLIGENT POWER ROUTER CONCEPT

Existing power delivery systems are designed with redundant power generators and delivery lines to make the system tolerant to failures on these elements. However, the control and coordination of the process to generate and distribute power still occur in a centralized manner, with only a few sites, or even one site, managing power generation and delivery. This scheme has a clear drawback: a failure in one of these *control centers* can impair the system. Therefore it is highly desirable that future power delivery systems have the capability of distributing the task of coordination and control of power generation and distribution when contingencies or emergency situations occur.

We are developing a model for the next generation power network control using a distributed concept based on scalable coordination by an intelligent power router (IPR). Our goal is to show that distributed network intelligence and control functions using the IPR can achieve improved survivability, security, reliability, and re-configurability. Our power network concept builds on our knowledge of power engineering, systems control, distributed computing, and computer networks.

In our scheme we detached control from central control sites and delegated it to intelligent power routers (IPR). The IPRs are strategically distributed over the entire electric energy processing network. By the power router's embedded intelligence we mean programmability, allowing the power router to switch power lines, shed load based on a priority scheme, activate auxiliary or distributed generation, isolate power region of the energy delivery network to prevent system cascade failures, and receive/broadcast local state variable information to and from other routers. The information exchange capability among the routers facilitates coordination that can reconfigure the network when the designated principal control center of the system has collapsed from a natural or human-made disaster. The IPR uses direct monitoring, area-limited online security assessment, and adaptive reconfigurable controls to establish a coordinated and local set of control actions as preventive countermeasures to anticipate a potential disturbance or provide corrective countermeasures following a disturbance.

Our approach follows a data-routing model in computer networks, where data can be moved over geographically distant nodes via *data routers* (or simply routers) [2–4]. When a flow of data needs to be established between two end points, the routers cooperate by moving pieces of data over the network until the data reaches the desired destination(s). At each step of this process, a router that receives a packet of data determines the next router that will forward that fragment of data. Notice that there can be many candidate routers, but the one that does the best forwarding job is the one that is selected. A power delivery system could operate the same way with due consideration of the physical differences between data exchange and energy exchange. In the event of a component or system failure, the IPR will make local decisions and coordinate with other routers to bring the system, or part of it, back into an operational state, though the system should be capable of degraded operation during major contingencies. The proposed scheme does not substitute current control protocols if there are no contingencies. However, under normal operating conditions the IPR would

provide additional information on system status to the central energy management system.

Figure 3.1 presents the proposed IPR system. Generation units $P_1, P_2, \ldots, P_n$ are connected via the power network with consumers $C_1, C_2, \ldots, C_m$. The producers and the consumers are connected via a series of power lines and intelligent power routers, $R_1, R_2, \ldots, R_k$, that take control of power routing over the lines when a major system disturbance occurs.

As Figure 3.1 shows, the IPR receives sensor data, processes the information, takes decisions, and sends commands to the flow control devices. The routers' network has multiple redundant power paths between producers and consumers, since the IPR organization is based in a peer-to-peer system (P2P) or a mesh.

Each IPR maintains information on the power flowing through its connecting power lines. This information is used to make local decisions on how to re-route power in the event of changes in the amount of power moving along the lines, such as might be caused by failures, changing power generation or demand. These routers could also signal that emergency power sources are needed online to meet demand and could gracefully bring down portions of the system in order to avoid further damage in the event of a contingency and maintain service to critical loads.

Since the power network has the infrastructure to react to changes in a decentralized and autonomous fashion, this approach is a departure from state-of-the-art schemes. The power network has enough redundancy and intelligence to find alternate paths to deliver power to the loads. The goal of the network is to survive failures and return critical loads to an acceptable level of operation. To achieve this, and reduce the risk associated with single-points of failures, the IPR operates following a distributed control scheme.

We envision IPRs to be strategically distributed over a power delivery network, a metropolitan area, or a naval ship that has been divided into several sectors, each

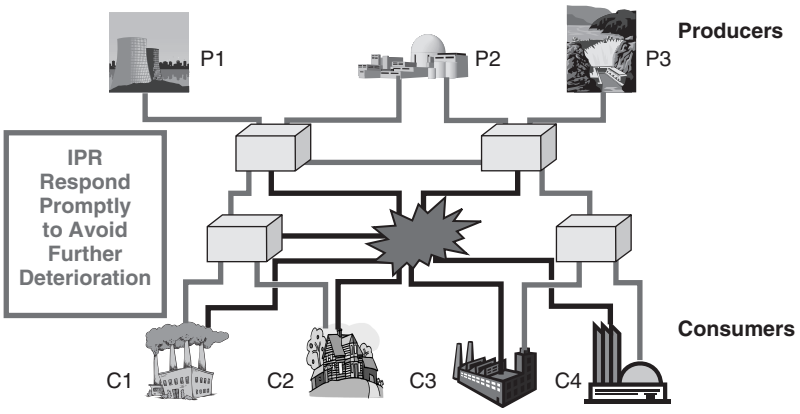

Figure 3.1 IPRs exchange information and take local decisions to avoid cascade failure when a major disturbance occurs, be it, natural or human-made.

one served by at least two routers. These IPRs are fundamental building blocks for the control scheme and are connected to a second layer of IPR that is in charge of controlling power delivery on the scale of regions formed by two or more sectors. The routers can in turn connect to a group of backbone routers that are directly connected to the power generators.

Our long-term goal is to architect a new type of scalable and decentralized power distribution infrastructure based on the concept of the IPR. This architecture should provide sustained operation in the presence of partial failures to power sources and communication lines through automatic reconfiguration. The fundamental engineering design principle behind the IPR system is *modular decentralized control*. Thus an IPR can be used as a simple yet fundamental building block upon which complex power distribution networks can be engineered in a disciplined fashion. In summary, our *design objectives* are as follows:

- *Survivability and fault tolerance.* Decentralized IPR modules control power routing based on local information. IPR capable of isolating failures.
- *Scalability.* IPR can be composed with other IPR to create complex distribution networks. The system can grow incrementally. Architecture admits graceful profile-based reengineering.
- *Cost-effectiveness.* Decentralized IPR modules avoid having to connect very producer to every consumer directly. Economies of scale reduce the cost of IPR.
- *Unattended 24/7 operation.* IPR are equipped with programmable computing capabilities. IPR incorporates algorithms that allow reconfiguration decisions without human intervention.

The rest of the chapter is organized as follows: Section 3.3 presents the project objectives, Section 3.4 shows the relation of the proposed work to the present state of the art in the field and work in progress, Section 3.5 discusses current IPR architecture and software module shows risk assessment of a system that operates with IPR. Section 3.6 presents IPR communication protocols, Section 3.7 studies distributed control modules, Section 3.8 explores the idea of defining the rendering of efficiency and security provided by IPR as an ancillary service. Section 3.9 presents our conclusions and final remarks.

3.3 IPR ARCHITECTURE AND SOFTWARE MODULE

The main goal of this component of the project is to design and test architecture for the IPR, the backbone of the new type of energy distribution network that we propose. Central to this architecture is the notion that IPR should eventually evolve into a new type of off-the-shelf component that energy network designers can use as building blocks in the construction of networks of all levels of complexity and capacity.

An IPR is in essence an energy flow controller with programmable intelligence. Figure 3.2 shows a proposed architecture for an IPR consisting of two main components: interfacing circuits (ICKT) that operates existing energy flow control and

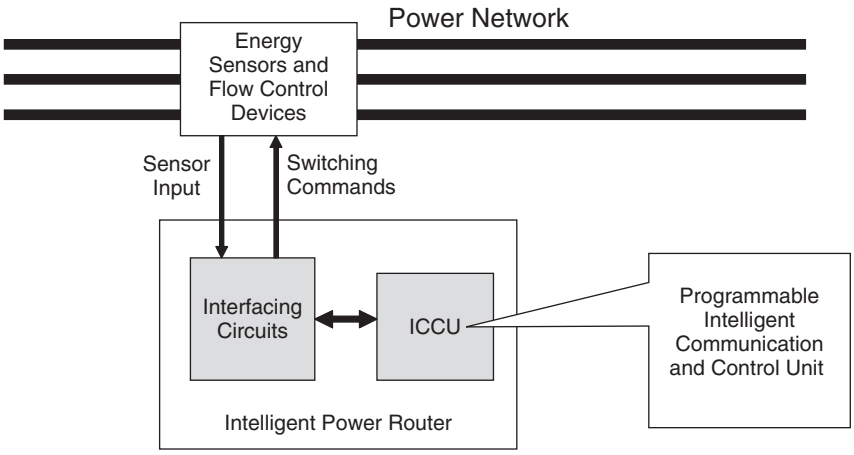

Figure 3.2 Proposed architecture for the intelligent power router.

sensing devices (EFCD), and an intelligent control and communication unit (ICCU). Example of EFCDs are circuit breakers, phase-shifting transformers, series compensation capacitors or their combination as flexible AC transmission (FACTS). The ICKT is the hardware component that interacts with the energy transfer components of the electric power system. Many devices that could act as EFCDs in an IPR-based system are already available in the market. They will work by controlling the power flow, opening and closing lines as needed, or regulating the amount of power that flows through a given interface. The interfacing circuits sends commands to the EFCD to dynamically change the behavior of the power system. Also the ICKT receives information collected by sensors (CTc, PTs) and dynamic system monitors (DSM) on the system state (phase currents, bus voltages, system frequency, generation levels, etc.) to assess the current status of the system.

The ICKT will operate under the direct control of the ICCU, which will have the necessary logic and software to determine how to re-route power, change load set point in generators, shed load, or take any other corrective or preventive action to enhance system security. As an embedded computer located inside the IPR, the ICCU could feature a RISC-type CPU, high-speed RAM, nonvolatile data storage, and a network interface. The ICCU should be made out of commodity components to keep its cost low, make it easy to fix or replace, and to leverage on the latest advances in the computing technology. For example, because the ICCU can run the latest version of the LINUX operating system for embedded systems, this scheme will not only make the IPR fully programmable but also simpler to upgrade with new versions of the system software. In short, the intelligent power router consists of two distinct elements: the intelligent control and communication unit (ICCU) and the interface circuits (ICKT). Existing energy flow controls and sensors will be managed by the IPR.

Figure 3.3 shows a simple switch-based IPR system that can illustrate the potential for survivability of an IPR-based network. For simplicity, assume that each of the two

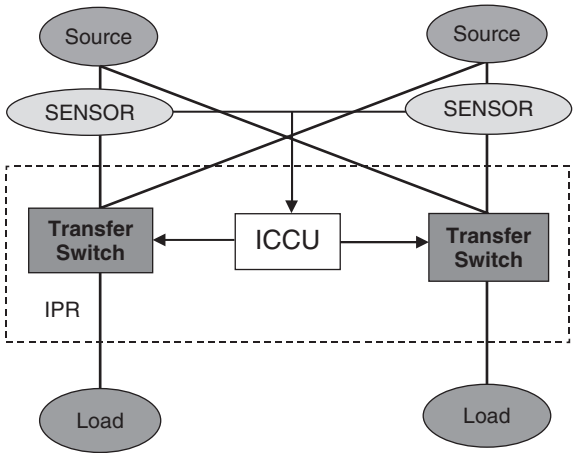

Figure 3.3 A simple switch-based IPR system.

sources can supply exactly one of the loads. In an ordinary power network and upon failure of a source, the system will attempt to continue serving both loads. This may result in a total failure once none of the loads receive enough power to operate. In an IPR system the ICCU can react to the source failure by reconfiguring the network to serve the load with highest priority with the power supplied by the surviving source. Load priorities may serve to model levels of criticalness or perhaps level of power quality purchased by different customers. Key to the IPR system is the ability to assign these priorities dynamically and without requiring costly and slow physical re-configuration of the network. Our goal is to discover distributed algorithms that do not require centralized control of a complex network with potentially many IPRs. The modularity of IPRs will make it possible to create configurations significantly more complex than the one shown above, requiring neither hardware modifications nor ad hoc devices.

Figure 3.4 shows a virtual test bed (VTB) [16] simulation of the system shown in Figure 3.3. The IPR module at the center of the figure continuously receives readings from current sensors connected to each of the two power sources. Initially the left source serves the left load and the right source serves the right load. The sinusoidal plot on the upper right shows the current drawn from the left source. At some point during the simulation the left source fails and stops generating current. The lower right plot depicts the current fed into the left (higher priority) load. In response to the failure of the left source the IPR re-configures the switches in order for the right surviving load to serve the left load. Therefore the current into the left load is restored after a short transient period. The goal of the IPR-based system is to harness the laws of physics in order to control energy flows based on dynamically reconfigurable load priorities with minimal human intervention.

Our next challenge was to find an appropriate simulation framework allowing us to conduct experiments in a setting significantly more realistic than the one used

for experimentation with the initial version of the IPR model illustrated above. We wanted, for instance, to work with realistic models of power generation sources and loads, as well as with more realistic models of switches and faults. The most suitable framework available to us was the SimPower system simulation package available for MatLab. To gain experience with the new simulation environment, we developed the simple model of a 3-bus power system depicted in Figure. 3.4, which consists of two generators and a single load. Each load is controlled by an IPR for a total of 3 IPRs (light blue boxes). We also designed a fault injection module (green boxes) as shown in Figure 3.5, that automatically generates a line-to-ground fault on phase A after a prespecified amount of time. This is an initial experiment and in the future other types of faults will be added to the model. The fault detection circuitry (dark blue in Figure 3.5) detects the line-to-ground fault by computing the zero-sequence component of the 3-phase signal. Part of this circuitry will eventually be packaged inside the IPR module. In particular, the portion of the circuitry that determines the action to be taken in response to the fault will be part of the IPR. Right now this portion of the circuitry is essentially nonexistent, since the very output of the zero-sequence analyzer is used to drive a relay that controls the switches that interconnect the two relevant buses. Although rather simple, this framework allows us to experiment with more complex IPR logic by inserting appropriate logic components between the zero-sequence analyzer and the relay.

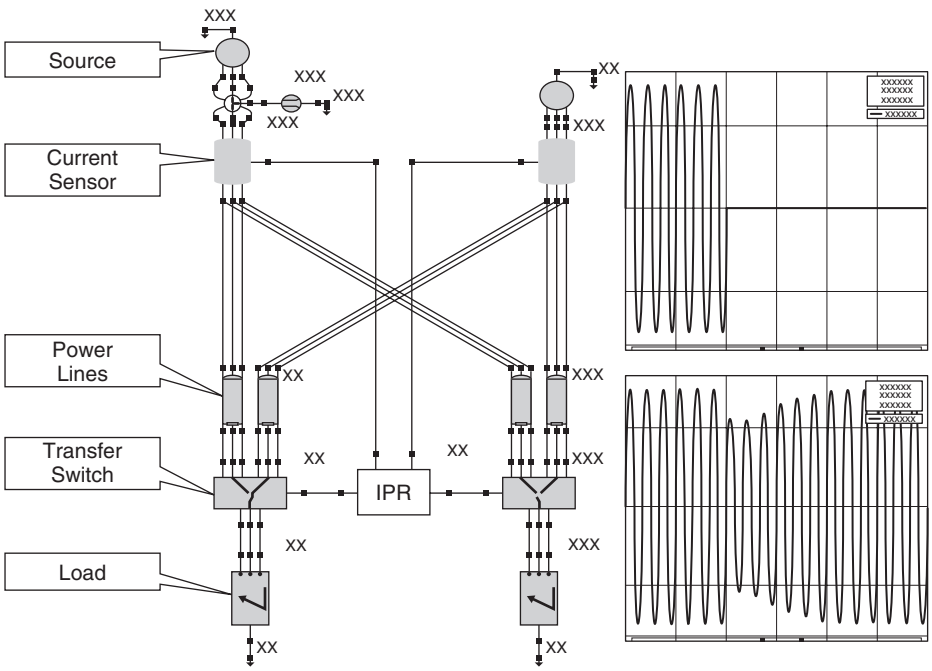

Figure 3.4 Virtual test bed (VTB) simulation of the simple IPR system of Figure 3.3.

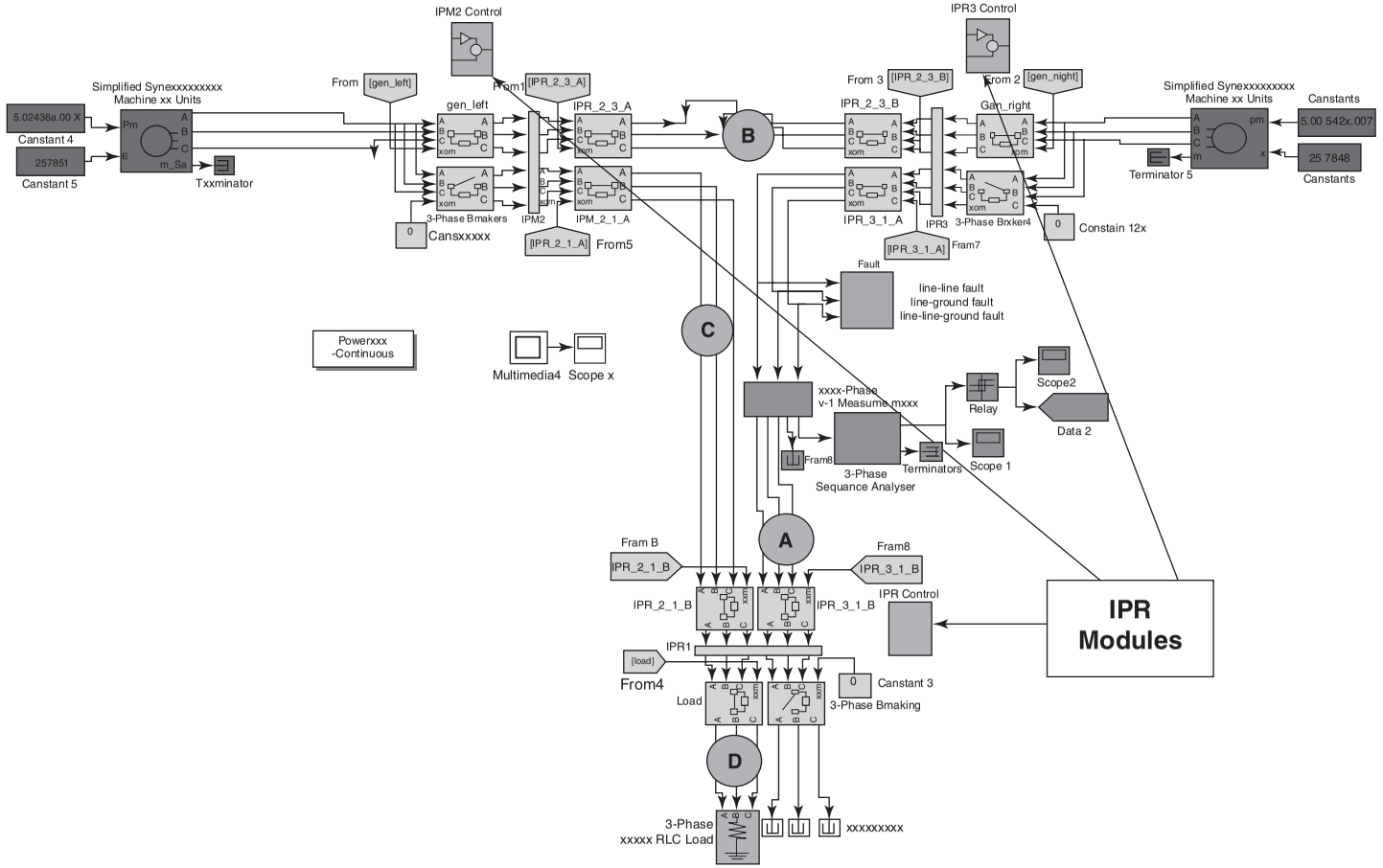

Figure 3.5 A SimPower model of a 3-bus system with 3 IPR.

Figure 3.6 shows the current at lines labeled A, B, C, and D in Figure 3.5. The upper left chart shows the phase-A current incident into the right port of the bottom bus. The line-to-ground fault occurs where the current drops to zero. The current at lines B and C rises in response to the opening of the breakers to supply the load without interruption. After a short transient the power to the load is reestablished. After about 100 ms the fault is fixed and the zero-sequence analyzer deactivates the relay, causing the breaker to close again. As depicted in Figure 3.6 the current in line A raises to its pre-fault level and the system overall is reestablished to its initial configuration.

Once we gained enough experience with the simulation framework, we shifted our focus to the creation of a modular SimPower model for an IPR and its application to the design of shipboard electric systems. After reviewing the different shipboard models considered in the literature, we decided to base our work on the DD(X) Navy Test Bed model developed at the University of Texas Center for Electromechanics (http://www.utexas.edu/research/cem/).1 Because of the unaccessibility of the SimPower model for the Test Bed, we proceeded to assemble the model depicted in Figure 3.7. This model is realistic in that it uses the turbine generators, engines, and other loads typically found on Navy ships.

Using this model, we developed a new type of computer controllable bus (large buses toward the lower center of Figure 3.7 enclosed by red circles). This bus serves the purpose of the EFCD in the IPR architecture. The internal structure of the controllable bus is shown in Figure 3.8 and it includes the sensor and actuator circuits that will be controlled by the ICCU. We are presently developing an IPR intercommunication subsystem that will implement the IPR protocols discussed in the following section.

3.4 IPR COMMUNICATION PROTOCOLS

3.4.1 State of the Art

In our framework for self-healing electrical networks, the intelligence used for control and coordination operations is embedded into the IPR. As shown in Figure 3.9, IPR are computing devices strategically deployed over the electric network at buses, power lines, power generators, and close to loads (i.e., power consumers). By controlling electronic power flow control devices (e.g., switches, FACTS), IPR can "route" power to various areas in a similar fashion as routers forward packets in a computer network. For example, when power is lost in a given region because of a generator failure, several IPRs in charge of that region might request another generator to increase its power output, and then coordinate to close alternate lines to route power into the affected region. Likewise IPRs can oversee *load-shedding* operations to remove low-priority loads (e.g., theaters) from the system in favor of other loads with higher priorities (e.g., hospitals). Groups of IPRs are responsible for executing distributed algorithms for disseminating system status information among fellow IPRs, and for using this information in making local decisions in the event of system failures. During a contingency, groups of neighboring IPRs work together to contain

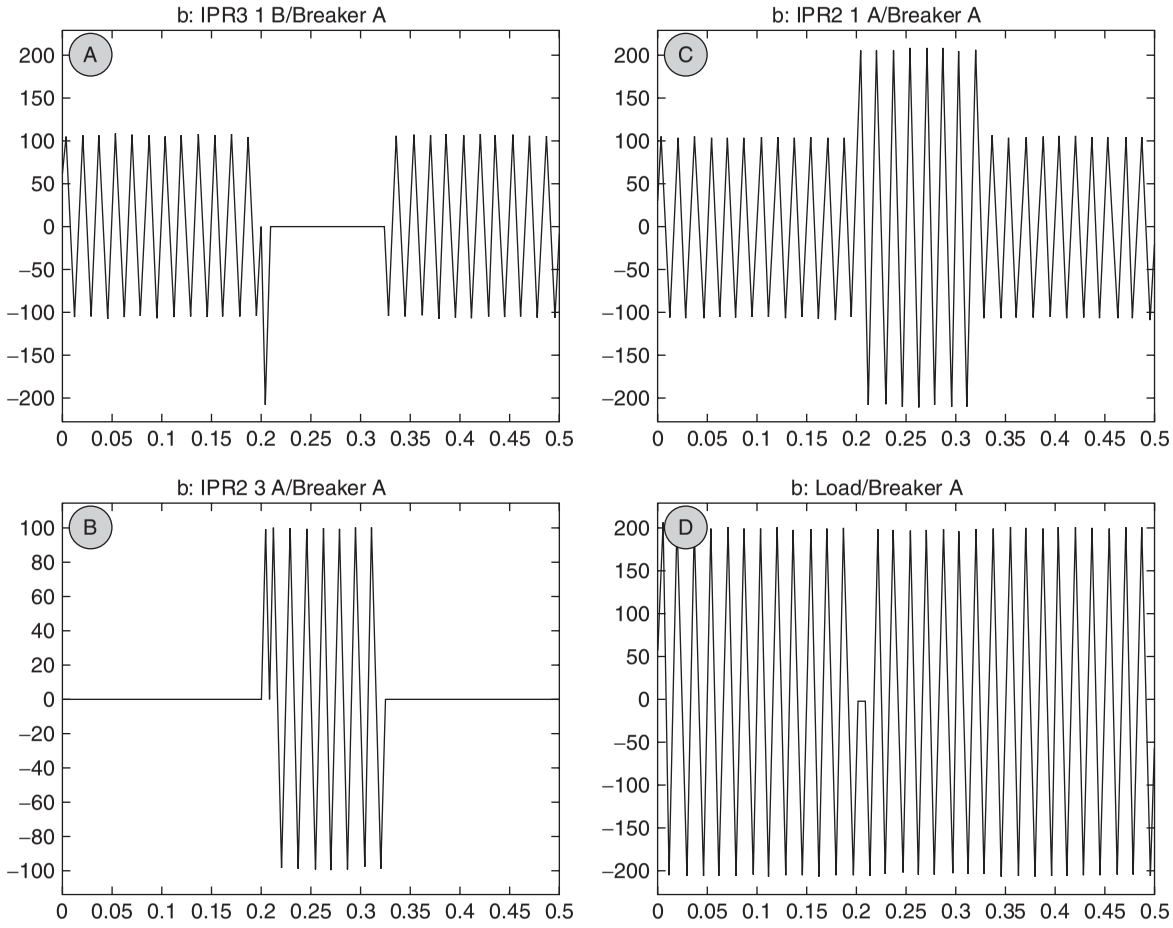

Figure 3.6 Current at indicated points in the example 3-bus system.

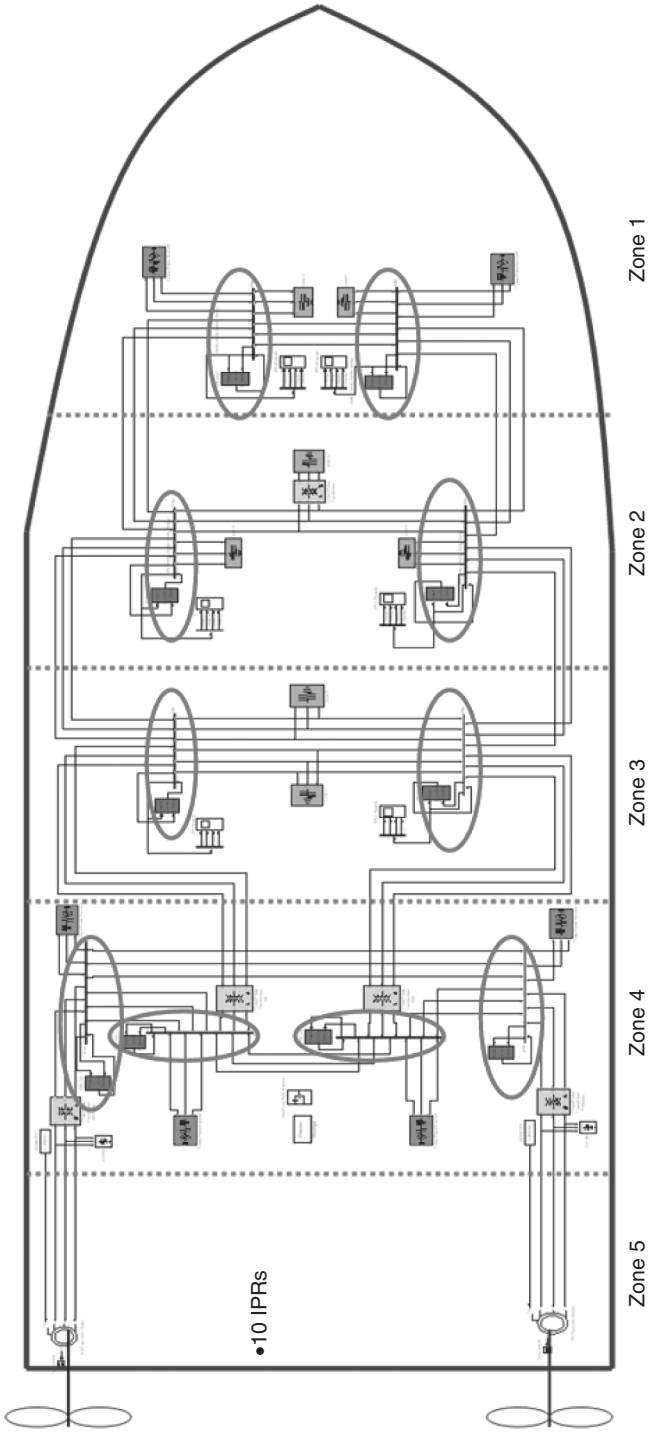

Figure 3.7 SimPower Model of DD(X) shipboard power system.

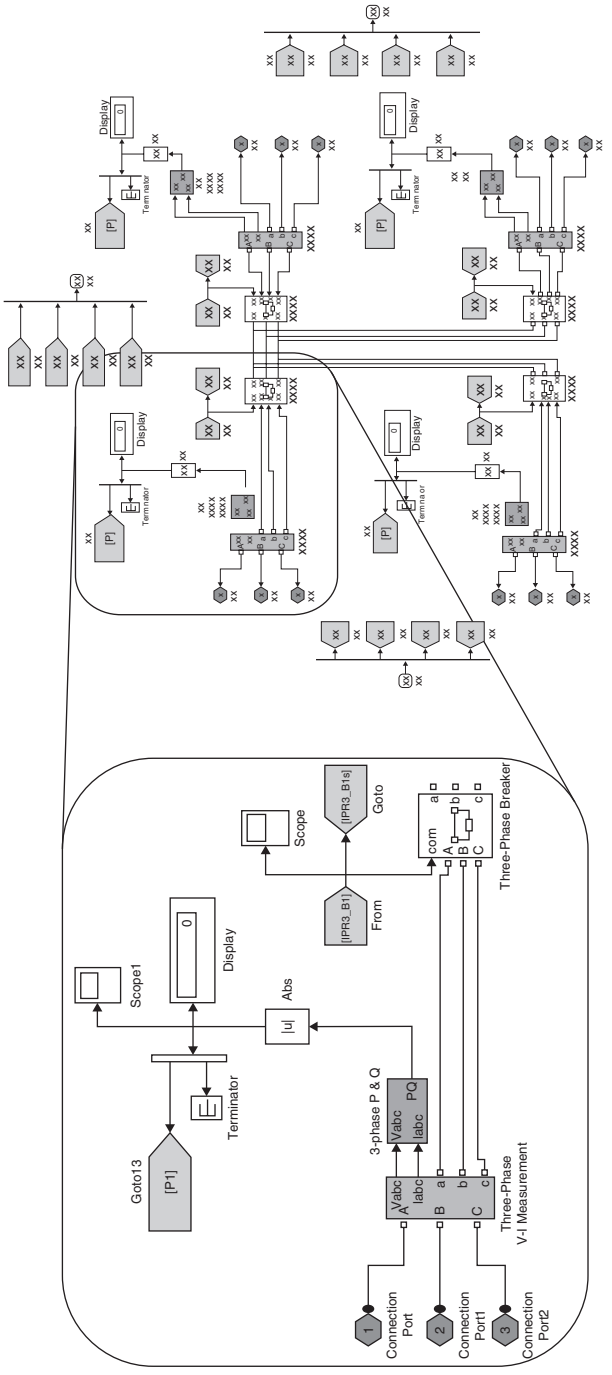

Figure 3.8 SimPower model of 3-phase computer controllable bus.

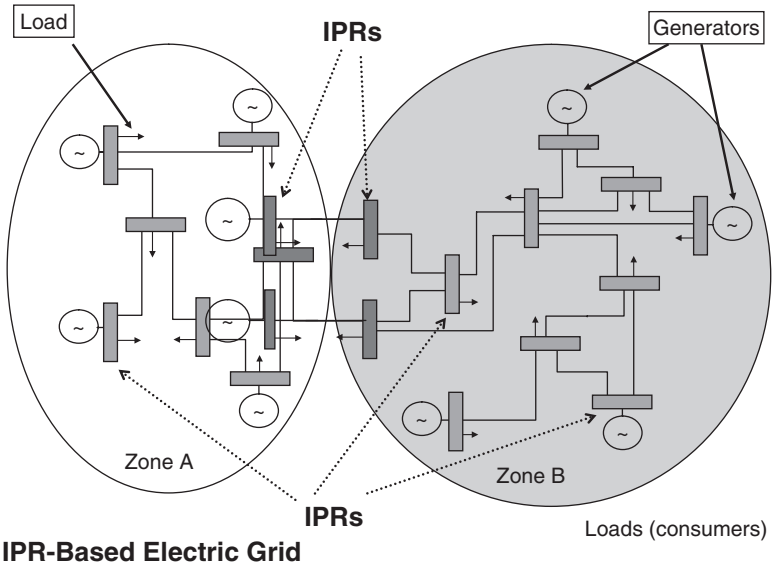

Figure 3.9 Electrical network featuring IPRs.

the damage, bring back critical lines, activate emergency generators, deliver power to critical loads, and continuously monitor the system to maintain an acceptable level of operation. Our goal is to show that by distributing network intelligence and control functions using the IPRs, we can improve the survivability, security, reliability, and re-configurability of the electrical network.

An IPR-based power delivery system scales much the same way as a computer network scales. Groups of *local* IPRs form "local area power networks" and are interconnected by border IPRs that enable the formation of larger networks of networks. Meanwhile *border* IPRs are responsible for attempting to contain countermeasures and recovery actions inside local area power networks to prevent a failure from cascading across large regions of the system. IPRs view currently existing relay-based load-shedding schemes as lower layer countermeasures in a multi-layer power delivery network.

3.4.2 Restoration of Electrical Energy Networks with IPRs

The worst-case contingency occurs, is a system *blackout* (e.g., August 2003 northeast USA blackout) whereby either the whole system or large sections of it are rendered inoperable. A *restoration* process must follow such an event to bring the system back into operation. This process must determine the *right order* of reconnection steps to re-energize power generators, transmission lines, distribution lines, and loads. Typically this problem is modeled as a network flow graph optimization problem [8]. We next

discuss how IPRs can be applied a decentralized restoration plan, unlike existing centralized schemes.

3.4.3 Mathematical Formulation

Our mathematical model derives from the mathematical formulations in [22,23]. Our objective for our power system's restoration is to maximize the number of restored loads with the highest priority values. We express this objective function as

$$\max \sum_{k \in R} L_k * y_k * (\alpha - \mathrm{Pr}_k)$$

where Pr_k is the load's priority factor (the highest priority load being $Pr = 1$, the second priority load $Pr = 2$, etc.), α is a natural number larger than the Pr value with less priority, L_k is each load in the system, y_k is a decision variable ($y_k = 1$ if load L_k is restored, $y_k = 0$ if load L_k is not restored), and R defines the current set of de-energized loads. The constraints associated with our mathematical model are similar to the constraints in the restoration model presented in [22]: limits on power sources available in each bus for restoration, balance in the power system between supply and demand, and limits on line capacity for power transmission.

3.4.4 IPR Network Architecture

The IPR are organized in a peer-to-peer (P2P) network [9,11,12]. In this architecture, for a given IPR, it is irrelevant whether the inputs come directly from power producers or other IPRs. For this propose we assume that there is one IPR in each of the buses in the system. It is important to recognize that the network for transmission or distribution of electrical energy is different from the communications network between IPRs. This scheme guarantees independency of communication during a contingency in the electric transmission system. But the IPR network communication must duplicate the electrical connections in the system. For this purpose we put an IPR in each bus of the system. Figure 3.10 shows the relation between the electric energy delivery network (EEDN) and the IPR network. We have developed three types of IPRs:

- *Source power router (SrcPR)* These routers provide an interface between power generator (drawn as circles) and the IPR network. They inform other IPRs about the status of the power generators.
- *Principal power router (PPR)* These routers re-configure the network during a high-risk operating condition or some type of system failure.
- *Sink power router (SnkPR)* These routers interface between loads and the IPR network. Their principal function is to connect and disconnect loads as necessary.

Each IPR has a set of lines classified as either *input* or *output* lines. These output and input lines correspond to transmission or distribution lines that move power between the buses associated with each IPR. The rest of this discussion will pertain

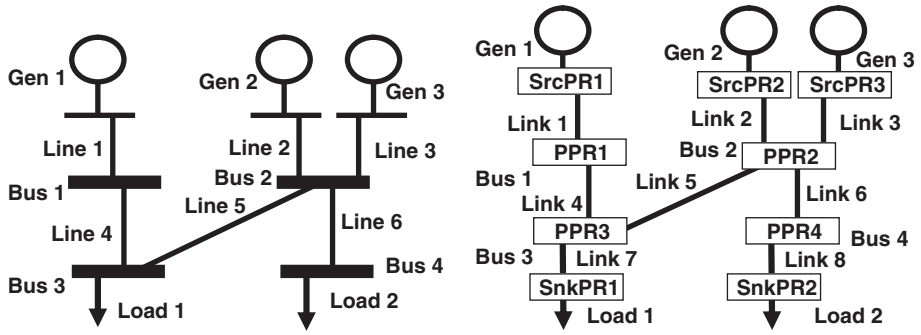

Figure 3.10 Relationship between EEDNs, IPR locations, and IPR logical connections (Gen n: generator n, SrcPR: source of power router, PPR: principal power router, SnkPR: sink power router).

to such a transmission system. Input lines model transmission lines that bring power into the bus associated with a given IPR. Likewise output lines model transmission lines (or branches) that feed from the bus associated with a given IPR. Decisions for the activation of contingency plans from IPR are based on two factors:

1. *Priority factors* Every output line has a priority factor that is similar to the priorities assigned to the loads. These priorities indicate which lines must be serviced first, in the event of a contingency.
2. *Reliability factors* Every input line has a reliability factor that indicates how reliable is the power source feeding the line.

Several message types are defined for IPR communications and interactions. Their purpose is to ensure that each IPR is aware of the conditions in its neighboring IPR. These message types are as follows:

- *Steady state messages* These messages are designed to exchange information between adjacent IPR while the EEDN is in normal operation state.
- *Contingency messages* When a fault occurs in the EEDN, these message types will be exchanged between IPRs during the system restoration process.

3.4.5 Islanding-Zone Approach via IPR

The key to the performance and quality of IPR decision making resides in the IPR's knowledge of the state of its neighbors. Hence all IPRs should exchange state messages continuously. Since, as the IPR network grows, the number of messages will grow exponentially, congestion in the communications network could make it difficult for IPRs to get the status messages necessary to maintaining current system conditions. In view of this, we divided the system into zones or geographical regions. Each zone has

a balance between capacity for energy generation and demand for consumption. Each zone behaves as an autonomous network of IPRs capable of exchanging messages with other zones, while also been able to contain and repair failures within the zone.

To support this zone concept, we developed a second IPR classification scheme. *Interior IPRs* are those that exchange messages within a given zone. *Border IPRs* exchange messages between different zones. Figure 3.11 shows an example of a power system divided in two zones (zone A and zone B). Zone A has nine buses and each bus has an IPR. Zone A has six interior IPRs and three border IPRs. Likewise zone B has 10 buses with eight interior IPRs and two border IPRs. The operation of each of IPR is as follows:

- Interiors IPR To establish a secure operational state in the interior of each zone, the Src-IPR informs the state of its generator in a message that is spread throughout that the zone. This way every other IPR knows the state of generators in its zone, allowing it to modify its reliability table to request power from generators with more probability of responding to a request. This scheme prevents wastage of time and resources in requests for power from generators that cannot satisfy such requests.
- Border IPR When zone X experiences a demand in power that cannot be served by its local generators, the border IPR of that zone issues the request to the neighboring zones so that the entirety of the loads in zone X can be served, or at least as many as the high-priority loads as possible. In the event of a catastrophic event that forces the partition of the systems in islands, the border IPR in each zone exchanges messages to coordinate the re-interconnection of those islands.

To simplify the negotiation scheme, border IPRs see each neighboring zone as a generator or as a load (network equivalent), depending on the power flow direction. If power is entering from zone A to zone B, then the border IPRs at zone B see zone A as a generator. Likewise the border IPRs in zone B see zone A as load. Figure 3.12 illustrates this idea; it shows the view of zone A for Border IPR of zone B as two generators and two Loads. These generators are the least reliable generators for zone B.

3.4.6 Negotiation in Two Phases

Although it is almost impossible to obtain optimal answers starting from local decisions, and although that it is not our objective, IPRs have the capacity to improve the state of the system via their negotiations at several stages when they restore the number of loads to serve high-priority needs.

Intra-zone Negotiation The first phase of IPR negotiation is performed at the intra-zone level. At this stage, the interior IPR works to satisfy the maximum number of high-priority loads within its zone. By a periodic exchange of messages, the interior IPR are able determine which loads should be served with the generation capacity in each zone, to make sure that the system operates in a secure way. The process of intra-zone negotiation is carried out in three stages, discussed below.

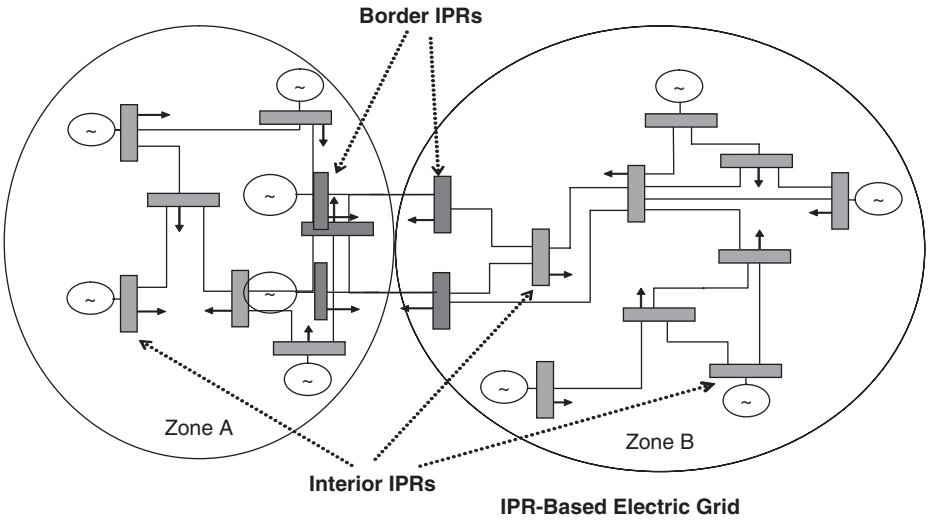

Figure 3.11 A zone-island approach.

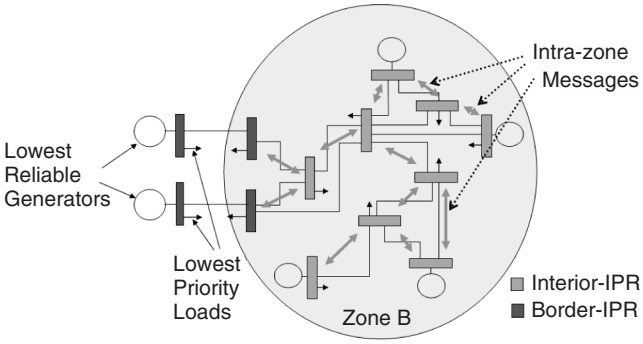

Figure 3.12 Interior and border IPRs.

1. *Friendly request stage* At this stage of the negotiation the IPR follows the standard negotiation process described in [23]. In this scheme each load uses its SnkPR to make requests for power to the IPR network. Each request is routed until an affirmative or negative answer is found, depending on current system conditions. Following the priorities scheme, IPRs choose which loads can be served and which cannot. Afterward the IPRs try to return the system to its previous safe operational state, maintaining request direction as the power flow was before the catastrophic event. But, if a high priority load sends a late request and the resources of the system are already committed and do not

allow this load to be served, then this high-priority load will receive a negative answer. At this first stage, loads of high priority might not be served at all. The second and third stages deal with such situation.

2. *Persistent request stage* The SnkPRs that receive a negative answer in the friendly request stage now send a *persistent service request*. This type of request forces the IPRs to attempt a system reconfiguration by changing the direction of the power flows necessary to satisfy most of the high-priority loads. When the request reaches a generator, the associated SrcIPR triggers a load shedding to ensure that power is directed to the highest priority loads.
3. *Load-shedding communication stage* When a SrcPR determines that it needs to disconnect a set of low-priority loads to guarantee service to a high-priority load, it sends a special disconnect message to the selected low-priority loads. To accomplish this, every request message is signed with a complete route to the load. The SrcPR sends a disconnect message following the path stored in the message to reach the SnkPRs servicing the low-priority loads. The SrcPR then awaits for a disconnect confirmation message. This message is routed by the IPR in the path between the SrcPR and the SnkPRs. When the SnkPR gets a disconnect message, it disconnects its associated load and sends a confirmation disconnect message to SrcPR that sent the original message. Then the SnkPR for the load just disconnected starts looking for power from alternative generators. When the SrcPR receives the disconnect message from all targets for disconnection, it sends an affirmative response to the high priority load to be serviced

Intra-zone Negotiation The objective of this phase is to bring power from another zone to try to restore the loads that were not served in the *intra-zone* negotiation because of insufficient generation capacity. When a SnkPR receives a deny response for a persistent request message, it sends an inter-zone assistance request, and this message is routed until it gets to a border IPR. This border IPR forwards this request to its peer border IPR in another zone. When a border IPR receives an inter-zone request, it stores this message and sends a friendly request message to the IPR in its local zone network. Notice that this message is treated as an intra-zone message, and it is processed as mentioned in the previous section. The idea is to handle the request as if it came from a load inside the zone of the border IPR.

When the border IPR receives the final response, it sends that response to the border IPR X in the zone that initiated the negotiation process. If this message is an affirmative response, border IPR X sent this response to the SnkPR that made the original request. Otherwise, the original power request is routed to another border IPR until an affirmative response is obtained, or a denial response is obtained from all border IPRs. In the latter case, a final denied response is sent to the SnkPR that made the original request. This SnkPR awaits a time interval T, and then begins the whole process again.

3.4.7 Experimental Results

To demonstrate the effectiveness of the proposed power distribution scheme, we have implemented a software library with all the protocols and communications for IPR operations and the intra-zone scheme presented above. We are still working on the implementation of the inter-zone scheme. Our computer simulation was built using the Java programming language, and it was run on several computers interconnected via a 100 Mbps LAN. In [23] we presented one of the simulation cases with its conditions that we ran on a modified version of the WSCC 9-bus model. The objective of our simulation consists in obtaining a reservation and allocation of power resources to enable system restoration after a total system blackout.

As [23] elaborates, after running the test cases four times, the power allocation negotiated by IPR can supply 100% of the power required by loads in each case. Moreover the allocation of power satisfies the constraints established in the mathematical formulation. All this was accomplished in a de-centralized manner and using only the local information available to each IPR.

3.5 RISK ASSESSMENT OF A SYSTEM OPERATING WITH IPR

For the purpose of calculating the reliability of an individual IPR, we divide the IPRs into three subsystems, namely power hardware (breakers or other power switching elements), computer hardware (the data router that permits communication between IPR and CPU functions), and software as depicted in Figure 3.1. We identify failure modes for each subsystem of the selected IPR structure to estimate the IPR reliability [24]. This estimate of failure probability for an IPR will be used in our work to measure the change in reliability of a power system operated with and without IPRs.

3.5.1 IPR Components

The operational relationship of IPR subsystems is shown in Figure 3.13

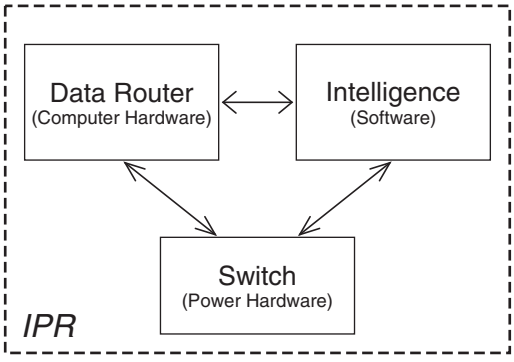

Figure 3.13 Basic operational relationship of IPR major subsystems.

1. *Software* The intelligence section (i.e., software) consists of the algorithm that will make and execute decisions while the IPR operates. The intelligence section will control the switching device of the IPR, depending on the network status.
2. *Power hardware* The switching device of an IPR can be a high-voltage circuit breaker, FACTS (flexible AC transmission systems), or another switching device capable of controlling the power flow in the transmission/distribution lines.
3. *Computer hardware* The data router section will handle the communication between IPRs. They have to communicate the status of the network and useful data obtained by the system sensors (PTs, CTs, etc.) for the intelligence section to analyze and take appropriate action.

3.5.2 Configuration

Figure 3.14 shows possible functional configurations for the internal components of an IPR. Figure 3.14*a* shows the basic series configuration. If any of the internal components fail, the IPR will fail. We assume that the probability of failure of each component (software, data router, and breaker) is independent of each other. Figure 3.14a,b,c,d, and e introduces a redundant path for the software, router, and software-router, respectively. If the main path fails, there is an auxiliary path allowing the IPR to maintain full functionality. We do not provide a redundant path for the breakers because we assume the cost of power breakers to be much higher than that of software or routers.

3.5.3 Example

In [25] Anderson reviews important concepts of reliability theory. Reliability is defined to be the probability that a component or system will perform a required function for

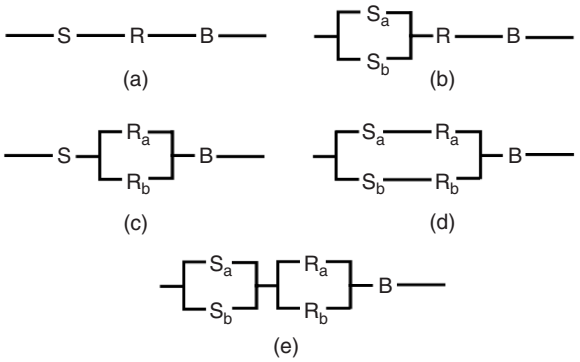

Figure 3.14 IPR internal configurations.

a given period of time when used under stated operating conditions [26]. It is the probability of non-failure over time. These concepts are the basis of our work. Let

$$R = P\{\text{successful IPR operation}\} = \text{reliability}$$

$$Q = P\{\text{unsuccessful IPR operation}\} = 1 - R = \overline{R}$$

$$B = \{\text{successful circuit breaker operation}\}$$

$$\overline{B} = \{\text{unsuccessful circuit breaker operation}\}$$

From the rules for series/parallel systems, the following equations are obtained for every configuration shown in Figure 6.14:

$$\text{Conf.(a)}, \mathbf{R} = \text{P(S)P(R)P(B)} \tag{3.1}$$

$$\text{Conf.(b)}, \mathbf{R} = \text{P(S)P(R)P(B)} = (1 - P(\overline{\text{S}}_\text{a})\text{P}(\overline{\text{S}}_\text{b})) \times \text{P(R)P(B)} \tag{3.2}$$

$$\text{Conf.(c)}, \mathbf{R} = \text{P(S)P(R)P(B)} = \text{P(S)} \times (1 - P(\overline{\text{R}}_\text{a})\text{P}(\overline{\text{R}}_\text{b})) \times \text{P(B)} \tag{3.3}$$

$$\text{Conf.(d)}, \mathbf{R} = (\text{P}(\text{S}_\text{b})\text{P}(\text{R}_\text{b}) + \text{P}(\text{S}_\text{a})\text{P}(\text{R}_\text{a}) - P(\text{S}_\text{a})\text{P}(\text{R}_\text{a})\text{P}(\text{S}_\text{b})\text{P}(\text{R}_\text{b})) \times \text{P(B)} \tag{3.4}$$

$$\text{Conf.(e)}, \mathbf{R} = \text{P(S)P(R)P(B)} = (1 - \text{P}(\overline{\text{S}}_\text{a})\text{P}(\overline{\text{S}}_\text{b})) \times (1 - \text{P}(\overline{\text{R}}_\text{a})\text{P}(\overline{\text{R}}_\text{b})) \times \text{P(B)} \tag{3.5}$$

To complete our example, reliability estimates of each component are needed. From [27] we have that "major failure per breaker year" estimate is 0.00672 for single-pressure high-voltage breakers above 63 kV (all voltages, from years 1988–1991). The reliability of high-voltage breakers can be calculated using the equation $\mathbf{R}(t) = \exp(-\lambda t)$, assuming a constant failure rate [26]. For a one-year period the estimate for the breaker's reliability is $\mathbf{R}(1) = P(B) = 0.99330$, or 99.330% of confidence.

From [28] we obtain the average MTBF (mean time between failure) of Ethernet routers to be 9.5 years, and for a price multiplier of 25, they are available with 35 years of MTBFs. From [26] the reliability can be calculated from the MTBF indexes using the equation $\mathbf{R}(t) = \exp(t/\text{MTBF})$, again, assuming a constant failure rate. For a one-year period, the reliability found is $\mathbf{R}(1) = P(R) = 0.90009$ for a 9.5-year of MTBF, or $\mathbf{R}(1) = P(R) = 0.97183$ for a 35-year of MTBF.

Estimation of software reliability is not an easy task. To make a good estimate, we need the total of code lines, loops, the frequency of each loops, the execution time, failure rate, fault density, and so on. Since software for an IPR is not available, an estimate of its reliability is not possible. Still we assume a reliability of 0.95 and 0.99 in our example. These values are conservative, since we believe that the controlling software on an IPR will not be all that complex and IPR decisions will be based on pre-established contingency tables.

Table 3.1 summarizes the results of reliabilities and failure probabilities for each configuration of Figure 3.14 using their respective equations. As we said before, reliability is defined as the probability that a system (component) will function over some time period t, and it can be expressed as $\mathbf{R}(t) = P\{T \geq t\}$, where T is a random variable of the time to failure of the system. If we define $F(t) = 1 - \mathbf{R}(t) = P\{T < t\}$,

TABLE 3.1 Reliabilities and failure probabilities of IPR configurations

	$P(S) = 0.95$, $P(R) = 0.90009$, $P(B) = 0.99330$		$P(S) = 0.99$, $P(R) = 0.90009$, $P(B) = 0.99330$	
IPR Configuration	**R**	**F**	**R**	**F**
(a)	0.84936	0.15064	0.88512	0.11488
(b)	0.89182	0.10818	0.89397	0.10603
(c)	0.93422	0.06578	0.97355	0.02645
(d)	0.97244	0.02756	0.98152	0.01842
(e)	0.98093	0.01907	0.98329	0.016713

then $\mathbf{F}(t)$ is the probability that a failure occurs before time t. The results show, as expected, that nonredundant configurations have lower reliabilities, or higher failure probabilities. As we introduce redundancy in just one component, the reliability of the system increases considerably, which reduces the probability of failure. The configurations shown in Figure 3.14*d* and Figure 3.14*e* showed the highest reliabilities.

The reliability of the each IPR configuration is lower than the reliability of the breaker alone. These results are not surprising because the reliability in a series system will be below the lowest reliability of its components. All our IPR configurations decompose to a series configuration. The only way that the reliability of IPR can be greater than the reliability of the breaker is if we provide a redundant path to the breaker. Does this mean that it is better to have only the breaker instead of the IPR? We believe not. A breaker will act based on local data, without regard to the system state outside its protection zone. The IPR, through its communication capabilities, will act based on local and regional data enhancing the system reliability. The classical methods do not capture appropriately the increase in the reliability of a power system when a special protection scheme (SPS) is included. However, it is known that when a SPS, like an IPR, is properly operating, system response significantly improves following a contingency and therefore so does the system reliability [29]. To capture appropriately the reliability increase in a power system, we will use the risk framework assessment developed by McCalley et al. [29]. In the following we give a summary of the reliability assessment for a section of a 179-bus system that includes an IPR. The system will suffer voltage collapse if lines L76–78 and L78–80 simultaneously have an outage. A solution to prevent system collapse is to install VAR compensators in buses 78 and 75. An IPR can be used to activate these compensators and prevent the collapse in the event that more than one line expenences outage.

Nomenclature

F_i: event there is a fault on ckt i (L76–78, L78–80)

A: fault type (1Φ, 2Φ, 3Φ, $\Phi - \Phi$)

N_C: # critical circuits

N_T: total number of events considered in the study

E_i: initiating events

N_C event → "N-1" outage

N_{C+1} event → No fault

$E_i, i > N_{C+1}$ → simultaneous outage two or more circuits

K: system collapse event

X: pre-contingency operating point

T: IPR switching event

Basic events:	Initiating Events
F_1, loss of line L76–78	E_1, loss of line L76–78
F_2, loss of line L78–80	E_2, loss of line L78-80
	E_3, no outage
	E_4, loss of both lines

Operation of an IPR (Categories)

1. IPR acts in a contingency $(T \cap E_i)$, $\quad i = 1, 2, \ldots, N_C, N_{C+2}, \ldots, N_T$.
2. IPR does not act in a contingency $(\overline{T} \cap E_i)$.
3. IPR acts when there is no contingency $(T \cap E_{N_C+1})$.
4. IPR does not act when there is no contingency $(\overline{T} \cap E_{N_C+1})$.

Risk Sources for a System with IPR

1. IPR fails to act in a contingency. The system may collapse depending on the pre-fault operating condition.
2. IPR works properly, no collapse, but nonzero impact.
3. IPR works unnecessarily when there is no outage, nonzero impact.

Risk of an event $E_i, i = 1, 2, \ldots$, which causes IPR to act or system collapse K:

$$Risk(K \cup T) = \sum_{i=1}^{N_T} Risk(E_i) = \underbrace{\sum_{i=1}^{N_T} \Pr(K \cap \overline{T} \cap E_i) \times \mathrm{Im}(K \cap \overline{T} \cap E_i)}_{Source\ 1}$$

$$+ \underbrace{\sum_{i=1}^{N_T} \Pr(T \cap E_i) \times \mathrm{Im}(T \cap E_i)}_{Sources\ 2\ and\ 3} \tag{3.6}$$

where

$$\Pr(K \cap \overline{T} \cap E_i) = \Pr(\overline{T} \cap E_i) \times \Pr\left(\frac{K}{\overline{T} \cap E_i}\right) \tag{3.7}$$

Each component (R, S, and B) can have two failure modes: 0–working, 1–failure. In this case the IPR can assume 16 states ($\underbrace{2}_{R} \times \underbrace{2}_{S} \times \underbrace{2}_{B} \times \underbrace{2}_{B} = 2^4 = 16$).

0000	0001	0010	0011
0100	0101	0110	0111
1000	1001	1010	1011
1100	1101	1110	1111

Some states are identical (e.g., 0010 and 0001), so we can merge them. The resulting states are

S_0–0000
S_1–0001, 0010
S_2–0011
S_3–0100
S_4–0101, 0110
S_5–0111
S_6–1000
S_7–1001, 1010
S_8–1011
S_9–1100
S_{10}–1101, 1110
S_{11}–1111

Now we classify the states into categories. There are four possible categories:

C_1: There is an active signal (AS, switching event). IPR works properly. If there is an inactive signal (IS, nonswitching event), IPR works unnecessarily.
C_2: There is an AS. IPR works properly. If there is an IS, IPR does not switch (works properly).
C_3: There is an AS. IPR does not work properly. If there is an IS, IPR works unnecessarily.
C_4: There is an AS. IPR does not work properly. If there is an IS, IPR does not switch (works properly).

Before we classify each state, we must characterize the failure mode for each component:

B → 0, the breaker switch properly
1, the breaker does not close
R → 0, the router communicates properly
1, the router does not send any information
S → 0, the software works properly
1, the software takes an incorrect decision

Now, the states can be classified in the following manner:

C_1: S_9
C_2: S_0
C_3: S_3, S_4, S_{10}
C_4: $S_1, S_2, S_5, S_6, S_7, S_8, S_{11}$

The resulting Markov chain is shown in Figure 3.16., where

$$\lambda_1 = \frac{1/9.5}{365} = \frac{0.10526}{365} = 0.000288392$$
$$\lambda_2 = 0.05129/365 = 0.00014053$$
$$\lambda_3 = 0.00672/365 = 0.0000184110$$

These values were obtained from the MTBF, MTTF, or the annual failure rate for each component. The failure rate of the router (λ_1) was obtained from its MTBF of 9.5 years. The daily rate of the software (λ_2) was calculated from the assumed reliability of 0.95 and converted to the failure rate per year of 0.05129. Finally, the failure rate of the breaker (λ_3) was obtained from literature.

To find the risk, the conditional probability $Pr(K/(\overline{T} \cap E_i))$ in equation (3.3) is needed. From simulations is known that the probability of collapse, given that event E_3 or E_4 occurred and there is no tripping action of the IPR, is 1 and 0 for E_3 and E_4, respectively. However, for events E_1 and E_2, the probability is not known. Right now we are working with a technique known as the voltage stability index to establish a probability function in order to compute these probabilities and finalize our risk assessment.

3.6 DISTRIBUTED CONTROL MODELS

3.6.1 Distributed Control of Electronic Power Distribution Systems

Today's complex electronic power distribution systems (EPDS) in data centers, automotive, ships, and aircrafts require sophisticated control techniques to support all aspects of operation, including failure. When a high degree of reliability is desired, the effects of failures must be mitigated and control must be maintained at survivable scenarios. In order to manage fault scenarios, we need to make a series of decisions and control actions:

1. The fault has to be detected.
2. The fault source has to be identified and its magnitude estimated (partial degradation vs. total failure).
3. Depending on the nature of the failure, a new control algorithm has to be selected that compensates for the failure.

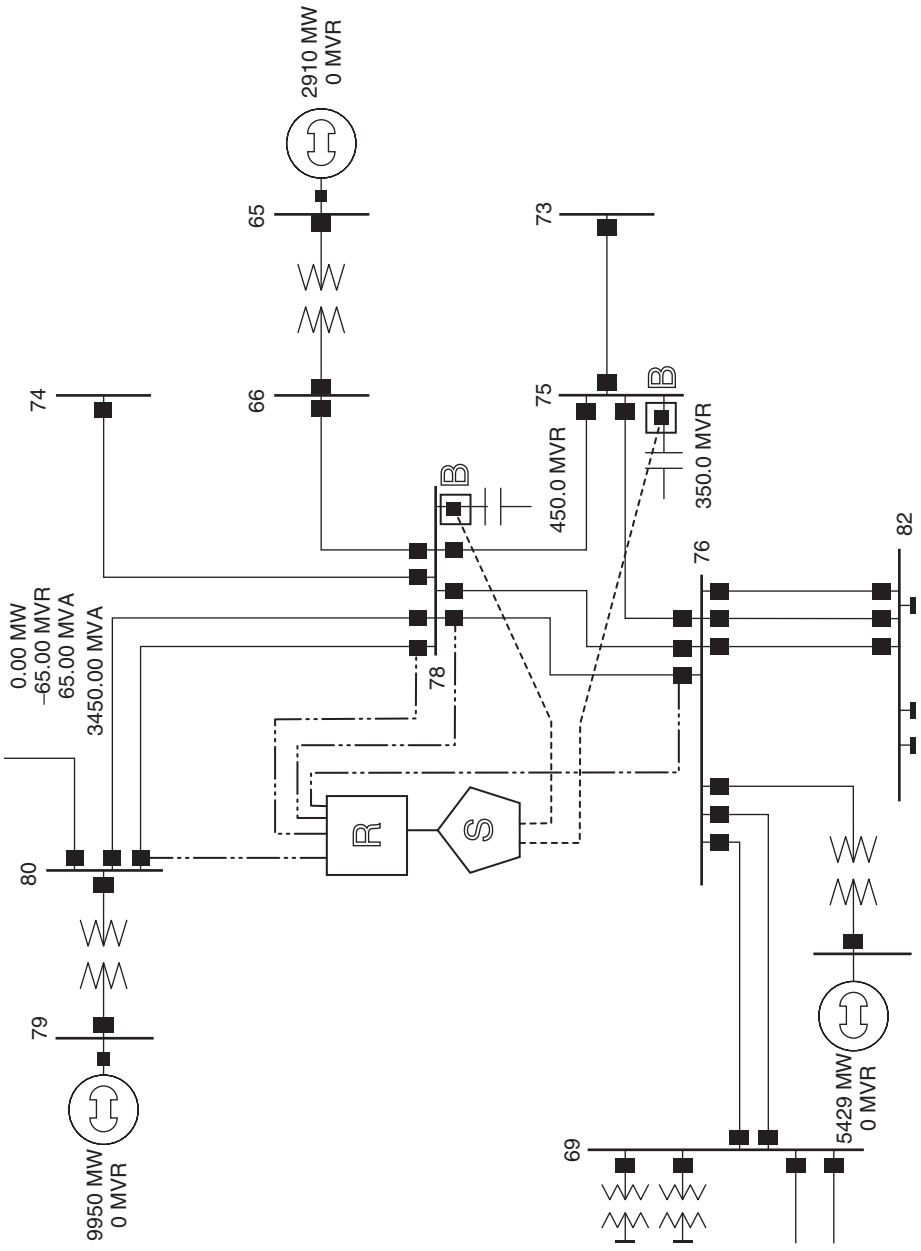

Figure 3.15 IPR configuration in a 179-bus section.

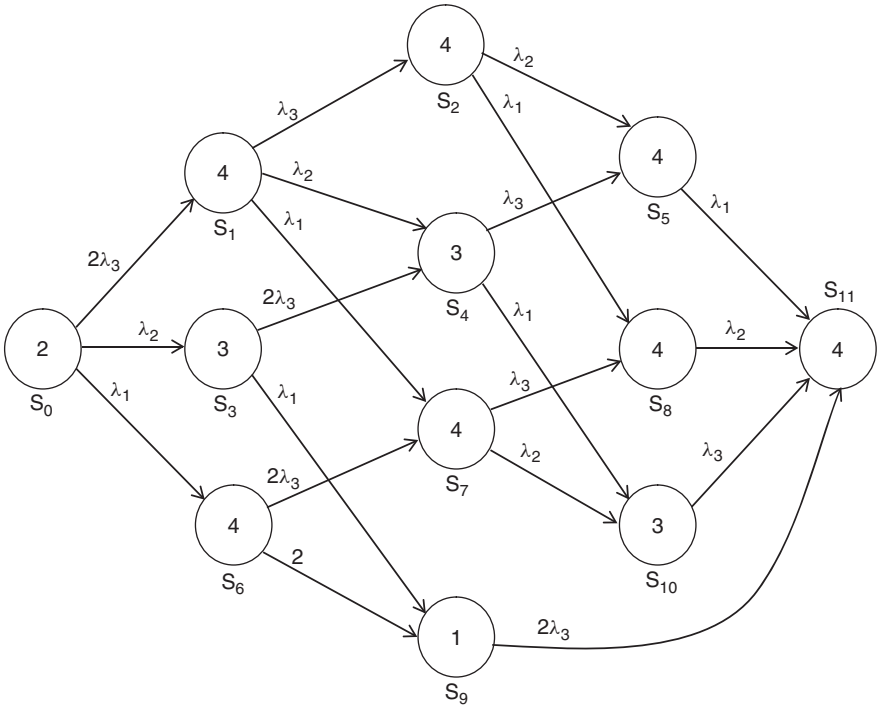

Figure 3.16 Markov chain.

4. The EPDS has to be reconfigured.
5. The new control algorithm has to be chosen.

All these decisions must be made by a control system that incorporates not only simple regulatory loops and the supervisory control logic, but also a set of components that detect, isolate, and manage faults in coordination with the control functions. A block diagram for a self-reconfigurable control system is shown in Figure **3.17**.

Hybrid dynamical systems theory offers a natural framework for the modeling and fault adaptive control problems in EPDS. Considerable research work has been dedicated to the study of various aspects of hybrid systems, including modeling, stability analysis, and control. Intelligence in the context of hybrid dynamic systems refers to the capability of these systems to adapt and reconfigure themselves to make significant changes to their operating environment and their own structure. An example of a self-reconfigurable control system is the fault adaptive control system described in [30]. Fault adaptive control systems, in particular, have been studied in the context of robotics [31] and manufacturing automation [32].

In general, autonomous systems are seen as one of the most important trends in control systems. Autonomous systems have initiated change of paradigm in the control of AC power systems [33,34] with similar trends are being investigated for EPDS in

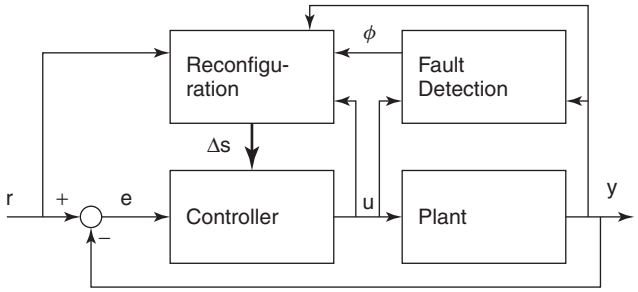

Figure 3.17 A self-reconfigurable control system.

ships [35], automotive [36], and space applications. Our research work is focused on studying the different approaches to realizing a self-reconfigurable control system for EPDS.

3.6.2 Integrated Power System in Ship Architecture

Integrated power system (IPS) is the term applied to a ship architecture where both ship service loads and ship propulsion are supplied by a common electrical source. In the IPS concept proposed by the Advanced Surface Machinery Program of the NAVY Naval Sea Systems Command, the power distribution is based on the zonal distribution architecture, which includes both AC backbone and DC zonal systems. Zonal architectures have advantages over traditional ring bus distribution systems supplying radial feeders, including better reconfigurability and greater survivability [37]. Compared to radial distribution, zonal distribution architectures provide maximum protection (fault tolerance), reduced cabling, and cost savings.

A diagram of the ONR reference IPS provided for self-reconfigurable control system studies is shown in Figure 3.18. This system contains the minimum elements to represent an advanced IPS [35]. System characteristics include the following:

1. Two finite inertia AC sources and buses.
2. AC bus dynamics, stability, and regulation.
3. Redundant DC power supplies and zonal distribution buses.
4. DC bus dynamics, stability, and regulation.
5. Three zonal distribution zones feed by redundant DC power buses.
6. A variety of dynamic and nonlinear loads.

An actual ship would typically have five to eight zones instead of the three as shown in Figure 3.18.

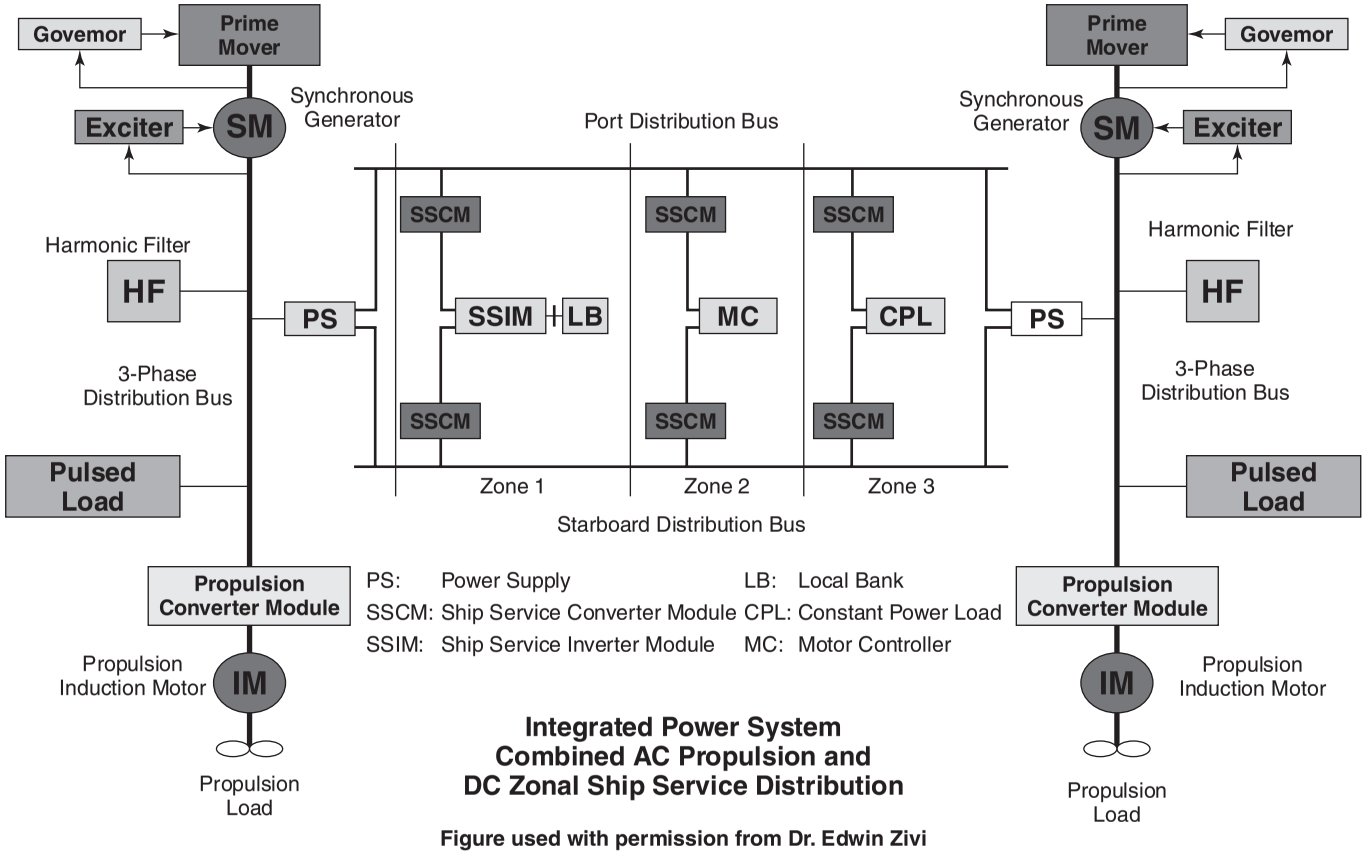

Figure 3.18 ONR reference system: Notional integrated power system (IPS).

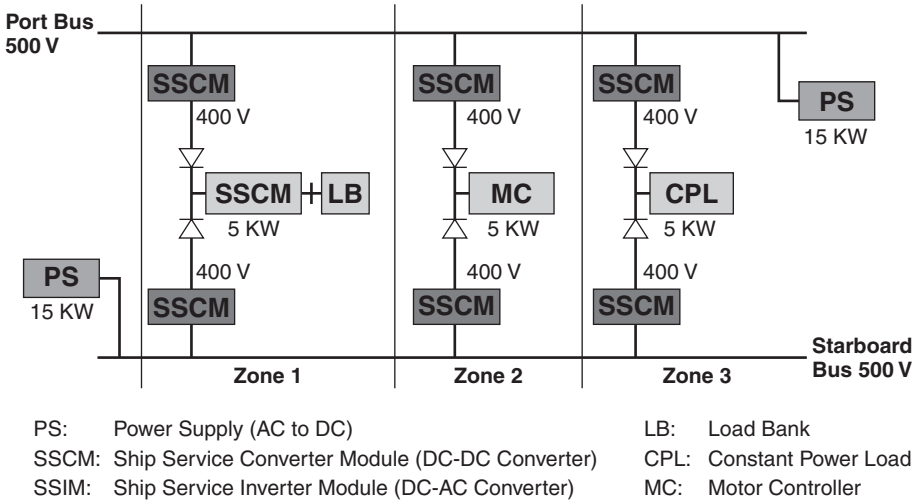

Figure used with permission from Dr. Edwin Zivi.

Figure 3.19 ONR IPS reference system DC zonal distribution system.

3.6.3 DC Zonal Electric Distribution System

Simulation will be our primary tool to test and validate the control algorithms to be developed in this work. In the initial stages we are using the Simulink™ implementation of the DC zonal electric distribution system (DCZEDS) described in [35,37,38], which is a simulation test bed for the control algorithms of the ship power distribution systems provided by the Office of Naval Research (ONR) to researchers in the NSF/ONR Electric Power Networks Efficiency and Security (EPNES) program [35].

Figure 3.19 shows an expanded version of the DCZEDS in Figure 3.18. The reference DCZEDS is fed by two 500-V busses: one on the starboard side and one on the port side. Each bus is connected to an electrical zone through a ship service converter module (SSCM) that serves to buffer the main bus and the intra-zone electrical loads and to provide a voltage level appropriate to the load. Diode networks are used for automatic bus transfer. AC loads are fed by ship service inverter module (SSIM). In addition to power conversion functions, the SSCM and the SSIM provide monitoring and protection functions.

The DCZEDS consists of two power supplies (PSs), six ship service converter modules (SSCMs), three diode networks, one ship service inverter module (SSIM) with an associated load bank (LB), one motor controller (MC), and one constant power load (CPL). The loads are divided into three zones as shown in Figure 3.19 All DCZEDS subsystems and modules have local controllers.

The components and subsystems of the DCZEDS have local conventional controllers. Our goal is to add to this system the fault detection and reconfiguration logic to develop a self-reconfigurable power distribution system.

Some Simulation Results Simulation studies using the DCZEDS model are being performed to understand how it functions and its limitations. Normal operation and fault scenarios are being evaluated. Figure 3.20*a* shows results of a system start-up simulation. As expected, under no faults, the system reaches steady state with no major problems. Examples of potential faults are as follows:

1. Isolated faults at the individual zonal loads.
2. Faults at the distribution buses.
3. AC propulsion bus fault (i.e., generator fault).

Figure 3.20*b* shows simulation results when there is a fault in the port distribution bus. As expected, the system can supply power to all loads from the starboard bus. A defect in the SIMULINK model is that loads are only connected through the corresponding SSCM to either the starboard or the port bus, which results in a limited number of potential faults and reconfiguration possibilities. An enhanced implementation of the DCZEDS system of Figure 3.19 has been implemented in the virtual test bed (VTB) environment and presented in [39]. We have obtained a copy of this model from Dr. Roger Dougal from University of South Carolina. We are also enhancing the SIMULINK model by including topological rules to limit the number of loads that can be connected to a bus and adding priorities to the system loads to include load shedding in the reconfiguration schemes.

3.6.4 Implementation of the Reconfiguration Logic

We selected MATLAB™ SIMULINK™ together with MATLAB™ Stateflow™ toolbox to conduct the simulation experiments and implement the reconfiguration logic. Stateflow is a graphical tool that works with Simulink. Stateflow lets you design and develop deterministic, supervisory control systems in a graphical environment. This program visually models and simulates complex reactive control to provide clear, concise descriptions of complex system behavior using finite state machine theory.

A finite state machine diagram can be used to represent new system configuration. Figure 6.21 shows a truth table for the modes for the system and Figure 3.21 shows a finite state transition diagram for the DCZEDS when a distribution bus fails. Our current work continues the simulation studies, and we are looking at different methodologies to design the logic control component of the supervisory system.

3.6.5 Conclusion

The future of power systems for ships will be based on zonal architectures, making them an ideal test bed where to evaluate potential concepts for self-reconfigurable systems for electronic power distribution systems. We have finished our evaluation of the DCZEDS as a potential simulation test bed, and the DCZEDS model has adequately met our demonstration objectives. Future work will be focused on the failure analysis and reconfiguration logic of the self-reconfigurable system using a centralized as well as the IPR distributed approach.

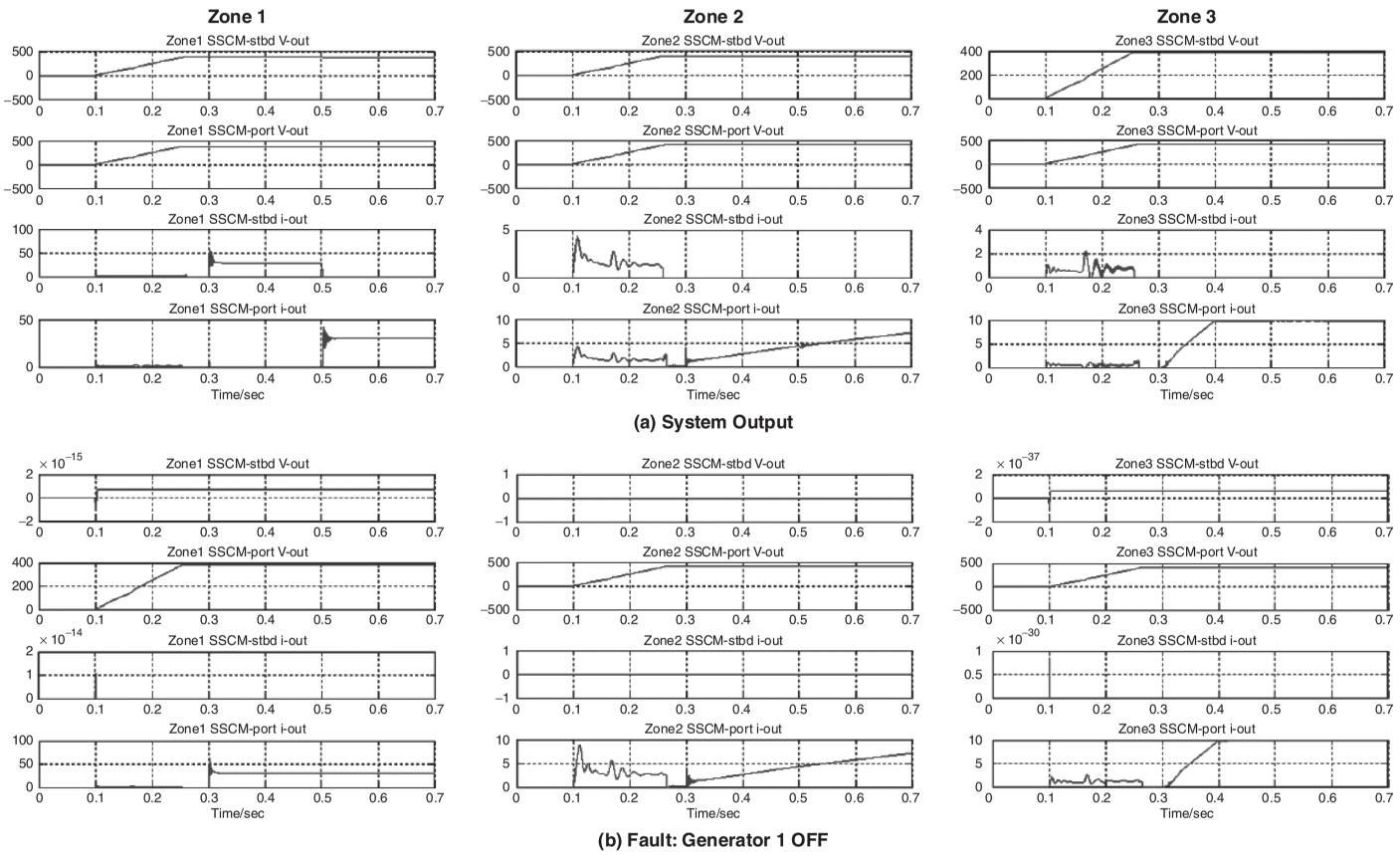

Figure 3.20 SIMULINK DCZEDS simulation results.

G1	G1	Z1	Z2	Z3
0	0	0	0	0
0	1	1	1	0
1	0	0	1	0
1	1	1	1	1

Figure 3.21 System truth table for distribution bus faults.

3.7 RECONFIGURATION

We chose to use the power system restoration (PSR) problem, an extreme condition in a power system, as a starting point to address the system reconfiguration problem. We are currently using the PSR problem global (centralized) solution as a benchmark against solutions obtained using the IPR approach.

The goal in the PSR problem is to rebuild a stable electric system and restore all unserved loads. Our restoration approach requires that at each stage of the restoration process the values for the control variables that minimize the unserved loads while satisfying the network operating constraints be obtained. The electric power system restoration problem was formulated as a multi-objective, multistage, combinatorial, nonlinear, constrained optimization problem, and a hybrid discrete and continuous particle swarm optimization (PSO) algorithm was implemented in order to handle the binary and continuous variables of the problem. The proposed method was tested on the well-known 9-bus WSCC equivalent system. The results obtained show the effectiveness and applicability of the proposed method [20].

We are currently developing a controlled islanding mechanism that will permit partial system preservation and rapid system recovery using IPR. The controlled islanding scheme will consider the inherent structural characteristics of the system, as well as the imbalance between generation and load. After the islands are created, appropriate control actions (e.g., underfrequency and/or undervoltage load shedding) will be executed to bring each island to a normal operating state. That way the extent and duration of a potentially catastrophic event can be effectively limited. The first step in the proposed approach will be to carry out a series of transient stability studies, which will provide valuable information regarding the coherent groups of generators, the quantities that should be monitored to assess the vulnerability of the power system with respect to possible cascading events and the proper location of the IPR throughout the system.

3.8 ECONOMICS ISSUES OF THE INTELLIGENT POWER ROUTER SERVICE

In this section we propose to define the IPR function as an ancillary service. To put this in context, we discuss the application of the IPR concept in an actual market

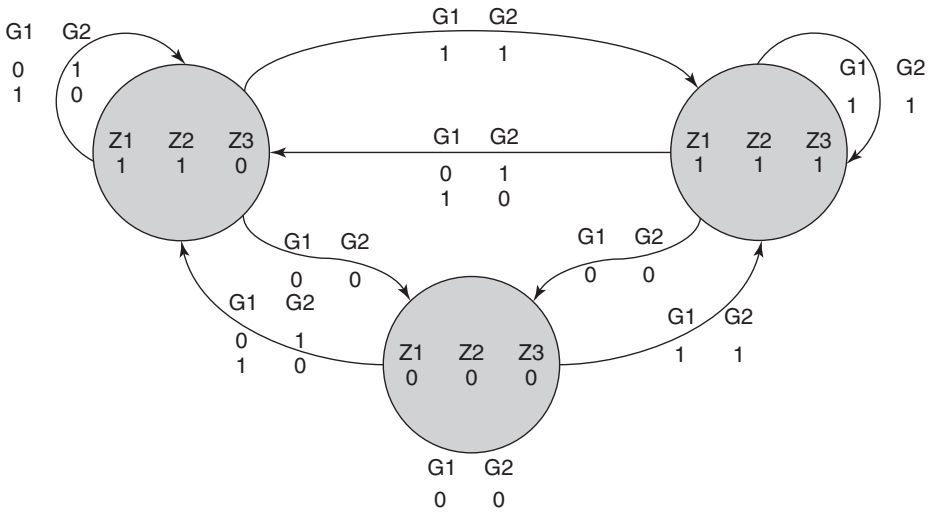

Figure 3.22 System operating modes for the distribution bus fault example.

structure, such as the standard market design (SMD), analyzing a locational marginal price (LMP) implementation.

3.8.1 The Standard Market Design (SMD) Environment

From an institutional point of view, the Federal Energy Regulatory Commission (FERC) has a strong commitment to establish a generalized standard market design (SMD) for the wholesale of electric power in the United States. This process will amount to a postderegulation effort to create a new a framework of standard guidelines, including the formation of regional transmission organizations (RTOs). The SMD proposal has considered both US and worldwide experiences, and the SMD is intended to improve the efficiency of the electricity marketplace.

The model key is found in the locational marginal price (LMP) feature. This concept is relevant to the notion of intelligent power routers, in particular its local nature, which parallels the one for IPR. The LMP can be simply defined as the cost to serve the next MW of load at a specific location using the lowest production cost of all available generation, while observing all transmission limits. It has three major components: generation marginal cost plus transmission congestion costs plus the cost of marginal losses.

The marginal cost to provide energy at a specific location depends on the marginal cost to operate generation, total load (demand), and cost of delivery on the transmission system. We should also mention that this pricing system internalizes the cost of system reconfiguration, plus the transaction curtailments and the re-dispatch of generation, in order to serve the next MW of load.

What is still missing is the load marginal-benefit component of LMP, except for some markets where load bidding is allowed and significant; for these hubs the price reflects rather well the marginal value of electricity from both supply and demand standpoints.

3.8.2 The Ancillary Service (A/S) Context

The A/S is a new essential concept/component of the modern power system. It is a consequence of the unbundling process taking place in the industry. In this context different products and services can be evaluated and priced separately from its original integrated matrix core. FERC defines A/S as those services that are necessary to support the transmission of capacity and energy from resources to loads, while maintaining reliable operation of the provider's transmission system in accordance with good utility practice. From this definition it is clear that the IPR function has a distinct potential to fall into the category of an ancillary service.

3.8.3 Reliability Aspects of Ancillary Services

A first insight into reliability stems from the very definition of A/S as previously stated. But good *utility practice* in the new era is somewhat undefined (in fact the very definition of *utility* has become a debatable matter in the new world) because of the complexity of the new deregulated environment, the fragmentation of the industry, and the difficulty of setting the responsibilities, cost, and benefits of security. Examples of relevant service as it relates to security can be found in [21].

3.8.4 The IPR Technical/Social/Economical Potential for Optimality

It is clear that the future electricity networks of the world will operate within some sort of market structure in a deregulated environment, most likely of the SMD type. Certainly this seems to be the trend both in North America and Europe. Therefore the LMP key feature will prevail for the pricing of electricity; this system will be topologically comprised of either zones or nodes to which such pricing will be referred to. Of course, such LMP will eventually evolve from its current basis to a more comprehensive one capable of synthesizing and impounding all the relevant technical/social/economical information with a quasi–real-time frequency (price minimum update-cycle time).

Furthermore the classical competitive model sets a random phenomenon capable of sustaining a sort of convolution between supply and demand stimuli. This basically amounts to the negotiating mobility between the players in order to improve their bargaining positions. The process becomes an exhaustive optimization, whether it applies to a pool or to a bilateral market framework; the attending outcome, as is well known, tends to clear a price that maximizes the efficiency and social welfare.

There are important parallels between the LMP and IPR fundamentals; this is a most favorable situation. First, regarding the power grid context, both are basically local/zonal in nature, actually by LMP's referencing of this very condition. Second,

within the IPR operating principles there is some active negotiation among IPRs, especially in order to act upon any disturbing event as was discussed here. Through this process, which can reasonably be assumed to be exhaustive, the router intelligence seeks to establish a grid reconfiguration, ideally retaining/upgrading generation by serving preferred loads in a stable postdisturbance environment. This IPR competitive negotiation resembles and compares favorably with that of players in the energy marketplace. It may even be considered an extension of market place competition.

But more important is the potential synergy between the two processes, for the local power router intelligence has also full access to the zonal/nodal LMP. That bit of information can be processed in the IPR algorithm as part of its negotiating position. As stated below, price theoretically overrides all the relevant updated information associated to the best rational use of energy the network is serving, with regard to the global/zonal marginal value of electricity for the period under scrutiny. Consequently these processes are bound to have an outcome of social optimality.

3.8.5 Proposed Definition for the Intelligent Power Router Ancillary Service

Power Routing Ancillary Service The functionality provided by distributed intelligent power routers (IPRs) relates to network security and efficiency. IPRs can perform in an emergency to switch power apparatus and lines, shed loads based on a priority scheme, activate auxiliary or distributed generation, isolate a power region of the energy delivery network to prevent system cascade failures, and receive/broadcast local state variable information to and from other routers.

3.8.6 Summary

Distributed IPRs may prove to be more efficient and secure if we apply to it a realistic market structure such as the standard market design with an LMP algorithm. In this economic model, the IPR routing function could be considered an ancillary service, but more work must be done on the market mechanism and pricing of such a service.

3.9 CONCLUSIONS

We began the design and testing of IPR architecture by developing a model of a computer controllable bus that serves as the energy flow control and sensing device of the IPR. To avoid congestion, since the IPRs are to be organized in a peer-to-peer (P2P) communication network that exchanges state messages continuously, we divided the communications network into zones. Each zone is an autonomous network of IPRs, of balanced generation capacity and demand. Each zone is capable of exchanging messages with other zones, while also being able to contain and repair its own failures. IPRs are for that reason classified as *interior IPRs*, those that exchange messages within a given zone and *border IPRs*, those that exchange messages between different zones. Using a two-stage inter/intra-zone negotiation scheme, we should be able to

restore power to high-priority loads after a contingency using a de-centralized approach with local information available to each IPR only.

Next we estimated the reliability of the IPRs according to the failure probabilities of their primary subsystems; software, communications and switching element, and a variety of possible functional relationships among these subsystems. Since an IPR has not been built yet, we estimated the failure probabilities of its subsystems from our knowledge of existing similar systems, using existing software, data routers, and reliability estimates of circuit breakers. As we expected, the configurations that provide redundancy achieved the highest reliabilities and lowest failure probabilities. To properly capture the reliability increase in a power system using an IPR, we took the risk framework assessment approach.

The zonal, approach we use for civilian power systems derives from a system used on naval ships. We used the US Navy's DCZEDS test bed to evaluate concepts of self-reconfigurable systems for electronic power distribution systems. Future work will focus on failure analysis and the reconfiguration logic of the self-reconfigurable system using a centralized as well as the IPR distributed approach.

To complement and expand our implemented IPR de-centralized restoration scheme, we are developing a controlled islanding mechanism that will permit partial system preservation and rapid system recovery, also using IPRs. The controlled islanding scheme will consider the inherent structural characteristics of the system as well as any imbalance between the generation and load.

We are also exploring the possibility of improving efficiency and security using IPRs by way of a realistic market structure such as the standard market design with an LMP algorithm. Within this economic model the routing function may be regarded as an ancillary service. More work remains to be done on the market mechanism and pricing of such a service.

ACKNOWLEDGMENTS

We acknowledge the support of the National Science Foundation (NSF) thru award number 0224743 as well as the support received from the University of Puerto Rico-Mayagüez. This project used facilities of the Center for Power Electronic Systems a National Science Foundation Engineering Research Center thru award EEC-9731677.

BIBLIOGRAPHY

1. Amin, M. "Modeling and Control of Complex Interactive Networks." *IEEE Control Systems Magazine* 22(1) (February): 22–27, 2002.
2. Cerf, V., and Kahn, R. "A Protocol for Packet Network Intercommunication." *IEEE Trans. Communications*, 22(5): 637–648, 1974.
3. Paxson, V. "End-to-end Routing Behavior in the Internet." *IEEE/ACM Transactions on Networking*, 5(5): 601–615, 1997.

4. Deering, S., Estrin, D., Farinacci, D., Jacobson, V., Liu, C., and Wei, L. "The PIM Architecture for Wide-Area Multicast Routing." *IEEE/ACM Transactions on Networking*, 4(2): 153–162, 1996.
5. Butler, K. L., Sarma, N. D. R., and Ragendra Prasad, V. "Network Reconfiguration for Service Restoration in Shipboard Power Distribution Systems." *IEEE Trans. Power Systems*, 16(4): 653–661, 2001.
6. Hsiao, Y. T., and Chien, C. Y. "Multiobjective Optimal Feeder Reconfiguration." *IEE Proc. Generation, Transmission, Distribution*, 148(4): 333–336, 2001.
7. Choi, J., and Kim, J. "Network Reconfiguration and the Power Distribution System with Dispersed Generations for Loss Reduction." *IEEE Power Engineering Society Winter Meeting*, 4: 2363–2367, 2000.
8. Curcic, S., Ozveren, V., Crowe, L., and Lo, P. K. L. "Electric Power Distribution Network Restoration: A Survey of Papers and a Review of the Restoration Problem." *Electric Power Systems Research*, 35(2): 73–86, 1995.
9. Camponogara, E., Jia, D., Krogh, B. H., and Talukdar, S. "Distributed Model Predictive Control." *IEEE Control Systems*, 22(1): 44–52, 2002.
10. Gribble, S., Halevy, A., Ives, Z., Rodríguez, M., and Suciu, D. "What Can Databases do for Peer-to-Peer?" *WebDB*, Santa Barbara, CA, 2001.
11. Stoica, I., Morris, R., Karger, D., Frans Kaashoek, M., and Balakrishnan, H. "Chord: A Scalable Peer-to-Peer Lookup Service for Internet Applications." *IEEE/ACM Transactions on Networking*, 11(1): 17–32, 2003.
12. Yang, B., and Garcia-Molina, H. "Comparing Hybrid Peer-to-Peer Systems." *Proc. 2001 VLDB Conf*., 2001, pp. 561–570.
13. Rodriguez-Martinez, M., and Roussopoulos, N. "MOCHA: A Self-extensible Database Middleware System for Distributed Data Sources." *Proc. ACM SIGMOD Conf*., Dallas, TX, 2000, pp. 213–224.
14. Taylor, C. W. "The Future in On-line Security Assessment and Wide-Area Stability Control." *IEEE Power Engineering Society Winter Meeting*, 1: 78–83, 2000.
15. Taylor, C. W. "Improving Grid Behavior." *IEEE Spectrum*, 36(6): 40–45, 1999.
16. Brice, V., Gökdere, L. U., and Dougal, R. A. "The Virtual Test Bed: An Environment for Virtual Prototyping." *Proc. Int. Conf. Electric Ship*, Istanbul, 1998, pp. 27–31.
17. Karady, G., Heydt, G., Michel, M., Crossley, P., Rudnick, H., and Iwamoto, S. "Review of Electric Power Engineering Education Worldwide." *Power Engineering Society Summer Meeting*, 2: 906–915, 1999.
18. Chowdhury, B. "Power Education at the Crossroads." *IEEE Spectrum*, 37(10): 64–69, 2000.
19. Padhke, V. "While We Are Sleeping: A Crisis in Power Engineering Education." *IEEE Computer Applications in Power*, 12(3): 10–15, 1999.
20. Jiménez, J. J., and Cedeño, J. R. "Application of Particle Swarm Optimization for Electric Power System Restoration." *Proc. IASTED Int. Conf. PowerCon*, New York, 2003.
21. Ramirez, A., Chen, M., and Shoults, R. "Ancillary Service Issues under Utility Deregulation." *Proc. 34th Annual TSDOS Transmission and Substation Design and Operation Symp*. (TSDOS). Texas Utility Industry, Arlington, November, 2001.
22. Nagata, T., and Sasaki, H. A. "Multi-agent Approach to Power System Restoration." *IEEE Trans. Power Systems*, 17(2): 457–462, 2002.

23. Vergara, I. J., and Rodriguez-Martinez, M. "IPR: A Decentralized Framework for Controlling Electrical Energy Distribution Networks with Intelligent Power Routers." *Proc. 2003 IASTED PowerCon Int. Conf*., New York City, December, 2002. pp. 104–112.
24. Torres-Ortolaza, C. M., and Irizarry-Rivera, A. A. "Failure Modes and Failure Probability of Intelligent Power Routers." *Proc. 8th Probabilistic Methods Applied to Power Systems (PMAPS) Int. Conf*., Ames, IA, September 13–16, 2004.
25. Anderson, P. M. "Relibility Modeling of Protective Systems." *IEEE Trans. Power Apparatus and Systems*, 103(8): 2207–2214, 1984.
26. Ebeling, C. E. *An Introduction to Reliability and Maintainability Engineering*. McGraw-Hill, New York, 1997.
27. Heising, C. R., Janssen, A. L. J., Lanz, W., Colombo, E., and Dialynas, E. N. "Summary of CIGRE 13.06 Working Group World Wide Reliability Data and Maintenance Cost Data on High Voltage Circuit Breakers above 63kV." *Industry Applications Society Annual Meeting*, 3: 2226–2234, 1994.
28. Scheer, G. W., and Dolezilek, D. J. *Comparing the Reliability of Ethernet Network Topologies in Substation Control and Monitoring Networks*. Schweitzer Engineering Laboratories, Inc. Pullman, WA. (no date).
29. Zhu, Z., Zhao, S., McCalley, J. D., Vittal, V., and Irizarry-Rivera, A. A. "Risk-based Security Assessment Influenced by Generator Rejection." *Proc. 5th Probabilistic Methods Applied to Power Systems (PMAPS) Int. Conf*., Vancouver, 479–484, 1997.
30. Simon, G., Karsai, G., Biswas, G., Abdelwahed, S., Mahadavan, N., Szemethy, T., Péceli, G., and Kovácshazy, T. "Model-Based Fault-Adaptive Control of Complex Dynamic Systems." *Proc. 20th IEEE Instrumentation and Measurement Technology Conf*., Vail, CO, 1: 176–181 May 20–22, 2003.
31. Ji, M., Zhang, Z., Biswas, G., and Sarkar, N. "Hybrid Fault Adaptive Control of a Wheeled Mobile Robot." *IEEE/ASME Trans. Mechatronics*, 8(2): 226–233, 2003.
32. Prabhu, V. V. "Stable Fault Adaptation in Distributed Control of Heterarchical Manufacturing Job Shops." *IEEE Trans. Robotics and Automation*, 19(1): 142–149, 2003.
33. Rehtanz, C. *Autonomous Systems and Intelligent Agents in Power System Control and Operation*. Springer-Verlag, Berlin, 2003.
34. Wilderberger, A. M. "Complex Adaptive Systems: Concepts and Power Systems Applications." *IEEE Control Systems*, 17(6): 77–88, 1997.
35. ONR Control Challenge Problem. http://www.usna.edu/EPNES.
36. Smith, S. M., An, P. E., Holappa, K., Whitney, J., Burns, A., Nelson, K., Heatzig, E., Kempfe, O., Kronen, D., Pantelakis, T., Henderson, E., Font, G., Dunn, R., and Dunn, S. E. "The Morpheus Ultramodular Autonomous Underwater Vehicle." *IEEE Journal of Oceanic Engineering*, 26(4): 453–465, 2001.
37. Ciezki, J. G., and Ashton, R. W. "Selection and Stability Issues Associated with a Navy Shipboard DC Zonal Electric Distribution System." *IEEE Trans. Power Delivery*, 15(2): 665–669, 2000.
38. Sudhoff, S. D., Pekarek, S., Kuhn, B., Glover, S., Sauer, J., and Delisle, D. "Naval Combat Survivability Testbeds for Investigation of Issues in Shipboard Power Electronics Based Power and Propulsion Systems." *Proc. 2002 Power Engineering Society Summer Meeting*, 1: 347–350, 2002.
39. Solodovnik, E., Gao, W., and Dougal, R. "Zonal Ship Power Systems." *Proc. of ASNE* 2002.

4

POWER CIRCUIT BREAKER USING MICROMECHANICAL SWITCHES

George G. Karady, Gerald T. Heydt, Esma Gel, Norma Hubele

Arizona State University

4.1 INTRODUCTION

Electric power distribution is an essential part of the infrastructure for delivering electric power from a generation and transmission system to a point of utilization. An important power system component is the circuit breaker, essentially a switch, used to automatically isolate and separate parts of the system under fault and permit switching on and off the loads if operation requires. The main function of a circuit breaker is to protect components from catastrophic failure. The distribution class circuit breaker (i.e., at voltages substantially less than about 35 kV) has not materially changed in design for several years. Typically the breaker contains stationary and moving contacts, which are surrounded by oil, SF6, or vacuum. The separation of the contact produces an electric arc that is extinguished by the oil, vacuum, or compressed SF6. In air-magnetic breakers, the magnetic field extends the arc till extinction. The basic idea is to use magnetism to "pull the arc" to a longer length thereby making extinction easier.

In this project a radical departure from mechanical circuit breakers is proposed: the large mechanical switch is replaced by an array of small micro-electro-mechanical (MEMS) switches. The MEMS switches operate at very high speed to effectuate rapid

Operation and Control of Electric Energy Processing Systems, Edited by James Momoh and Lamine Mili

system operating configuration changes. The use of MEMS switches will allow the application of advanced optimal operating strategies to permit rapid disconnection of faulted components, rerouting of power from faulted segments to unfaulted segments, utilization of DC distribution in naval applications, and minimization of system losses. Some motivational factors include:

- better characterization of distribution system performance (including power quality),
- identification of the proper trade-off between investment and service,
- optimization of the investment in distribution equipment,
- improved power quality,
- improved reliability, and
- improved hardness to power quality problems, less vulnerability.

MEMS devices have inherently low voltage and current ratings, and a key part of the project is to assemble these devices in series and parallel to build up the required distribution class ratings. A medium voltage circuit breaker requires several hundred devices connected in series and parallel. The nonsimultaneous opening of the switches can generate overvoltages or overloads. An additional problem is that the MEMS device is designed for cold switching. The term *cold switching* refers to switching when the current passing through the switch is essentially zero. The MEMS device cannot interrupt current because even a small arc destroys it. This problem is mitigated by connecting diodes in parallel with the MEMS switches. The opening of the MEMS switch transfers the current to the diodes. At zero crossing the diodes interrupt the current. These results in a small, fast operating combined micromechanical and electronic device, which modernizes the dormant circuit breaker technology.

The project objective includes an educational component: to bring innovative topics in power distribution engineering to practicing engineers (e.g., continuing education) as well as beginning engineering students. Another premise of the educational component is the value of cross-fertilization in engineering education. The objective is to utilize cross-disciplinary topics for motivation as well as education—at the undergraduate, graduate, and continuing education levels. The intent is to expose industrial engineers to electrical engineering topics, engineering students of all disciplines to MEMS technologies, and electrical engineers to optimization and uncertainty. The material presented here will be used for short courses and will be integrated in graduate courses.

4.2 OVERVIEW OF TECHNOLOGY

4.2.1 Medium Voltage Circuit Breaker

The construction of circuit breakers used by electric power distribution has not changed in the last few decades [1,2]. Figure 4.1 shows a typical 15 kV medium voltage level circuit breaker used in an indoor metal enclosed switchgear. This device is intended

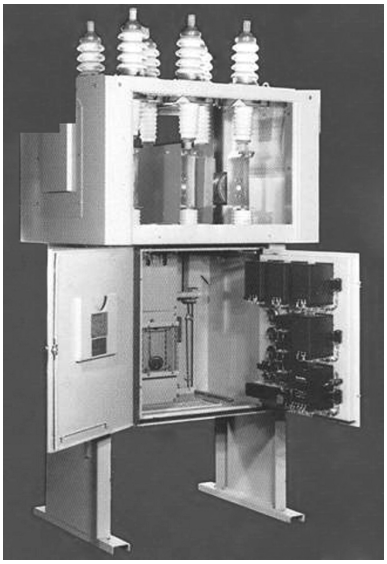

Figure 4.1 Medium voltage (15 kV class) circuit breaker (courtesy of General Electric).

for three-phase use, AC, at 60 Hz, and the 15 kV rating refers to the root mean square value of the line–line voltage. The upper part of the cabinet houses the three interrupting elements. At the top of the breaker are the six porcelain bushings for the incoming and outgoing conductors. The lower part of the cabinet is the control circuit, including relays.

Figure 4.2 shows a vacuum bottle interrupter that interrupts the short circuit current. A three-phase circuit breaker has three interrupters, one for each phase. The vacuum bottle interrupter has two electric terminals: a moving and a stationary terminal. At the end of the terminals are electric contacts.

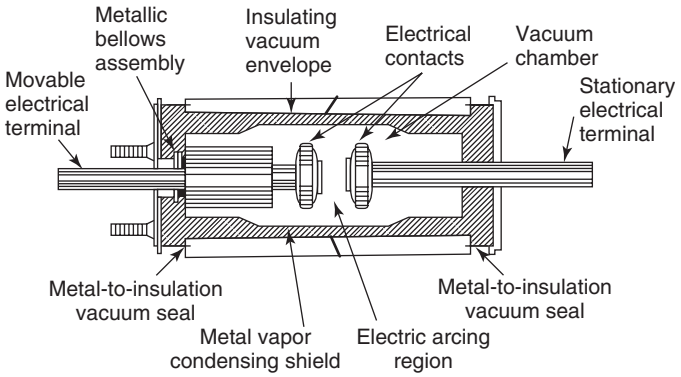

Figure 4.2 Vacuum-bottle circuit breaker (courtesy of General Electric).

The terminals and contacts are placed in a vacuum chamber. The exit of the moving terminal is sealed by a metallic bellow. In closed position the contacts are pressed together by strong springs, to ensure low contact resistance and small conduction losses.

Discussion now turns to short circuits (faults) in distribution systems. Traditionally these are analyzed as phase to ground of phase to phase, or three phase (i.e., three phases connected together). Obviously these are undesired events. A short circuit increases the current suddenly. The high current activates the protection circuit, which triggers the circuit breaker operating mechanism. The movable terminal is released, and a strong spring pulls the movable terminal backward to open the contacts. The contact opening produces arcing between the terminals. In the first few cycles, when the distance between the contacts is small, the arc extinguishes at each zero crossing and reignites when the supply voltage appears between the contacts. However, as the distance increases, the high dielectric strength of the vacuum prevents the re-ignitions and the circuit breaker interrupts the short circuit current and separates the supply from the faulty part of the circuit.

The vacuum bottle interrupter is the most frequently used circuit breaker at medium voltage level, but oil and magnetic circuit breakers are also used. At high power levels, exotic technologies are used and SF6 (an insulating gas) may be used.

This project presents a novel concept for circuit interruption. The distribution class breaker is replaced by an array of micro-electro-mechanical (MEMS) switches and diodes. This leads to faster operation and smaller size. The proposed new type of circuit breaker merges the conventional technology with the latest microelectronic techniques. This will lead to significant improvement of distribution system reliability. The other advantages include better control of the circuit breaker, potentially lower losses, potentially better reliability, ohmic connection when the breaker is closed, and insensitivity to the bandwidth of the disturbance (e.g., the rise time of the disturbance). However, there are many unknowns such as the sensitivity of such a device to mechanical vibration.

4.2.2 Micro-Electro-Mechanical Switches (MEMS)

Recently several companies have attempted the development of an electronic circuit breaker, using thyristors. These units interrupt the current within a half cycle, but their steady state conduction losses are very high because the voltage drop on a typical semiconductor is more than one volt and the breaker requires several devices connected in series. Micro-electro-mechanical switches have low conduction losses. Typically the voltage drop on a conducting MEMS switch is less than a hundred mV. The problem with these switches is that they are not designed to interrupt current. The combination of an electronic device (diode) with a MEMS switch ensures low conduction losses and fast current interruption. The low voltage and current ratings of the MEMS devices requires the series and parallel connection of a large number of devices to achieve the required distribution class ratings [4].

MEMS switch technology is in a fast development stage. The current and voltage rating of the devices are increasing rapidly. For a circuit breaker the most advantageous

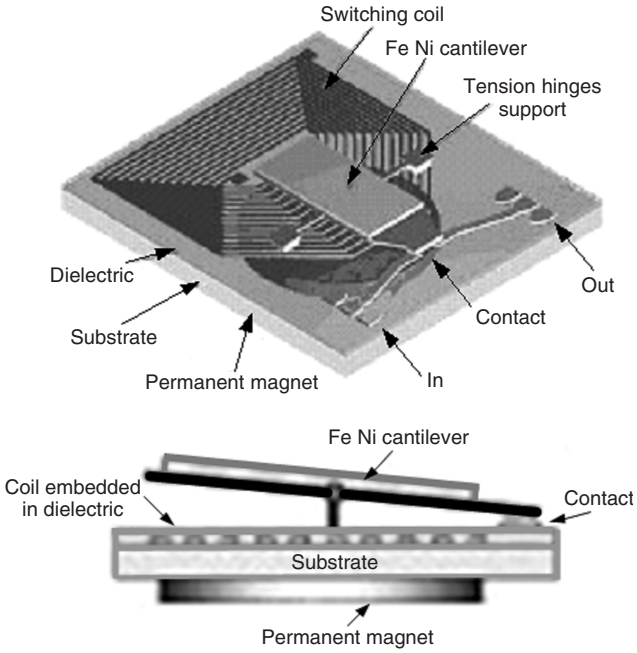

Figure 4.3 Construction of the MEMS micro-switch [7].

switch is a latching type device. A positive impulse closes and a negative impulse opens the switch. But the switch remains in open or closed position without any signal. No current or voltage is needed to maintain switch position. This minimizes the control current requirement because of the infrequent circuit breaker operation.

Figure 4.3 shows the components of a MEMS switch. The switch is built on a silicon substrate. The moving part of the switch is a Fe Ni cantilever placed on a beam etched out from the silicon substrate. A gold contact and a two tension hinges are mounted on the moving part.

With reference to Figure 4.3, the operating coil is at the top of the substrate. This coil is embedded in dielectric that insulates the coil from the switch. On the front of the substrate two contacts are placed. Supplying the coil with a current generates electromagnetic force, which moves the hinge downward and closes the contacts at the front.

The cross-sectional view of the switch shows a permanent magnet placed on the bottom of the switch. This magnet ensures that the switch is latched in either open or closed position. A current pulse driven through the operation coil flips the switch, and the force between the permanent magnet and the Fe Ni cantilever keeps the switch in this position. A current pulse with opposite polarity flips the switch back. The micro switch is packaged in an enclosure and requires surface mounting. Figure 4.4 shows the photograph of the packaged microswitch showing the terminals. The chip is about 10 times enlarged in the photo.

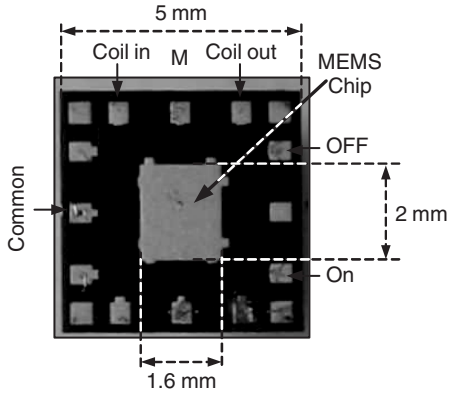

Figure 4.4 Packaged MEMS switch chip.

Specification of the selected MEMS device is as follows:

- Maximum voltage between the contacts: 60 V
- Insulation voltage between the contacts and the operating coil: 400 V
- Closed contact resistance: 0.5 Ω
- Open contact resistance: >1000 MΩ
- Steady state conduction current: 100 mA
- Short duration current pulse: 1A
- Closing time: >100 ns
- Opening time: >100 ns
- Operating coil current: 100 mA
- Operating coil voltage: 5 V
- Operating coil current duration: 100 μs
- Operating coil resistance: 50 ohm
- The dimensions of the packaged switch: 5 × 5 mm.

The fast development of MEMS technology increases the voltage and current ratings; latest information obtained from manufacturer gives voltage ratings of 100 to 200 V and current rating around 1 A. The higher rating reduces the required number of switches connected in series and parallel. Figure 4.5 shows an electrical connection diagram of the selected microswitch.

4.3 THE CONCEPT OF A MEMS-BASED CIRCUIT BREAKER

4.3.1 Circuit Description

The basic building block of the circuit breaker is a MEMS switch shunted by a diode and a large (1 Mohm) resistance. Several units connected in series form a switching

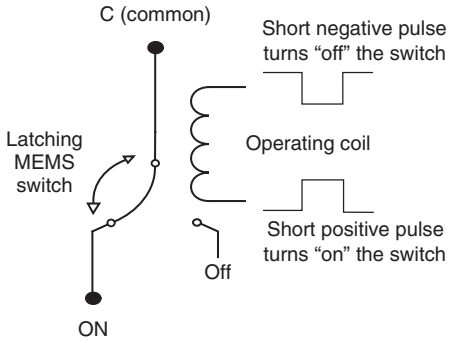

Figure 4.5 MEMS switch electrical circuit diagram.

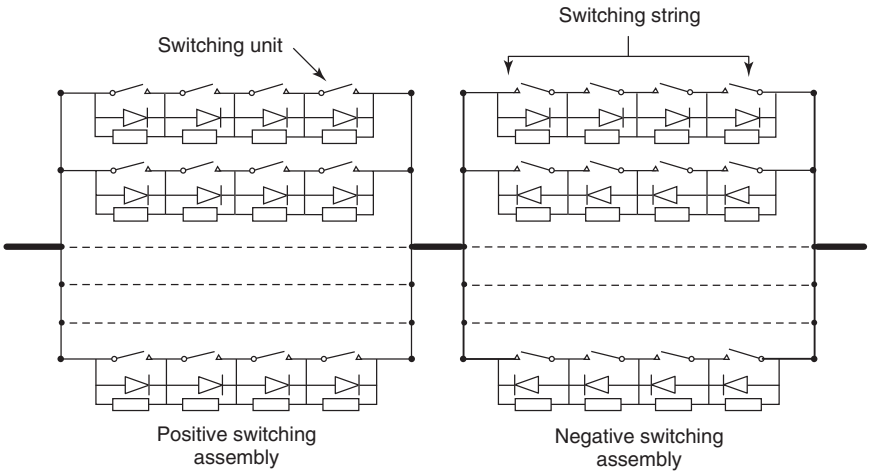

Figure 4.6 MEMS-based electronic circuit breaker.

string, and several switching strings are connected in parallel to form the switching assembly. The diodes determine the conduction direction in a switching assembly, when the MEMS switches are open.

Two switching assemblies are connected in series to form the circuit breaker. The conduction directions in the series-connected switching assemblies are opposite. Figure 4.6 shows the conceptual connection diagram of the proposed MEMS-based electronic circuit breaker. The positive switch assembly operates in the positive and the negative switch assembly in the negative cycle.

4.3.2 Operational Principle

The MEMS switches are operated by magnetic coils. These coils activate all switches practically simultaneously in a switching assembly. The typical operation time of a

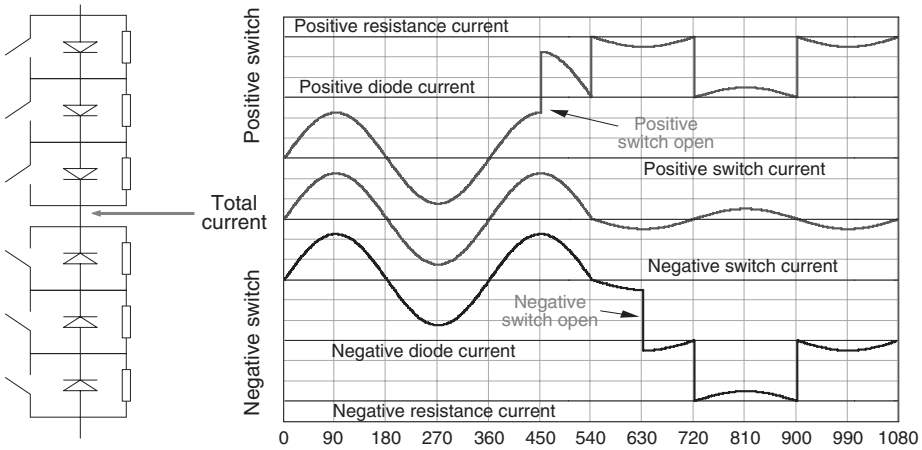

Figure 4.7 Illustration of current interruption.

MEMS switch is between 10 and 300 μs. This suggests that maximum operation time difference is around 1 to 10 μs, which is negligible in a 60 Hz system. The opening of the MEMS switches transfers the current from the MEMS switch to the diodes. The closing of the MEMS switch transfers the current from the diode to the MEMS switch. The resistances ensure uniform voltage distribution in a switching string when the MEMS switches are open. The resistances act as snubber circuits.

4.3.3 Current Interruption

The most important function of the circuit breaker is the short circuit current interruption. Figure 4.7 shows a section of the circuit breaker, a switching assembly. All MEMS switches are closed, and the current flows through the MEMS switches because the voltage drop on the diodes is around 0.8 V and the voltage drop on the MEMS switches only few hundred millivolts.

In the event of a short circuit, the current polarity is identified and the MEMS switches are opened in the appropriate switching assembly. If the short circuit occurred in the positive cycle, the positive switches open. This transfers the current to the diodes. At current zero the diodes interrupt the current.

In the follow-up negative cycle, the switches open in the negative switching assembly. The opening of the negative switches completes the switching operation. However, this occurs after current interruption. Figure 4.7 illustrates the described current interruption process and shows that this switch interrupts the current within a half cycle. The figure shows that after the current interruption a small, few milliamp leakages current flows due to the 1 Mohm snubber resistance. These calls for the use of a (mechanical) disconnect switch.

4.3.4 Switch Closing

The switch described above must be closed manually or automatically for energization or reconfiguration of a circuit. When the MEMS switches are open, the diodes block

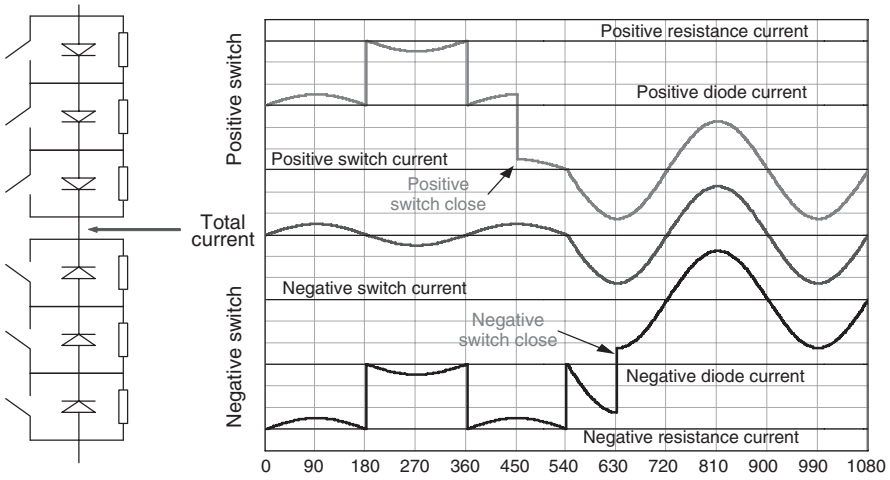

Figure 4.8 Illustration of switch closing.

the current. The snubber resistances ensure the uniform voltage distribution among the switches. In open position, in the positive cycle, a small current flows through the diodes in the positive assembly and the snubber resistances in the negative assembly. In the negative cycle the current flow is the opposite. The closing of the switch is illustrated in Figure 4.8.

The closing of the switches in the positive cycle transfers the small leakage current to the microswitches but does not turns on the circuit breaker. After zero crossing in the negative cycle, large load current flows through the diodes of the negative switch and through the closed microswitches of the positive switch assembly. This turns on the circuit breaker. During the follow-up negative cycle the MEMS switches are closed in the negative switch assembly, which completes the closing of the circuit breaker. Figure 4.8 shows that the diodes turn the breaker on within a half cycle.

4.4 INVESTIGATION OF SWITCHING ARRAY OPERATION

A medium voltage circuit breaker requires several hundred devices connected in series and parallel. The nonsimultaneous opening of the switches can generate overvoltages or overloads. The series and parallel connected switch assemblies form a switching array. The operation of these types of switching arrays is not documented in the literature. The switching-generated transients in an array can endanger the MEMS switches. For the investigation of the transients a model circuit was developed and analyzed using PSPICE

Figure 4.9 shows the connection diagram of a generalized positive switching array consisting of a 10×10 switching matrix. The circuit consists of 10 switching units connected in series. Each switching unit consists of 10 MEMS switches connected in parallel and shunted by a diode and a 1 Mohm snubber resistance. The MEMS switches are controlled by a current pulse injected through terminal P1. The input terminal is A1; the output terminal is K1.

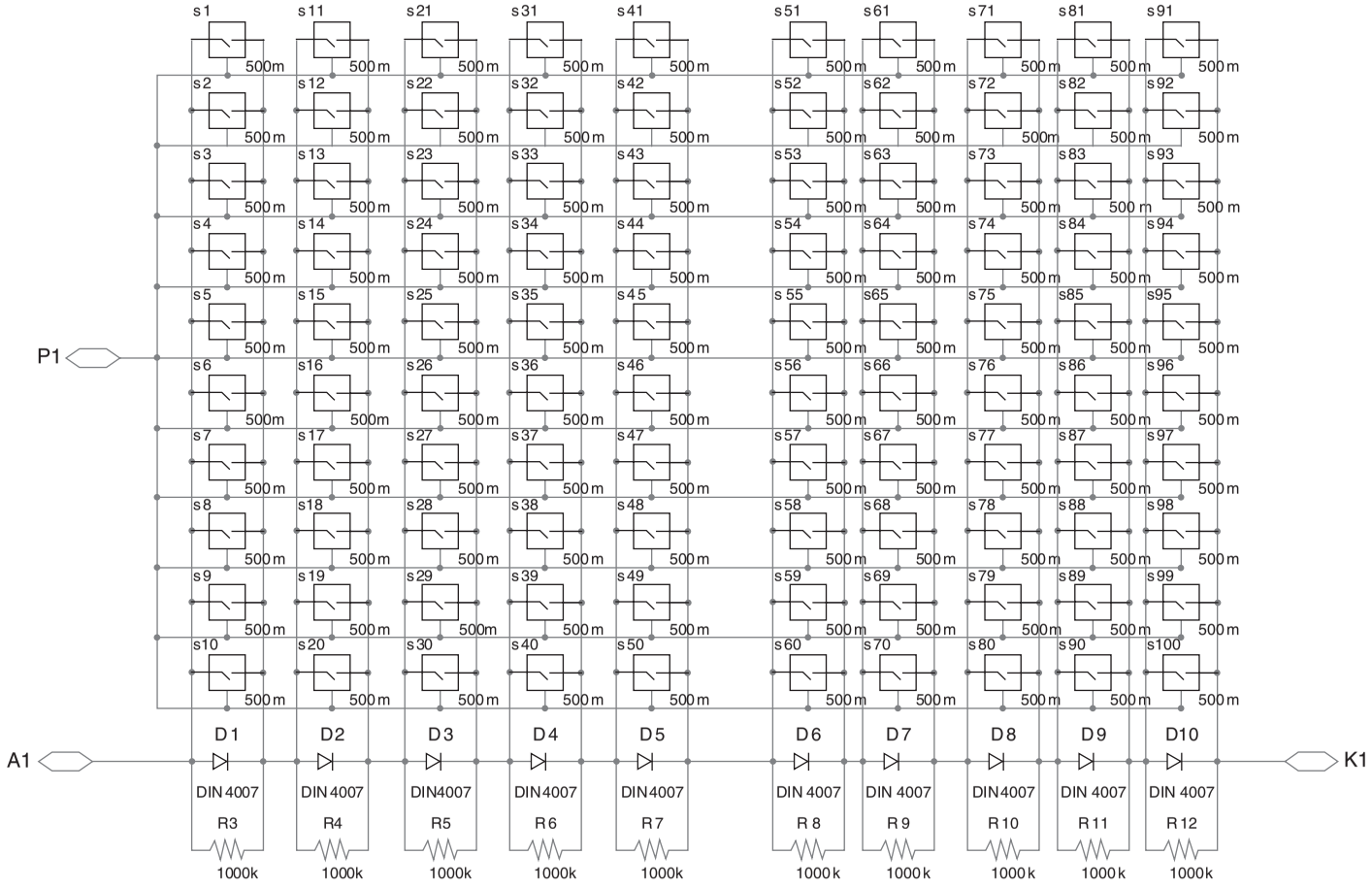

Figure 4.9 Circuit diagram of a switching array.

The circuit breaker requires a positive and a negative array connected in series. The negative array is similar to the positive array shown in Figure 4.9. The difference is that the diodes are in reverse direction. The negative array is connected to terminal K1.

4.4.1 Model Development

For the investigation of the array operation several switching matrices were connected in series and parallel, and the operation of the array was modeled using PSPICE. The model is built with a positive and negative switch consisting of 4500 switches each, arranged in a matrix of 150 × 30 as shown in Figure 4.10. In this figure, 15 switching matrices are connected in series to form a switching string. Three such switching strings are connected in parallel.

For a case study, a 7.2 kV distribution system was considered. Due to the simulation limitations only a 3 A full load current was considered. For simulation purposes the following system parameters were used:

System AC voltage	7200 V
Supply resistance	1 ohm
Supply inductance	10 mH
Load resistance	1.9 k ohms
Load inductance	3.81 H
Load power (lagging) factor	0.8

Several different operating conditions were simulated, and all the results are published in [3]. Because of space limitation, only a few selected "worst-case scenarios" will be presented here to demonstrate the feasibility of the system. First the normal operation, load energization, and current interruption were investigated to prove the feasibility of the system's operation.

During load energization or closing of the switch, the typical failure mode is that switches in the array fail to close or close with delay. During current interruption or opening of the switch, the failure mode is that switches fail to open or there is a delayed opening of few switches. These cases were modeled on the assumption that one switching matrix in the model shown in Figure 4.10 fails to open or fails to close, or the operation is delayed.

4.4.2 Analysis of Current Interruption and Load Energization

The inherent 0.8 V drop on the diodes can affect the current transfer from the diode to the switch, and vice versa. Figure 4.11 shows the results of the simulation, when the circuit breaker interrupted the current and re-closed with few cycles.

A "turn-off" signal is given to positive switches (PC) during a positive current cycle, and hence the current from the positive switches transfers to forward-biased diodes at time t_1. Since the negative switches (NC) are still closed, the load current continues to flow through forward-biased diodes and negative switches.

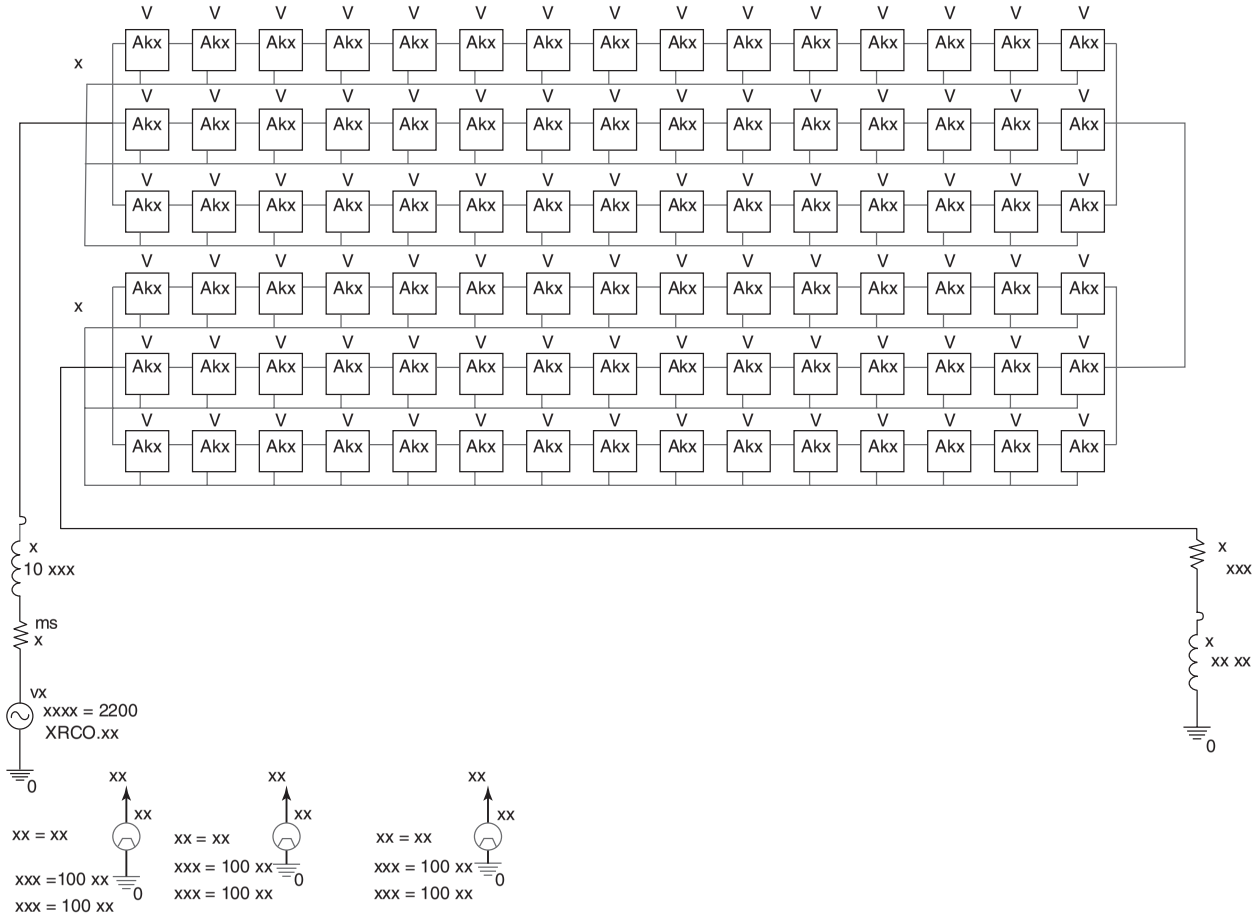

Figure 4.10 PSPICE model of the switching matrix.

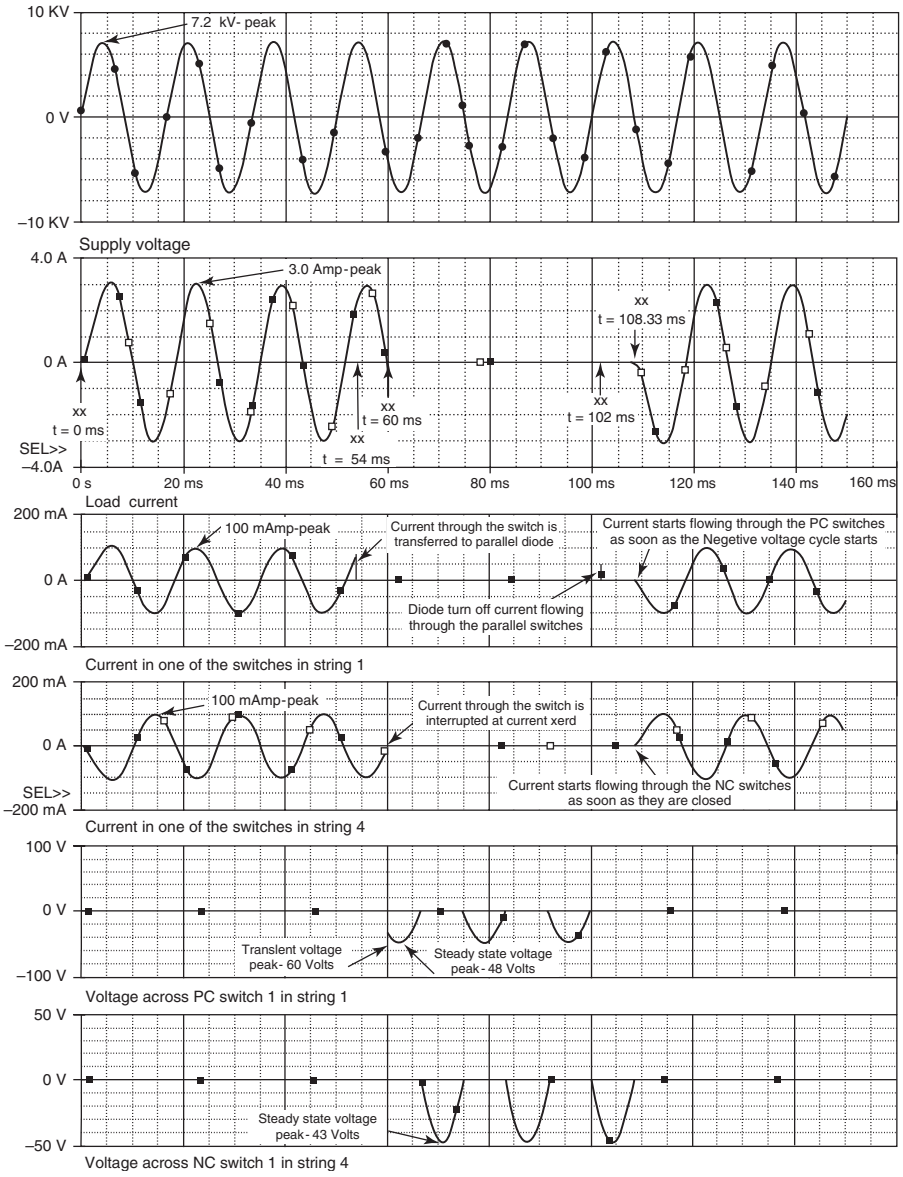

Figure 4.11 Demonstration of MEMS switch operation.

At time t_2 ($t = 60$ ms), the diode interrupts the load current at current zero and then soon after time t_2 the "turn-off" signal is given to the negative switches. During this sequence of operation all the switches in parallel strings operate synchronously, and the current through each parallel strings is 100 mA. Figure 4.11 shows the interval when the switches are open between time t_2 and t_3. Note that the switches connected

in series share the system voltage equally (48 V each). It is also evident that the diodes do not stop conducting at exact current zero. The diode turns off before a zero current, which produces current chopping. The interruption of small inductive current (i.e., current that lags voltage) generates short duration overvoltage across the switches. The approximate peak value of the overvoltage is 60 V, which is less than 1.5 times the steady state peak voltage. This overvoltage can be regulated by a parallel snubber circuit. A typical parallel snubber could be a as simple as a single capacitor.

At time t_3, the "turn-on" signal is given to the positive switches to re-close the breaker. Since the negative switches are open, the current does not start conducting. At time t_4, the negative voltage cycle starts, and the current starts to flow through the forward-biased diodes and the closed positive switches. A "turn-on" signal is given to the negative switches soon after time t_4 to complete the re-closing. It is evident from Figure 4.11 that the closing of the positive switches produces small approximately 50 mA transient current through the switches. No transient current was observed in the line current.

This and similar simulations proved that the switching array operates properly regardless of the small overvoltages generated by the diodes. These overvoltages will be controlled by a snubber circuit or by increasing the number of switching units connected in series. The simulation results are used for the design of the circuit breaker with large switching arrays.

4.4.3 Effect of Delayed Opening of Switches

The proper operation of the circuit breaker requires the simultaneous operation of all switches. The effect of a delayed opening of a set of switches was investigated. In the circuit breaker model three strings are connected in parallel and 15 switching matrices are connected in series. The delayed operation was simulated by delaying the opening of the MEMS switches in a switching matrix in string 2. In the switching matrix 10 MEMS switches are connected in series and 10 in parallel. Figure 4.12 shows the effect of delayed switch opening. The delay is 7 ms, an entirely pessimistic assumption.

Figure 4.12 shows that the opening of MEMS switches in strings 1 and 3 transfers the current to the diodes, but in string 2, where the delayed opening occurs, the current increases from 100 mA peak value to 150 mA peak value, which represents an overcurrent of 50%. When finally the switches open, the current transfers to the diode and the diodes interrupt the current at zero crossing. The investigation revealed that the overcurrent occurred because the voltage drop on the closed switches was less than on the diodes. The figure shows that the voltage across the switches that open first is just the forward voltage drop of a diode, which is in the range of 0.6 to 1.2 V.

The delayed opening of switches causes a short duration overload of the delayed switches. The overload depends on the number of switches that failed to open. This must be considered at the design of the circuit breaker by increasing the number of switches connected in parallel. That is, the redundancy in the series string length is determined, in part, in the delay-to-open consideration.

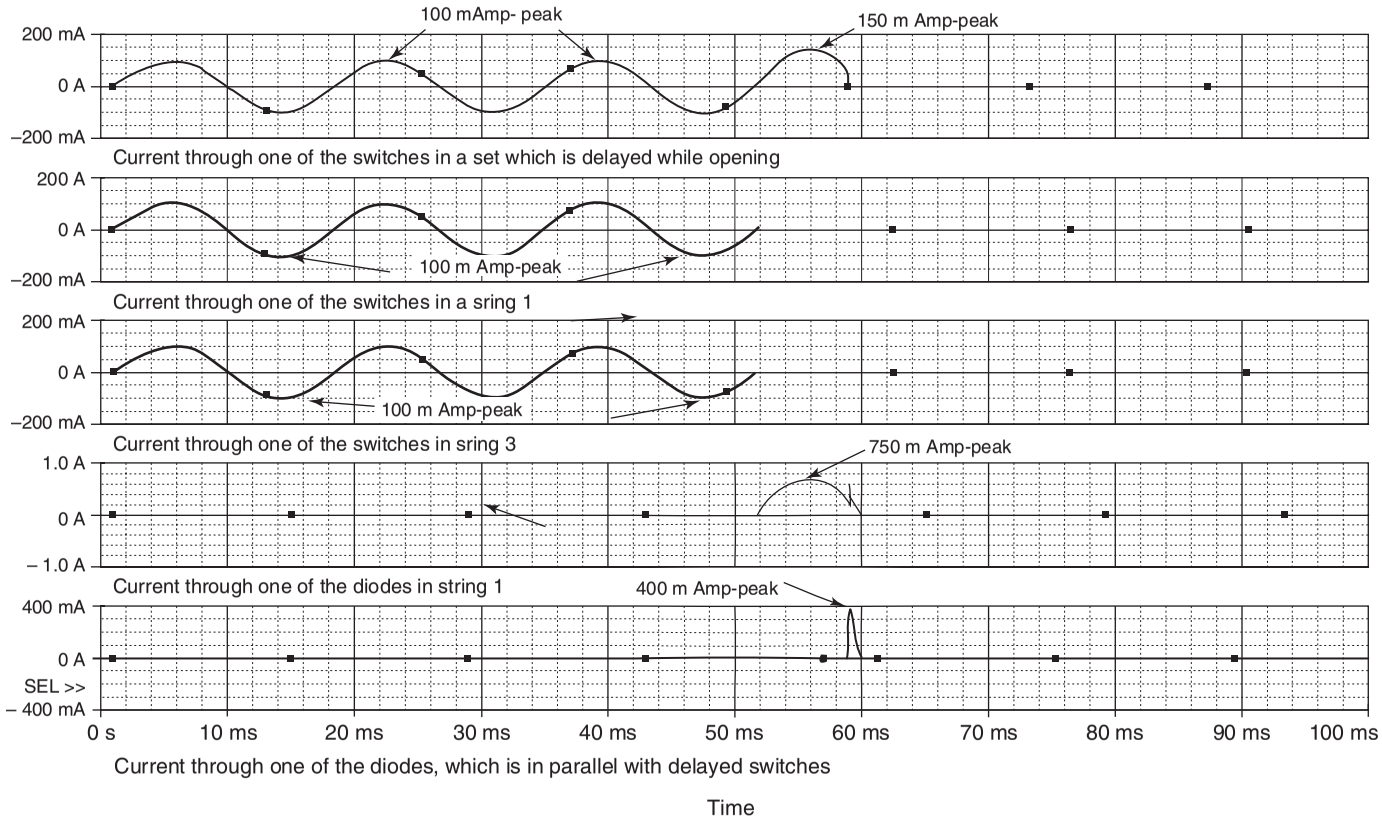

Figure 4.12 Effect of delayed opening of a block of switch.

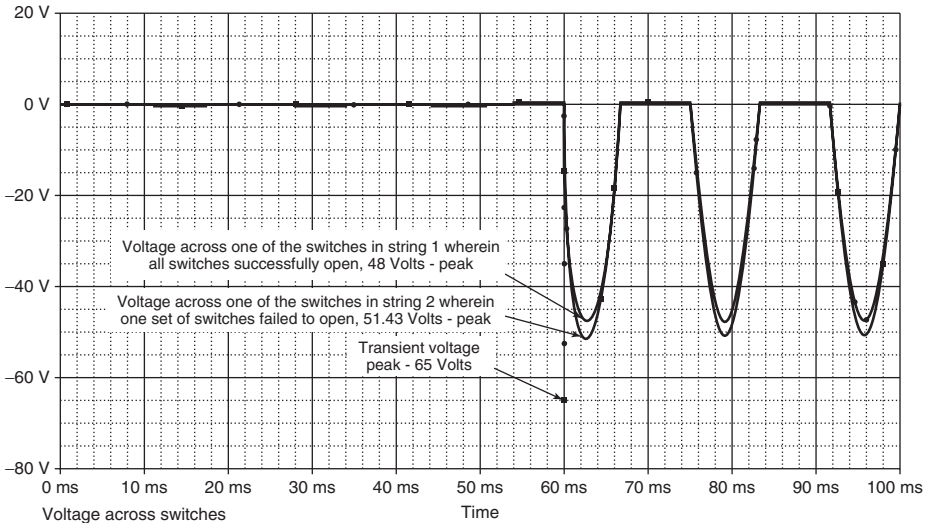

Figure 4.13 Effect of a block of switches fails to open.

4.4.4 A Block of Switch Fails to Open

All the switches in string 1 and string 3 open successfully while one set of switches (10 by 10 MEMS switch matrix) in string 2 fails to open during the opening operation. Figure 4.13 shows the voltage across the individual MEMS switches in the string where all switches opened and in string 2 where one block of switches failed to open. Figure 4.13 shows the comparison of the two curves. The results are as follows:

- Increase of steady state peak voltage from 48 to 51.4 V in string 2 across switches that are opened. This corresponds to a small increase of 11%.
- Increase of short duration transient overvoltage from 60 to 65 V, which corresponds to an 8% increase.

We also investigated the change of current distribution due to the failure of the opening of switches in string 2. It was observed that the switches failed to open in string 2, causing more current in the other parallel strings. The overcurrent is less than 50%. This difficulty is the *dual* of the overvoltage consideration discussed earlier. Despite the failure of a block of switches, diodes interrupt the current at zero crossing. Since all the switches except one set of switches opened successfully, the results show that the load current was successfully interrupted, as is the case during normal conditions.

The effect of switch opening failure results in overvoltages and short durations of overcurrent. These results are used to design the circuit breaker. We calculated the number of switches that can fail before the overvoltage causes a catastrophic cascading failure. The generation of overvoltage can be explained by the fact that the failure to

open switches reduces the number of switches in the string, which in turn increases the voltage across the remaining switches.

4.4.5 Effect of Delayed Closing of Switches

In the case where the switches in string 2 closed first during the positive cycle, there followed the closing of all remaining switches simultaneously with a delay of 7 ms. This delay causes the closing of both the positive and the negative switches during the negative cycle. Figure 4.14*a* shows the currents in selected switches in strings 1, 2, and 3, Figure 4.14*b* shows the transient current produced by the early closing of the switches in string 2.

Closing the switches in string 2 produces a large short duration transient current pulse in both the switches that closed and the diodes connected in parallel with theses switches. Figure 4.14*b* shows a peak current of 1 A, (10 times the rated current) through the switches and 3 A through the diodes. This large current could endanger the switches or diodes. The current surge is caused by the sudden reduction of system impedance when the switches in string 1 are closed. Before closing the switches in the positive cycle the sum of the forward-biased diodes voltage restricted the current. The closing of switches in string 2 shorted the diodes and replaced the diode voltage by the low contact resistance of the MEMS switches. This suddenly changes the total system impedance that generates the transient current.

After the attenuation of the transients the reverse-biased diodes in the negative switch block the current until the zero crossing. The reversal of the current direction initiates all current flow through the diodes in the negative switch and the closed MEMS switches in string 2. Figure 4.14*a* shows that the switches in string 2 carry a current of 300 mA, which is three times the rated current.

When the rest of the switches are closed, the current distribution improves and each string will carry the same current of 100 mA. The simulation results show that switching generated a large short duration transient current. The MEMS switches can carry about 10 times its rated current for a short period of time; this mitigates the overload caused by the transient current.

4.4.6 One Set of Switches Fails to Close

In this case the circuit breaker closing is initiated in the positive cycle. All the switches in strings 1 and 3 closed, but due to a failure one set of switches (a matrix of 10×10 MEMS switches) in string 2 fail to close.

Figure 4.15 shows that the closing of the switches produces a very short duration transient current surge but no immediate current flow. The transient current is due to the sudden change of system impedance when the switches are closed.

The closing of the switches does not initiate current flow immediately because the diodes in the negative switch block the current. However, after the zero crossing, in the negative cycle the current starts to flow in strings 1 and 3, but no current flows in string 2 because the diodes in a positive switch block the current. During the negative cycle all switches are closed in the negative branch of the switch. Figure 4.15 shows that the current in strings 1 and 2 is 150 mA, which represents a 50% overload.

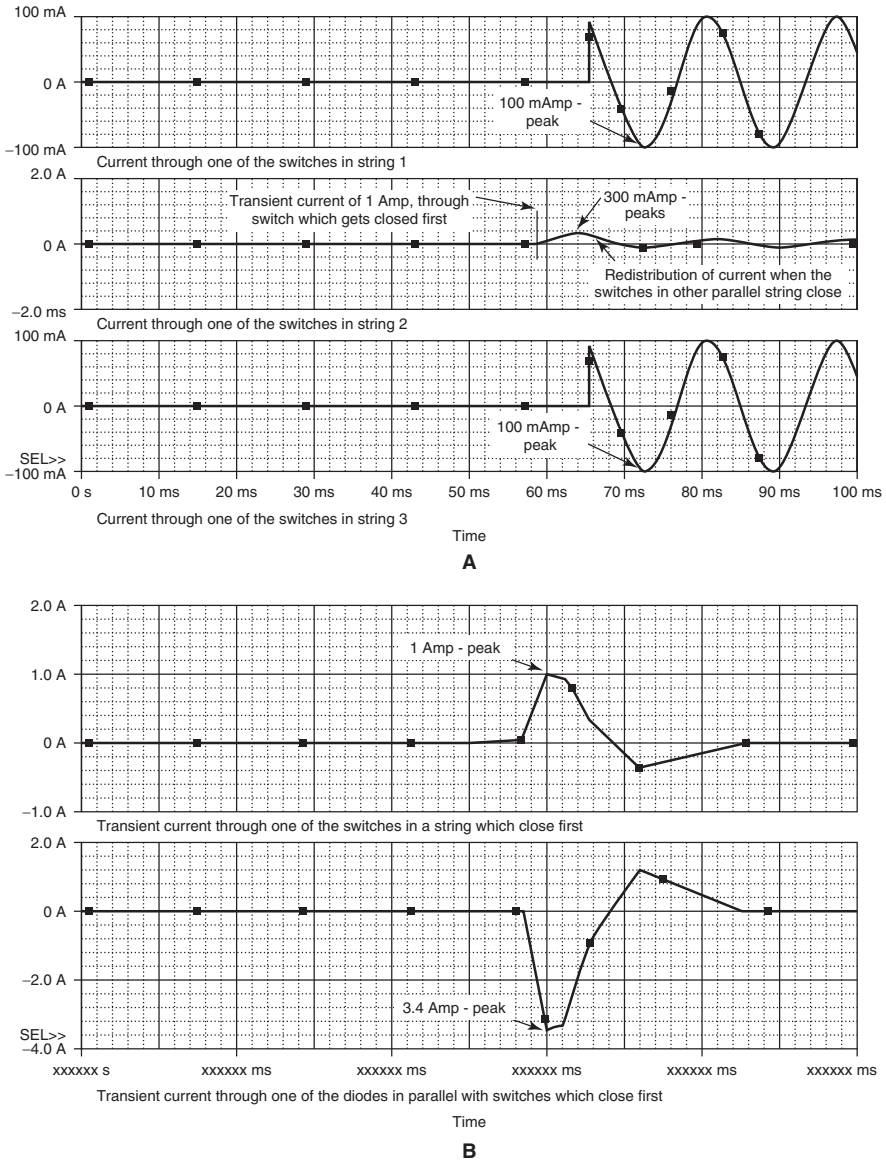

Figure 4.14 Effects of switch closing delay.

4.4.7 Summary of Simulation Results

The modeling study showed that:

- The MEMS switch operation produces short duration overvoltages, which must be considered in the system design.

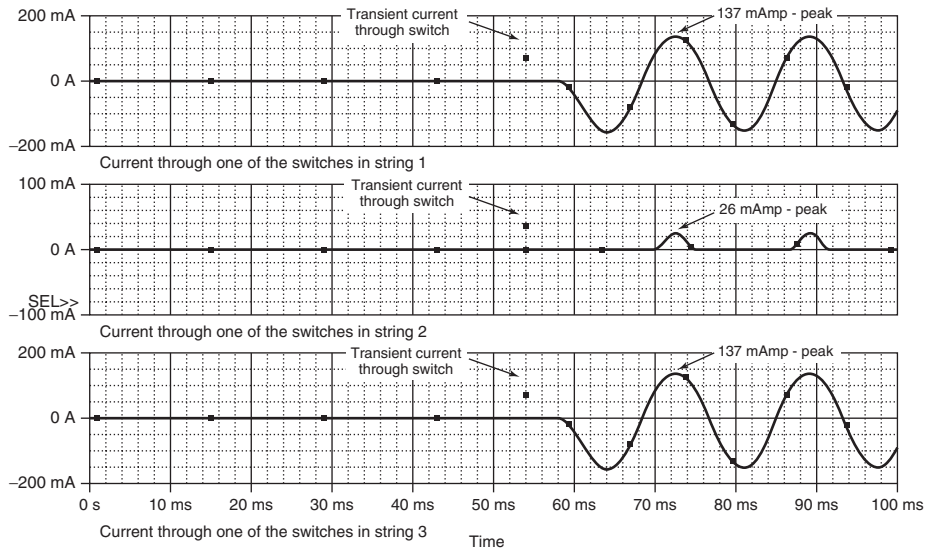

Figure 4.15 Effects of one set of switch failing to close.

- The delay of switch operation causes short duration uneven current distribution. These overcurrents must be considered at the design stage, although the MEMS switch can withstand up to 10 times the rated current for a few milliseconds.
- The switch failures generate permanent overload, which must be considered at the design stage.

4.5 RELIABILITY ANALYSES

The objective of the reliability analysis is determination of the number of redundant switches needed for long-term operation of a switching array. The practical questions are as follows:

- How many switches can fail before the failure of the system?
- How many hours of operation cause system failure?

In this section we present a typical expected lifetime result of the MEMS base circuit breaker as well as a description of the analysis technique. In calculating the expected lifetime of the switch, we consider the failures that occur during switching operations due to overvoltage or overcurrent, since they represent the main modes of failures. In particular, two types of failures: fail to open (when switching from closed to open) and fail to close (when switching from open to closed) are addressed.

Fail-to-open and fail-to-close failures occur mainly because of a switching or lightning overvoltage but also when a large short circuit current damages some of the MEMS devices. Hence the failure probabilities are directly affected by the voltage

and the current on the unit. For this reason it is more accurate to model the failure probability of a MEMS unit as a function of the voltage and/or current. Generally, this failure probability is a nondecreasing function of voltage and/or current, which can be modeled as a piecewise linear function. In particular, for a given voltage (or current), it can be anticipated that the failure probability will remain constant up to a critical current value, after which the failure probability increases linearly. Furthermore the probability of failure can safely be modeled as one, after some maximum current value.

The fact that the failure probabilities are a function of the voltage and current on the MEMS unit presents important challenges for the reliability analysis of the switch. As more and more MEMS devices on a switching string fail, the voltage on each MEMS unit increases, which results in an increased likelihood of failure of the remaining MEMS devices and the whole switching string. Similarly, as switching strings (branches) fail, the current on the other remaining strings increases, increasing the failure likelihood. This implies that the failure probabilities of the MEMS units are not stationary (i.e., they change over time as more and more MEMS units fail), since they are directly affected by the status (failed or functional) of all other MEMS units in the system.

This dependency among the units necessitates the need for a Markov model that captures the dynamics of the switch system over time. In particular, it is important to maintain, as part of the system state, the status of each MEMS device on the switch matrix and model each switching operation as a system transition that takes the system to a new state, depending on the number and identity of the MEMS units that fail (i.e., fail to open or fail to close) during a switching operation. The system failure can be modeled by an absorbing state, and the distribution of the first passage time to this absorbing state represents the distribution of the system lifetime. One complexity in this Markov model is the computation of the transition probabilities, which are not stationary, since the failure probability of each MEMS unit depends on the status of the other MEMS units.

While the Markov model developed here can accurately estimate the lifetime of the system, it is not practical for realistic size systems due to the large state description and space. Hence, due to the number of MEMS devices that need to be used in parallel and series to attain the required distribution ratings, the analysis of the Markov model by an exact algorithm is computationally inefficient. Therefore, rather than using an exact algorithm, an approximation algorithm to estimate the reliability of the MEMS switch was developed. In the next section we present this effective approximation to calculate the expected lifetime for realistic size systems. We finish with some numerical results that are representative of the switch that the team has designed and manufactured as part of a sponsored project to modernize power distribution systems in US Navy ships and urban areas.

4.5.1 Approximations to Estimate Reliability

As an introduction to the reliability calculations, the design of the circuit breaker is briefly summarized. The MEMS switch consists of units connected in series and parallel. Each unit consists of five positive and five negative MEMS switches connected in

series. To achieve the required voltage rating, a number (typically around 170) of these units are then connected in series to form a string. Around 6000 strings are connected in parallel to attain the required current rating for power distribution systems.

Denote the number of units on a branch as n, and the number of parallel branches in the circuit breaker as m. In developing the approximation to estimate the reliability, it is necessary to make the following simplifying assumptions for the system:

- *Failure probabilities* The failure probability of a MEMS switch (positive or negative) is constant. That is, we neglect the effect of voltage and/or current increases on the failure probability. We denote the failure probability as q.
- *Failure of a Unit* A unit is said to fail when at least k_1 out of five of the switches in a unit fail, which helps generate a current in the same direction (either positive or negative).
- *Failure of a branch* A string fails when the number of functional units falls below a certain level, meaning a string is functional if the number of unit failures on this branch is not more than k_2.
- *Failure of circuit breaker* Finally, the circuit breaker fails when the number of functional strings falls below a certain number, meaning the number of branch failures has to be less than or equal to k_3 in order for the circuit breaker to operate as desired.

Step 1 Calculate the lifetime distribution of a single unit (consisting of five positive and five negative MEMS switches shunted by diodes) by an absorbing Markov chain in which the unit state may change (due to failures of MEMS devices or diodes) in each switching operation.

Step 1.1 Generate the state space for a unit. State (i,j) denotes that there are i positive and j negative functional switches in the unit, where $i,j \in \{5,4,\ldots,5-k_1+1\}$. We denote the failed state of a unit as state 0.

Step 1.2 Calculate the transition probabilities by using the binomial distribution. The transition probability from (i_1,j_1) to (i_2,j_2) can be calculated as

$$p_{(i_1,j_1)(i_2,j_2)} = \begin{cases} \binom{i_1}{i_2} q^{(i_1-i_2)}(1-q)^{i_2} \binom{j_1}{j_2} q^{(j_1-j_2)}(1-q)^{j_2} & \text{if } i_2 \le i_1 \text{ and } j_1 \le j_2 \\ 0 & \text{otherwise} \end{cases}$$

and the transition probability from (i_1,j_1) to state 0 is

$$p_{(i_1,j_1),0} = 1 - \sum_{i_2=5-k_1+1}^{i_1} \sum_{j_2=5-k_1+1}^{j_1} p_{(i_1,j_1)(i_2,j_2)}$$

Step 1.3 Calculate the cumulative failure probability distribution by the following:

$$P(\text{fail by the } n\text{th transition}) = P^n_{(5,5),0}$$

Note that, as the state 0 is the absorbing state $P^n_{(5,5),0}$ gives the probability of a unit's failure by the nth transition. Therefore probability of a unit's failure at exactly the nth transition can be calculated by

$$P(\text{fail at the } n\text{th transition}) = P^n_{(5,5),0} - P^{n-1}_{(5,5),0}$$

where $P^n_{(i,j),0}$ is the n-step transition probability from state (i,j) to the absorbing state 0.

Step 2 Using a Monte Carlo simulation model, estimate the lifetime of the complete MEMS circuit breaker using the failure probability distribution of a unit generated in step 1. Note that the failure probability distribution of a unit is dependent on several factors and does not have a common form. The failure of an individual string is determined by the order statistics of unit failures on the string and the system failure is determined by the order statistics of string failures. Finding the lifetime of the system analytically is complicated as it involves order statistics on a collection of order statistics. Therefore simulation approach is employed.

Step 2.1 For each of the m branches, generate n random variables from a uniform (0,1) distribution.

Step 2.2 Find the $(k_2 + 1)$st smallest number among each set of n numbers, and obtain a set of m numbers

Step 2.3 Among these m numbers pick the $(k_3 + 1)$st number L.

Step 2.4 The expected lifetime of the circuit breaker is equal to the smallest n such that $P^n_{(5,5),0} \geq L$.

In the next section we present the results of the experimental studies to approximate the lifetime of the MEMS circuit breaker for typical values of q, n, m, k_1, k_2, and k_3. The algorithm above, which was coded in Matlab, is available upon request from the authors.

4.5.2 Computational Results

The number of MEMS units is one of the most important issues in the design of the circuit breaker. Different size breakers can generate different current ratings and have different reliabilities. Intuitively large-size systems are supposed to be more reliable than small breakers. In this study the values of n and m (number of units on a branch and number of branches in the system, respectively) are set equal to 170 and 6000, as these values satisfy the requirements for the application addressed in this project. In this section we describe an experimental study to estimate the reliability, equivalently the lifetime of a 170×6000 AC circuit breaker, using the algorithm discussed in Section 5.1.

To employ the algorithm proposed, values for q (constant failure probability for a switch in a unit), k_1 (number of positive or negative switch failures that lead to the failure of the unit), k_2 (maximum number of defective units that will keep a branch functioning), and k_3 (maximum number of defective strings that will not cause system failure) have to be set properly. In this numerical study for a modest estimate of

TABLE 4.1 Levels for the parameters in the numerical study

Parameter	Levels		
k_1	2	3	4
k_2	155	160	165
k_3	5975	5950	5925

TABLE 4.2 Approximate number of switching operations for the AC breaker prior to failure

	$k_2 = 165$			$k_2 = 160$			$k_2 = 155$		
k_1	$k_3 = 5975$	$k_3 = 5950$	$k_3 = 5925$	$k_3 = 5975$	$k_3 = 5950$	$k_3 = 5925$	$k_3 = 5975$	$k_3 = 5950$	$k_3 = 5925$
2	9500	9280	9120	7700	7560	7460	6760	6620	6600
3	15100	14680	14520	12540	12300	12200	11200	11060	10920
4	23260	22720	22560	19680	19360	19160	17820	17580	17400

failure probabilities $q = 10^{-4}$ is chosen and the other parameters are varied at three different levels as shown in Table 4.1.

As a result, in total, we have $3^3 = 27$ design points. For each design point, five replications of the Monte Carlo simulation were executed to obtain a better estimate of the average lifetime of the circuit breaker. Table 4.2 presents the results of the numerical study.

As expected, higher values for k_1, k_2, and k_3 result in longer average lifetimes, since higher values for these parameters imply higher tolerance of MEMS devices to high voltage and current. Another observation from the numerical results is that the lifetime of the system is sensitive to changes in k_1. Increasing k_1 to 4 from 2 increases the expected lifetime more than 100%. However, note that a value of 4 for k_1 may not be realistic, since this means that a single MEMS device would be sufficient to keep the unit functional.

The approximation algorithm presented in this section represents a fast, efficient way to compute the system reliability. While some simplifying assumptions have been made, the numerical results in smaller systems (for which for which it is possible to compute the exact lifetime distributions) show that the expected lifetime values are accurate enough to safely base maintenance and repair cost estimates and power system reliability.

The current reliability investigations involve further numerical tests with a wider range of operating parameters as well as optimal or effective strategies to maintain the MEMS circuit breaker so that its operation in Navy ships and urban power distribution systems are cost effective.

4.6 PROOF OF PRINCIPLE EXPERIMENT

4.6.1 Circuit Breaker Construction

The medium voltage circuit breaker requires about 300 MEMS switches connected in series in each switching string and a few thousand switching strings are connected in

parallel. The operation of each MEMS switches requires 5 V, 100 mA pulses. The insulation between the operating coil of the MEMS switch and moving part is 400 V. Accordingly 400 V/80 V = 5 series-connected MEMS switches can be supplied with one auxiliary power supply. We selected a slightly reduced (80 V) operating voltage for each microswitch, rated at 100 V.

The limited dielectric strength (400 V) of the insulation between the operating coil and moving part requires the development of a building block for the switch. The series and parallel connection of several building blocks will form the switch. In a building block the MEMS switches are connected in series, but their operating coils are connected in parallel. The MEMS switches in the building block will be opened by a negative DC impulse and closed by positive dc impulse. The generation of these pulses requires a floating local power supply, which will be connected to the operating coils of the MEMS switches by a transistor bridge for a short period (100 μs) to operate the switch. A control pulses will be sent from the ground level through a fiber optic cable to control the transistor bridge.

Figure 4.16 shows the connection diagram of a building block switching module. The module contains:

- Five MEMS switches connected in series, with their operating coils connected in parallel
- Battery-powered operating circuit, with a transistor bridge
- Charging circuit for the battery
- Fiber-optic links for control the operating circuit
- Control circuit at the ground level ("switching control" in Fig. 4.16)

The five parallel connected operation coils are supplied by the transistor bridge. The turn on of transistors 1 and 2 for a short period (100 ms) connects the battery to the coils in the positive direction. The current pulse turns on the MEMS. In a similar way the turn on of transistors 3 and 4 connects the battery to the coils in the negative direction. The current pulse turns off the MEMS. In our prototype the battery was replaced by a super capacitor.

The control pulse is transmitted from the ground level by fiber-optic links. The control pulse is generated by the "switching control" unit.

The battery charger is supplied by small current transformer connected in series with the module. A small ferrite coil with a few turns forms a current transformer. The transformer is terminated by a resistance. The voltage across the resistance is rectified by a diode, which charges the 5 V battery or supercapacitor. In our prototype a small solar cell charged the supercapacitor. In both cases the power supply trickle charges the battery or supercapacitor.

The circuit breaker operates infrequently and needs only a 100 μs duration current pulse. Consequently battery use is minimal. The charger keeps the battery voltage constant by replacing the self-discharge causing depletion. Figure 4.17 shows the prototype switching module.

This module has a positive and a negative switch connected in series. Each switch has five MEMS switches connected in series. These switches are surface mounted. The

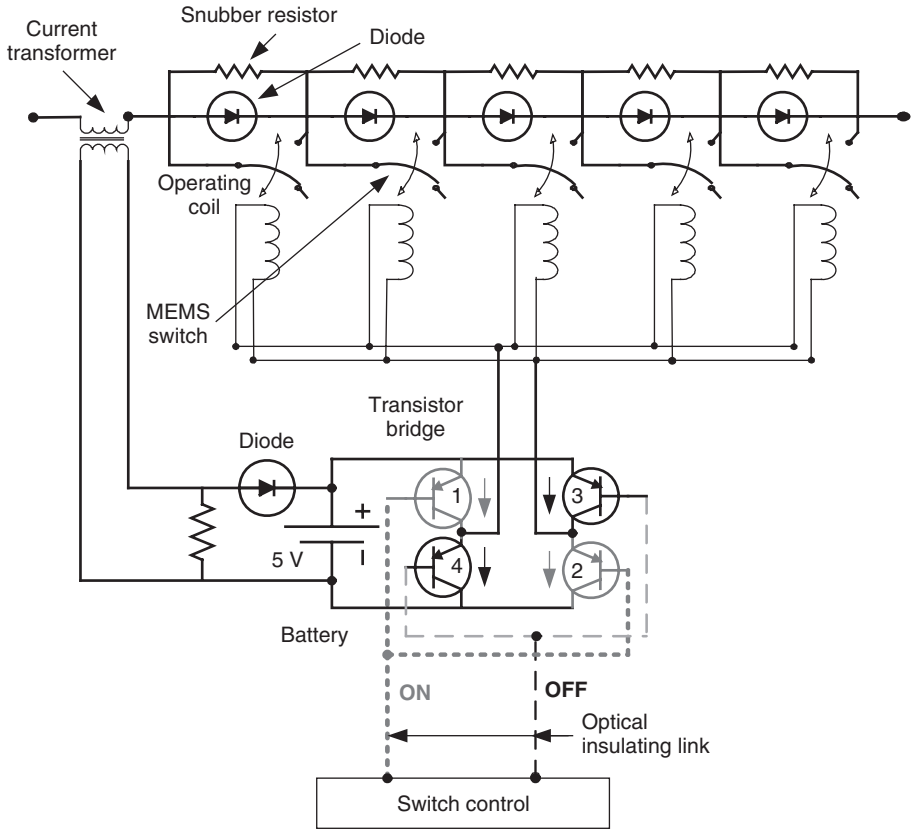

Figure 4.16 Building block of the switching module.

control coils of the MEMS are connected in parallel. Each MEMS switch is shunted by a diode and a snubber resistance. A transistor bridge (H-bridge) supplies the control coils. The charger is powered by a flexible solar cells (not shown), which charges a supercapacitor. This capacitor can be replaced by a battery. This capacitor provides DC voltage for the electronics and optical links provide insulation and connects the control signal to the transistor bridge. The control signal is a 5 V, 100 mS impulse, which is generated by the "switch control" unit.

4.6.2 Control Circuit

The operation analysis shows that when the current is positive the positive switch operates first, and the negative switch operates after the current polarity is reversed, approximately a half cycle later. In the case of a negative current, the operation sequence is reversed. A control circuit has been developed for the proper operation of the circuit breaker. Fiber-optic links transmit the control signal to the switching modules. Figure 4.18 shows the block diagram of the developed control circuit.

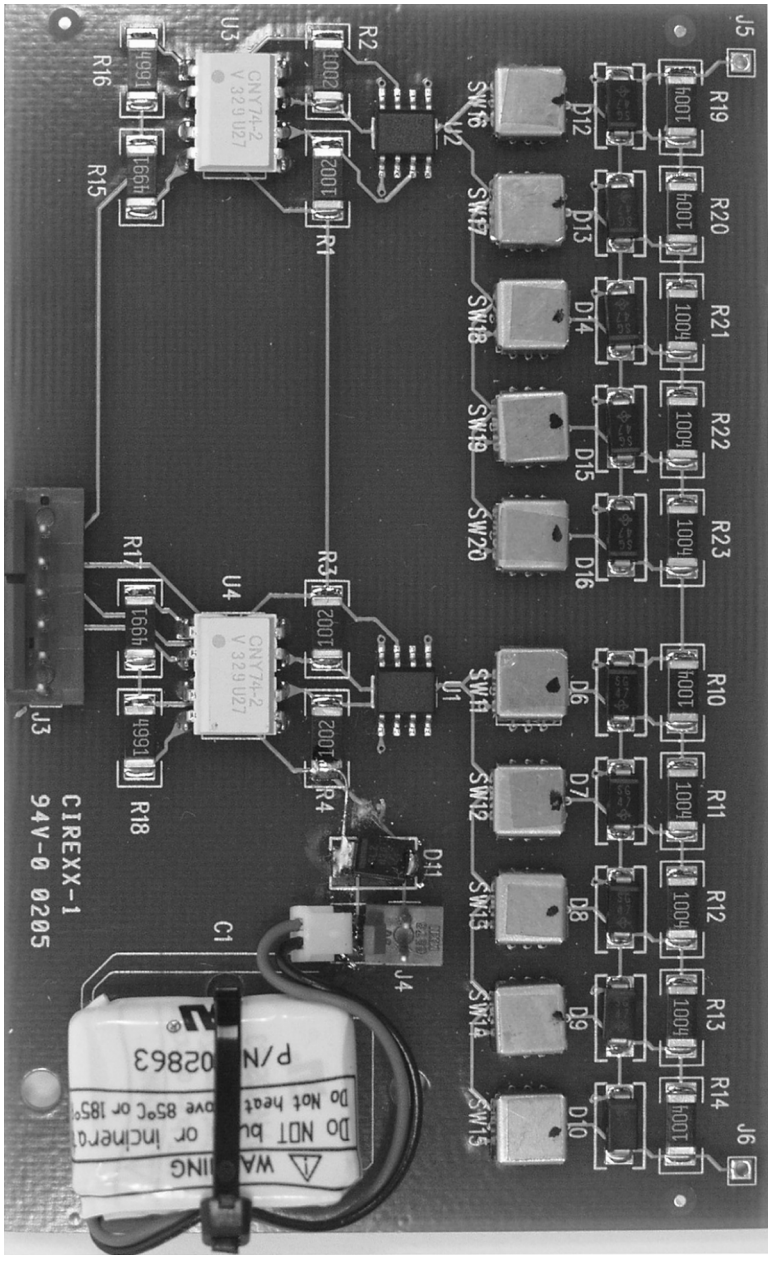

Figure 4.17 Prototype switching module.

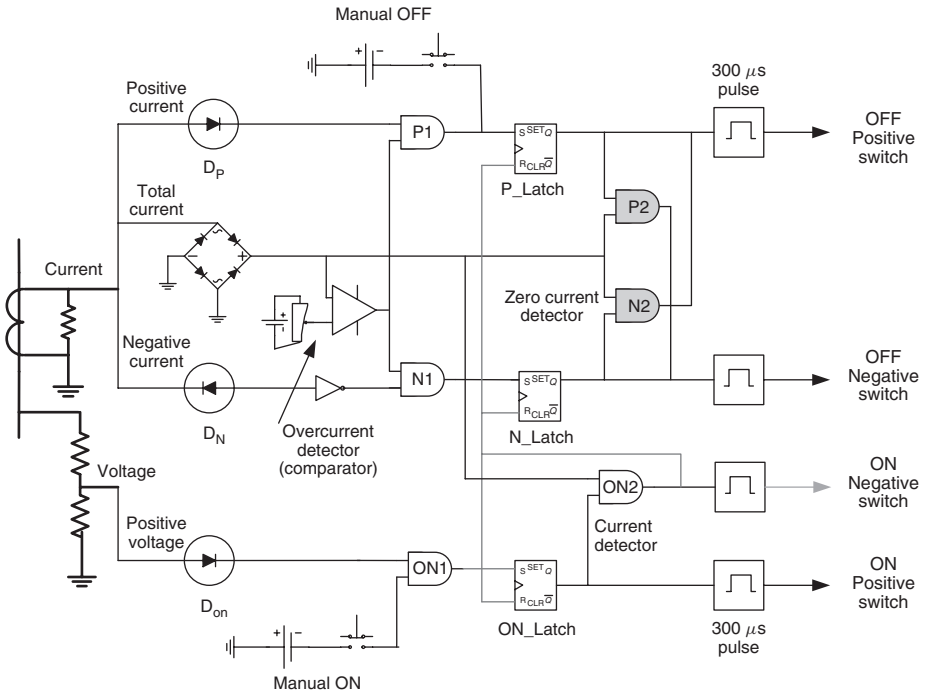

Figure 4.18 Block diagram of the control circuit.

In the case of a current interruption, the current transformer produces a signal. Responding to this signal, the full-wave bridge rectifier generates a DC signal proportional with the total current. In addition the positive and negative components of the current signal are separated by two diodes (D_P and D_N). The total current signal supplies a comparator that produces a signal if the current is above a predetermined level. The typical value is 1.5 times the rated current. The comparator signal supplies two AND gates ($P1$ and $N1$). These gates determine the polarity of the current. The output signal from the appropriate AND gate triggers a latching circuit (P_Latch or N_Latch), which activates a pulse generator that produces a 100 µs square pulse. This pulse is transmitted through the optical links to the positive switches in all switching modules. After this $P2$ or $N2$ logic block detects the current zero and activates the microswitches in the negative switches of the circuit breaker.

In the case of manual operation, the ON switch directly activates the positive latching circuit (P_Latch). Manual closing activates the AND gate ON1, which produces a signal if the voltage is positive. This signal activates a latching device (Latch_ON) that triggers a pulse generator. The 100 µs square pulse operates the microswitches in the positive switch. After this, the AND gate ON2 detects the current flow and triggers the microswitches in the negative switch. The switch can be opened manually or automatically if an overcurrent occurs or the off push-bottom is activated. The switch

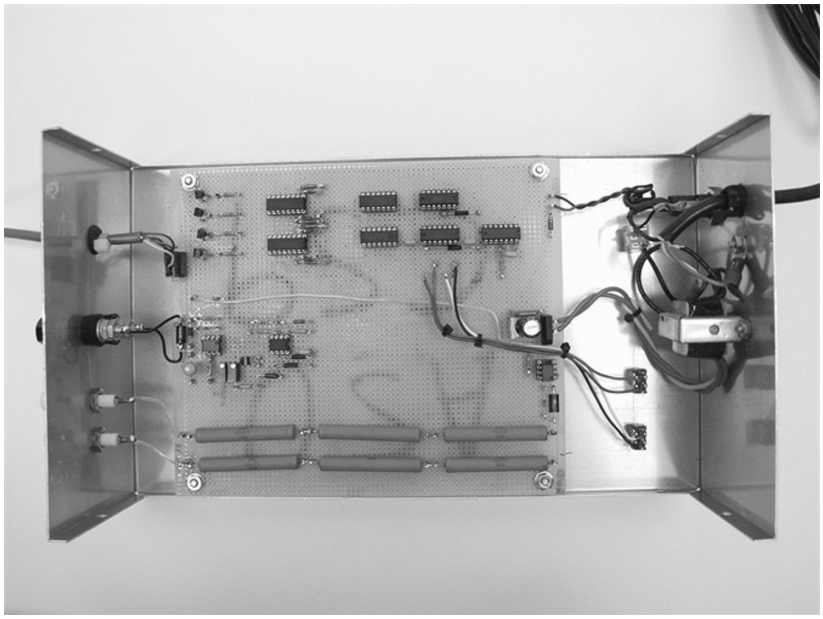

Figure 4.19 Control circuit prototype.

opening process can be followed using the block diagram in Figure 4.18. Figure 4.19 shows the prototype control unit.

Because of financial limitations, three switching units and one control unit were built. The switching units were tested as follows:

- All three units in connected in parallel.
- All three units are connected in series.

The tests included turn on and off in resistive and inductive loads. The tests verified that the units interrupt the current in the first half cycle. Also the units turned on within a half cycle. Relatively small (2.5 times the supply) transient voltage were observed during the switch-opening test. This overvoltage can be controlled by an RC snubber network, which will be developed in the future.

The MEMS switches operated fast, and we were unable to detect any delay of turn on or turn off. The results proved that the MEMS-based circuit breaker is feasible. However, actual circuit breaker development requires further research and development work.

4.7 CIRCUIT BREAKER DESIGN

A medium voltage circuit breaker must withstand lightning caused overvoltages as well as switching produced overvoltages. The MEMS-based switch interrupts the

short circuit current in the first half cycle, without arcing at current zero. This ensures that the transient recovery voltage is twice the peak line to neutral voltage. The design of a breaker requires detailed engineering work, which is beyond the scope of this project.

Another consideration is the fast growing state of MEMS technology. The new devices are more powerful. Manufacturers have indicated that a latching device of 200 V, 1 A will be available very soon. This device nevertheless is close in dimensions, when packaged, to the device used for this project.

It is useful in this regard to establish the technical data of a hypothetical medium voltage breaker as a starting point for the design of a practical beaker. The rating of a typical distribution system circuit breaker is 7.2 kV and 600 A. The breaker has to interrupt a short circuit current of 6 kA, and withstand of an over voltage of 34 kV.

The building block of the described switching string assembly is a MEMS switch. A review of the literature and a market survey shows that MEMS switches can be built for 150 V and 100 mA. The closing and opening time is less than a millisecond. The distribution switch requires a string built with minimum of $34{,}000/150 = 227$ MEMS connected in series. The number of strings connected in parallel is $600/0.1 = 6000$. It is assumed that the switches can conduct about 1 A for a half cycle. This ensures that the breaker can interrupt a short circuit current of 6000 A.

The estimated dimensions of a MEMS switch, diode, and snubber resistance is 0.3×3 mm. About 500 switching units could be connected in series and 50 strings in parallel on a 300 mm silicon wafer. One wafer can carry two 250×50 switch assembly, which can be used as a positive and negative switch. This requires 120 wafers connected in parallel. The switch has to be packaged. One concept is to place the switch in vacuum in a glass enclosure or filing the enclosure with SF6. It can be foreseen that both method results in a miniaturized circuit breaker.

4.8 CONCLUSIONS

Out study proved that a MEMS-based medium voltage circuit breaker is feasible. Our switching model offers small size, zero current switching, and interruption of short circuit current within the first half cycle. The specific results are as follows:

- Development of a novel concept for CBs, where the large mechanical switch is replaced by an array of MEMS switches and diodes.
- Development of a switching string, which contains a positive and a negative switch. This string is the building block of a MEMS based circuit breaker.
- Modeling the failure of MEMS switches in a switching array.
- Analysis of nonsimultaneous operation of MEMS switches in a switching array.
- Reliability analysis of switching matrix.
- A proof of principles model is constructed using switching string assembly to experimentally prove the validity of the concept.

ACKNOWLEDGMENTS

The authors would like to acknowledge the support of NSF, particularly to James Momoh (NSF) and Katherine Drew (ONR) for their efforts to clarify the project goals and for their encouragement of our work. In addition the authors thank Prof. B. Kim, and graduate students: Neil Shah, Daniel S. James II, and Rahim Kasim for their contributions.

BIBLIOGRAPHY

Circuit Breakers

1. Heinrich, C., Schmitt, H., and Hoever, I. "New Switching Technologies in Medium-Voltage Systems-Application and Requirements." *Proc. 7th IEEE Conf. on AC-DC Power Transmission*, l: 282–287, 2001.
2. Yanabu, S., Zaima, E., and Hasegawa, T. "Recent Development of High Voltage Circuit Breaker for High Voltage Transmission and Distribution System." *IEEE/PES Transmission and Distribution Conference and Exhibition 2002, Asia Pacific*, 2(l): 1438–1443, 2002.
3. Chung, Y.-H. "Medium Voltage Hybrid Transfer Switch." *Proc. IEEE Power Engineering Society Winter Meeting*, 2: 1158–1163, 2002.

MEMS Switches

4. Tilmans, H. A. C., Fullin, E., et al. "A Fully-Packaged Electromagnetic Micro-Relay." *Proc. 12th IEEE International Conf. Micro Electro Mechanical Systems*, January, 25–30, 1999.
5. Qiu, J., Lang, J. H., and Slocum, A. H. "A Centrally-Clamped Parallel-Beam Bi-stable MEMS Mechanism." *Proc. 14th IEEE Int. Conf. Micro Electro Mechanical Systems*, January, 352–356, 2001.
6. Pelesko, J. A., and Bernstein, D. H. *Modeling MEMS and NEMS*, CRC Press, Boca Raton, FL, 2002.
7. Gardner, J. W., Varadan, V. K., and Awadelkarim, O. O. *Microsensors, MEMS and Smart Devices*. Wiley, New York, 2002.

Series Parallel Connection of Switches

8. Watanabe, E. H., Aredes, M., de Souza, L. F. W., and Bellar, M. D. "Series Connection of Power Switches for Very High Power Applications and Zero Voltage Switching." *Proc. IEEE Int. Symp. Industrial Electronics*, 2(1): 399–404, 1997.
9. Karady, G., and Gilsig, T. "The Calculation of Turn-off Overvoltages in a High Voltage Thyristor Valve." *IEEE Trans. Power Apparatus and Systems*, 91(2): 565–574, 1972.
10. Karady, G., and Gilsig, T. "The Calculation of Transient Voltage Distribution in a High Voltage DC Thyristor Valve." *IEEE Trans. Power Apparatus and Systems*, 92(3): 893–898, 1973.
11. Karady, G., and Gilsig, T. "The Calculation of Turn-on Overvoltages in a High Voltage Thyristor Valve." *IEEE Trans. Power Apparatus and Systems*, 90(1): 2802–2809, 1971.

12. Park, I.-G., and Lee, S.-M. "Hybrid Series Connection of a Controllable Switch and Thyristors." *IEEE Trans. Industry Applications*, 36(1): 206–211, 2000.
13. Hofer-Noser, P., and Karrer, N. "Monitoring of Paralleled IGBT/Diode Modules." *IEEE Trans. Power Electronics*, 14(3)1: 438–444, 1999.

Shipboard Power System

14. Momoh, J. A., and Kaddah, S. "Comparative Study between Two Voltage Stability Methods for Integrated Shipboard Power System with DC Zonal Protection." *34th North American Power Symp*., l: 294–299, 2002.
15. Ciezki J. G., and Aston, R. W. "Selection and Stability Issues Associated with Navy Shipboard DC Zonal Electric Distribution System." *IEEE Trans. Power Delivery*, 15(1): 665–669, 2000.
16. Butler, K. L., Sarma, N. D. R., Whitcomb, C., Carmo, H. D., and Zhang, H. "Shipboard Systems Deploy Automated Protection." *IEEE Computer Applications in Power Systems*, 11(1): 31–36, 1998.

Reliability Analysis

17. Heydt, G. T., James, D. S., Gel, E., Albu, M., and Hubele, N. F. "The Reliability Analysis of High Power Switches Composed of Series and Parallel Branches." *IEEE Power Engineering Society General Meeting*, l: 1–8, 2003.
18. Chaudhuri, G., Hu, K., and Afshar, N. "A New Approach to System Reliability." *IEEE Trans. Reliability*, 50(1): 75–84, 2001.
19. Moustafa, M. "Reliability Model of Series-Parallel Systems." *Microelectronics and Reliability*, 34(1): 1821–1823, 1994.
20. Lesanovsky, A. "Systems with Two Dual Failure Modes—A Survey." *Microelectronics and Reliability*, 33(1): 1597–1626, 1993.

5

GIS-BASED SIMULATION STUDIES FOR POWER SYSTEMS EDUCATION

Ralph D. Badinelli, Virgilio Centeno, Boonyarit Intiyot

Virginia Tech

5.1 OVERVIEW

In this chapter we prescribe computer simulation as a robust tool that should be integrated into any comprehensive educational curriculum in the field of power systems design, engineering, and management. Our advocacy of computer simulation is based on the essential role that this methodology plays in two foundational elements of power systems education: case studies and decision modeling. These elements, in turn, are necessary in the education of future power system designers, engineers, and managers who need to understand the ever-expanding complexities of these systems from the points of view of their many stakeholders. Computer simulation is unique among modeling techniques to support case analysis and decision modeling for such complex systems. In conjunction with case studies, text and lecture materials computer simulation forms a flexible educational support system (ESS). In this chapter we provide an overview of the role of case analysis and decision modeling in power systems education and the basic elements of simulation models along with an explanation of the essential role they play in this education.

We are motivated by two concomitant features of the educational landscape. First, the important role played by power systems in the economic health, environmental

Operation and Control of Electric Energy Processing Systems, Edited by James Momoh and Lamine Mili

quality, and national security of the United States and other countries has become evident. As a consequence operation, design, and management of power systems have become disciplines that are gaining in popularity and importance. Second, the operation, design, and management of power systems involve large numbers of interrelated systems that are mutually dependent in mathematically complex ways. New developments in generation technologies, market deregulation, environmental regulations, reliability standards, and security concerns are aggravating the complexity and interdisciplinary nature of this topic. New and existing personnel in the fields of power system engineering, grid operation, power plant control, energy portfolio management, public policy, and consulting demand up-to-date and holistic education in the rapidly changing power systems discipline.

Decision making is the common foundation of all of the challenges in the fields mentioned above, and we view all learners as future decision makers. Hence our design of educational tools will revolve around decision analysis. Examples of the decision domains that our educational tool must support include:

- *Public policy decision problems* Environmental policy planning, market regulation planning, and infrastructure planning
- *Engineering decision problems* Protection system design, generation, and transmission technology selection
- *Business decision problems* Generation capacity planning, unit commitment, optimal dispatch, demand side response, trading strategy, and financial risk management

For each of these decision areas the cause–effect relationship between decision alternatives and key performance indicators (KPIs) such as cost, reliability, pollution, and market equity must be understood and analyzed by the decision maker. For the learner, modeling the decision of a case study is the most effective method for identifying the trade-offs inherent in the KPIs. The learning process can be brought to fruition only by quantifying these trade-offs and experimenting with the cause–effect relationship inherent in each decision—a task that demands computer simulation.

Electric generation units, power grids, and energy markets form a complex system that evolves over time through the decisions of system managers, engineers, unit operators and market participants as well as through the influence of weather, load variation, market prices, forced outages, and the physical behavior of network components. Some of these influences have a random component to their variations over time, making the trajectory of the power system stochastic. Computer simulation is unique among modeling techniques in its ability to capture the effects of numerous interacting influences as well as of randomness on the performance of a system. Furthermore the raw output of a simulation in the form of the trajectory of performance measures over time can be summarized in statistically valid ways to evaluate the long-run behavior of a system over time and over a representative sample of random scenarios.

5.1.1 Case Studies

A case study is a presentation of a problem in the context of realistic conditions, people and events. Unlike traditional textbook problems, a case study does not present a well-formulated problem but rather a situation of conflicting needs and desires instigated by the disparate points of view of various stakeholders. Each case presents the learner with a situation in which a decision is needed. The learning process is pursued through the learner's attempts to create a model of the decision problem and to use the model to determine the best choice of alternatives (see [7]).

Case studies are the most effective form of learning assignment for the education of professionals for several reasons (see [2,3,4,6,21]):

- Students become active instead of passive learners. Students learn by doing.
- Students are forced to define questions, not just answers.
- Students must identify, respect, and consider a problem from several points of view.
- Students are forced to apply theory in order to create structure for the case as opposed to applying a structured method to a well-defined, contrived problem.
- Students are forced to compromise and look for workable, feasible solutions when there are conflicting needs and constraints.
- Students acquire general problem-solving skills within a field of study instead of mere formulaic solution methods that, in real situations, must be applied with modifications and adjustments in consideration of assumptions that are not met and factors that were ignored in the development of the methods.
- Students gain maturity and confidence by facing the ambiguity of realistic cases.

In every industry the decision problems that comprise the public policy, engineering and management naturally fall into a hierarchical order. The solutions to decision problems that have long-term consequences and that are updated infrequently become parameters that influence decisions that have shorter term consequences and that can be updated more frequently. For example, the choice of technology for a new generation unit will influence the way that this unit is committed and dispatched. Hence a hierarchy of decisions emerges in which longer range, less frequent decisions are placed above shorter range, more frequent decisions. We assert that a holistic understanding of a subject such as the design, engineering, and management of power systems requires the learner to attempt to solve all of the essential decision problems associated within this subject as well as to see these decision problems in their hierarchical order. A collection of case studies in hierarchical order integrated with text and lecture material comprises a well-designed educational experience for future professionals in the field of powers systems.

The list below forms such a collection. These cases include problems of operating a conventional power system as well as problems of designing and operating power systems of the future.

Level 1: Public Policy Cases

- How to set the emissions limits on generation units in a given power grid.
- How to limit the prices that can be cleared in a given power market.
- How to limit the prices that can be charged to different consumer groups in a given power market.
- Where to install new transmission lines, gas pipelines, or publicly owned generation in a given power grid.

Level 2: Power Systems Design Cases

- How to select nontraditional generation technologies for distributed generation (DG).
- How to select the best location for DG.
- How to select the type of generation plant to add to a given power grid.
- How to plan the installation of new capacity in a given power grid.
- How to coordinate protective devices for a given power grid.
- How and where to change protection coordination for DG.
- How to select fast, alternating-current transmission (FACT) devices to strengthen transmission systems.
- How to coordinate protections and placement of FACT devices for voluntary islanding during catastrophic events.
- How to determine locations that are exposed to catastrophic hidden failures.

Level 3: Power Systems Management Cases

- How to set circuit breaker limits in a given power grid.
- How to configure FACT controllers (see [1]).
- How to commit the generation units to a given power grid.
- How to dispatch the generation units in a given power grid.
- How to bid or offer energy in a wholesale energy market for a given power grid.
- How to configure a portfolio of financial derivatives to support the risk management of an energy trading position within a given power market.
- How to commit and dispatch generation units to a power grid that is practicing various forms of DSR, environmental restrictions, market regulations, demand growth rates, and fuel cost volatility.
- How to encourage consumers to shape loads in order to balance cost and convenience.

The educational cases have several unique characteristics that carry the learner through these decisions in a realistic manner:

- *Interactive* Students are able to change different aspects of a power system's elements, markets, or regulatory environment in order to experiment with different scenarios for the configurations of physical assets, time series of loads

and failures, location and type of generation, contractual arrangements between customers and suppliers, and regulatory constraints. For each scenario entered by a student, the KPIs of the system must be computed by a computerized model.

- *Realistic* The educational cases are based on prototypes of real and proposed power systems, markets and regulatory environments.
- *Configurable* The development of a case-based ESS will yield not only a sample of case studies for use in courses but also structures for the database, student interface, and cases that can be modified with new data for the development of new case studies.

Clearly, a qualitative overview of the decision problems listed above does not prepare a prospective power systems engineer, manager, or regulator for the real world. An understanding of the trade-offs presented by these decision problems requires a quantitative analysis of them. Decision support systems that are more sophisticated than a collection of simple formulas are necessary. Specifically, our case analyses require decision support systems that embody mathematical decision models.

Many powerful methodologies for building and optimizing decision models have been developed over the last 50 years. The lexicon of modeling tools includes computer simulation, linear programming, integer programming, nonlinear programming, dynamic programming, and many others. For a comprehensive overview of decision models for power-system cases and their associated optimization methods, see [14,20]. Although these methodologies have been available for several decades, they have not enjoyed rapid adoption by businesses and institutions. One reason for their slow adoption is that most people find model formulation very difficult. The computerized tools for describing and prescribing solutions can be applied only after a descriptive decision model has been created—a task that generally is accomplished through the art and science of an operations researcher who understands the problem domain and the structure of decision models. For the practicing manager or analyst, model application is the process that delivers business performance. Therefore our educational goal is to teach the application of models to the decision problems described earlier.

A general understanding of the structure of decision models and their application is necessary for both the learner and the teacher. We provide such an overview below.

5.1.2 Generic Decision Model Structure

A decision model quantifies the cause–effect relationships between actions and outcomes. The outcomes of an action are expressed in terms of performance measures, which, for any decision alternative, are used by the decision maker to determine the alternative's feasibility and desirability. For example, the performance measures for the unit dispatch decision in a given time period include the total cost of generation across all dispatched units, the total grid power loss, the line load on each transmission line, the load coverage for each load bus, and the reliability of the system. To the challenge of quantifying these performance measures, we propose the application of

decision models. Models are the brains within a decision support system that transform masses of data into knowledge.

In order to specify the scope of the decision, the modeler categorizes the causative factors into two sets: a set of controllable factors that are used to define the alternatives available to the decision maker and a set of uncontrollable influences on the performance measures.

The alternatives of a decision represent the choices, options, or actions that a decision maker is empowered to execute within the scope of a given decision. Mathematically we can represent these alternatives in terms of a well-defined set of data elements that we call decision variables. For example, the alternatives for the unit dispatch decision in a given time period could be represented by the set of power output values for each generation unit that is available. This vector of power output values would constitute the decision variables for this decision. Among all of the possible sets of values for the decision variables, the decision maker then seeks the one that yields the most desirable, feasible performance. This solution is called the optimal solution to the decision problem for which the model is built.

The uncontrollable factors of a decision are the influences on the performance measures that cannot be chosen by the decision maker. We call these uncontrollable factors parameters. For example, the parameters of the unit dispatch decision for a given time period include the capacities of each available generation unit, the thermal capacity of each transmission line, the real and reactive load at each load bus, and the coefficients of the operating cost function of each available generation unit. A parameter could remain constant throughout the analysis or could be a random variable. If some parameters are random variables, then the performance measures that depend on these parameters also are random variables—a characteristic of the model that earns it the label "stochastic." Parameters, or their probability distributions, must be measured, estimated or forecasted in order to build the database for a decision model.

Contrary to common belief, the presence of random parameters does not preclude the application of decision models. In fact the ability to model decision-making under conditions of uncertainty can be considered the highest form of the modeler's science. In order to construct a stochastic model we must make use of the probability distributions of the random parameters. Doing so requires specification of these probability distributions as, for example, the estimates of the mean and the standard deviation define the probability distribution of a normally distributed parameter and the coefficients and volatility of a mean-reversion forecasting formula define the probability distribution of a future commodity price.

Performance measures that cannot be predicted with certainty introduce the element of risk into the decision. In these cases the distributions of random performance measures must be summarized over all scenarios into measures that capture both risk and reward. For example, for the unit dispatch decision in a given time period the total cost of generation is a random variable because the total load is not known with certainty in advance. Variations in the load from its forecasted value are handled by automatic dispatch of reserve power. Consequently the actual total cost of power generated during the given time period can be predicted by a decision model only up to the probability distribution of this cost. Summarizing this probability distribution

over all possible load scenarios in terms several summary measures such as the distribution's mean and its upper and lower quartile points gives the decision maker a representation of expected financial cost as well as the risk associated with this cost.

Most decision alternatives associated with the design and management of a power system have ramifications that extend over long time horizons. The trajectory of a performance measure over a time horizon can exhibit various kinds of cyclic, trended, or memory-influenced behavior. In order to provide useful indicators of the performance of an alternative, a decision model must summarize these trajectories over a time horizon that is long enough to capture all of the time-varying behavior of the performance measures. For example, for the unit dispatch decision over *multiple* time periods, the total cost of generation will exhibit fluctuations and memory due to load variation over time, load momentum, generator start-up costs, and ramping constraints. Summarizing the time series of generation cost in terms of its time average provides the decision maker with a useful indicator of overall cost performance. When a model summarizes performance measures over random scenarios and over time, as necessary, the resulting measures are called key performance indicators (KPI) as they are used directly to evaluate the feasibility and desirability of each alternative.

In order to specify the feasibility and desirability of performance, the decision maker imposes a decision criterion on each KPI. There are two possible forms for each criterion: a KPI can be constrained from above or below in order to impose bounds on performance, or a KPI can be maximized or minimized in order to pursue performance to its greatest possible extent.

The cause–effect relationships from decision variables and parameters to KPIs form a descriptive decision model. The qualifier "descriptive" indicates that the model's value is to predict or describe the performance of a system for a hypothetical set of inputs to that system. Hence a computerized descriptive model provides the decision maker with an efficient means to test any proposed alternative and a trial-and-error capability for searching for the best alternative. Given enough time, the decision maker can arrive at an alternative that yields optimal or near-optimal, feasible performance.

Some decision models can also help select the best course of action from among an overwhelmingly large set of alternatives. An extension of a descriptive model engages a computerized search algorithm that, in effect, automatically performs an intelligent trial-and-error procedure for the decision maker. Such an extended model is called a prescriptive model. Prescriptive models provide dramatically enhanced decision support when a decision involves so many feasible alternatives that manual trial-and-error is impractical.

The first step in building a decision model is to define data elements and to derive the mathematical relationships that constitute the descriptive model. The categories of data elements are:

- Decision variables
- Parameters
- Performance measures
- KPIs
- Criteria

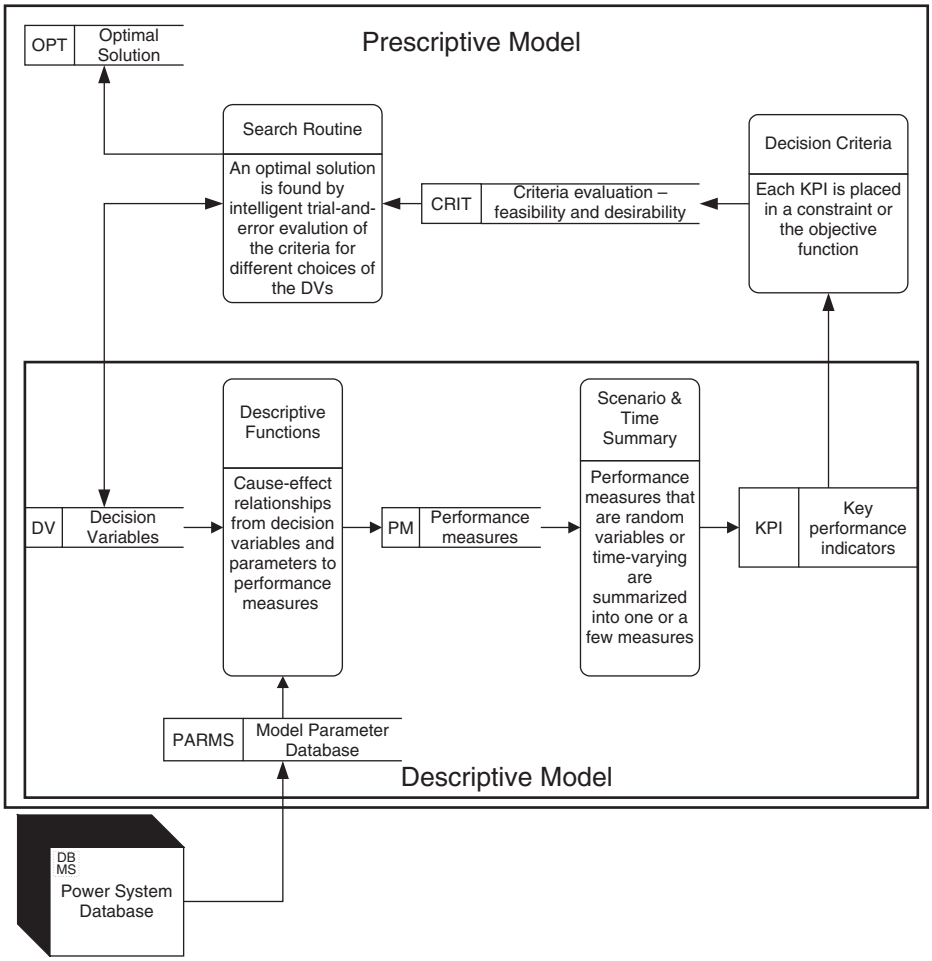

Figure 5.1 Data flow of descriptive and prescriptive models.

Figure 5.1 shows the general structure of a decision model. The most important perspective to draw from Figure 5.1 is the fact that a descriptive model forms the core of a prescriptive model. Furthermore the search routine of the prescriptive model is usually performed by a commercially available code of a search algorithm (linear programming, integer programming, etc.). However, the rest of the construction in Figure 5.1, without which the search routine is useless, is the responsibility of the modeler.

5.1.3 Simulation Modeling

Decisions related to power systems have outcomes (performance measures) that play out over a long time and that can take on many scenarios due to randomness in system parameters such as loads and market prices. Furthermore the relationship between

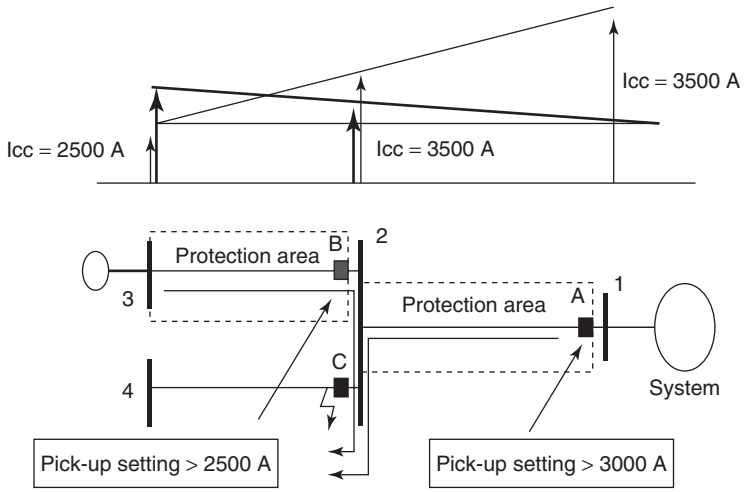

Figure 5.2 Effect of DG insertion in the coordination of protective devices.

decision variables and performance measures for power systems decision problems is typically very complex and nonlinear. Of all of the forms of decision modeling, simulation is uniquely capable of capturing complex cause–effect relationships, time varying performance measures and stochastic effects. In fact, for many of the decision problems that the learner needs to model, simulation is the only modeling technique that can produce a reasonably accurate descriptive model. For example, simulation can be used to identify the vulnerabilities of the protection system prompted by the interconnection of DG to a distribution feeder. By comparing the total DG short circuit contribution passing through protection devices with the pick-up settings of the devices the required protection coordination changes for a specific DG location can be determined [9]. Figure 5.2 shows a simulation of a fault at bus 2 that results in a DG short circuit contribution greater than the pickup setting of the protective device B. This will clearly result in misoperation of unit B and unnecessary loss of load.

Every simulation model is a computerized description of a system. A system can often be visualized as a collection of interacting operations with flows of material, power, cash, or other commodities among them. The simulation model tracks the state of the system as it evolves over time through the occurrence of events such as changes in load, outages, unit dispatching, short circuits, and the passage of time. In order to do this, a simulation model is created in the form of a computer program that consists of the following fundamental elements:

- Random Number Generator
- Event Scheduler
- State Transition Procedures
- System State Data Management
- Performance Measure Output

Through the creation of an artificial clock that marks simulated system time, the simulation program schedules the events that cause the system to evolve. Transitions in the state of the system take place at points in time determined by the Event Scheduler. In the case of a typical simulation of a power grid, the Event Scheduler would be programmed to update the time on an hourly basis. At each of these transition times, the State Transition Procedures update the state of the simulated power system to reflect changes caused by the events that occur at the transition time. The current state of the system is represented by the System State Data. The System State Data is used by the Performance Measure Output routines to store values of performance measures over the time period that has just ended. Once the updated performance measures are filed, the simulation program returns to the Event Scheduler to process the next system-changing event.

Some of the state-changing events, such as load variations and outages, may be the result of random effects. Computer simulation models are able to introduce random events into the event schedule through the use of random number generators. Through this mechanism, computer simulation models can represent realistically the performance that results from planned system interventions as well as unplanned system influences.

Events are defined by the modeler in terms of the simplest changes that can take place in the system that is modeled. By modeling the detailed interactions of system components over small intervals of time and aggregating the results of these interactions, complex behavior can be described through the use of numerous, relatively simple transition procedures. In fact computer simulation is the only modeling technique that can capture the complexity and randomness of a typical power system.

In a simulation model of a power system, the power flows through each network element and the cash flows associated with the power flows can be modeled for each hour of each day. From hour to hour the simulation program updates the status of each generation unit, load, and network element and stores this status in computer memory. The performance measures of the power system are computed, and the results filed.

Another simple example of simulation modeling is found in the case of the unit dispatch decision. The simulation model for this decision would compute, for any given dispatching plan and for any given scenario of loads, the total generation cost as well as other performance measures. Figure 5.3 portrays a time series of generation costs over a 24-hour period for one scenario of loads. This time series would be summarized most appropriately in terms of its average. A simulation model could generate this time series if the scenario of loads was provided as input parameters. We call the computation of performance measures over a time horizon for one scenario of parameters a "replication" of the simulation model.

In order to assess the KPIs of risk and expected cost of a dispatching plan, we would compute the generation cost over many 24-hour time horizons, each one of which represents one possible scenario. This way we would obtain a representative sample of system performance from the population of all possible scenarios. Figure 5.4 shows a sample of scenarios of the time series of generation cost. By computing the time average of each of these time series, we obtain an overall measure of performance for that scenario. Table 5.1 shows these time averages, and Figure 5.5 shows the

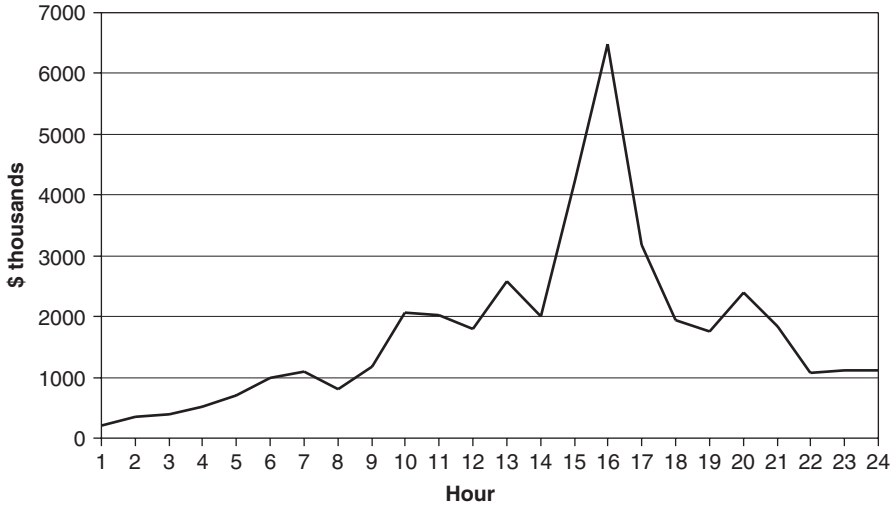

Figure 5.3 Generation cost time series example.

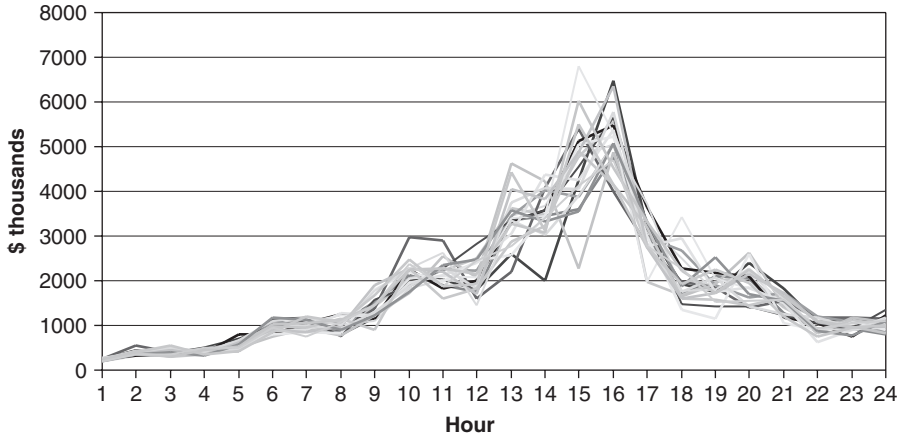

Figure 5.4 Generation cost scenarios.

distribution of the sample of costs given in Table 5.1. Finally, we summarize the data in Table 5.1 by computing their average and the value at risk evidenced by these data. Value at risk is a measure of financial risk that is commonly used in the energy industry. In this case we compute VAR as follows:

$$\text{VAR} = C_{90} - \mu_c$$

where μ_c = the mean cost, estimated from the sample to be 1774 and C_{90} = the cost at the 90th percentile point of the distribution of costs, estimated from the sample to

TABLE 5.1 Scenario averages

Scenario	Average Cost
1	1742
2	1683
3	1807
4	1778
5	1782
6	1847
7	1791
8	1790
9	1734
10	1875
11	1799
12	1724
13	1757
14	1632
15	1875
16	1794
17	1753
18	1841
19	1793
20	1692
Average	1774
VAR	76

be 1850. The two measures of expected cost and VAR are KPIs for the dispatching decision model that capture the expected financial value of the dispatching plan and a measure of financial risk associated with the dispatching plan.

5.1.4 Interfacing

A computerized educational support system is effective only if its interfaces for learners and teachers are transparent and easy to learn. To these users of a simulation program, the simulation is a tool for analyzing trade-offs associated with decisions related to the design and management of a power system. Clearly, the underlying details of the simulation model, such as random number generators, statistical evaluation of performance measures, and event scheduling, should be hidden from these users. The learner's interface to the simulation package should be designed for entry of decision variables and viewing of KPIs that result from these settings of the decision variables. The teacher's interface should include the ability to modify the parameter database in order to create different configurations of a power system for different sets of learners.

One of the most natural representations of the assets of a power system is that of a geographic information system (GIS). A GIS is fundamentally a database of objects, each of which can be indexed by a location in terms of an x-coordinate,

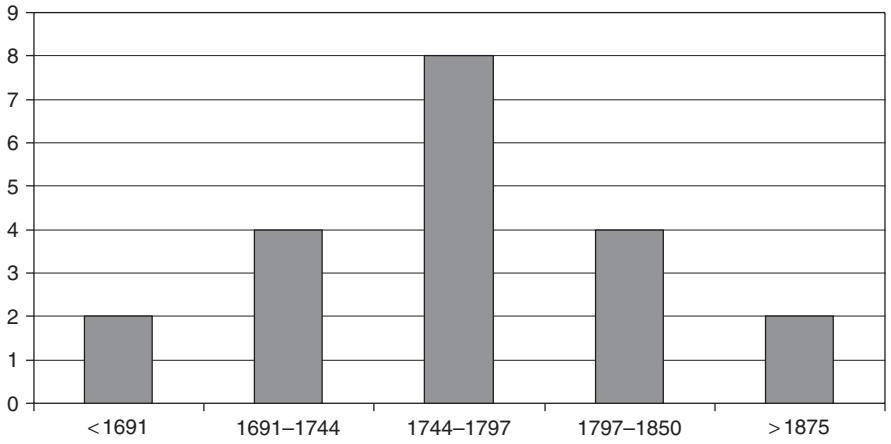

Figure 5.5 Distribution of sample of costs.

a y-coordinate, and elevation coupled with a graphical interface that displays these objects on a map. Generation units, power lines, transformers, substations, and buildings or other sites where loads occur can be represented in a GIS database and displayed on a computer screen so that a learner or a teacher can see clearly the components that make up the power system under study. In addition GIS provides a connection that permits linking the physical and economic databases of the electric grid to available sociopolitical databases, opening the possibility to study the effect of public policy, public perception, and other sociopolitical factors that influence decision makers in real systems. Coupling the GIS system to the simulation program provides a seamless interface for the user between data entry and KPIs. Figure 5.6 shows a flowchart of the kind of ESS that we advocate in this chapter.

The Electricity Grid and Market Simulator (EGMS) is a crucial part of the simulation program. Because of the modular nature of the components in an energy grid, object-oriented programming (OOP) is a good choice of coding paradigm for EGMS. In OOP, the computer program consists of *objects*. An object packages data (or *properties*) and data processing functions (or *methods*) into one unit. For example, a Time object may contain hour, minute, and second as its properties. The methods of the Time object may include assigning values to these properties and printing them in different time formats. The way an object-oriented program works is that the objects communicate with one another by sending and receiving messages among them. A message that an object receives can be an inquiry for a property of the object or a request for the object to perform one of its methods. After receiving messages from other objects, an object will process the data, and send the result to other objects. OOP has been widely used in large-scale software development for years because of the modularity, expandability, and reusability of the code. Unlike the traditional programming, keeping the OOP code up to date is relatively easy and cost effective. These advantages are so compelling that we cannot imagine coding an EGMS without OOP.

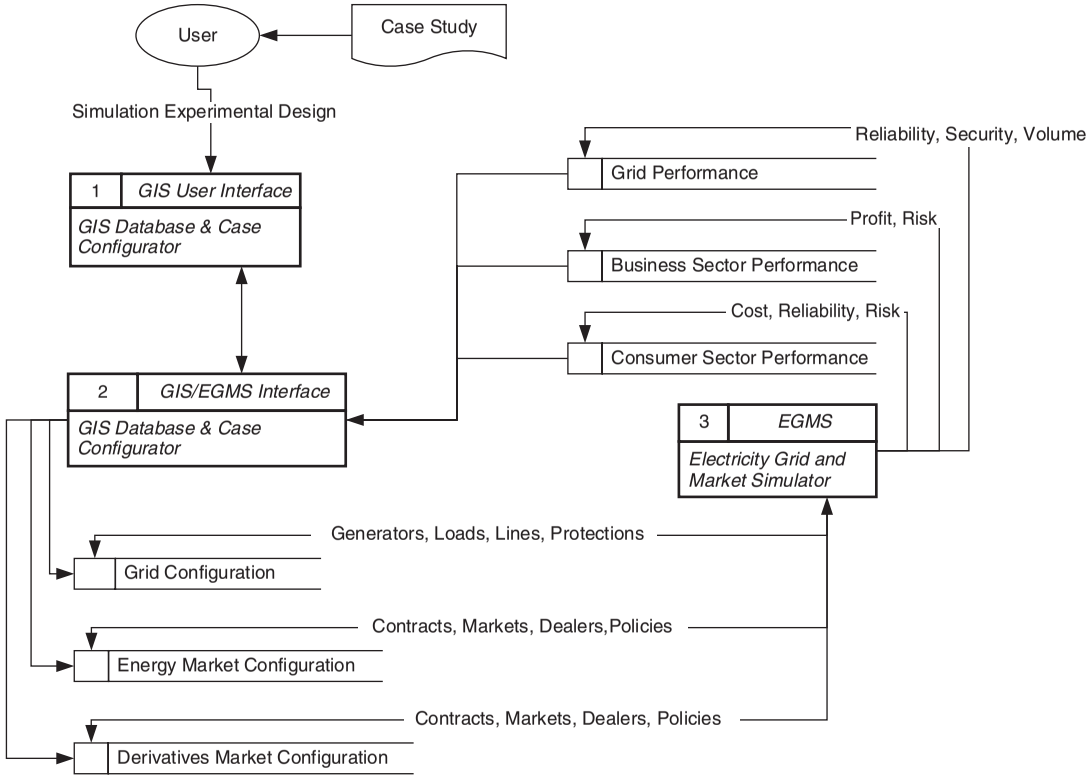

Figure 5.6 Data flow diagram of ESS.

In order to program EGMS using OOP, we define the following main objects:

1. *Grid operations model (GOM)* Simulates planning, scheduling, dispatching and controlling an electrical grid.
2. *Risk management model (RMM)* Assesses the financial risk and develops strategies to manage it.
3. *Energy market model (EMM)* Evaluates market performance.
4. *System configuration model (SCM), simulation controller (SC), output stream summarizer (OSS), output statistical analyzer (OSA)* Manage the simulation program, data entry, and output reporting.

Figure 5.7 depicts the relationships among these objects. When the simulator runs, GOM reads the grid configuration, simulates the electricity flows, and updates the grid performance. RMM reads the grid performance and derivatives market configuration, performs risk analysis, and updates the risk portfolio performance. EMM reads the risk portfolio performance as well as the market configuration and grid performance and outputs the consumer sector performance and business sector performance. All these events are executed for each time interval of the simulation.

To simulate the power flows with GOM, we need to solve a set of power-flow optimization problems (see [14,20]). Solving such optimization problems is the most computationally intensive part of the simulator. Since the flows must be updated for every simulated time interval, the speed of the simulator could become a problem if the code for solving the optimization problems is not efficient. Writing an efficient optimization routine from scratch could be very time-consuming. Fortunately, some proprietary software packages, such as CPLEX and IMSL, provide routines for these purposes. With years of research and development invested in these software packages, their routines have proved to be efficient and reliable. Consequently the construction of EGMS should be integrated with these routines.

5.2 CONCEPTS FOR MODELING POWER SYSTEM MANAGEMENT AND CONTROL

The determination of optimal power flow in a grid over a sequence of time periods can be modeled as a set of decisions and actions that execute the workings of the energy markets and the technical control of the electricity grid. In the operation of real energy markets and grids as well as in a simulation of these systems, the operational decisions are supported by computerized models. These models manifest several challenging features of mathematical modeling and optimization, which we describe below in a constructive sequence.

5.2.1 Large-Scale Optimization and Hierarchical Planning

The control of markets and electricity grids requires coordinated decision-making across five decision domains:

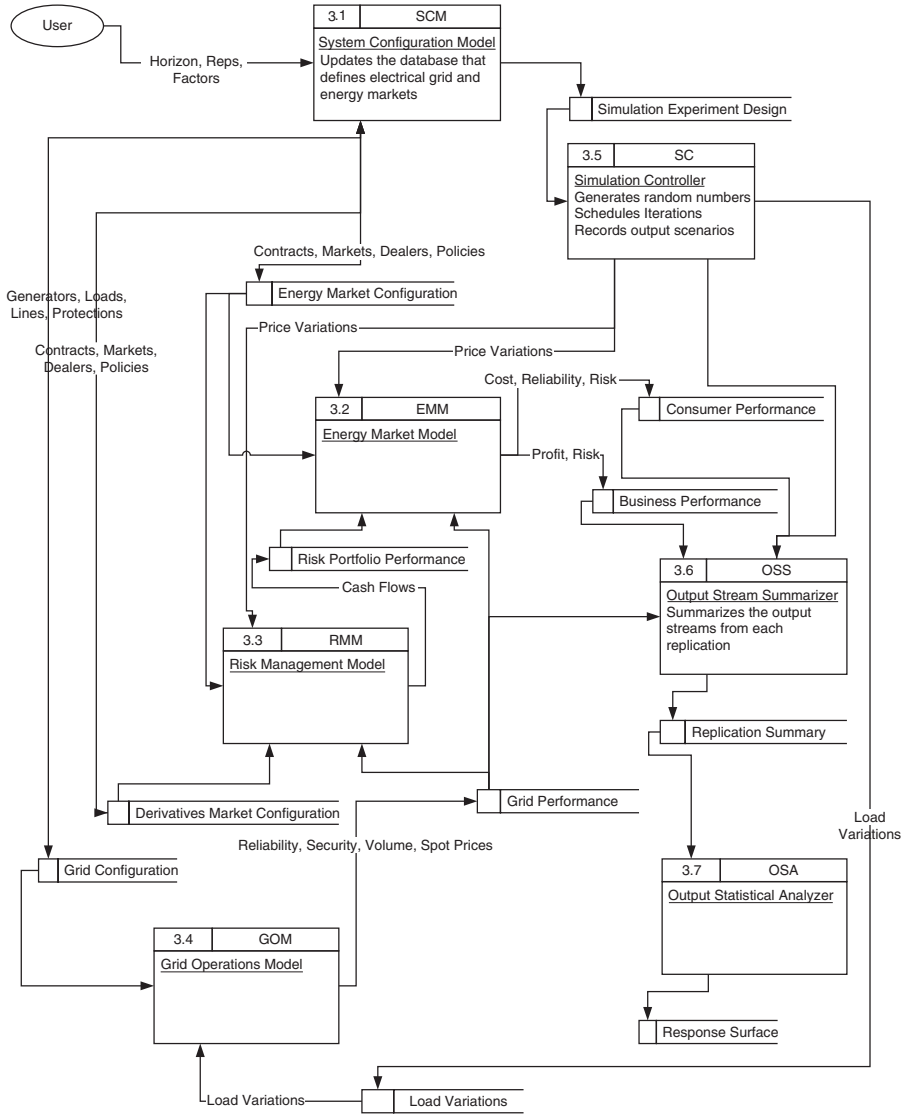

Figure 5.7 Data flow diagram of EGMS.

1. *Configuring* Installed generation capacity, grid configuration, and market regulations
2. *Planning* Bilateral contracts, wholesale bids and offers, and unit availability
3. *Scheduling* Unit commitment, ancillary service contracts, and reserve requirements

4. *Dispatching* Unit dispatch, demand management, and regulation
5. *Controlling* Voltage control, frequency control, and circuit protection

The large number of variables that these decisions encompass classifies this collection of decisions as a large-scale optimization problem. There is no practical decision-support system that can simultaneously optimize all these decisions. Consequently power grid and market management is carried out through the application of some conventional heuristic approaches.

A heuristic approach that is often used is one that is based on a hierarchical sequence of decisions that lead, through successive levels of detail, to a final solution. The basic idea behind hierarchical planning is that the solution to a rough-cut representation of a decision in terms of aggregated decision variables can serve as a set of guidelines and constraints for a refined decision in terms of detailed decision variables. In other words, the final solution to a problem can be achieved by first "coarse-tuning" the solution and then "fine-tuning" the solution.

In the case of energy grid management, the conventional hierarchy of decision making conforms to the ordered list shown earlier. For example, the problems of determining the unit availability, unit commitment, and unit dispatch are all related through performance measures such as profit and service level, which depend on all three decisions. Rather than attempt to find solutions to these three decisions simultaneously so that a globally optimal solution is obtained, a hierarchical planning approach would specify three separate decisions to be solved in stages. The determination of unit availability, based on approximate representations of total demand over the upcoming week, provides capacity constraints on the commitment and dispatching decisions. The commitment decision, based on a forecast of load variations over the next 36 hours for which real-time dispatching will be needed, consumes the bulk of the generation capacity and leaves a judicious amount of capacity for support of the imbalance dispatching decisions.

The intuitive appeal of this approach is found in the selection of decision variables for each level of the hierarchical planning process. The first level generally involves strategic decisions that have long-term effects such as unit availability. The second level involves decision variables that describe how the available assets are to be committed. The third level involves decision variables that describe how committed assets are to be dispatched. The fourth level and fifth levels involve decision variables that describe how dispatched assets are to be controlled. Under the hierarchical scheme long-range strategic decisions are made first. These decisions then impose constraints on the shorter range, more detailed decisions that follow. At each level the plan for the entire system is developed in more detail.

The approximation inherent in hierarchical planning is introduced in the modeling of the performance of lower level solutions at any stage in the hierarchy. In order to simplify each stage's problem, the effects of the lower level decision variables on the current stage's constraints and the objective function are approximated. In turn the solution to a higher level problem specifies constraints on the next lower level problem, and so on.

Using the "hat" notation to indicate approximations, the hierarchical planning approach is described as follows: suppose we have four sets of decision variables x_1, x_2, x_3, x_4 for the decision model,

$$\begin{aligned}
&\max\ f(x_1,\ x_2,\ x_3,\ x_4)\\
&\text{subject to :}\\
&g_1(x_1,\ x_2,\ x_3,\ x_4) \le 0\\
&g_2(x_1,\ x_2,\ x_3,\ x_4) \le 0\\
&\cdots\\
&g_n(x_1,\ x_2,\ x_3,\ x_4) \le 0
\end{aligned}$$

By approximating the effects of variables x_2, x_3, x_4, we construct the aggregate planning problem:

$$\begin{aligned}
&\hat{f}_1(x_1) \approx f(x_1,\ x_2,\ x_3,\ x_4)\\
&\hat{g}_{1j}(x_1) \approx g_j(x_1,\ x_2,\ x_3,\ x_4) \quad \text{for } j = 1, \ldots, n
\end{aligned}$$

The first optimization in the hierarchy is

$$\begin{aligned}
&\max_{x_1}\ \hat{f}(x_1)\\
&\text{subject to :}\\
&\hat{g}_{11}(x_1) \le 0\\
&\hat{g}_{12}(x_1) \le 0\\
&\cdots\\
&\hat{g}_{1n}(x_1) \le 0
\end{aligned}$$

The resulting solution, x_1^*, becomes a parameter in all the succeeding problems. The second approximate decision model is

$$\begin{aligned}
&\hat{f}_2(x_2) \approx f(x_1^*,\ x_2,\ x_3,\ x_4)\\
&\hat{g}_{2j}(x_2) \approx g_j(x_1^*,\ x_2,\ x_3,\ x_4)\\
&\max_{x_2}\ \hat{f}(x_1^*,\ x_2)\\
&\text{subject to :}\\
&\hat{g}_{21}(x_1^*,\ x_2) \le 0
\end{aligned}$$

$$\hat{g}_{22}(x_1^*,\ x_2) \leq 0$$

$$\ldots$$

$$\hat{g}_{2n}(x_1^*, x_2) \leq 0$$

The remaining optimization problems are formulated in a similar manner.

5.2.2 Sequential Decision Processes and Adaptation

The control of markets and electricity grids must be done on a continuous basis, which necessitates ongoing decision-making regarding the supply availability, demand management, unit commitment, dispatching, ancillary services, and regulation. For practical reasons, the planning horizon is divided into discrete time periods and the planning decisions are expressed and solved in terms of actions for each period. Of course, this discrete representation of the time scale for a process that changes continuously introduces an approximation. However, the notion of developing a plan in finer and finer detail as each level of hierarchical planning is executed applies to the time scale as well. Higher level, more strategic decisions are given a longer planning horizon and longer planning periods. By their nature these decisions can be made more crudely than tactical or operational decisions. As one moves down the hierarchy of decisions, the planning horizons and the planning periods are made shorter. Table 5.2 shows the basic scope and definition of the five levels of hierarchical planning that make up our model of power grid management.

A sequential decision process (SDP) is sequence of decisions made over time in a way that each decision can adapt to the effects of all previous decisions and adapt to the outcomes of uncontrollable influences on the performance measures. A general methodology for optimizing SDPs is known as decomposition or dynamic programming.

Dynamic programming decomposes an optimization by segregating the decision variables into subsets and creates a group of nested optimization problems. For example, suppose that we have four sets of decision variables x_1, x_2, x_3, x_4 representing the actions that can be taken at each of four time periods that make up the planning horizon and p_1, p_2, p_3, p_4 are the probability distributions of the random variables that influence the performance measures of the system that is to be controlled. Each performance measure may be expressed in terms of some measure of risk with respect to

TABLE 5.2 Planning horizons and periods

Decision Domain	Planning Horizon (typical)	Planning Period (typical)
Configuring	>1 year	>1 month
Planning	1 day - 1 year	1 day
Scheduling	36 hours	1 hour
Dispatching	1 hour	5 minutes
Controlling	0.5 hour	<5 seconds

these random influences. The decision model for optimizing the plan can be stated as

$$\max\ f(x_1,\ x_2,\ x_3,\ x_4;\ p_1,\ p_2,\ p_3,\ p_4)$$

subject to :

$$g_1(x_1,\ x_2,\ x_3,\ x_4;\ p_1,\ p_2,\ p_3,\ p_4) \leq 0$$

$$g_2(x_1,\ x_2,\ x_3,\ x_4;\ p_1,\ p_2,\ p_3,\ p_4) \leq 0$$

$$\ldots$$

$$g_n(x_1,\ x_2,\ x_3,\ x_4;\ p_1,\ p_2,\ p_3,\ p_4) \leq 0$$

The dynamic programming methodology transforms this optimization into a nested sequence of optimization problems with the decisions of later time periods nested with the decisions of earlier time periods. The optimization procedure starts with the innermost nested problem (last time period) and works in stages to the outermost problem (first time period). A dynamic programming formulation of the problem described above is built from the following nested set of optimizations:

$$\max_{x_1}\left(\max_{x_2}\left(\max_{x_3}\left(\max_{x_4} f(x_1,\ x_2,\ x_3,\ x_4;\ p_1,\ p_2,\ p_3,\ p_4)\right)\right)\right)$$

At each stage the optimization procedure derives optimal decision rules as opposed to optimal decisions. A decision rule is a set of contingency-based decisions. In this case the contingencies at any stage are the combined effects of all outer decisions (not yet determined by the optimization procedure) as well as the range of uncontrollable influences on the performance measures over the time periods prior to the stage's decision. Through this methodology we can explicitly express the decision rule for each time period in terms of the outcomes of the random variables of all previous periods. Such a representation of the decision rule accurately portrays the real situation that is faced by the decision maker in each time period.

The correct solution to a stochastic, sequential decision process consists of the state-contingent decision rules generated by the dynamic programming solution. However, the derivation of the large number of such decision rules that would be necessary for a problem as complex as that of unit commitment and dispatch precludes the use of dynamic programming. Instead, planning for stochastic load and generation levels is achieved through the use of a control heuristic known as rolling horizon and adaptation. This procedure is used commonly in the commitment and dispatching of generation units.

Rolling horizon and adaptive control is executed through the combination of three planning techniques:

- *Rolling the plan* Plans are updated at regular intervals. The time between updates is called the planning interval.
- *Planning over a horizon* Each plan extends over a number of future time periods. The time over which a plan is derived called the planning horizon.

- *Adapting the plan* At each update of the plan, the plan is adjusted within limits that are determined by the system's constraints on the rates at which resource flows can change. The planning horizon for each plan consists of a horizon over which the plan must be "frozen" followed by a horizon over which adjustments are allowed. The boundary between the fixed portion of a plan and the adjustable portion of a plan is called the planning "fence."

In the case of electricity scheduling and dispatch, there are four adaptation options. Table 5.3 defines these options. Each option is constrained to be exercised within the capacities that are set by the capacity reservation decisions made at a higher level of the decision-making hierarchy (see the previous section). The update intervals, planning horizons and time fences given in Table 5.3 are typical values in the operation of a large power grid.

The approximation that is inherent in a rolling horizon and adaptation procedure stems from the use of a deterministic forecast for each plan update. The accuracy of this forecast increases as the forecast horizon decreases. Consequently the adaptation options with the shortest time fences enjoy the most accurate forecasts and can be viewed as "fine-tuning" actions with respect to the "coarse-tuning" of the plans produced by the longer fence options.

TABLE 5.3a Capacity and demand constraints on scheduling options

Scheduling Option	Capacity Constraint	Demand Constraint
Day-ahead unit commitment	Day-ahead offers	Day-ahead bids
Imbalance commitment	Imbalance offers	Imbalance bids
Regulation reserve commitment	Regulation reserves offers	Regulation forecast
Spinning reserve commitment	Spinning reserves offers	Control error forecast

TABLE 5.3b Scheduling option parameters

Scheduling Option	Update Interval	Planning Horizon	Time Fence
Day-ahead unit commitment	24 hours	36 hours	12 hours
Imbalance commitment	24 hours	30 hour	6 hours
Regulation reserves	8, 16 hours	9, 17 hours	1 hour
Spinning reserves	8, 16 hours	9, 17 hours	1 hour

TABLE 5.3c Capacity and demand constraints on dispatching options

Dispatch/Control Option	Capacity Constraint	Demand Constraint
Day-ahead dispatch	Day-ahead commitments	Day-ahead commitments
Real-time dispatch	Imbalance commitments	Demand forecast
Ancillary service regulation	Regulation reserve commitments	Regulation error
Voltage/frequency control	Spinning reserve commitments	Control error feedback

TABLE 5.3d Dispatching option parameters

Dispatch/Control Option	Update Interval	Planning Horizon	Time Fence
Day-ahead unit commitment	8, 16 hours	9, 17 hours	1 hour
Real-time dispatch	1 hour	1.5 hours	30 minutes
Ancillary service regulation	5 minutes	30 minutes	5 minutes
Voltage/frequency control	4 seconds	30 seconds	4 seconds

5.2.3 Stochastic Decisions and Risk Modeling

Demand for electricity and, to a lesser degree, supply are not known with complete certainty, a priori. For this reason decisions regarding supply availability, demand management, unit commitment, dispatching, ancillary services, and regulation involve some risk. Such decisions are labeled stochastic. There are several approaches to coping with risk, all of which incorporate some combination of buffering and adaptation.

In our model we use a measure of financial risk known as value at risk (VAR). For every business decision the decision maker has some desired level of financial performance that is considered satisfactory. However, due to the uncertainties of the real world, the financial performance of any decision is a random variable that can take on a range of values with probabilities given by a distribution that is known through the modeling of the decision. Ranking all of the scenarios for this random variable according to their associated financial performances, the decision maker can apply his/her own perspective on risk by specifying a probability that identifies the portion of these scenarios that constitute the "downside" risk of the decision. For example, a decision maker could consider the lowest performing 10% of scenarios as the downside potential of a decision. Once this probability is set, the minimum financial loss that the downside scenarios can generate, measured relative to the pre-defined satisfactory level of return, is called the value at risk. VAR is typically computed over a risk horizon of one day and suffices to represent the exposure of a portfolio of contracts to downside risk from falling prices or falling demand. Figure 5.8 illustrates the concept of VAR.

Mathematically, pursuing the minimization of VAR or constraining VAR below some tolerable limit is equivalent to adopting the key performance indicator of the cumulative probability of returns:

V = satisfactory return

C = actual cash flow

$V - C$ = financial loss

α = risk level

L = tolerable loss

F_C = cumulative distribution of cash flow

$V - F_C^{-1}(\alpha)$ = value at risk

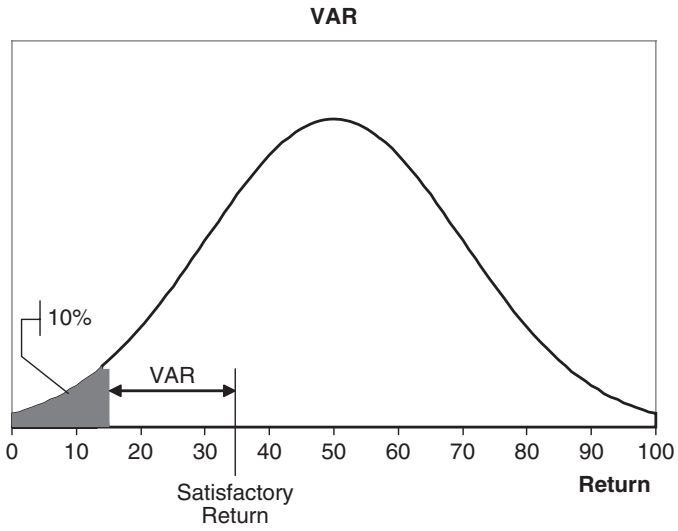

Figure 5.8 Value-at-risk example.

The constraint on *VAR* is $V - F_C^{-1}(\alpha) \leq L$, which can be expressed more simply as $F_c(V - L) \leq \alpha$.

Risk measures have received much research attention over the last several decades and this brief discussion of VAR does not do justice to the depth of understanding of the nature of risk that this research has revealed. The interested reader is referred to [18].

5.2.4 Group Decision Making and Markets

In a regulated power industry, the reservation, commitment, and dispatching decisions are made by a single authorized manager of the power grid. In the case of a single decision-making authority, a decision can be modeled with a single objective function and accompanying constraints. However, in the case of partially regulated power grid, supply-availability decisions and demand-management decisions involve numerous decision makers, each pursuing his/her own self-interests. Hence markets are born and the decision models that describe the choices of market participants must recognize the different objectives and constraints of each market participant.

We model each market with a hierarchy of decision models in which capacity reservations are achieved in the form of bids and offers that are entered into each market by load-serving entities and suppliers of electricity, respectively. The grid operator then executes the commitment and dispatching decisions by clearing the markets, which sets the market-clearing prices at each basis point in such a way that all demand constraints are met and the total cost of power to the entire grid is minimized. Table 5.4 lists the markets that typically drive the management of the grid.

TABLE 5.4a Wholesale markets

Market	Transaction	Price	Buyer	Seller	Delivery Node
LTC	Bilateral contract	Bilateral	ISO/DSO	IOU/SA	Gen bus
	Bilateral contract	Bilateral	LSE	ISO/DSO	Load bus
Day ahead	Unit commitment	LMP	ISO/DSO	IOU/SA	Gen bus
	Load commitment	LMP	LSE	ISO/DSO	Load bus
Imbalance	Unit dispatch	Real-time LMP	ISO/DSO	IOU/SA	Gen bus
	Load dispatch		LSE	ISO/DSO	Load bus
Regulation	Operating reserves	Real-time LMP	ISO/DSO	IOU/SA	Gen bus
AS	Ancillary service		LSE	ISO/DSO	Load bus
Spinning	Reserve allocation	Reserve LMP	ISO/DSO	IOU/SA	Gen bus
AS	Ancillary service		LSE	ISO/DSO	Load bus

TABLE 5.4b Retail markets

Market	Transaction	Price	Buyer	Seller	Delivery Node
Bilateral, Regulated	Long-term contract	Bilateral	Consumer	LSE	Load bus

AS = ancillary services

DSO = distribution service operator, distribution grid manager

IOU = investor owned utility

ISO = independent service operator, grid manager

LMP = locational marginal price

LSE = load-serving entity or load aggregator

SA = supply aggregator

5.2.5 Power System Simulation Objects

A simulation of a power system that portrays the behavior of the system hour by hour over a period of many days must mimic the behavior of the power grid's hardware as well as the decision-making of the customers, suppliers, and grid operators who collectively manage the power system. In order to execute the simulated actions of market bidding/offering, unit commitment, and unit dispatch in the same sequence with which these actions take place in the real system, a computer simulation of must contain software objects that behave as the decision-making agents and the grid controllers. In this section we describe the objects that form the building blocks of a typical power-grid simulation. Specifically, we present the design of a simulation package called the Virginia Tech Electricity Grid and Market Simulator (VTEGMS). Figure 5.9 shows a flowchart of the interactions of these objects within VTEGMS.

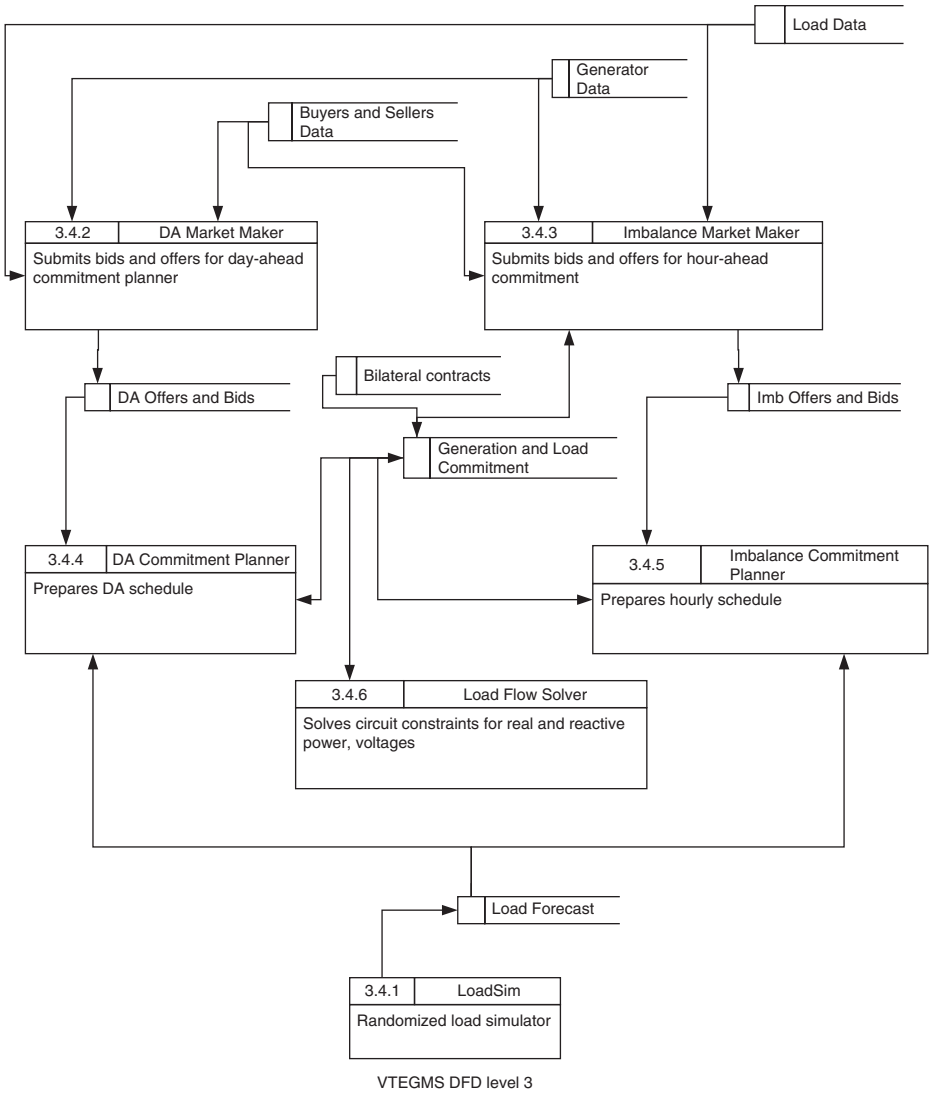

Figure 5.9 Simulation of grid-driving decisions.

5.3 GRID OPERATION MODELS AND METHODS

In this section we describe the models and optimization methods that are used in VTEGMS, which are also typical of any EGMS. The reader should refer to Figure 5.9 to see how each of the each of the models described in this section is integrated into the EGMS.

5.3.1 Randomized Load Simulator

A time series of demand as well as a time series of demand forecasts initiates the decisions of market bidding and offering. As we stated earlier, random parameters and random events are represented in a computer simulation through the use of random number generators (RNG). A simple example of the need for random numbers in a simulation is the requirement to represent randomly varying load over the time horizon modeled by the simulation. Formulas (5.1) through (5.3), adapted from [19], shows a typical load-forecasting formula that would be used to represent load for hour h of day d of a simulated horizon.

$$L_{h,d} = L^P_{h,d} + L^S_{h,d} \tag{5.1}$$

where

$$L^P_{h,d} = \alpha_0 + \rho\, d + \sum_{r=1}^{H} \alpha_r \cos(\omega r d + \theta_r) + \sum_{i=1}^{K} \mu_i \delta_i \tag{5.2}$$

$$L^S_{h,d} = \phi_0 + \sum_{i=1}^{p} \phi_i z_{h,d} + \varepsilon_{h,d} \tag{5.3}$$

$L_{h,d}$ = total load

$L^P_{h,d}$ = potential load

$L^S_{h,d}$ = irregular load

α_0 = initial base load

ρd = trend component of load

$\sum_{r=1}^{H} \alpha_r \cos(\omega r d + \theta_r)$ = cyclical variations in load represented by H harmonics of an annual cycle

$\sum_{i=1}^{K} \mu_i \delta_i$ = load adjustments for the day of the week, holidays, etc.

$\phi_0 + \sum_{i=1}^{p} \phi_i z_{h,d}$ = autoregressive components of load

$\varepsilon_{h,d}$ = random component of load assumed to be normally distributed with a mean of zero and a standard deviation of $\sigma_{h,d}$

For any day d and hour h, all of the terms in these formulas except $\varepsilon_{h,d}$ would be known parameters that the modeler would enter into the simulation program's database. The random component of load must be represented in the simulation

program as a different value each time the load for day d and hour h is simulated. To do this, the simulation program generates a stream of numbers that have the properties of random drawings of numbers from a normal distribution with a mean of zero and a standard deviation of $\sigma_{h,d}$.

A RNG is a computer program that can produce a stream of numbers that appear to have come from a specified probability distribution. These streams are actually computed deterministically by a recursion formula, so they are more appropriately called pseudorandom numbers. However, pseudorandom numbers have all of the statistical properties of numbers that are randomly generated from a physical process as well as some nonrandom properties that make them very useful for simulation studies. The essential properties of RNGs are as follows:

1. RNGs generate numbers that are uniformly distributed between 0 and 1. A uniformly distributed stream of numbers can be transformed into a stream of numbers that appears to come from any other probability distribution through standard computational techniques.
2. Each number generated in a stream of numbers should be statistically independent of all numbers generated previously and independent of all numbers to be generated afterward. This ensures that we are not instilling unwanted memory into the behavior of the simulated system.
3. A stream of random numbers should be reproducible. This allows one to perform multiple simulation runs in the context of a simulation experiment in which all factors, including the random influences, are controlled except those that we wish to change for the sake of the experiment.
4. The computer program that generates the random numbers should be efficient in terms of computing time and data storage requirements.

Pseudorandom numbers are not truly random. They have a "period" or "cycle length," so a stream of pseudorandom numbers will at some point repeat itself. The pseudorandom number generators embodied in simulation models are constructed so that the length of the period is very long, alleviating concern about this property causing the numbers to be dependent on one another.

The pseudorandom numbers are generated by a deterministic formula. This makes them well defined and also gives them the reproducibility property that we desire. The linear congruential method, which we describe in its simplest form below, is the most common method for generating pseudorandom numbers in the interval [0, 1). Consider a stream of numbers $x_0, x_1, \ldots$, such that

$$x_{i+1} = (ax_i + b) \text{mod} c$$

$$r_{i+1} = x_{i+1}/c$$

$$x_0 = \text{seed}$$

a, b, and c are chosen in order to give the stream the longest period possible. For example, let $w =$ the number of bits/word on the computer used to generate the

random numbers. Then

$$c = 2^w$$

$$b = \text{relatively prime to } c$$

$$a = 1+4k, \text{ where } k \text{ is an integer}$$

Once a stream of pseudorandom numbers in the interval [0, 1) are generated they can be translated into a stream of numbers that appears to have been drawn from any specified probability distribution such as the normal distribution of mean 0 and standard deviation $\sigma_{h,d}$ in the load-forecasting example described earlier. Although it is beyond the scope of the treatment of simulation offered in this chapter, this transformation is straightforward and is easily coded into a simulation software package.

The interested reader is referred to [5] for more information about the structure of simulation programs and simulation modeling. An overview of simulation models specifically for modeling electricity markets is provided in [2].

5.3.2 Market Maker

Following the hierarchy of decisions, we model the planning decisions in terms of the market strategies of buyers and sellers. In the day-ahead and imbalance wholesale markets, each supply aggregator offers generation capacity in the form of a "stack," which is a list of ordered pairs of power quantities and associated offer prices. When the market clears, any power that was offered at or below the market-clearing price will be sold by the supply aggregator at the market-clearing price. Similarly each load aggregator bids on power in the form of a stack in terms of power quantities and associated bid prices. When the market clears, any power that was bid at or above the market-clearing price will be purchased by the load aggregator at the market-clearing price.

The market maker object of the simulation applies the auction rules described above for determining the optimal offer and bid functions of each player in the market. That is, for the simulation of a power market associated with a particular power grid we construct an instance of the market for each buyer and seller of power and for each type of energy auction. We can specify these instances using the following notation:

m = market identification = *ltc* (long-term, bilateral contract), *da* (day-ahead wholesale), *imb* (imbalance, wholesale), *reg* (regulation reserve), *con* (control reserve)

M_z^m = market-clearing price for zone z in market m

$\overline{M}_z^m$ = price cap for M_z^m

$\underline{M}_z^m$ = price floor for M_z^m

$z(k)$ = zone to which generator or load element k belongs

$B_{kj}^m = j$th bid price for power in market m from load element k

$O_{kj}^m = j$th offer price for power in market m from generator k

S_G = set of all generator circuit branches
S_A = set of all transmission lines
S_S = set of supply aggregators
S_L = set of load aggregators
S_{Gn} = set of generators marketed by supply aggregator n
S_{Gn} = set of loads represented by load aggregator n
S_B = set of all busses
$P_{kj}^m = j$th power segment bid or offered in market m at load or generator element k
P_k^m new power commitment in market m in the planning period at load or generator element k

The market model for availability planning ($m = da$, rt) for each $n \in S_S$ is

$$\max_{\{(O_{kj}^m, P_{kj}^m) | k \in S_{Gn}\}} \sum_{k \in S_{Gn}} E[R_k]$$

subject to:

$$\text{Prob}\left(\sum_{k \in S_{Gn}} R_k < V_n \right) < \alpha_n$$

where

$$R_k = M_{z(k)}^m P_k^m$$
$$P_k^m = \sum_{O_{kj}^m \le M_{z(k)}^m} P_{jk}^m$$

The market model for demand planning $(m = da, rt)$ for each $n \in S_L$ is

$$\min_{\{(B_{kj}^m, P_{kj}^m) | k \in S_{Gn}\}} \sum_{k \in S_{Ln}} E[R_k]$$

subject to :

$$\text{Prob}\left(\sum_{k \in S_{Ln}} R_k > V_n \right) < \alpha_n$$

where

$$R_k = M_{z(k)}^m P_k^m$$
$$P_k^m = \sum_{B_{kj}^m \ge M_{z(k)}^m} P_{jk}^m$$

Solution Method In this section we propose a simple generic market model for the simulation object that represents the decision of an individual market player. This object is then instantiated in the simulation for each market participant in each market type. We assume a market for the buying and selling of power over a particular future time period that we will call the sale period.

c_i = internal capacity, or maximum volume, of an asset that the market player can offer (bid) for sale (purchase)

c_e = external capacity, or maximum volume, of the asset that the rest of the market can offer (bid) for sale (purchase) over the sale period

m = future market-clearing price of the asset, a random variable at the time offers (bids) are made

$\overline{m}$ = price cap for the market

$\underline{m}$ = price floor for the market

F_m = cumulative distribution function of m

d = maximum demand for the asset over the sale period

The decision that the market player must make is the set of prices at which each unit of volume will be offered (bid). In effect each market player presents a supply or demand function to the market. We define these decisions in terms of distribution functions:

$o_x(p)$ = fraction of the asset$'$ s maximum volume offered at prices $\leq p, x = e, i$

$b_x(p)$ = fraction of the maximum demand bid at prices $\geq p, x = e, i$

$0 \leq o_x(p) \leq 1$

$0 \leq b_x(p) \leq 1$

Note that $o(p)$ is right continuous and increasing and $b(p)$ is decreasing and left continuous. Conventional offer and bid mechanisms allow for the presentation of a "stack" of power to the market. The stack is a finite set of power volumes with associated prices. $\{(v_i, p_i)\}_{i=1}^{n}$. For offers, $o(p) = \sum_{p_i \leq p} v_i$, and for bids, $b(p) = \sum_{p_i \geq p} v_i$. For the purpose of this model, we assume that $o_i(p)$ is continuous and do_i/dp is continuous except at the point of contact with the boundaries of the constraints, $0 \leq o_i(p) \leq 1$

In what follows we derive the decision facing an individual power supplier. The model for an individual power buyer is analogous. The market clears at a price that matches supply to demand. This condition is expressed as

$$c_i o_i(p) + c_e o_e(p) = db(p)$$

We re-state the market-clearing condition as

$$o_i(p) = \frac{db(p) - c_e o_e(p)}{c_i}$$

We define the right-hand side of this expression as the normalized, residual-demand random process, $\hat{d}(p)$. The market-clearing condition is then

$$\hat{d}(p) = \frac{db(p) - c_e o_e(p)}{c_i}$$

$$o_i(p) = \hat{d}(p)$$

Note that $\hat{d}(p)$ is a random process that is decreasing and left-continuous in p and the market-clearing condition induces a market-clearing price that is a random variable. In other words, the residual demand process is a function of scenarios, $\omega \in \Omega$, which implies that the market-clearing price is also a function of scenarios, $m(\omega)$. The distribution of market prices can then be expressed in terms of the distribution (forecast) of residual demand:

$$F_m(p) = F_{\hat{d}}(o_i(p))$$

Figure 5.10 provides an example of a supply function and several scenarios for residual demand. The intersections of the supply function with the residual demand functions indicate the scenarios for market-clearing prices. When the market clears, the revenue (cost) that is accrued by a seller (buyer) can be evaluated as

$r(m) = mc_i o_i(m)$

$m =$ random variable, so r is a random variable

$F_r =$ cumulative distribution function of the cash flow $r(m)$ over the random variable, m

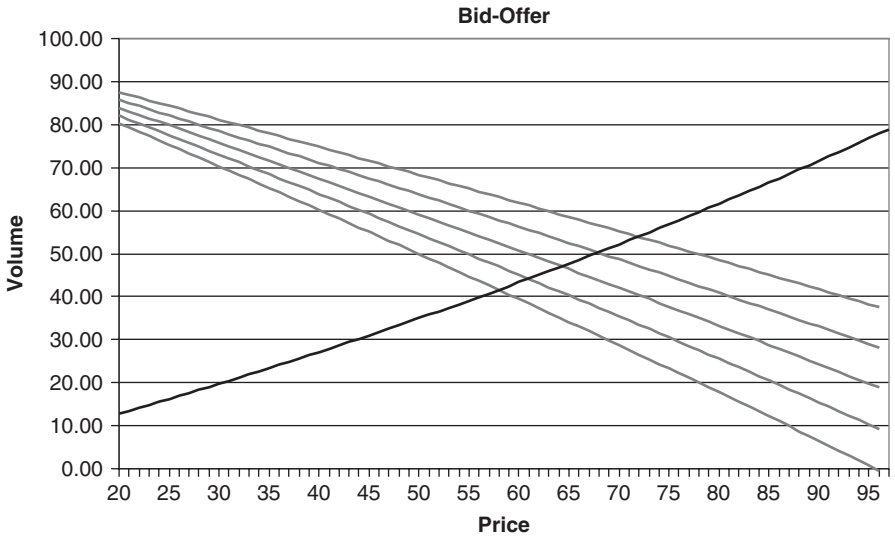

Figure 5.10 Example of residual demand scenarios and offer fraction versus price.

Note that

$$F_r(r(p)) = F_m(p) = F_{\hat{d}}(o_i(p))$$

The market player's key performance indicators are return and risk. The former measure is evaluated as the expected cash flow:

$$E[r] = \int_0^{\infty} r dF_r = \int_{\underline{m}}^{\overline{m}} c_i mo_i(m) dF_m = \int_{\underline{m}}^{\overline{m}} c_i mo_i(m) f_{\hat{d}}(o_i(m)) \frac{do_i}{dm} dm$$

In energy markets, risk is most commonly incorporated in the market decisions in terms of a constraint on value at risk:

$$F_r(V - L) \leq \alpha \quad \text{or} \quad \int_0^{V-L} dF_r \leq \alpha$$

By the monotonicity of $o_i(m)$, for any policy, o_i, there is a well-defined market-clearing price β for which

$$r(\beta) = V - L \quad \text{or} \quad o_i(\beta) = \frac{V - L}{\beta c_i} = \hat{d}(\beta)$$

Note that β is a function of the policy o_i. Furthermore the monotonicity of $r(m)$ implies that the risk constraint can be written equivalently as

$$F_m(\beta) \leq \alpha \quad \text{or} \quad \int_{\underline{m}}^{\beta} f_{\hat{d}}(o_i(m)) \frac{do_i}{dm} dm \leq \alpha$$

The risk constraint is incorporated into an objective function with a lagrange multiplier, μ.

$$J = \int_{\underline{m}}^{\overline{m}} c_i mo_i(m) f_{\hat{d}}(o_i(m)) \frac{do_i}{dm} dm - \mu \int_{\underline{m}}^{\beta} f_{\hat{d}}(o_i(m)) \frac{do_i}{dm} dm + \mu\alpha$$

Badinelli (2006) provides an optimal solution for the supply function by using optimal control theory.

5.3.3 The Commitment Planner

The market maker object is used in the simulation to determine the "stacks" of generation offers and load demands for each time period. The next stage in the planning and scheduling hierarchy is that which clears the market and the selects from the

generation and load stacks the power that will be supplied. However, in making this selection, the currents, voltages, generation, loads, and prices must satisfy numerous constraints. Subject to these constraints, minimizing the total cost of power that is needed to cover all of the loads is a typical objective function for power pools and grid operators. See PJM [15,16,17]. Hence we have an optimal power flow (OPF) problem that we must solve at every instance of commitment planning, which can be formulated approximately in terms of real power and capacity constraints (DC load flow model) as follows:

$\overline{P}_k$ = maximum allowed total power at load element or generator element k

$\underline{P}_k$ = minimum required total power at load element or generator element k element k

U_k = maximum upward ramp rate of generator element k

D_k = maximum downward ramp rate of generator element k

C_o^m = overhead cost of operating the grid for market m

λ_k = congestion cost charged to load element k

P_k^c = total currently committed power in the planning period at load or generator

$$P_k^c = \sum_{k \in S_{mk}} P_{kj}, \quad m = ltc$$

$$P_k^c = P_k^{ltc} + \sum_{k \in S_{mk}} P_{kj}, \quad m = da$$

$$P_k^c = P_k^{ltc} + P_k^{da} + \sum_{k \in S_{mk}} P_{kj}, \quad m = imb$$

$$P_k^c = P_k^{ltc} + P_k^{da} + P_k^{rt} + \sum_{k \in S_{mk}} P_{kj}, \quad m = reg$$

$$P_k^c = P_k^{ltc} + P_k^{da} + P_k^{rt} + P_k^{res} + \sum_{k \in S_{mk}} P_{kj}, \quad m = con$$

$\boldsymbol{I}^{\text{bus}}$ = vector of all *external* current phasors at each bus = currents injected to the grid by generators and currents drawn from the grid by loads

$\boldsymbol{Y}^{\text{bus}}$ = bus admittance matrix constructed from the admittances of all circuit elements

$\boldsymbol{V}^{\text{bus}}$ = vector of voltages at all generator and load busses

Note:

- The index k used in the notation for generators and loads refers to the unique circuit branch of the generator or load as opposed to the numerical identifier of the generator or load.
- Bilateral contracts can be modeled as bids and offers at the contract price.
- Must-serve loads (from bilateral contracts) can be modeled as bids at the price cap.

- Load shaping through the discretionary use of power can be modeled in terms of the bids.
- Load shaping through the use of islanded DG can be modeled in terms of the bids.
- Must-run generators (from self-scheduled generators) can be modeled as offers at the price floor.

Problem: OPF (*m = ltc, da, imb, reg, con*)

$$\min \sum_{k \in S_G} M_k^m P_k^m$$

Subject to:

Constraint Set 1

$P_k^c \geq \underline{P}_k$ for all generators, $k \in S_G$

$P_k^c \leq \overline{P}_k$ for all generators, $k \in S_G$

$U_k \geq P_k^c - P_k^c(t-1) \geq -D_k$ for all generators, $k \in S_G$

Constraint Set 2

$\underline{M}_z^m \leq M_z^m \leq \overline{M}_z^m$ for all zones, z

$P_k^m = \sum_{O_{kj}^m \leq M_{z(k)}^m} P_{kj}^m$ for all generators, $k \in S_G$

$P_k^m = \sum_{B_{kj}^m \geq M_{z(k)}^m} P_{kj}^m$ for all loads, $k \in S_L$

$\sum_{k \in S_L} (M_{z(k)}^m + \lambda_k) P_k^m - \sum_{k \in S_G} M_{z(k)}^m P_k^m \geq C_o^m$

Constraint Set 3

- Emissions constraints
- Regulatory constraints
- Inventory constraints for storable power generators

Constraint Set 4

$P_k \leq T_k$ for all lines $k \in S_A$

Constraint Set 5

$\mathbf{Y}^{\text{bus}} \mathbf{V}^{\text{bus}} = \mathbf{I}^{\text{bus}}$

$Q_k^{\min} \leq Q_k \leq Q_k^{\max}$ for all generators, $k \in S_G$

$V_k^{\min} \leq |V_k| \leq V_k^{\max}$ for all busses, $k \in S_B$

$\alpha_k^{\min} \leq \alpha_k \leq \alpha_k^{\max}$ for all busses, $k \in S_B$

Constraint set 1, expressed in terms of real power, reflects general physical limitations of generators. Several market constraints, shown in constraint set 2, are necessary

to model the behavior of the auctions that mechanize the day-ahead and imbalance markets. The last constraint in this set ensures that the power that is actually bought or sold is that which the market-clearing process selects and that revenues cover costs.

Constraint set 3 reflects special considerations of a particular power grid. Constraint set 4 consists of the thermal limits on the power lines of the grid. These constraints determine the congestion charge, λ_k, that is assigned to any load that cannot obtain power from the cheapest source of generation because of thermal limits on transmission lines that connect the load to this generation.

Finally, we must enforce the physical laws that govern real and reactive power within a circuit as well as limits on the phase and voltages of generator outputs. We assume that all voltages and currents attain their steady state, forced-response values during each interval. We do not include transient behavior in the solution. To this end we impose Kirchoff's current law and Kirchoff's voltage law on all circuit elements, leading to constraint set 5. We also impose quality conditions on the power that is made available throughout the grid in terms of the voltage magnitude and the amount of reactive power that is allowed.

Solution Method The rather large OPF problem is traditionally solved in two stages, following the decomposition approach described earlier. The first stage consists of constraint sets 1, 2, and 3. The optimization method can be any robust nonlinear programming method. The values of real power at all generation and load busses that this stage produces are used to solve the equality constraints in constraint set 5.

Stage 2 consists of solving constraint set 5 using the Newton–Raphson load flow method (see [12]). The solution to the load flow problem is then checked against constraint set 4. Violations are recognized via updated congestion charges that are applied to constraint set 3. Then the two-stage process is repeated until convergence is achieved.

5.3.4 Implementation

To date, there are several versions of simulation packages for modeling power systems. Each of these packages was designed for specific purposes and exhibits particular strengths as Table 5.5 indicates.

The fields of energy engineering, management and policy are burgeoning with the challenges of new technologies, business models, and regulatory changes. Education of future professionals in the energy economy will require intensive exposure to realistic problems and decisions that the future holds. The breadth of this exposure, as is indicated by our hierarchical list of decision problems, is broad enough to require ESS packages of widely varying scopes—from decision models for multiple-year horizons to models for hourly and minute-by-minute horizons and from decision models for broad public policy regulations and massive capital investments to models for control of small distributed generation units. We conclude that more simulation-based ESS packages are needed.

Finally, we emphasize the need for case studies in the education of professionals in the energy field. Computerized decision support systems alone are useful only

TABLE 5.5 Comparison of simulation packages

Package Name	Creator/Vendor	Scope	Key Features	Applications
VTGIS/EGMS	Virginia Tech [3]	Distribution grids & distributed generation	Interfaced with ESRIs ARCGIS package	Future application in university courses in electrical engineering, business, public policy
GE Maps	General Electric [11]	Regional grids	LMP computation, transmission constraints	Bid strategy, unit commitment, market studies, economic analysis
Aurora	EPIS, Inc. [10]	Regional grids	Nodal and zonal LMP computation, transmission constraints	Power flow computation; valuation of generation & transmission assets, FTRs, LTCs
SimRen	ISUSI [13]	Multi-region grids	Dispatches wind, solar, cogen as well as conventional generation	Generation technology selection, installed capacity planning
EMCAS	CEEESA [8]	Adaptive systems model of regional energy markets	Agent-based modeling and simulation	Electricity trading strategies, economic analysis
STEMS	EPRI	Short-term markets	Agent-based modeling and simulation	Energy market design, trading strategies

to professionals who already understand the decision problems to which they apply these systems. However, learners must view each decision problem in a holistic, multidisciplinary manner in order to understand fully the trade-offs inherent in the problem. Only well-crafted case studies that are supported by companion computerized decision support systems can impose this view.

BIBLIOGRAPHY

1. Acha, E., Fuerte-Esquival, C., Ambriz-Perez, H., and Angeles-Camacho, C. *FACTS Modelling and Simulation of Power Networks*. Wiley, Hoboken, NJ, 2004.
2. Amelin, M. *On Monte Carlo Simulation and Analysis of Electricity Markets*. PhD dissertation. Royal Institute of Technology Department of Electrical Engineering, Stockholm, 2004.

3. Badinelli, R. "Unit Commitment and Market Strategies for Distributed Generation," Presentation at National INFORMS meeting, Pittsburgh, November, 2006.
4. Badinelli, R., Centeno, V., and Gregg, M. "A Technological Tool and Case Studies for Education in the Design and Management of a Secure and Efficient Distributed Generation Power System." NSF supplemental grant proposal No. ECS-0323344, 2004.
5. Banks, J., Carson, J., Nelson, B., and David, N. *Discrete-Event System Simulation*, 4th ed. Prentice Hall, Upper Saddle River, NJ, 2005.
6. Barnes, Christensen, and Hansen. *Teaching and the Case Method*, 3rd ed. Harvard Business School Press, Boston, 1994.
7. Bodily, Caraway, Frey, and Pfeifer. *Quantitative Business Analysis Text and Cases*. McGraw-Hill, New York, 1998.
8. Center for Energy, Economic, and Environmental Systems Analysis (CEEESA). *Electricity Markets Complex Adaptive Systems (EMCAS)*. Argonne National Laboratories, 2002. http://www.dis.anl.gov/CEEESA/downloads/emcas_brochure.pdf.
9. Depablos, J., DeLaRee, J., and Centeno, V. "Identifying Distribution Protection System Vulnerabilities Prompted by the Addition of Distributed Generation." *Proc. CRIS Conf. Protecting Critical Infrastructures*, Grenoble, France, October 25–27, 2004.
10. EPIS. *Auroraxmp® and PowerWorld® Simulator*, 2005. http://www.epis.com/Products/OneSheet-APWSI%20050412.pdf.
11. General Electric. *MAPS™ Software, GE*. 2005. http://www.gepower.com/prod_serv/products/utility_software/en/ge_maps/index.htm.
12. Grainger, J. J., and Stevenson, W. D. *Power Systems Analysis*. McGraw-Hill, New York, 1994.
13. Herbergs, S., Lehmann, H., and Peter, S. *The Computer-Modelled Simulation of Renewable Electricity Networks*. Institute for Sustainable Solutions and Innovations, Aachen, Germany. 2005. http://www.susi-con.com/downloads/simren.pdf#search='simulation%20%20electricity.
14. Momoh, J. A. *Electric Power System Applications of Optimization*. Dekker, New York, 2001.
15. PJM. *Manual #10, Revision 16: Pre-Scheduling Operations* (12/24/2003).
16. PJM. *Manual #11, Revision 23: Scheduling Operations* (12/07/2004).
17. PJM. *Manual #12, Revision 11: Dispatching Operations* (01/01/2005).
18. Smithson, C. *Managing Financial Risk*. McGraw-Hill, New York, 1998.
19. Soares, L., and Medeiros, M. Modeling and Forecasting Short-Term Electricity Load: A Two-Step Methodology. *Working paper 495*. Department of Economics, Pontifical Catholic University of Rio de Janeiro.
20. Soman, S., Khaparde, S., and Pandit, S. *Computational Methods for Large Sparse Power Systems Analysis, an Object Oriented Approach*. Kluwer Academic, Dordrecht, 2002.
21. Wasserman, S. *Introduction to Case Method Teaching*. Teachers College Press, New York, 1994.

6

DISTRIBUTED GENERATION AND MOMENTUM CHANGE IN THE AMERICAN ELECTRIC UTILITY SYSTEM: A SOCIAL-SCIENCE SYSTEMS APPROACH

Richard F. Hirsh, Benjamin K. Sovacool, Ralph D. Badinelli

Virginia Tech

6.1 INTRODUCTION

The past several decades have witnessed significant change in the American electric utility system. The once-stable, secure, and regulated system no longer retains as much government oversight as in the past; it is being moved increasingly by the invisible hand of a competitive marketplace. While proponents of the evolving new system laud many of its benefits, others point to disturbing signs of increased susceptibility to terrorist attacks (and other disruptions) and decreased overall reliability. Novel approaches for restructuring the utility system continue to be made, reflecting the uncharacteristically fluid state of affairs that exists today.

This chapter explores the long-term trends in the electric utility system and the beginning of efforts to restructure it. To frame the analysis, the chapter draws on a nonengineering version of the systems approach that has been fruitfully developed for understanding sociotechnical endeavors. The social-science systems approach provides a macroscopic way to view long-term trends. Going beyond consideration of engineering concerns, it encourages an understanding of the stakes, interests, and actions of a host of participants who make and use technologies. Such a view

Operation and Control of Electric Energy Processing Systems, Edited by James Momoh and Lamine Mili

suggests that engineering concerns held by managers and technical leaders often do not necessarily determine the way a technological system emerges. Rather, economic, social, and political factors may play more important roles in moving elements of a system.

Applying the social-science systems approach, the chapter views the present time as a rare opportunity in which entrepreneurs can pursue implementation of a non-traditional type of generation technology. Known as distributed generation (DG), the family of technologies consists of small-scale, decentralized hardware that, if structured properly, can provide greater reliability, security, and efficiency to the utility system.

The chapter begins with a discussion of the social-science systems approach, highlighting the notion of momentum, a combination of technical and social components that give a system an apparent direction, speed, and inertia. It describes the origins of momentum in the system and explores the reasons why that momentum has diminished dramatically starting in the 1970s. To help create new momentum, proponents of distributed generation seek to gain acceptance for a host of potential benefits while eliminating impediments and uncertainties. The chapter concludes with an analysis of DG within the business environment and a suggested model that may succeed in advancing the new technology within a system that develops new momentum.

6.2 OVERVIEW OF CONCEPTS

6.2.1 Using the Systems Approach to Understand Change in the Utility System

To gain a sense of the development of electric utilities, we employ the social-science version of the systems approach that was originally conceived of by Thomas Hughes. In his influential *Networks of Power: Electrification in Western Society* [1] and other publications, Hughes posits that the generation, transmission, and distribution of power takes place within a technological system. The system, however, goes beyond consideration of engineering elements (though they are components), including a "seamless web" of factors characterized as economic, administrative, educational, legal, and technical. Modern technological systems weave these considerations into one fabric, as system-builders (often business managers) seek to "construct or ... force unity from diversity, centralization in the face of pluralism, and coherence from chaos" [2]. When successful, the managers help the system expand and flourish. At the same time, the system closes itself. Put differently, as the system grows, the influence on it from the outside environment diminishes, largely because the system's scope has enveloped elements that might have altered it [2].

The systems approach also comprehends the notion of momentum, which Hughes describes as a mass of "machines, devices, structures" and "business concerns, government agencies, professional societies, educational institutions and other organizations" that contains "a perceptible rate of growth or velocity" [1]. In other words, momentum

can be viewed as a "mass of technological, organizational and attitudinal components [that tend] to maintain their steady growth and direction" [3]. The inclination of a system to evolve in a certain direction stems from the actions of a host of participants, such as regulatory bodies, educational institutions, the investment of money in operating hardware, and the efforts and industry culture of people working within the system. Momentum may also be aided by barriers to entry that favor established players, market and corporate dominance in an industry, and the lengthy lead times needed to develop new technologies. At the same time, momentum can grow due to the inertia of customers who may see few motivations to change buying habits, as well as due to market education and difficult-to-alter product life cycles. Together, these elements encourage business as usual and the noticeable demonstration of momentum. Hughes further argues that momentum can be abetted through employment of "conservative" inventions, namely new hardware that maintains the existing system. Leaders of system momentum clearly seek to preserve their dominance, and they avoid encouragement of novel and "radical" technologies that would displace their control. For example, Internet telephony and cell phones could be considered radical inventions by the corporate leaders of the conventional wired communications network.

In short, the social-science systems approach views the development of systems as the result of managers' efforts to command elements that exploit the human, natural, and technical environment. As systems gain momentum and mature, they resist change. Even so, momentum does not imply determinism (which suggests that social or technical elements determine technological development) or autonomy (which implies that technologies evolve independent of human action). Instead, system momentum can often be changed due to a confluence of technical, economic, and political factors. As will be described in this chapter, the electric utility system has recently seen its momentum change in a way that provides opportunities for the introduction of distributed generation facilities.

6.2.2 Origins and Growth of Momentum in the Electric Utility System

The electric utility system had humble beginnings near the end of the nineteenth century when the United States saw creation of a flourishing corporate-based economy. Large multi-level companies exploited the potentials of new communications and transportation technologies to manage production and distribution of quantity-produced goods, thus overthrowing the once-common family-owned and operated businesses. The railroad industry served as the epitome of modern enterprises that exploited new technologies to eliminate regional competition, to gain octopus-like political and economic power, and to earn the contempt of many of its customers [4].

The fledgling electric utility companies that emerged after Thomas Edison opened his small Pearl Street, New York City power station in 1882 did not appear to be in the same class as the large, and often reviled, railroad corporations. After all, Edison conceived of a decentralized system within cities that included scores of relatively small generation plants, each providing direct-current (DC) power to individual

businesses. But rapid innovation in electric power production equipment altered the relatively benign character of business. Adopting alternating-current (AC) transmission and steam-turbine technologies, early utility entrepreneurs quickly found they could emulate trends in other industries. Through the use of transformers made available in the late 1880s, AC transmission allowed companies to distribute high-voltage power over long distances. And in the first decade of the twentieth century, utility managers began employing compact steam turbines as prime movers, which further encouraged centralization because the new machines offered tremendous economies of scale. (Put simply, as the turbines, connected to generators, produced larger capacities of power, the unit cost of electricity declined over a broad range of output.) Becoming the core conservative technologies used in the electric utility system, steam-turbine generators and alternating-current technologies yielded exponentially growing supplies of power, produced at higher thermal efficiencies and at lower costs and prices. Electricity changed from being viewed as an expensive product used only in special situations to a cheap commodity that Americans considered a necessity and right. While residential customers in 1892 paid about 520 cents per kWh (in adjusted 2009 terms), they only paid 12 cents for the equivalent amount of electricity in 1970 [5]; see Figure 6.1.

Employment of conservative, slowly improving hardware enhanced the utility system's momentum. But nonengineering elements also did. Because it explicitly addresses such elements, the social-science systems approach focuses attention on the social nature of technological evolution. In the case of the utility system, the creation of regulatory bodies constituted a major driver of momentum. Unlike the railroad industry, which became regulated by government to stem perceived abuses,

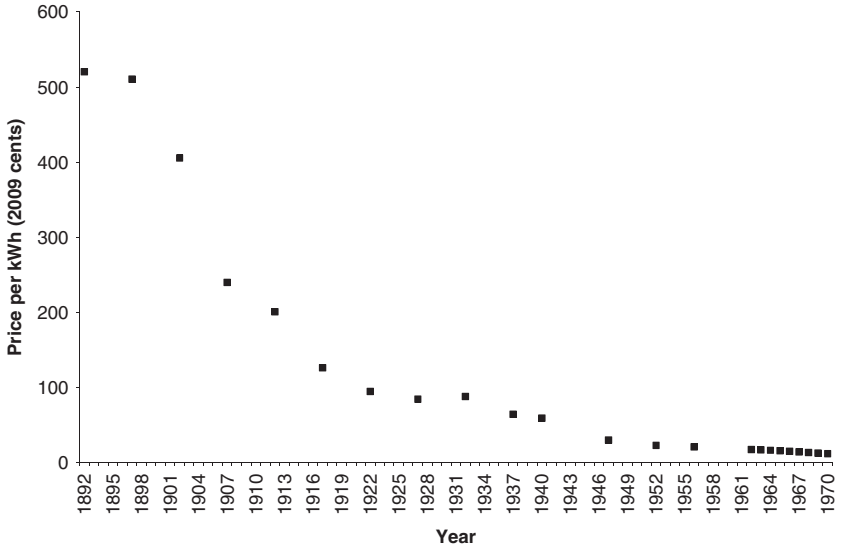

Figure 6.1 Average residential price of electricity, 1892 to 1970.

the electric utility industry actually sought oversight by state officials. As early as 1898, industry leader Samuel Insull argued that government supervision would offer legitimacy to power companies as monopolies. Once companies won dominance in a region, regulation would effectively create a barrier to entry and allow them to solidify their control. Government oversight would also reduce financial risks because utility commissions would be required not only to protect customers against monopoly abuses but to ensure that utilities earned enough money from customers to provide good service [6]. Winning the day, Insull saw state regulation spread rapidly after New York and Wisconsin created the first public utility commissions in 1907. Soon after the Progressive era ended during World War I, the quality of state regulators declined markedly, enabling utility managers largely to run the power system with only the appearance of dutiful oversight. Utility managers had effectively "captured" the regulatory mechanism, which helped them control a system that was developing significant momentum [7].

The system's momentum also grew because of the support of other stakeholders within society. Investment bankers, manufacturers of electrical equipment, educational institutions, and customers found reason to encourage development of an industry that employed large-scale technologies and appeared to bring universal benefits [8]. In other words, a variety of social groups implicitly supported a big, technology-dominated and regulated electric utility system. By the 1970s the utility system had gained a huge amount of momentum that appeared unalterable.

6.2.3 Politics and System Momentum Change

And yet, momentum changed significantly, starting in the 1960s and 1970s. First, for a number of managerial and technical reasons, manufacturers could no longer obtain significantly higher thermal efficiencies or economies of scale from new steam-turbine generators. This phenomenon, called "technological stasis" or an apparent end to progress, became critical during the "energy crisis" of the 1970s, when fuel costs (especially oil costs, but also costs of other fossil fuels) skyrocketed. Unlike in the past, when improvement in the power-producing technologies mitigated hikes in labor and capital costs, stasis meant that utilities needed to request rate increases from formerly quiescent (but now increasingly activist) regulatory bodies (Figure 6.2). Higher prices motivated conservation and energy-efficiency efforts. Electricity consumption grew at negative rates for a few years, while the long-term annual growth rate from 1974 to 2009 dropped from the decades-old rate of about 7% to just 2.3% [9].

The economic turmoil created by the energy crisis spurred politicians into action. Making energy policy a top priority, President Carter won passage in 1978 of several laws that sought to encourage energy efficiency and to increase domestic energy production. Though viewed as fairly tame, one of the laws, the Public Utility Regulatory Policies Act (PURPA), had at least three unintended consequences: it unexpectedly spurred creation of radical technologies, it began the process of deregulation, and it challenged the control held by power company managers. In the process the law helped change the momentum of the utility system.

The salient portion of PURPA initially appeared to offer no threat to utility companies. It primarily offered incentives for the use of cogeneration plants—units that

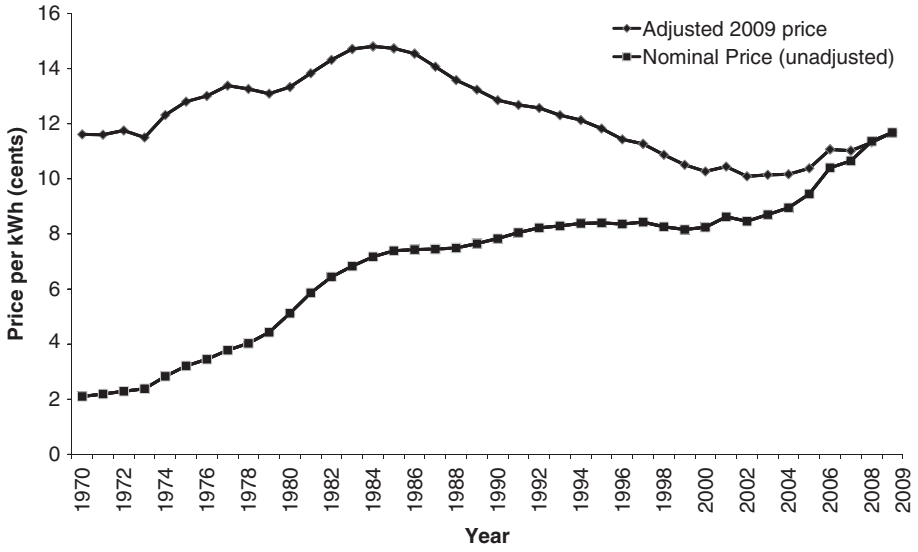

Figure 6.2 Average residential price of electricity, 1970 to 2009.

often generated less than 100 MW of power—about one-tenth the capacity that new utility-owned nuclear and fossil units yielded. But the smaller plants proved economically practical, even without economies of scale, because they employed waste heat for industrial processes or space conditioning. Obtaining double duty from raw fuel in the form of two valuable products (electricity and process steam), cogeneration plants demonstrated an overall thermal efficiency rate of 50% or higher, which compared favorably to the 40% figure achieved by the best utility-owned power plants. President Carter hoped more widespread use of such plants would reduce the amount of energy used in power production. A related portion of the law also encouraged development of renewable technologies that used water, wind, or solar power to generate electricity. Unusually successful, this portion of PURPA (along with incentives offered by some states) helped spur technological innovation and drive down the cost of power produced by solar photovoltaic panels by about 70% between 1980 and 1995 [10] and wind turbines by a similar margin. Most significant, cogeneration plants and some wind plants offered power at costs that compared favorably with (or was priced cheaper per unit output than) power generated by conventional utility plants [11].

In the language of Hughes's systems approach, these PURPA-inspired, small-scale technologies constituted radical technologies to the utility system's momentum. Through their use, the technologies enabled nonutility companies to compete (at least in the generation sector) with utilities that previously enjoyed vertically integrated monopolies. At the same time the unintended experiment with competition encouraged some regulators and legislators in the 1980s—a period when several other industries (i.e., the airline, telecommunications, and natural gas industries) had been

deregulated—to suggest that increased competition and less regulation would benefit participants in the electric utility business. The Gulf War of 1991 spurred further legislative changes, as Congress passed a modified form of President George H. W. Bush's energy plan that opened up the electricity transmission network so it would serve as a common carrier. The Energy Policy Act of 1992 also allowed states to begin competition on the retail level. Taking advantage of the law, 23 states (and the District of Columbia) had established mechanisms by September 2001 for a competitive marketplace for electricity.

As these events suggest, by the 2000s the momentum of the utility system has been altered significantly. Perhaps most important, the shifting momentum has displaced utility managers as the key controllers of the system. No longer in charge of the large-scale, gradually improving, and conservative generation technologies, the managers ceded political and economic power to entrepreneurs who, in some cases, use small-scale conventional and renewable energy technologies. From 1992 to 2003 the portion of the country's power capacity managed by nonutility firms grew from 1.5% to 34.7% percent [12]. At the same time utility managers lost the legitimacy provided by regulation of their companies' status as natural monopolies and have been forced to alter their business culture and practices to deal with life in the competitive market. And as other stakeholders (e.g., financiers, equipment manufacturers, and educators) saw momentum change, they shifted their allegiances to reflect the new environment. New stakeholders also entered the arena. Environmental advocates in many states, for example, won seats at negotiating tables and influenced the terms of restructuring laws, which often included expenditures of funds for renewable energy and energy-efficiency technologies [13]. Meanwhile the California electricity crisis of 2000 and 2001, along with the Enron scandal and the massive blackout of 2003, focused new attention on the changed nature of the utility system and caused policy makers to rethink their enthusiasm for a free market of electricity. In the years following the blackout the Federal Energy Regulatory Commission and state policy makers kept on feuding about new scenarios for operation of the system and for dealing with specific problems, such as the underinvestment of capital in an increasingly fragile-looking transmission network [14]. Using the language of the social-science systems approach, it appears that the human and technical components of the utility system have been severely altered, forever changing what had been substantial momentum.

6.3 APPLICATION OF PRINCIPLES

The semi-chaotic state of affairs that exists in the early twenty-first century has enabled distributed generation to gain a foothold. In fact the present time may be viewed as a rare inflection point as stakeholders have started to negotiate a new paradigm (or at least part of a new paradigm) and begin establishing momentum that diverges from what existed for almost a century. Distributed generation facilities constitute a collection of decentralized, modular, smaller, and on-site power production technologies. Supporters of DG argue that the decentralized plants offer less expensive, more efficient, more reliable, more flexible, and less environmentally damaging alternatives to traditional utility-owned power plants.

6.3.1 The Possibility of Distributed Generation and New Momentum

DG technologies are often classified by net generation capacity (ranging from 1 kW to more than 100 MW) and location. Because a significant number of electricity generators can be located on site, DG encompasses a wide range of technologies. Many renewable energy systems—such as wind turbines and photovoltaic technologies—are small and decentralized, and they serve as examples of DG technologies. Even generation equipment that employs fossil fuels, such as natural gas and coal, can be considered valuable DG resources, especially when they exploit waste heat generated through combustion or fuel conversion. These include cogeneration plants (also known as combined heat and power [CHP] facilities) that were originally encouraged by PURPA. They may also consist of very small steam turbines known as microturbines that produce power in the range of 25 to 500 kW while employing waste steam for water or space heating needs [15]. Phosphoric acid fuel cells are also being pursued as DG technologies. The devices (which are being tested in 200 kW to 11 MW sizes) take in hydrogen-rich fuel and create electricity through a chemical process rather than by combustion, thus yielding few particulate wastes [16]. The process also yields heat, which can be used as a profitable by-product. Beyond these DG technologies are modular internal combustion engines that run on diesel fuel or gasoline. In their smallest versions (about 1 kW), they provide backup power for recreational vehicles and homes. In larger packages, these engines provide backup power for hospitals and other large commercial enterprises. DG facilities may be established as isolated "islands"—disconnected from the transmission grid—or attached to it. In the latter case they may constitute the primary producers of power for a user or serve as backup units. They can also be set up to add power to the grid for use by other customers.

The economic viability of these DG technologies has improved in recent years. Technological advances in microturbines and reciprocating gas engines have lowered the cost and increased the efficiency of the small-scale generation technologies [17]. Advances in net metering, fuel conversion technology, and thermal engineering have accompanied developments in automation and control, improving the economy of small units and reducing the need for periodic maintenance and inspection [18]. Small system technology can also be mass produced at a lower unit cost. For example, numerous companies offer fuel cell technology, which is viewed as having virtually no emissions, in ready-to-connect packages. Many policy makers also perceive gas turbines as having low initial investment, steam generation capabilities, and installation flexibility [19].

The broad variety of DG technologies presents challenges for accurately measuring the extent that such technologies have become employed. For instance, the Electric Power Research Institute estimated in 1999 that more than 50 GW of electricity in the United States came from DG units [20]. In the same year, Arthur D. Little consultants noted that the capacity for reciprocating engines and small gas turbines *alone* in North America stood at roughly 60 GW [21]. Three years later, the generating capacity of diesel DG technologies in the United States exceeded 100 GW, according to the International Energy Agency [22]. And by 2004, Electric Utility Consultants concluded that the country's 12.3 million distributed generation

units—classified as decentralized generators sized between 1 and 60 MW—provided an aggregate capacity of 234 GW [23].

Nevertheless, proponents of distributed generation emphasize that DG technologies should not be viewed as a replacement for the current power grid. The US Combined Heat and Power Association notes that DG would not serve as a reliable substitute for all large, centralized power plants, since it is unlikely to meet the needs of customers in urban areas with severe land, permitting, and siting constraints. Moreover the fact that small and modular generators can be more efficient and less costly does not negate the useful role of large and centralized generators on the power grid, since in many situations large plants placed near points of consumption maximize thermal efficiency. Gary Mittleman, President and CEO of Plug Power, a fuel cell manufacturer and advocate of DG, acknowledged that power "plants and the grid will remain a part of our infrastructure" [24]. Similarly the American Wind Energy Association clarifies that the use of wind turbines is primarily intended to augment, rather than replace, the grid [25].

Consumer advocates note that DG technologies can also provide more efficient electrical power. The transmission of electricity from large and centralized plants typically wastes between 4.2% and 8.9% of the electricity, since wire resistance, inconsistent enforcement of reliability guidelines, and growing bottlenecks all degrade the effectiveness of transmission systems [26]. Since customers pay a share of the cost of the transmission system in their electricity bills, employment of localized generation equipment can conceivably yield affordable and higher quality power. Moreover self-generators can sell excess power to the grid and earn revenues, especially during times of peak demand.

Additionally industrial managers, commercial business owners, and contractors have begun to recognize advantages of local power generation. Combined heat and power technologies permit these power users to recycle thermal energy that would normally be wasted. Energy-intensive industries, including iron and steel foundries, chemical processing facilities, and paper and pulp manufacturers already use CHP technologies to maximize the efficiency of their on-site electricity generation. Office and industrial managers have also begun to use CHP technologies to reuse energy normally needed for district heating (where excess heat is pumped through buildings in lieu of electrically produced heat) and surplus power provision (where the extra thermal energy from combustion is reused to produce more electricity). CHP technologies have been proved to enhance industries working in aquaculture, greenhouse heating, desalination of seawater, increased crop growth and frost protection, and air preheating [27].

Beyond efficiency, DG technologies can provide more reliable power for digital and telecommunications industries that require uninterrupted service. One study conducted by the Electric Power Research Institute noted that power outages and quality disturbances cost $119 billion in 1999, with between $21.2 and $33 billion lost in California and New York alone [28]. A comparable study undertaken by the American Superconductor Industry estimated that power outages cost California more than 1010 billion every year [29]. The cost of a two-hour blackout for chip manufacturing and semi-conductor industry alone can cost as much as $48 million [30]. These numbers

help explain why several companies already rely on DG facilities to ensure consistent power supplies.

Surprisingly, perhaps, DG facilities offer enhancements for the transmission of power. By producing local power for users, DG technologies can decongest the grid by reducing demand during peak times, one of the causes of the 2000–2001 California crisis and the 2003 blackout on the Eastern seaboard [31]. Most important, by constructing large numbers of decentralized power facilities rather than a few large plants located distantly from load centers, DG use can reduce the need to upgrade and expand transmission facilities during a period when investment in such facilities remains restricted due to siting policies and local opposition. And in an increasingly security-minded era, proponents further argue that DG technologies may enhance protection of the grid. Decentralized power generation reduces the terrorist targets that large nuclear and conventional facilities and natural gas refineries offer. It also helps the system by diversifying fuels, enhancing emergency stand-by generation, and better insulating the grid from failure if a large power plant goes down due to an accident or attack [32].

Finally, some environmentalists and academics have argued that DG technologies provide ancillary benefits to society at large. Large, centralized coal- and gas-fired power plants emit pollutants, such as carbon monoxide, dioxins, sulfur oxides, particulate matter, hydrocarbons, and nitrogen oxides. For many years, the Environmental Protection Agency (EPA) has reported the correlation between high levels of sulfur oxide emissions and significant health effects, including cancer and asthma. Moreover, combustion of fossil fuels tends to create acid rain, which suppresses crop growth and leeches nutrients from the soil. Because larger plants concentrate the amount of power they produce, they center their pollution and waste heat, which destroy fragile ecosystems and reduce marine biodiversity. On the other hand, some recent investigations have confirmed that widespread use of DG technologies substantially reduces emissions: A British study estimated that domestic CHP production cut carbon dioxide emissions by 41% in 1999. A report on the Danish power system argued that widespread use of DG technologies have reduced emissions by 30% from 1998 to 2001 [33].

6.3.2 Impediments to Decentralized Electricity Generation

Despite its potential benefits, the transition to a new DG paradigm will not occur effortlessly because of the existence of social, technical, political, and business-related impediments. The most significant impediment may be the belief that decentralized units cost more than large centralized facilities. Cost projections for electricity often only include the capital cost of a generator, maintenance, and fuel. Such estimates exclude "external costs" in the form of pollution, decommissioning, and price swings for fuel and labor. These pricing schemes also fail to include many of the potential benefits—such as reliability, efficiency, and security—that DG systems can provide. Consequently policy makers and consumers often think that renewable technologies (in particular) cannot compete effectively on costs with traditional fossil fuel sources of electricity [34].

The largest technical impediment consists of problems related to the connection of DG technologies to the grid. This interconnection conundrum really constitutes a

set of aggregated technical problems: voltage control (keeping voltages within acceptable ranges), the balancing of reactive power (properly synchronizing power within the grid), and safety (ensuring the protection of people working on the grid, especially when parts of it fail). Customers using DG technologies today often rely on custom-designed electronics packages to resolve these problems. But the high cost to create such packages serves as a disincentive for many users. Recognizing this problem, an IEEE Standards Coordinating Committee has begun developing rules for interface technologies that would enable DG users to "plug" into the grid directly and safely. However, agreement on the specific details of the new standards remains years away. As of January 2, 2002, the list of committee members included 385 names of people, representing scores of investor-owned and public power utilities, manufacturers, government laboratories, state agencies, and consultants. Each player sees advantages and disadvantages to acceptance of any single technical standard, meaning that a consensus will be difficult to fashion. The problem again illustrates the social nature of technological change, as different players in the system view benefits and costs differently [35].

Possibly more important, regulatory and political inertia within the United States, in the form of financial subsidies, still favors fossil fuels, which are used to produce most of the nation's electricity. A recent study performed by the Environmental Law Institute found that federal government subsidies (which consist of direct spending and tax incentives) to fossil fuels totalled $72.5 billion over a seven-year period from 2002 to 2008. Meanwhile, subsidies for renewable fuels amounted to $29 billion in the same period. (More than half of the subsidies for renewable fuels went to corn-based ethanol, little of which is used to produce electricity.) [36] A 2007 U.S. Government Accountability Office report suggested a similar lack of balance of direct spending from the Department of Energy for electricity-related research and development: between 2002 and 2007, the DOE spent $6.2 billion on nuclear programs, $3.1 billion on fossil fuel efforts, and $1.4 billion on renewable energy R&D. This asymmetric subsidization means, for instance, that wind energy technologies may not improve as rapidly as they did in the past [37]. Similarly, lingering monopoly rules and discriminatory rate structures (often taking the form of exit fees, backup tariffs, and connection surcharges) still exist in many states and create political obstacles to investments in DG technologies. Customers who seek to use DG often face extra charges imposed by utilities that seek to recover stranded costs.

In addition many old coal-fired power plants have been exempted from the 1972 Clean Air Act. This exemption gives them a further advantage because it allows them to operate under older environmental standards, unlike DG technologies that must meet current (and more stringent) permitting and siting requirements [38]. Similarly the Congressional Budget Office notes that the costs of environmental monitoring for DG technologies would be more costly than enforcement of regulations for large central plants because power generators would be more dispersed, and that utilities would have to invest large amounts of money in computer software and transmission upgrades to manage DG facilities on the grid.

To be sure, some of these impediments can be mitigated by effective public policy. As noted, DG implementation suffers because some of the costs involved

in producing power in the conventional sense are not borne directly by the companies that create those costs. Known generally as "externalities," these costs are imposed on society and are not included in the cost of conventional methods to produce power, thereby skewing conventional analyses of alternative power choices. However, government policies can impose taxes and other disincentives on activities that cause perceived harm to society. At the same time they may provide incentives for use of technologies that will enhance public health, security, power reliability, and welfare—benefits that are difficult to quantify using traditional economic analyses. Several policy initiatives have been suggested for improving the likelihood of obtaining the societywide benefits of DG implementation. They include creation of interconnection standards and contractual requirements so that DG owners can gain access to the power grid at a fair cost and with reasonable, uniform technical requirements. Such an approach would minimize the need for expensive, time-consuming efforts to manufacture custom-designed interfaces. At the same time DG implementation would benefit from establishment (by policy makers) of hourly retail markets for the trading of power between DG owners and the distribution grid. Such a market would allow DG owners and other consumers to profit from the value of DG in reducing peak-load generation from utilities. Such markets remain in the experimental stage, though similar markets have been shown to provide useful incentives to small-scale generation technology users and energy-efficiency technologies. Finally, some argue that creation of a level "playing field" among all types of generators (owned by utilities and nonutilities) would help eliminate unseen subsidies, costs, and benefits, and encourage proper consideration of alternatives. Government policy would establish standardized requirements for emissions allowances, land use, building codes, and other key components of the production of power, helping users choose the most efficient design of a power delivery network. It would aid in the analysis of energy-efficiency alternatives as well by elucidating the true costs of all supply-side and demand-side alternatives.

6.4 PRACTICAL CONSEQUENCES: DISTRIBUTED GENERATION AS A BUSINESS ENTERPRISE

In the "real" world these potential benefits and impediments are evaluated by men and women in the business community who seek to exploit opportunities in the altered electric utility system. This section examines in more detail the ways business people consider these factors and develop business decisions. The discussion ends with an analysis of a business model that incorporates economic and strategic factors to create a possible niche for DG in the evolving utility system.

Four different categories of business entities appear likely to consider the implementation of DG technology as an element of a strategic plan. These include:

- Investor-owned utilities (IOUs) and publicly owned utilities that may want to install DG units for supplying peak demand in areas that are located behind congested transmission lines.

- Manufacturers of DG systems that have already advanced the technologies for DG on several fronts and, with the exception of large gas turbines, appear to be pacing their capacity growth by market growth.
- The new generator and consumer (NGC) that sees operation of DG units as a potential substitute for some or all of its purchases of electricity from utilities. Included in this category are industrial sites, apartment complexes, government agencies, military bases, universities, hospitals, shopping malls, and the like. On the horizon, NGCs may also become wholesale energy suppliers by interconnecting DG units.
- The contractor industry (CI) that performs one or more of the functions of designing, building, installing, and operating DG units. The viability of contractors depends on the rate of adoption of DG by the above-mentioned categories of business entities.

For any organization, strategic business planning begins with an analysis of the organization's mission and the threats and opportunities that exist in the external environment. It continues with an examination of the firm's weaknesses and strengths (i.e., its internal environment). External threats include uncertain and rising electricity costs and the unreliability of power supplied by utilities. As managers scope out opportunities for changing their organization and developing a new strategic plan, they often consider four general categories: redesign and repositioning in the marketplace of the organization's products and services, improved selection and design of the processes that the organization uses to pursue its mission, expansion or contraction and the reallocation of capacity, and improvements to operations control systems [39].

Among these categories of action, managers view process improvement as the mechanism through which they often take advantage of technological innovation. But technological innovation is neither deterministic nor autonomous. It results from a series of choices pursued by managers and events occurring in the marketplace (which is itself affected by others' choices and actions). In the strategic business plan of new customers and generators, DG is viewed as a potentially new process for the creation of electricity, a basic commodity that serves as a critical input into business activities. Its price, availability, security, and quality may affect an organization's ability to produce the products or services that define its mission.

The most common business model for DG adoption and growth may consist of one that partners new consumers and generators with DG contractors. By doing so, companies seeking electricity and heat do not need to develop extensive expertise outside their core competencies. Rather, they can depend on contractors who have developed the skills and knowledge from operating DG units for other firms and who can provide other services. The employment of DG would therefore not become a distraction to a company's core competencies or become a burden to its mission.

Even with a competent contractor working to develop DG units for a firm, an array of risks confronts the nontraditional new player in the utility system. The list of risk factors includes the impediments noted earlier. However, business managers may look at them differently, combining several into these general categories:

- *Technological uncertainty* Owners must deal with the chance that the DG technology will not perform as reliably or as efficiently as its specifications. In particular, interconnected DG systems may actually reduce the reliability of a distribution grid due to the inability of grid operators to control unit dispatches under rapidly changing conditions.
- *Fuel cost uncertainty* The price of natural gas, coal, and oil will affect the financial performance of any DG unit that uses these fuels. Owners of renewable energy technologies (e.g., wind turbines) will not need to worry about the cost of energy resources, but the price they receive for surplus power will depend, to a large extent, on the price of conventional fuels that provide competitive benchmarks prices.
- *Load uncertainty* The growth and volatility of electricity demand within the transmission grid that serves the NGC must be considered. Ironically, efforts to reduce the cost of electricity in the form of demand-side response could reduce the value of DG units that are most beneficial in supplanting expensive peak-load power from utilities [40].
- *Electricity price uncertainty* The financial performance of a DG unit depends on the cost of electricity from utilities that the unit supplants. Future prices of electric power in the United States remain highly uncertain due to variability in fuel costs, regulation, and technological change.
- *Regulatory and public policy uncertainty* The viability of DG projects depends, to a certain extent, on the treatment by government entities. NGCs need to consider the chance that tax incentives, subsidies, or easements associated with a DG implementation may be offered or repealed by future legislatures and executives. Given the spotty history of utility system restructuring and deregulation, it is difficult to predict the effects of government policies on evolving electricity markets.

These uncertainties create financial (and nonfinancial) risks for NGCs. As with any capital investment option, the cash flows of a proposed DG facility must be viewed as random variables, and measures of financial risk must be computed from the probability distributions of these variables. Investments that look acceptably profitable on the basis of expected cash flows may be deemed unworthy when the risk associated with these cash flows is estimated. The energy industry is a motivating force behind new methods for assessing risk, and it currently is replacing the traditional evaluation of net present value with the view of investments in generation capacity as real options. This more enlightened view of financial risk directs the investor's attention to both the downside loss potential as well as the upside gain potential [41].

6.5 AGGREGATED DISPATCH AS A MEANS TO STIMULATE ECONOMIC MOMENTUM WITH DG

This analysis suggests a host of potential and real problems faced by businesses considering use of DG technologies, making the novel approach viewed as a somewhat

risky, marginally profitable opportunity. Nevertheless, opportunities for the use of DG exist, especially if structured in a new fashion, namely as an element of an aggregated entity that can dispatch power to the grid. In such a way a DG owner might obtain a significant revenue stream while also enhancing grid reliability and reducing pollution. The business would employ electricity and waste heat for its own needs when power remains cheap, and it would sell surplus power to the grid when spot prices for electricity are high. To participate in the market for power, DG units must be dispatched at times and locations where they are most needed. This kind of dispatch requires coordination of all DG units in a distribution grid. By doing so, owners provide society with some of the promised benefits of DG while also making financial profits for themselves.

Is such dispatch possible? An experiment in New York, funded by the New York State Energy Research and Development Authority (NYSERDA) and the US Department of Energy, suggests that such dispatch can occur efficiently. The experiment engaged the services of a private contractor, ELECTROTEK, to link 50 backup generators (providing a capacity of 35 MW) to centralized control points for dispatch to the power grid. Not only technically feasible, the aggregated system demonstrated its economic value by saving $1.5 million in one year through the use of DG only for load curtailment [42].

The experiment highlights the new business model of aggregated dispatching for DG. In this model, DG owners would submit, under contractual limitations, their units to the control of a central dispatcher who trades off the cost of generation from the DG units against the spot prices available from the wholesale market. In addition the volatility of spot prices motivates financial risk management through the trading of derivatives. Given the special expertise and close attention that such trading requires, DG owners would probably assign these duties to a contractor as well. Here again, DG owners would most likely try to avoid moving beyond their core competencies. An experienced contractor would design, install, maintain, and operate DG units for the owners. It would also trade the power produced by the units and manage risks associated with their operation within an integrated distribution grid. The contractor further would play (as in the NYSERDA experiment) the role of a load serving entity (LSE) for a group of DG owners. It would purchase bulk electricity from utilities and sell it in the day-ahead market in different parts of New York. When real-time prices exceed the cost of generation from the DG units, the LSE would dispatch the DG units and earn revenues. This complex business operation has proved financially successful and illustrates clearly the viability of a contractor industry in the DG economy. As the financial benefits of this business model become recognized, members of the contractor industry might even benefit from economies of scale. They would collect, under one roof, the broad expertise necessary for coordinated management of DG resources.

Parenthetically, it should be noted that this analysis currently focuses on the profit-seeking new consumer and generator segment of the market. Perhaps in a later study, the authors will examine in greater detail the potentially large interest in DG by government entities, such as federal, state, and municipal agencies. Decision makers in these bodies may (or should) evaluate energy situations differently than do managers in profit-making corporations. For example, a city manager may look to the

increased reliability and security benefits of DG technologies as a prime consideration of a government that needs to maintain emergency services during a blackout caused by accident or by terrorists. DG technologies would provide backup power at critical times for the city to provide critical communications and rescue functions, displacing economic factors (e.g., the simple cost of electricity per kilowatt-hour) as top considerations. As another example, the US Department of Energy's Federal Energy Management Program, operated by Oak Ridge National Laboratories, may desire to employ DG technologies as a way to obtain secure electrical supplies for government facilities to deal with potential terrorist attacks or natural disasters. In fact, because government managers may view DG positively for such uses, they may be among the largest (and quickest) adopters of the new small-scale technology, thereby providing its proponents with a substantial market.

6.6 CONCLUSION

Made up of a diverse set of economic, educational, legal, administrative, and technical components, the American electric utility system developed much momentum during most of the twentieth century. Supporting the use of large-scale hardware that exploited economies of scale, the system's stakeholders generated huge amounts of power at declining costs and produced financial and social benefits for millions of people. The system's momentum, a metaphor for the social and technical components aligned in such a way as to resist change, grew consistently and seemed to favor everyone.

But starting in the 1960s, problems with the standard (and previously improving) generating technology became evident. Combined with the energy crisis of the 1970s and the political response to it, however, momentum change began occurring. The monopolistic utility industry first saw competitors generate power using small-scale and cost-effective equipment that employed raw energy more efficiently. Government incentives also spurred increased production of power from environmentally preferable equipment such as wind turbines. Following passage of the Energy Policy Act of 1992, the existing structure of the utility system changed further, with wholesale and retail competition further eroding the momentum of the former system.

Efforts to restructure and partially deregulate the utility system have not occurred without difficulties. It appears that, like in other industries, restructuring the utility system will remain a messy business and may take a long time for stakeholders to work out a new paradigm. The inherent messiness highlights the notion that momentum in the system has changed and that stakeholders—some new ones in particular, such as those that employ distributed generation technologies—have an occasion to introduce new ideas for how the utility system will emerge in the near future.

This chapter has suggested that at a time when momentum change is occurring, opportunities exist for the increased employment of DG technologies in the utility system. Focusing on possible strategies for various business entities, it concludes that ominous risks appear for companies that seek to generate power largely for themselves. In many cases it is understandable why DG has not yet seen greater penetration into the marketplace. However, some of those risks would diminish if government policy

makers recognized better the subsidies offered to conventional fuel users and also made companies pay for the significant external costs they impose on society. Such a policy may be difficult to pursue for political and economic reasons. Still policy should provide incentives for DG enterprises to recognize the real, but difficult-to-quantify benefits to society overall, such as increased reliability, heightened security of the grid, and reduced (or stabilized) transmission costs.

Even if policy makers fail to pursue some of these measures, DG could be embraced by the business community in a novel form. This chapter suggests a business model that employs experienced contractors to serve as load-serving entities for DG units owned by several parties. The contractors would dispatch the units in a real-time marketplace and earn revenues when spot prices surpass the cost of producing power. Recent experiments with this business model appear promising. The authors plan to continue to explore ways to make DG a larger element in a utility system whose momentum continues to shift.

BIBLIOGRAPHY

1. Hughes, T. P. *Networks of Power: Electrification in Western Society, 1880–1930*. Johns Hopkins University Press, Baltimore, 1983.
2. Hughes, T. P. "The Evolution of Large Technological Systems." In Bijker, W. E., Hughes T. P., and Pinch, T. J., eds., *The Social Construction of Technological Systems: New Directions in the Sociology and History of Technology*. MIT Press, Cambridge, p. 52, 1987.
3. Hughes, T. P. *American Genesis: A Century of Invention and Technological Enthusiasm 1870–1970*. Penguin Books, New York, p. 460, 1989.
4. Chandler, A. D. Jr. *The Visible Hand: The Managerial Revolution in American Business*. Harvard University Press, Cambridge, 1977.
5. Unadjusted data from Edison Electric Institute, *EEI Pocketbook of Electric Utility Industry Statistics*, 34th ed., Edison Electric Institute, Washington, DC, p. 33, 1988; Edison Electric Institute, *EEI Pocketbook of Electric Utility Industry Statistics*, 43rd ed. Edison Electric Institute, Washington, DC, p. 37, 1997; and US Department of Energy, Energy Information Administration, at http://www.eia.doe.gov/cneaf/electricity/epm/table5_3.html. Adjusted prices based on "all items" category of Consumer Price Index found in US Department of Labor, Bureau of Labor Statistics, at ftp://ftp.bls.gov/pub/special.requests/cpi/cpiai.txt. (January 15, 2010).
6. McDonald, F. *Insull*. University of Chicago Press, Chicago, p. 114, 1962.
7. Regulatory capture is described in D. D. Anderson, *Regulatory Politics and Electric Utilities: A Case Study in Political Economy*, Auburn House, Boston, pp. 1–4, 1981. Also see Stigler, G. J. The Theory of Economic Regulation, *Bell Journal of Economics and Management Science* 2: 3–21, 1971.
8. Hirsh, R. F. *Technology and Transformation in the American Electric Utility Industry*. Cambridge University Press, New York, pp. 26–35, 1989.
9. Rates determined from data at US Department of Energy, Energy Information Administration, Monthly Energy Review, January 2010, Table 7.1, at http://www.eia.doe.gov/emeu/mer/elect.html.
10. Hirsh, R. F. *Power Loss: The Origins of Deregulation and Restructuring in the American Electric Utility System*. MIT Press, Cambridge, pp. 114–15, 1999.

11. Smith, R. "Not Just Tilting Anymore." *Wall Street Journal*, October 14, 2004, p. C1. See also American Wind Energy Association (AWEA). "Wind Energy Costs," at http://www.awea.org/faq/tutorial/wwt_costs.html, and AWEA, "The Economics of Wind," at http://www.awea.org/pubs/factsheets/EconomicsOfWind-Feb2005.pdf.
12. US Department of Energy. Energy Information Administration, Electric Power Annual, Table 13. 2.1, 14. 2003, from http://www.eia.doe.gov/cneaf/electricity/epa/epa.pdf.
13. For example, California Assembly bill AB 1890, for amending Chapter 2.3, "Electrical Restructuring," of the state's Public Utilities Code, Article 1, General Provisions and Definitions, Section 17. 330(e), Chapter 2.3, signed into law September 23, 1996.
14. Rigby, P. "Deregulation's Dysfunctional Markets Strike Back; The Blackout of '03 Intensifies Political and Regulatory Risk for U.S. Transmission.'' *Platts Energy Business and Technology* 5(8): 28, 2003.
15. Capehart, B. L., and Barney, L. "Microturbines." In *Whole Building Design Guide*, August 4, 2003, from http://www.wbdg.org/design/microturbines.php. See also US Department of Energy. "Microturbine Program," 2005, from http://www.eere.energy.gov/de/program_areas/det_microturbine_prgrm.shtml.
16. Yacobucci, B. D. and Curtright, A. E. "A Hydrogen Economy and Fuel Cells: An Overview." CRS Report for Congress, Library of Congress: Congressional Research Service, January 14, 2004.
17. Learner, H. A. "Cleaning, Greening, and Modernizing the Electric Power Sector in the Twenty-First Century." *Tulane Environmental Law Journal* 14: 277–314, 2001. Iannucci J. "Electricity Competition: Volume 1." *Hearing before the Subcommittee on Energy and Power of the Committee on Commerce, House of Representatives*, Washington, DC, March 18–May 6, pp. 214–221, 1999.
18. Willis, L., and Scott, W. G. *Distributed Power Generation: Planning and Evaluation* Dekker, New York, pp. 4–6, 2000.
19. Capehart, B. L., Mehta, P., and Turner, W. "Distributed Generation and Your Energy Future." *Cogeneration and Distributed Generation Journal* 18(4): 17–33, 2003. See also Blustein, J., et. al. "The Impact of Air Quality Regulations on Distributed Generation." *National Renewable Energy Laboratory Technical Monitor* (October): iii, 2002.
20. Yeager, C. "Perspective on the Current Status and Research Needs for Distributed Resources in the Evolving U.S. Energy Industry." *Hearing before the Senate Committee on Energy and Natural Resources*, Washington, DC, June 22, p. 55, 1999.
21. Arthur D. Little. "Distributed Generation: System Interfaces." *An Arthur D. Little White Paper*, ADL, Boston, MA, p. 2, 1999.
22. International Energy Agency. *Distributed Generation in Liberalized Electricity Markets*. International Energy Agency, Paris, p. 48, 2002.
23. Electric Utility Consultants. *The Installed Base of U.S. Distributed Generation*, EUC Publishing, Greenwood, CO, 2004.
24. Mittleman, G. "Electricity Competition: Volume 3." *Hearing before the House Subcommittee on Energy and Power*, September 13, 1999, Washington, DC, p. 15.
25. Fallek, M. "Distributed Generation: Electric Utility Perspective," 2004, from http://uschpa.admgt.com/Rdmap03Fallek.pdf; and American Wind Energy Association, "Distributed Generation: Revolutionizing the Grid," 2004, from http://groups.msn.com/AAEA/utilities.msnw.

26. Halverson, M. "Downturn in Demand Gives Contractors Time to Get in the DG Game." *EC&M*, February 2002, from http://www.ecmweb.com/mag/electric_downturn_demand_gives/.
27. Kleinbach, P., and Hinrichs, H. *Energy: Its Use and the Environment*, Harcourt, New York, p. 311, 2002.
28. Hinrichs, D., Conbere, S., and Lobash. M. "Taking Control of Power Supplies," in *Building Operating Management*, July 2002, from http://www.findarticles.com/p/articles/mi_qa3922/is_/ai_n9110155.
29. Yurek, G. "Electricity Competition: Volume 1." *Hearings before the Subcommittee on Energy and Power of the Committee on Commerce, House of Representatives*. March 18–May 6, 1999, Washington, DC.
30. Lin, J. "Power Outage Hits Industrial Park Hard." *Taipei Times*, April 11, p. 10, 2004.
31. Congressional Budget Office. "Prospects for Distributed Electricity Generation," September 2003, from http://www.cbo.gov/showdoc.cfm?index=4552&sequence=2.
32. Friedman, S. J., Homer-Dixon, S. and T. "Out of the Energy Box." *Foreign Affairs* 83(6): pp. 72–83, 2004.
33. International Energy Agency. *Distributed Generation in Liberalized Electricity Markets*. International Energy Agency, Paris, p. 92, 2002.
34. Pepermans, G., et. al. "Distributed Generation: Definition, Benefits, and Issues." *Energy Policy* 33(6): 787–798, 2005.
35. IEEE. "IEEE 1547 Standard for Interconnecting Distributed Resources with Electric Power Systems," http://grouper.ieee.org/groups/scc21/1547/1547_index.html.
36. Environmental Law Institute. *Estimating U.S. Government Subsidies to Energy Sources: 2002–2008*. Washington, DC, Sept. 2009, at http://www.elistore.org/Data/products/d19_07.pdf. U.S. Government Accountability Office. *Federal Electricity Subsidies: Information on Research Funding, Tax Expenditures, and Other Activities That Support Electricity Production*. GAO-08-102. Washington, DC, Oct. 2007, at http://www.gao.gov/new.items/d08102.pdf.
37. Rosta, P. "Wind Development Flags with Tax Credit's Expiration." *Engineering News–Record*, 252 (June 14): 19–23, 2004.
38. Casten, T. R. *Turning Off the Heat: Why America Must Double Energy Efficiency to Save Money and Reduce Global Warming*. Prometheus Books, New York, p. 203, 1998.
39. Slack, N., and Lewis, M. *Operations Strategy*, Prentice Hall, Upper Saddle River, NJ, 2003.
40. Congressional Budget Office. "Prospects for Distributed Electricity Generation," pp. 12–13, September 2003, from http://www.cbo.gov/showdoc.cfm?index=4552&sequence=2.
41. Smithson, C. *Managing Financial Risk*. McGraw-Hill, New York, 1998.
42. National Renewable Energy Laboratory. *Aggregated Dispatch of Distributed Generation Units*. US Department of Energy, Oak Ridge, TN, 2004.

INDEX

Accommodation procedure, of the detuning operation, 27
AC/DC power flow program, 8
AC generation and propulsion test bed, 8
Adaptation, sequential decision processes and, 137–139
Adaptation options, 139–140
Adaptive control, 138–139
Admittance bus matrix, 38, 40
Advanced Systems Theory, 4
Aggregated dispatch, 170–172
Aggregate planning problem, 136
Alternating-current (AC) transmission, 160
American electric utility system
  distributed generation and momentum change in, 157–175
  momentum of, 172
Analytic redundancy, fault detection via, 17
Ancillary services (A/S), 81. *See also* Intelligent power router ancillary service
Angular displacements, 30
Approximation, in hierarchical planning, 135–136
Approximation algorithm, 106
Armature MMF distributions, 20
Autonomous systems, 73–74
Availability planning, market model for, 147

Badinelli, Ralph D., xi, 119, 157
Barriers to entry, 159
Beard-Jones detection (BJD) filter, 17
Behavior and Market Model Tool module, 7
Benchmark systems, 3
Benchmark test systems, 7
  challenges related to, 5
Bilateral contracts, 151
Block switch failure, 102–103
Border IPRs, 59, 62, 63, 64, 82. *See also* Intelligent power routers (IPRs)
Branch failure, 107
Breaker reliability, 68
Broken rotor bar detection, on IFOC-driven induction motors, 28–35
Broken rotor bars
  residual generator to detect, 31–35
  squirrel cage induction motor model with, 29–31
Building block switching module, 110, 111
Bus admittance matrix, 38
Business community, DG in, 173
Business decision problems, 120
Business entities, DG technology implementation by, 168–170
Bus load change, 37, 42, 43

California electricity crisis, 163
Case analysis, 119
Case studies, 121–123
  importance of, 153–154
Cedeño, José R., xi, 47
Centeno, Virgilio, xi, 119
Circuit breakers, 87
  construction of, 109–111
  control circuit for, 111
  design of, 106–107, 114–115
  failure of, 107
  medium voltage, 88–90, 95
  proper operation of, 100
Circuit breaker technology, 88–92
Civil Test Bed, 10
Coal-fired power plants, 167
Cogeneration plants, 161–162, 164
Cold switching, 88
Combined heat and power (CHP) facilities, 164–166
Commitment planner, 150–153
Communications network congestion, 61

Operation and Control of Electric Energy Processing Systems, Edited by James Momoh and Lamine Mili

Commutation, mechanical, 20
Comparator signal, 113
Computer controllable bus, 55
Computer hardware IPR subsystem, 65–66. *See also* Intelligent power routers (IPRs)
Computerized educational support system, effectiveness of, 130
Computerized descriptive model, 125
Computerized tools, 123
Computer simulation
  benefits of, 120
  as a robust tool, 119
"Conservative" inventions, 159
Consumer behavior, challenges related to, 4
Contingency messages, 61
Contractor industry (CI), 169
Control centers, 48
Control circuit, 111–114
Controlled induction motors, detuned operation of, 20–24
Controlled islanding mechanism, 79, 83
Cortés, Hugo Rodrıguez, xi, 15
Cost-effectiveness, as an IPR design objective, 50
CPLEX software, 133
Current distribution, switch failure and, 102
Current-fed indirect field-oriented controlled induction motors, detuned operation of, 20–24
Current interruption, 94
  analysis of, 97–100
Current pulse, 110
Current transformer, 110
Current transformer signal, 113
Curricula
  innovative and integrated, ix, 3, 5
  interdisciplinary, 6
  interdisciplinary research-based, 2

Damage tolerance analysis, 16
Data-routing model, 48
DC pulses, 110
DC signal, 113
DCZEDS model, simulation studies using, 77. *See also* DC Zonal Electric Distribution System (DCZEDS)
DC Zonal Electric Distribution System (DCZEDS), 76–77
  enhanced implementation of, 77
DC zonal ship service distribution test bed, 10
DD(X) Navy Test Bed model, 55
DD(X) shipboard power system, 57
Decentralized electricity generation, 166
  impediments to, 166–168
Decision alternatives, ramifications of, 125
Decision analysis, 120
Decision/control actions, 71–73
Decision hierarchy, 121
Decision making, coordinated, 133–135
Decision model hierarchy, 141
Decision modeling, 119
Decision models
  building and optimizing, 123
  data elements in, 125
  general structure of, 126
  performance measure trajectories in, 125
Decision model structure, generic, 123–126
Decision problem, optimal solution to, 124
Decisions
  simulation model for, 128
  stochastic, 140–141
  uncontrollable factors of, 124
Decision support systems, 123
Decision variables, 124
  selection of, 135
Demand planning, market model for, 147
Descriptive decision models, 125–126
Descriptive models, data flow of, 126
Deterministic forecasts, 139
Detuned indirect field-oriented controllers, residual generator to detect, 24–26
Detuned operation, detection of, 24–26
Detuning, consequences of, 22
Detuning detection/accommodation, on IFOC-driven induction motors, 19–28
Detuning effect model, 22–24
Detuning operation, accommodation of, 27
DG adoption, business model for, 169. *See also* Distributed generation (DG)
DG facilities, 166
DG insertion, in protective device coordination, 127
DG paradigm, transition to, 166
DG system manufacturers, 169
DG technologies, 164
  connection to the grid, 166–167
  environmental issues related to, 166
  opportunities for, 172–173
  as a power grid replacement, 165
  reliability of, 165
DG units, dispatch of, 171
Differential equations, 36–37
Dispatching option parameters, 140
Dispatching options, capacity and demand constraints on, 139
Distributed algorithms, 52

Distributed control, of electronic power distribution systems, 71–74
Distributed control models, 71–79
Distributed generation (DG), 158, 163. *See also* DG entries
  in the American electric utility system, 157–175
  as a business enterprise, 168–170
  new momentum and, 164–166
  opportunities for the use of, 171
  stimulating economic momentum with, 170–172
Distribution systems, short circuits in, 90
Dynamic model-based state estimation approaches, 35
Dynamic models, 16
  in fault tolerant operation, 15–45
Dynamic programming, 137–138
Dynamic residual generator, 18
Dynamic security assessment, 16
Dynamic state estimating, 16
Dynamic system monitors (DSM), 51

Economic market efficiency, funded research for, 12
Economic momentum, stimulating with DG, 170–172
Economics
  challenges related to, 4
  interdisciplinary research in, 12
Edison, Thomas, 159
Educational case studies, characteristics of, 122–123
Educational support system (ESS), 119. *See also* ESS entries
Efficiency, challenges related to, 4
EGMS data flow diagram, 134. *See also* Electricity Grid and Market Simulator (EGMS)
Electrical energy networks, restoration with IPRs, 59–60
Electric drives, high-performance applications of, 19–20
Electric energy delivery network (EEDN), 60
Electric energy processing networks, distributed coordination for, 47–85
Electric energy processing systems, operation and control of, ix
Electricity, cost projections for, 166
Electricity generation, decentralized, 166–168
Electricity Grid and Market Simulator (EGMS), 131–133. *See also* EGMS data flow diagram
Electricity price uncertainty, 170
Electric power
  distribution of, 87
  efficient, 165
Electric power networks
  analysis, planning, and operation of, 1
  interdisciplinary curriculum for, 6
  security of, 2
Electric power networks efficiency and security (EPNES) framework, 1, 3, 4. *See also* EPNES entries
  future directions of, 13–14
Electric utility companies, early, 159–160
Electric utility industry, regulation of, 160–161
Electric utility system
  distributed generation and momentum change in, 157–175
  origins and growth of momentum in, 159–161
Electromechanical torque, 21
Electronic power distribution systems (EPDS), distributed control of, 71–74
Electronic power flow control devices, 55
Embedded intelligence, 48
Energy crisis, 161
Energy flow control devices (EFCD), 50–51
Energy grid management, 135
Energy industry, 170
Energy market model (EMM), 133
Energy policy, 161–162
Energy Policy Act of 1992, 163, 172
Energy processing systems, 15
  fault detection problems in, 16
Engineering decision problems, 120
Environment, interdisciplinary research in, 12
Environmental advocates, 163
Environmental issues, challenges related to, 4–5
Environment Issues and Control module, 7
EPNES architecture. *See also* Electric power networks efficiency and security (EPNES) framework
  modular description of, 6–7
  solution of, 6–8
EPNES award distribution, 12–13
EPNES benchmark test beds, expectations of studies using, 7–8
EPNES goals, 13
EPNES initiative, interdisciplinary education component of, 12
EPNES solicitation, funded research work in response to, 10–13
ESS data flow diagram, 132. *See also* Educational support system (ESS)
ESS packages, 153
Estimation error, 26
Estimation error dynamics, 27
Event Scheduler, 128
"Externalities," 168

Fail-to-open/close failures, 105–106
Failure detection filters, 17–19
Failure modes, 70
Failure probability, modeling, 106
False alarms
  identification of, 35
  rate of, 16
Fault adaptive control systems, 73
Fault detection
  induction motor dynamics for, 32
  key to, 43
  on power systems, 35–43
  via analytic redundancy, 17
Fault detection circuitry, 53
Fault detection, isolation, and accommodation (FDIA) procedure, 17
Fault detection schemes, 39–41
  basic function of, 16
Fault detector, 34
Fault injection module, 53
Fault scenarios, managing, 71–73
Fault tolerance, as an IPR design objective, 50
Fault tolerance enhancement framework, 15
Fault tolerant operation, dynamical models in, 15–45
Federal Energy Management Program, 172
Federal Energy Regulatory Commission (FERC), 80, 81
Field flux, 20
Field orientation, implementation of, 21–22
Field-oriented (vector) control, 19–20
Field-oriented controllers, 20
Field-oriented induction machine, dynamic response of, 21
Filters, failure detection, 17–19
Financial risk, 140–141. *See also* Risk entries
Finite state machine diagram, 77
Flexible AC transmission system (FACTS) devices, 5
Flux and torque control, decoupled, 20–21
Flux linkages, 31
Fossil fuels, 167
Friendly request negotiation stage, 63–64
Fuel cell technology, 164
Fuel cost uncertainty, 170
Funded research, under the EPNES award, 10–12
Fuzzy logic, 29

Gain-scheduled nonlinear observer, 35
Gel, Esma, xi, 87
Generation cost scenarios, 128–129
Generation technologies
  non-traditional types of, 158
  small-scale, 164
Generators
  constraints related to, 152
  "level playing field" among, 168
Generic decision model structure, 123–126
Generic market model, 148–150
Geographic information system (GIS), 130–131. *See also* GIS-based simulation studies
Geometric techniques, 29, 34, 44
GIS-based simulation studies, for power systems education, 119–155. *See also* Geographic information system (GIS)
Global sustainability technology, 5
Government entities, interest in DG, 171–172
Government policies, 172–173
  DG implementation and, 167–168
Grid-driving decisions, simulation of, 143
Grid operation models/methods, 143–154
Grid operations model (GOM), 133
Group decision making, markets and, 141–142

Hadjicostis, Christoforos N., xi, 15
Harmonic filter (HF), 10
Heuristic approaches, 135
Heydt, Gerald T., xi, 87
Hierarchical planning, 133–137
High confidence systems architecture, challenges related to, 4
High-performance electric power system model, 8
High-performance electric power systems (HPEPS), 6
High-voltage breakers, reliability of, 67
Hirsh, Richard F., xi, 157
Hubele, Norma, xi, 87
Hughes, T. P., 158–159
Hybrid dynamical systems theory, 73

IFOC-driven induction motors
  broken rotor bar detection on, 28–35
  detuning detection and accommodation on, 19–28
IMSL software, 133
Indirect field-oriented control (IFOC) diagram, 22. *See also* IFOC-driven induction motors
Indirect field-oriented controlled induction motor model, 23–24
Indirect field-oriented controller, 22
Inductances, 31
Induction machines, flux pattern disturbances in, 29
Induction motor dynamics, 32
Induction motors
  IFOC-driven, 19–28, 28–35
  parameters of, 28, 34
Industry-government partnerships, 13
Input (UI) observer approach, 17

Input lines, 60, 61
Integrated power system (IPS), 1, 8
  in ship architecture, 74–76
Intellectual disciplines, existing barriers between, 3
Intelligent control and communication unit (ICCU), 51–52
Intelligent power router ancillary service, defined, 82
Intelligent power router concept, 48–50
Intelligent power routers (IPRs), 47–85. *See also* IPR entries
  described, 48, 51
  distributed, 82
  electrical network featuring, 59
  islanding-zone approach via, 61–62
  local, 59
  restoration of electrical energy networks with, 59–60
  risk assessment of a system operating with, 65–71
  risk sources for a system with, 69
  strategic distribution of, 49–50
  synergy with LMP, 81–82
  technical/social/economical potential for optimality, 81–82
  types of, 60
Intelligent power router service, economic issues related to, 79–82
Interdisciplinary approach, 2
Interdisciplinary curriculum, 6
Interdisciplinary research
  framework for, 1–14
  in systems, economics, and environment, 12
Interdisciplinary research work, 14
Interface technologies, 167
Interfacing, 130–133
Interfacing circuits (ICKT), 50–51
Interior IPRs, 62, 63, 82. *See also* Intelligent power routers (IPRs)
Internal combustion engines, modular, 164
Inter-zone assistance request, 64
Intiyot, Boonyarit, xi, 119
Intra-zone negotiation, 62–64
Investor-owned utilities (lOUs), 168
IPR architecture, 50–55, 82. *See also* Intelligent power routers (IPRs); IPR network architecture
IPR communication protocols, 55–65
IPR components, 65–66
IPR configurations
  in a 179-bus section, 72
  reliabilities and failure probabilities of, 67–68
IPR decision making, performance and quality of, 61
IPR intercommunication subsystem, 55
IPR internal configurations, 66
IPR modules, decentralized, 50
IPR negotiation phases, 62–64
IPR network architecture, 60–61
IPR network communication, 60
IPR operation, 69
IPR reliability, 83
IPR software module, 50–55
IPR states, 70–71
IPR subsystems, 65
IPR system, 49
  switch-based, 51–52
  virtual test bed (VTB) simulation of, 52–53
Irizarry-Rivera, Agustín A., xii, 47
Islanding-zone approach, via IPR, 61–62

Karady, George G., xi, 87
Key performance indicators (KPIs), 120, 125
Kirchoff's current law, 153
Kirchoff's voltage law, 153
Knowledge
  broader dissemination of, 3–4
  unification of, 2

Lagrange multiplier, 150
Large-scale optimization, 133–137
Latching circuit, 113
Latching type switch, 91
Legislative changes, 161–163
Linear congruential method, 145–146
Line-to-ground fault, 55
Load change, 39
Load conditions, influence of, 29
Load energization, analysis of, 97
Load-flow equations, 36
Load-forecasting formula, 144, 146
Load priorities, 52, 55
Load serving entities (LSEs), 171, 173
Load shaping, 152
Load-shedding communication stage, 64
Load-shedding operations, 55
Load torque conditions, 44
Load uncertainty, 170
Local area power networks, 59
Local power generation, 165
Locational marginal price (LMP) concept, 80, 81–82
Lost line, 37–38, 42

Machine parameters, 42
Magnetic coils, 93
Magnetizing flux, 25
  estimation of, 26–27

Magneto-motive force (MMF), 20
Market-clearing condition, 148–149
Market-clearing price, 146, 149
Market constraints, 152–153
Market maker, 146–150
Market model, 147
  for demand planning, 147
  generic, 148–150
Markets, group decision making and, 141–142
Markov chain, 71, 73
Markov model, 106
Mathematical Analysis Toolkit module, 6–7
MATLAB Stateflow toolbox, 77
Mean time between failure (MTBF), 67
Medium voltage circuit breaker, 88–90, 95, 109–110, 114–115
MEMS-based circuit breaker, 92–95. *See also* Micro-electro-mechanical systems (MEMS)
  feasibility of, 114, 115
  operational principle of, 93–94
MEMS devices
  higher tolerance of, 109
  failure of, 106
MEMS switches, 115. *See also* Micro-electro-mechanical switches (MEMS)
  building blocks for, 110
  estimated dimensions of, 115
  failure probability of, 107
  opening of, 100–101
MEMS switch operation, 99
  overvoltages and, 104
MEMS switch technology, 90–91
MEMS technology, fast growth of, 115
MEMS units, number of, 108–109
Micro-electro-mechanical switches (MEMS), 87–88, 90. *See also* MEMS switch entries
  components of, 91
  specifications for, 92
Micro-electro-mechanical systems (MEMS), 10. *See also* MEMS entries
  funded research for, 11–12
Micromechanical switches, power circuit breaker using, 87–117
Microswitches, 113
Minimal unobservability distribution, 18, 19, 33
Model-based broken rotor bar detection techniques, 29
Model-based fault detection, 16–19
Model-based fault detection scheme, 35–43
Model-based fault detection techniques, 16
Modeling, computational techniques for DC/AC systems, 6
Modeling tools, 123
Modern technological systems, 158
Modular decentralized control, 50
Momentum, 158–159
  distributed generation and, 164–166
  in the electric utility system, 159–161
  of the American electric utility system, 172
  stakeholders and, 161, 163
Momentum change, in the American electric utility system, 157–175
Momoh, James, xi, 1
Monte Carlo simulation model, 108
Motor current signature analysis (MCSA) method, 29
Motors, residual behavior for, 34
Multidisciplinary approach, 3
Multimachine state estimation, 35
Must-run generators, 152
Must-serve loads, 151

Naval Integrated Power System, 1
Navy Electric Ship example, 38–39
Navy power system model, 8–10
Navy power systems baseline ship architecture, 5
Navy power system topology, 9
Negative array, 97
Negative switches (NC), 94, 97, 100
Negative voltage cycle, 100
Nested optimization problems, 137–138
Network flow graph optimization problem, 59
Network intelligence, distributing, 47, 48
Network intelligence/control functions, distributing, 59
Network operation conditions, 35
Network parameters, 42
Networks of Power: Electrification in Western Society (Hughes), 158
New generators and consumers (NGCs), 169
  risks for, 170
Newton-Raphson load flow method, 153
New York State Energy Research and Development Authority (NYSERDA), 171
Next-generation power network control model, 48
9-bus WSCC equivalent system, 79
Noisy measurements, 34
NSF initiatives, EPNES as a benchmark for, 13–14
NSF/ONR awards, 10
NSF-ONR EPINES initiative, ix
Nuisance fault modes, 32
Nuisance faults, 17, 18, 24
Numerical simulations, 28, 34, 41–43, 44

Object-oriented programming (OOP), 131–133
Objects, 131, 133
Observer error, 42–43
Observer performance, 42–43, 44

Office of Naval Research (ONR), 76. *See also* ONR reference system
179-bus reduced WSCC electric power system, 11
179-bus section, IPR configuration in, 72
179-bus WSCC benchmark power system, 10
O'Neill-Carrillo, Efraín, xi, 47
ONR reference system, 74–75. *See also* Office of Naval Research (ONR)
Optimal decision rules, 138
Optimality, IPR potential for, 81–82
Optimal power flow determination, modeling, 133
Optimal power flow (OPF) problem, 151
  constraints related to, 152–153
  stages of, 153
Optimal solution, 124
Optimization, large-scale, 133–137
Optimization problems, nested, 137–138
Organizations, analysis of, 169
Output diffeomorphism, 19
Output lines, 60, 61
Output statistical analyzer (OSA), 133
Output stream summarizer (OSS), 133
Overcurrents, 100, 102
Overvoltages, 95, 100, 102–103, 114
  MEMS switch operation and, 104

Parallel snubber circuit, 100
Parameters, 124
Particle swarm optimization (PSO) algorithm, 79
Pedagogy, innovative and integrated, 5
Peer-to-peer (P2P) communication network, 82
Performance measures, 123–124, 126–127
Persistent request negotiation stage, 64
Planning, hierarchical, 133–137
Planning horizons, 137
Positive array, 97
Positive switches (PC), 97
Power circuit breaker, using micromechanical switches, 87–117
Power delivery systems, future, 48
Power distribution infrastructure, decentralized, 50
Power distribution scheme, experimental results of, 65
Power electronic switching devices, 20
Power engineering education, 2
Power flow information, 49
Power-flow optimization problems, 133
Power grid, constraints related to, 153
Power hardware IPR subsystem, 65, 66. *See also* Intelligent power routers (IPRs)
Power network, 49
Power outages, 165–166
Power routers, intelligent, 47–85
Power routing, 55
Power system management/control, concepts for modeling, 133–142
Power system model, Navy, 8. *See also* Navy power system entries
Power system modeling, 5–6
  implementation of, 153–154
Power system restoration (PSR) problem, 79
  mathematical formulations for, 60
Power systems
  architectures for, 5
  automation technology in, 3
  challenges to, 4–6
  dynamic equations for, 41
  evaluating the performance of, 5
  fault detection on, 35–43
  important role of, 119–120
  parameters for, 41–42
  reform in, 13
  simulation models of, 128
  systems related to, 120
Power systems design, case studies in, 122
Power systems education, GIS-based simulation studies for, 119–155
Power system simulation objects, 142
Power systems management case studies, 122
Prefault states, assessment of, 16
Prescriptive models, 125–126
  data flow of, 126
Principal power router (PPR), 60
Priority factors, 61
Probability distributions, 124
Proof of principles experiment, 109–114, 115
Pseudomeasurements, 35
Pseudorandom numbers, 145–146
PSPICE model, 98
Public policy
  case studies in, 122
  decision problems in, 120
  DG implementation and, 167–168
  uncertainty in, 170
Public utility commissions, early, 161
Public Utility Regulatory Policies Act (PURPA), 161–162
Pulse generator, 113

"Radical" technologies, 159
Ramirez-Orquin, Alberto R., xi, 47
Randomized load simulator, 144–146
Random number generators (RNGs), 144–145
Random number stream, reproducibility of, 145
Random performance measures, 124
Random variables, 124
Reconfiguration logic, implementation of, 77
Reconnection steps, right order of, 59

Redundant switches, determining the number of, 105–109
Regulatory constraints, 4
Regulatory inertia, 167
Regulatory uncertainty, 170
Reliability, approximations to estimate, 106–108
Reliability analyses, 105–109
  computational results of, 108–109
Reliability assessment, 68–71
Reliability estimates, 67
Reliability factors, 61
Reliability theory, 66–71
Research, multidisciplinary, ix. *See also* Interdisciplinary research entries
Residual behavior, 34
Residual candidate, 39–40
Residual demand functions, 149
Residual generation problem, 18–19
Residual generator, 25
  validating, 28
Residual generator dynamics, 33
Residuals, 17
Residual signal, 40, 41–42
Restoration process, for electrical energy networks, 59–60
Restricted diagonal detection (RDD) filter, 17
Retail markets, 142
Risk, challenges related to, 4. *See also* Financial risk
Risk assessment, of a system operating with IPR, 65–71
Risk constraint, 150
Risk factors, in DG adoption, 169–170
Risk framework assessment, 68
Risk management model (RMM), 133
Risk modeling, stochastic decisions and, 140–141
Risk sources, for a system with IPR, 69
Robust systems architectures/configurations, challenges related to, 4
Rodríguez-Martínez, Manuel, xi, 47
Rolling horizon, 138–139
Rotating frames, 43
Rotor flux dynamics, 32
Rotor speed, 25, 33
Rotor time constant, 22, 26, 28, 34
Rotor windings, 30
Routers, information exchange capability among, 48

Scalability, as an IPR design objective, 50
Scheduling options
  capacity and demand constraints on, 139
  parameters for, 139
Security
  challenges related to, 4
  funded research for, 10–12
Self-reconfigurable control system, 73, 74
Self-reconfigurable systems, 83
Sequential decision processes (SDP), 137–140
Series configuration, 68
Series/parallel system equations, 67
Ship architecture, integrated power system in, 74–76
Ship power systems
  example of, 38–39
  future of, 77
Ship service converter module (SSCM), 76
Ship service inverter module (SSIM), 76
Ship service power supply (PS), 8
Short circuits, 90
SimPower model, 54, 55, 57, 58
SimPower system simulation package, 53
Simulated system time, 128
Simulation controller (SC), 133
Simulation framework, 52–53
Simulation model, "replication" of, 128
Simulation modeling, 126–130
Simulation packages
  comparison of, 154
  interface to, 130
  for power system modeling, 153–154
Simulation results, 77
Simulink, 76
Simulink DCZEDS simulation results, 78
Simulink model, enhancing, 77
Sink power router (SnkPR), 60, 63, 64
Slip frequency, 21
Small-scale technologies, 162
Snubber resistances, 95
Social-science systems approach, 157–175
  utility system change and, 158–159
Socioeconomic principles, convergence with new system theories, 2
Sociopolitical databases, 131
Software IPR subsystem, 65, 66. *See also* Intelligent power routers (IPRs)
Software library, 65
Software module, IPR, 50–55
Software reliability estimates, 67
Source power router (SrcPR), 60, 64
Sovacool, Benjamin K., xii, 157
Special protection scheme (SPS), 68
Squirrel cage induction motor model, with broken rotor bars, 29–31
"Stacks," 146, 148, 150
Standard market design (SMD), 83
Standard market design environment, 80–81

Stankovic, Aleksandar M., xi, 15
State diffeomorphisn, 19
State estimation, 35
Stateflow toolbox, 77
State transition procedures, 128
Stator currents, 21, 23
Stator steady state values, 27
Stator windings, 30
Steady state messages, 61
Steam-turbine generators, 160
Stochastic decisions, risk modeling and, 140–141
Stochastic model, 124
Strategic business planning, 169
Strategic decisions, long-range, 135
Subsidization, 173
  asymmetric, 167
Supercapacitor, 111
Supply function, 149
Survivability, as an IPR design objective, 50
Swing model, structure-preserving internal-node, 35
Switch closing, 94–95
Switches
  building blocks for, 110
  calculating expected lifetime of, 105–109
  delayed closing of, 103–104
  delayed opening of, 100
Switching arrays
  circuit diagram of, 96
  model development of, 97
  operation of, 95–105
Switching matrix, PSPICE model of, 98
Switching module, 112
Switching strings, 115
Symmetrical line short circuit, 37
Synchronous machine (SM), 8
System blackout, 59
System collapse, 68, 69
System components, modeling detailed interactions of, 128
System configuration model (SCM), 133
System engineering concepts, 13
System impedance, reduction of, 103
System momentum, 158–159
System momentum change, politics and, 161–163
System performance, representative sample of, 128–129
System reconfiguration problem, 79
Systems
  challenges related to, 4
  computerized descriptions of, 127
  interdisciplinary research in, 12
System state data, 128
System status information, distributed algorithms for disseminating, 55
Systems theory, funded research for, 11–12
System truth table, 79

Target fault modes, 32
Target faults, 17–18, 24
Technological evolution, social nature of, 160
Technological innovation, 169
"Technological stasis," 161
Technological systems, 158
Technological uncertainty, 170
Technology/communications, funded research for, 11–12
Test beds, EPNES benchmark, 7–8
3-bus power system, 53, 54, 56
Three-phase circuit breaker, 89
3-phase computer controllable bus, 58
Time object, 131
Time rotor constant, 28
Transient current surge, 103
Transistor bridge (H-bridge), 111
Transition probabilities, 107–108
"Turn-off" signal, 97–100
"Turn-on" signal, 100
24/7 operation, as an IPR design objective, 50

Unit failure, 107
Units
  failure probability distribution of, 107–108
  number of, 108–109
Utility managers, 163
Utility practice, 15–16, 81
Utility system
  approaches for restructuring, 157–175
  restructuring, 172
Utility system change, social-science systems approach and, 158–159

Vacuum-bottle circuit breaker, 89–90
Value at risk (VAR), 129–130, 140–141, 150
Vélez, Bienvenido, xii, 47
Vélez-Reyes, Miguel, xi, 47
Vienna monitoring method (VMM), 29, 34
Virginia Tech Electricity Grid and Market Simulator (VTEGMS), 142, 143
Virtual test bed (VTB) simulation, 52–53

Wholesale markets, 142
WSCC 9-bus model, 65. *See also* 179-bus WSCC benchmark power system

Zonal distribution architecture, 74, 76

Books in the IEEE Press Series on Power Engineering

Principles of Electric Machines with Power Electronic Applications, Second Edition
M. E. El-Hawary

Pulse Width Modulation for Power Converters: Principles and Practice
D. Grahame Holmes and Thomas Lipo

Analysis of Electric Machinery and Drive Systems, Second Edition
Paul C. Krause, Oleg Wasynczuk, and Scott D. Sudhoff

Risk Assessment for Power Systems: Models, Methods, and Applications
Wenyuan Li

Optimization Principles: Practical Applications to the Operations of Markets of the Electric Power Industry
Narayan S. Rau

Electric Economics: Regulation and Deregulation
Geoffrey Rothwell and Tomas Gomez

Electric Power Systems: Analysis and Control
Fabio Saccomanno

Electrical Insulation for Rotating Machines: Design, Evaluation, Aging, Testing, and Repair
Greg Stone, Edward A. Boulter, Ian Culbert, and Hussein Dhirani

Signal Processing of Power Quality Disturbances
Math H. J. Bollen and Irene Y. H. Gu

Instantaneous Power Theory and Applications to Power Conditioning
Hirofumi Akagi, Edson H. Watanabe, and Mauricio Aredes

Maintaining Mission Critical Systems in a 24/7 Environment
Peter M. Curtis

Elements of Tidal-Electric Engineering
Robert H. Clark

Handbook of Large Turbo-Generator Operation Maintenance, Second Edition
Geoff Klempner and Isidor Kerszenbaum

Introduction to Electrical Power Systems
Mohamed E. El-Hawary

Modeling and Control of Fuel Cells: Disturbed Generation Applications
M. Hashem Nehrir and Caisheng Wang

Power Distribution System Reliability: Practical Methods and Applications
Ali A. Chowdhury and Don O. Koval

Economic Market Design and Planning for Electric Power Systems
James Momoh and Lamine Mili

Operation and Control of Electric Energy Processing Systems
James Momoh and Lamine Mili

Restructured Electric Power Systems: Analysis of Electricity Markets with Equilibrium Models
Xiao-Ping Zhang

An Introduction to Wavelet Modulated Inverters
S.A. Saleh and M. Azizur Rahman